

**Development of Ligand Conjugated Nano Drug Delivery
System to Prevent Lymphatic Metastasis of Breast Cancer**



A Thesis

submitted to

The Tamil Nadu Dr. M.G.R. Medical University

Chennai

In partial fulfillment for the award of degree of

DOCTOR OF PHILOSOPHY

in

Pharmacy and Pharmaceutics

By

Siram Karthik, M. Pharm.,

Ref. No. EXII(1)/54272/2013

Reg. No: 141440019

Under the Guidance of

Dr. V. SANKAR, M. Pharm., Ph.D.,

Professor and Head

Department of Pharmaceutics

PSG College of Pharmacy

Coimbatore

December 2017

Certificates

**Dr. V. SANKAR, M. Pharm, Ph.D.,
Vice Principal and Head,
Department of Pharmaceutics,
PSG College of Pharmacy,
Coimbatore.**

Certificate

This is to certify that the Ph.D. thesis entitled “**DEVELOPMENT OF LIGAND CONJUGATED NANO DRUG DELIVERY SYSTEM TO PREVENT LYMPHATIC METASTASIS OF BREAST CANCER**” being submitted to the Tamil Nadu Dr. MGR Medical University, Chennai, for the award of degree of **DOCTOR OF PHILOSOPHY** in **PHARMACY & PHARMACEUTICS** was carried out by **Mr. SIRAM KARTHIK**, at **PSG COLLEGE OF PHARMACY**, Peelamedu, Coimbatore, under my direct supervision and guidance to my fullest satisfaction. The contents of this thesis, in full or in parts, have not been submitted to any other Institute or University for the award of any degree or diploma.

Place: Coimbatore

Dr. V. SANKAR, M. Pharm, Ph.D.,

Date:

(Centre Head)

**Dr. V. SANKAR, M. Pharm, Ph.D.,
Vice Principal and Head,
Department of Pharmaceutics,
PSG College of Pharmacy,
Coimbatore.**

Certificate

This is to certify that the Ph.D. thesis entitled “**DEVELOPMENT OF LIGAND CONJUGATED NANO DRUG DELIVERY SYSTEM TO PREVENT LYMPHATIC METASTASIS OF BREAST CANCER**” being submitted to the Tamil Nadu Dr. M.G.R Medical University, Chennai, for the award of degree of **DOCTOR OF PHILOSOPHY** in **PHARMACY & PHARMACEUTICS** was carried out by **Mr. SIRAM KARTHIK**, at **PSG COLLEGE OF PHARMACY**, Peelamedu, Coimbatore, under my direct supervision and guidance to my fullest satisfaction. The contents of this thesis, in full or in parts, have not been submitted to any other Institute or University for the award of any degree or diploma.

Place: Coimbatore

Dr. V. SANKAR, M. Pharm, Ph.D.,

Date:

(Supervisor & Guide)

**Dr. M. RAMANATHAN, M. Pharm., Ph.D.,
Professor and Head,
Department of Pharmacology,
PSG College of Pharmacy,
Coimbatore.**

Certificate

This is to certify that the Ph.D. thesis entitled “**DEVELOPMENT OF LIGAND CONJUGATED NANO DRUG DELIVERY SYSTEM TO PREVENT LYMPHATIC METASTASIS OF BREAST CANCER**” being submitted to the Tamil Nadu Dr. M.G.R Medical University, Chennai, for the award of degree of **DOCTOR OF PHILOSOPHY** in **PHARMACY & PHARMACEUTICS** was carried out by **Mr. SIRAM KARTHIK**, at **PSG COLLEGE OF PHARMACY**, Peelamedu, Coimbatore, under the direct supervision and guidance of **Dr. V. SANKAR, M. Pharm., Ph.D.**, Professor & Head, Department of Pharmaceutics, PSG College of Pharmacy, Coimbatore.

Place: Coimbatore

Dr. M. RAMANATHAN, M. Pharm., Ph.D.,

Date:

(Principal)

DECLARATION

I hereby certify that I am the sole author of this thesis entitled **“DEVELOPMENT OF LIGAND CONJUGATED NANO DRUG DELIVERY SYSTEM TO PREVENT LYMPHATIC METASTASIS OF BREAST CANCER”** and that neither any part of this thesis nor the whole of the thesis has been submitted for a degree to any other University or Institution. I certify that, to the best of my knowledge, my thesis does not infringe upon anyone’s copyright nor violate any proprietary rights and that any ideas, techniques, quotations, or any other material from the work of other people included in my thesis, published or, are fully acknowledged in accordance with the standard referencing practices. I declare that this is a true copy of my thesis, including any final revisions, as approved by my thesis review committee.

Place: Coimbatore

SIRAM KARTHIK

Date:

Acknowledgement



Dedicated to

My beloved Parents,

Innocent Rats, Teachers,

Friends & Nation

ACKNOWLEDGEMENT

Behind every achievement there are many helping hands that aid in reaching an objective.

“**LEARNING FIRST BEGINS AT HOME**”. Hence it is my privilege to thank my dearest lovable **Parents, Sister** and **brother-in-law** whose unconditional love and support has been the driving force throughout this process of my learning.

I would like to express my sincere gratitude to my dynamic and supportive guide, **Dr. V. Sankar., M. Pharm., Ph.D.**, Head of the Department of Pharmaceutics and Vice Principal, PSG College of Pharmacy, for his guiding force and intellectual ideas throughout this work. His innovative and constructive ideas have been very invaluable and enlightening which made the work interesting and easy. His kind help during crisis was very valuable.

I extend my special heartfelt thankfulness and deep respects to my beloved co-supervisor **Dr. C. Vijaya Raghavan, M. Pharm., Ph.D.**, for providing me ample freedom, motivation and all the support to express myself.

I would like to express my sincere gratitude to my generous and supportive Principal, **Dr. M. Ramanathan., M. Pharm., Ph.D.**, for providing facilities and moral support from time to time for the completion of this work.

I would like to thank my department teachers **Dr. S. M. Habibur Rahman., Ph.D., Dr. S. Subramanian., Ph.D., Mr. Vaiyana Rajesh, M.Pharm., Mr. S. Kartikeyan, M. Pharm., Mrs. Nithya, M. Pharm., Mrs. Vijayalakshmi and Mr. Nikhil., Ph.D., Department of Pharmaceutics**, for their constructive and valuable ideas at various stages of the work.

I express my sincere thanks to **Mr. R. Hari Prasad, M. Pharm.**, Assistant Professor, PSG CP, Coimbatore, **Mr. Siva Selva Kumar, M. Pharm.**, Assistant Professor, PSG CP, Coimbatore, **Dr.N.Tamilselvan, Dr. Darshit Shah, Mr. Balakumar Krishnamoorthy, Dr. R. Ranjith Kumar., Ph.D.**, Assistant Professor, PSG CP, Coimbatore, **Dr. K.G Prasanth., Ph.D., King Khalid University., and Dr. B. Balaji., Ph.D.**, for their timely suggestions and help.

I specially thank **Dr. Imran Ahmad, President and CEO, Jina Pharmaceuticals Inc, United States of America, Dr. Franklin Gregory, Poland, and Dr. Marslin Gregory, China**, for keeping me inspired throughout the research period through his valuable ideas and advice.

Special thanks to **Dr. Mansi K. Shah**, Postdoctoral Fellow, University of Texas Medical Branch, Texas, United States of America for her support in various stages of the work.

I express my deepest thanks to my colleagues, **Mr. S. Divakar, Mr. Mrinmoy Gautam, Mrs. R. Lavanya, Mr. K. Arjunan, Mr. Ravi Kumar Rajan, Mr. Abdul Khayyum, Dr. Kalpana, and Mr. Manikandan**, for their valuable support and for creating a wonderful working environment.

I owe my gratitude to **Dr. Anuradha Ashok., Mr. Kartikeyan and Mr. Vijayarghavan** for helping me in carrying out TEM and AFM analysis.

I am thankful to my friends **Harsha, Raghava Chandra, Vamshi Krishna Karanam, Kamal Sagar, J. Bhanu Ramakrishna, Mounika, Venkateswara Rao, Subramaniam, Akkineni Sriram, V. Sai dutt, Vithunes Mani, Jeeva, Akash, Harish**, for keeping me in high spirits.

I would like to thank **Mr. Karthik Kumar, Mrs. Nithya, Mr. Asad Kumar, Mrs. Chithra, Mrs. Chithra Priya and Mr. Murugan** for helping me in providing various chemicals and glasswares during the project.

I wish to thank **Mrs. Mini Nair**, Saraswathi Computer Centre, Coimbatore, for helping me in shaping the book to perfection.

I gratefully acknowledge the **Tamil Nadu State Council for Science and Technology, Government of Tamil Nadu**, for providing me the financial assistance for carrying out my research work under the “**Research Funding for Research Scholars**” scheme.

I owe my most sincere gratitude to **PSG Sons and Charities** for providing financial support and all the facilities to carry out this work.

I would like to acknowledge Gattefosse, Germany, Subhash Chemicals, India and Lipoid, Germany, for providing me the gift samples.

Siram Karthik

Contents

CONTENTS

Chapter No.	Title	Page No.
	LIST OF ABBREVIATIONS	vii
	LIST OF TABLES	x
	LIST OF FIGURES	xii
1	INTRODUCTION	1
1.1	BREAST CANCER: MOTIVATION AND STATISTICS	1
1.2	METASTASIS OF BREAST CANCER AND THE ROLE OF LYMPHATICS IN ASSISTING THE SPREAD:	1
1.3	LYMPHATICS AND THEIR ROLE	5
1.4	NANOTHERAPEUTICS FOR CANCER CHEMOTHERAPY	6
1.5	LIPID BASED NANOTHERAPEUTICS	7
1.6	VARIOUS KINDS OF LIPID BASED COLLOIDAL DRUG CARRIERS	8
1.7	LIPID BASED NANOTHERAPEUTICS FOR PREVENTION OF CANCER METASTASIS BY TARGETING THE LYMPHATICS	11
1.8	SOLID LIPID NANOPARTICLES	12
1.9	ADVANTAGES OF SLNs	13
1.10	TOXICITY AND REGULATORY STATUS OF LIPID EXCIPIENTS	13
1.11	METHODS OF PREPARATION OF SOLID LIPID NANOPARTICLES	15
1.12	SCALE UP FEASIBILITY	19
1.13	STABILITY OF SOLID LIPID NANOPARTICLES	19
1.14	TARGETING LIGAND AND THEIR RECEPTORS	20
1.15	QUILLAJA SAPONIN (QS) AND ITS ROLE AS A SURFACTANT	22
2	AIM AND OBJECTIVES	23

Chapter No.	Title	Page No.
3	REVIEW OF LITERATURE	26
3.1	METASTASIS OF BREAST CANCER	26
3.2	LYMPHATIC TARGETING OF DRUGS USING NANOPARTICLES	27
3.3	DIFFERENT TYPES OF NANOPARTICLES	29
3.4	APPLICATION OF LIPIDS IN LYMPHATIC DELIVERY	33
3.5	SOLID LIPID NANOPARTICLES AND THEIR APPLICATION IN LYMPHATIC TARGETING	37
3.6	IMATINIB MESYLATE	39
3.7	QUILLAJA SAPONIN	40
3.8	IMPORTANCE OF DRUG SOLUBILISATION IN THE LIPIDS	42
3.9	PREPARATION AND CHARACTERISATION OF SOLID LIPID NANOPARTICLES AND CONJUGATION USING VARIOUS LIGANDS	49
3.10	PHARMACOKINETIC STUDIES	51
4	SCOPE AND PLAN OF WORK	53
4.1	SCOPE	53
4.2	PLAN OF WORK	54
5	MATERIALS AND METHODS	56
5.1	MATERIALS	56
5.2	INSTRUMENTS	58
5.3	IMATINIB MESYLATE (IM)	59
5.4	QUILLAJA SAPONIN (QS)	61
5.5	VITAMIN B12	62
5.6	HYALURONIC ACID	64
5.7	PALMITIC ACID	66
5.8	STEARIC ACID	67
5.9	GLYCERYL PALMITOSTEARATE	69

Chapter No.	Title	Page No.
5.10	GLYCERYL MONOSTEARATE	70
5.11	GELEOL MONO AND DI GLYCERIDES	72
5.12	DETERMINATION OF LAMBDA MAX (λ_{\max}) FOR IM USING UV SPECTROPHOTOMETER	73
5.13	CONSTRUCTION OF CALIBRATION CURVE FOR IM USING UV SPECTROPHOTOMETER AT 256 nm	73
5.14	DEVELOPMENT OF ANALYTICAL METHOD USING HIGH PERFORMANCE LIQUID CHROMATOGRAPHY	73
5.15	SOLUBILITY OF IM IN VARIOUS LIPIDS	77
5.16	CALCULATION OF TOTAL SOLUBILITY PARAMETERS, POLARITY OF IM AND LIPIDS	77
5.17	IDENTIFICATION OF DESCRIPTORS AND DEVELOPMENT OF QUANTITATIVE STRUCTURE SOLUBILITY RELATIONSHIP (QSSR) MODEL	78
5.18	DETERMINATION OF PARTITIONING COEFFICIENT OF IMATINIB MESYLATE IN DIFFERENT LIPIDS AND WATER	79
5.19	INFRARED (IR) ABSORPTION SPECTROSCOPY	79
5.20	CHEMICAL CONJUGATION OF LIPID WITH LIGANDS	80
5.21	PREPARATION OF IM LOADED SOLID LIPID NANOPARTICLES (SLNs)	80
5.22	PREPARATION OF SLNs ADSORBED WITH HYALURONIC ACID	81
5.23	PREPARATION OF SLNs CONJUGATED WITH LIGANDS	81
5.24	FREEZE DRYING	81
5.25	NMR SPECTROSCOPY	81
5.26	DETERMINATION OF PARTICLE SIZE AND POLY DISPERSITY INDEX (PDI)	81
5.27	DETERMINATION OF ZETA POTENTIAL	82
5.28	TRANSMISSION ELECTRON MICROSCOPY	82

Chapter No.	Title	Page No.
5.29	ATOMIC FORCE MICROSCOPY	82
5.30	ENTRAPMENT EFFICIENCY	82
5.31	<i>IN VITRO</i> DRUG RELEASE	83
5.32	<i>IN VITRO</i> HAEMOLYSIS TEST	83
5.33	<i>IN VITRO</i> CYTOTOXICITY STUDIES	83
5.34	APOPTOSIS ANALYSIS	84
5.35	STERILITY TESTING	84
5.36	<i>IN VIVO</i> PHARMACOKINETIC STUDIES	85
5.37	STABILITY STUDIES AS PER ICH GUIDELINES	87
5.38	STATISTICAL ANALYSIS	87
6	RESULTS AND ANALYSIS	88
6.1	DETERMINATION OF LAMBDA MAX (λ_{\max}) OF IMATINIB MESYLATE USING UV SPECTROPHOTOMETER	88
6.2	CONSTRUCTION OF CALIBRATION CURVE FOR IMATINIB MESYLATE USING UV SPECTROPHOTOMETER AT 256 nm	88
6.3	ANALYTICAL METHOD DEVELOPMENT	89
6.4	SCREENING OF LIPIDS FOR IM SOLUBILITY	95
6.5	SOLID STATE CHARACTERISATION USING DIFFERENTIAL SCANNING CALORIMETRY	97
6.6	QUANTIFICATION OF SOLUBILITY OF IMATINIB MESYLATE IN THE LIPIDS	100
6.7	ESTIMATION OF TOTAL SOLUBILITY PARAMETERS, POLARITY OF IMATINIB MESYLATE AND LIPIDS	101
6.8	IDENTIFICATION OF DESCRIPTORS AND DEVELOPMENT OF QUANTITATIVE STRUCTURE SOLUBILITY RELATIONSHIP MODEL	102
6.9	DETERMINATION OF PARTITIONING COEFFICIENT OF IMATINIB MESYLATE IN DIFFERENT LIPIDS AND WATER	106
6.10	INFRARED (IR) ABSORPTION SPECTROSCOPY	107

Chapter No.	Title	Page No.
6.11	CHEMICAL CONJUGATION OF STEARIC ACID WITH LIGANDS	114
6.12	PREPARATION OF IM LOADED SOLID LIPID NANOPARTICLES (SLNs)	117
6.13	PHYSICAL ADSORPTION WITH HYALURONIC ACID	119
6.14	FREEZE DRYING	119
6.15	DETERMINATION OF PARTICLE SIZE AND POLY DISPERSITY INDEX	120
6.16	DETERMINATION OF ZETA POTENTIAL	125
6.17	TRANSMISSION ELECTRON MICROSCOPY	125
6.18	ATOMIC FORCE MICROSCOPY	130
6.19	MEASUREMENT OF ENTRAPMENT EFFICIENCY	134
6.20	DIFFERENTIAL SCANNING CALORIMETRY FOR FORMULATIONS	134
6.21	<i>IN VITRO</i> DRUG RELEASE	136
6.22	RELEASE KINETICS	139
6.23	<i>IN VITRO</i> HAEMOLYSIS TEST	140
6.24	<i>IN VITRO</i> CYTOTOXICITY STUDIES	142
6.25	APOPTOSIS ANALYSIS	145
6.26	STERILITY TESTING	146
6.27	<i>IN VIVO</i> PHARMACOKINETIC STUDIES	147
6.28	STABILITY STUDIES	151
7	DISCUSSION	156
7.1	PREFORMULATION AND ANALYTICAL STUDIES	156
7.2	SOLUBILITY OF IMATINIB MESYLTE IN LIPIDS: INFLUENCE OF MOLECULAR, CHEMICAL AND PHYSICOCHEMICAL PROPERTIES AND DEVELOPMENT OF A PREDICTORY MODEL	160
7.3	FORMATION OF LIGAND- LIPID CONJUGATES	168
7.4	SOLID LIPID NANOPARTICLES OF IMATINIB MESYLATE PREPARED USING STEARIC ACID AS LIPID CARRIER	169

Chapter No.	Title	Page No.
7.5	SOLID LIPID NANOPARTICLES OF IMATINIB MESYLATE PREPARED USING PALMITIC ACID AS LIPID CARRIER	176
7.6	SOLID LIPID NANOPARTICLES OF IMATINIB MESYLATE PREPARED USING GLYCERYL PALMITOSTEARATE AS LIPID CARRIER	179
7.7	SOLID LIPID NANOPARTICLES OF IMATINIB MESYLATE PREPARED USING GLYCERYL MONOSTEARATE AS LIPID CARRIER	186
7.8	SOLID LIPID NANOPARTICLES OF IMATINIB MESYLATE PREPARED USING GELEOL MONO AND DIGLYCERIDES AS LIPID CARRIER	188
7.9	PHARMACOKINETIC STUDIES TO QUANTIFY THE CONCENTRATION OF IMATINIB MESYLATE IN PLASMA AND SENTINAL LYMPH NODES	190
7.10	STABILITY STUDIES	192
8	SUMMARY AND CONCLUSION	194
9	IMPACT OF THE STUDY	197
10	BIBLIOGRAPHY	
11	ANNEXURES	

List of Abbreviations

LIST OF ABBREVIATIONS

AFM	-	atomic force microscopy
B12-IGPN	-	vitamin B12 conjugated solid lipid nanoparticles of imatinib mesylate prepared using palmitic acid as lipid carrier
B12-ISN	-	vitamin B12 conjugated solid lipid nanoparticles of imatinib mesylate prepared using stearic acid as lipid carrier
B12-SA	-	vitamin B12 conjugated stearic acid
BSN	-	blank solid lipid nanoparticles
DMSO	-	dimethyl sulfoxide
DSC	-	differential scanning calorimetry
EDC	-	1-Ethyl-3-(3-dimethylaminopropyl) carbodiimide
F	-	Fisher's value
FBS	-	Fetal bovine serum
FBS	-	fetal bovine serum
FDA	-	Food and Drug Administration
FTIR	-	fourier transform infrared
GPS	-	glyceryl palmitostearate
HA	-	hyaluronic acid
HAC	-	IGPN- hyaluronic acid coated solid lipid nanoparticles of imatinib mesylate prepared using palmitic acid as lipid carrier
HAC	-	ISN- hyaluronic acid coated solid lipid nanoparticles of imatinib mesylate prepared using stearic acid as lipid carrier
HAI-IGPN	-	hyaluronic acid conjugated solid lipid nanoparticles of imatinib mesylate prepared using palmitic acid as lipid carrier

HAI-SA	-	hyaluronic acid conjugated stearyl amine
HPLC	-	High Pressure Liquid Chromatography
ICH	-	International Conference on Harmonisation
IGEN	-	solid lipid nanoparticles of imatinib mesylate prepared using geleol mono and di glycerides as lipid carrier
IGMN	-	solid lipid nanoparticles of imatinib mesylate prepared using glyceryl monostearate as lipid carrier
IGPN	-	solid lipid nanoparticles of imatinib mesylate prepared using glyceryl palmitostearate as lipid carrier
IM	-	Imatinib mesylate
IM-PBS	-	imatinib mesylate in pH 7.4 PBS
IPN	-	solid lipid nanoparticles of imatinib mesylate prepared using palmitic acid as lipid carrier
IR	-	infrared
ISN	-	solid lipid nanoparticles of imatinib mesylate prepared using stearic acid as lipid carrier
LOD	-	Limit of Detection
LOO	-	leave one out model
LOQ	-	Limit of Quantification
MLR	-	multiple linear regression
MTT	-	3-[4,5-dimethylthiazol-2-yl]- 2,5-diphenyl-tetrazoliumbromide
NMR	-	nuclear magnetic resonance
P	-	Probability
PA	-	palmitic acid

PBS	-	Phosphate buffer saline
PCA	-	principal component analysis
PDI	-	polydispersity index
PI	-	Propidium iodide
PLS	-	partial least square
Q^2	-	cross validated R^2
QS	-	Quillaja saponin
QSSR	-	quantitative structure solubility relationship
R^2	-	squared correlation coefficient
R^2_m	-	multiple correlation coefficient
R^2_{pred}	-	predictive correlation coefficient
RBCs	-	red blood cells
RMSE	-	root mean square error
RP-HPLC	-	reverse phase-high performance liquid chromatography
RSD	-	relative standard deviation
SA	-	stearic acid
SD	-	standard deviation
SLNs	-	Solid lipid nanoparticles
TEM	-	transmission electron microscopy
UV	-	Ultra visible

List of Tables

LIST OF TABLES

Table No	Title	Page No
1	Calibration curve data for IM by UV spectroscopy	89
2	Optimised chromatographic conditions for HPLC	90
3	Calibration curve data for IM in aqueous samples	92
4	Calibration curve data for IM in plasma samples	92
5	Accuracy of IM in aqueous samples	93
6	Accuracy of IM in plasma samples	94
7	Interday and intraday precision of IM in aqueous and plasma samples	94
8	Stability of IM at different temperatures and after freeze thaw test	95
9	Assessment of solubility of IM in various lipids	96
10	Quantitative solubility of IM in the lipids and their melting points.	100
11	Solubility parameter and polarity of IM and lipids along with their difference in solubility parameters.	101
12	Details of the three MLR models developed	104
13	Molecular and physicochemical descriptors of the lipids.	104
14	Statistical results of the three QSSR models developed to predict solubility of IM.	104
15	Functional groups corresponding to IM, lipids and physical mixture as observed in FT-IR spectroscopy.	113
16	Optimised conditions for the formation of solid lipid nanoparticles	117
17	Composition of different batches of SLNs	118
18	Particle size, polydispersity index, zeta potential and entrapment efficiency of the formulations.	121
19	Mechanism of release of IM from ISN	139

Table No	Title	Page No
20	Mechanism of release of IM from IPN	139
21	Mechanism of release of IM from IGPN	140
22	IC ₅₀ values of the samples	142
23	Pharmacokinetic parameters of IM in blood	147
24	Pharmacokinetic parameters of IM in lymph nodes	150
25	Particle size of the formulations over a period of 12 months	151
26	Polydispersity index of the formulations over a period of 12 months	152
27	Zeta potential of the formulations over a period of 12 months.	153
28	Entrapment efficiency of formulations over a period of 12 months.	154

List of Figures

LIST OF FIGURES

Figure No	Title	Page No
1	Metastatic dissemination of cancerous cells through the lymphatics	3
2	Diagrammatic steps representing the metastasis of breast cancer to different organs	4
3	Overview of the lymphatic system	6
4	Structure of Imatinib mesylate	59
5	Structure of quillaja saponin	61
6	Structure of vitamin B 12	62
7	Structure of hyaluronic acid	64
8	Structure of palmitic acid	66
9	Structure of stearic acid	67
10	Structure of glyceryl monostearate	70
11	Wavelength of maximum absorbance for IM using UV spectrophotometer	88
12	Calibration curve for the estimation of IM by UV spectroscopy.	89
13	Representative chromatogram of IM in aqueous sample (a) and rat plasma (b).	91
14	Calibration curve of IM in aqueous samples.	92
15	Calibration curve of IM in rat plasma.	93
16	DSC thermograms of Imatinib mesylate, bulk lipids and mixture of Imatinib mesylate and lipid.	99
17	Three dimensional molecular structures of IM and lipids.	103
18	Experimentally determined plot representing solubility of IM in lipids against predicted solubility of IM in lipids as observed in (i) model 1, (ii) model 2 and (iii) model 3.	106
19	IR spectrum of IM: pure sample	107
20	IR spectrum of QS: pure sample	108
21	IR spectrum of stearic acid: pure sample.	108
22	IR spectrum of palmitic acid: pure sample	109

Figure No	Title	Page No
23	IR spectrum of glyceryl palmitostearate: pure sample	109
24	IR spectrum of glyceryl monostearate: pure sample	110
25	IR spectrum of Geleol mono and di glycerides: pure sample	110
26	IR spectrum of physical mixture: IM, stearic acid and QS	111
27	IR spectrum of physical mixture: IM, palmitic acid and QS.	111
28	IR spectrum of physical mixture: IM, glyceryl palmitostearate and QS	112
29	IR spectrum of physical mixture: IM, QS and glyceryl mono stearate	112
30	IR spectrum of physical mixture: IM, QS and Geleol mono and diglycerides	113
31	NMR spectra of stearic acid	114
32	NMR spectra of the conjugate: HAJ-SA	115
33	NMR spectra of the conjugate: B12-SA	115
34	FT-IR spectra of the conjugate: HAJ-SA	116
35	FT-IR spectra of the conjugate: B12-SA	116
36	Freeze dried powder samples of the prepared SLNs	120
37	Particle size distribution and polydispersity index for HAC-IGPN3	124
38	Zeta potential for HAC-IGPN3	125
39	Transmission Electron Microscope Image of ISN	126
40	Transmission electron microscope image of HAC-ISN	127
41	Transmission electron microscope image of B12-ISN	127
42	Transmission electron microscope image of IPN	128
43	Transmission electron microscope image of IGPN	128
44	Transmission electron microscope image of B12-IGPN	129
45	Transmission electron microscope image of HAC-IGPN	129

Figure No	Title	Page No
46	Transmission electron microscope image of IGMN	130
47	Transmission electron microscope image of IGEN	130
48	AFM phase image and topographic image of ISN	131
49	AFM phase image and topographic image of IPN	131
50	AFM phase image and topographic image of IGPN	132
51	AFM phase image and topographic image of HAC-IGPN	132
52	AFM phase image and topographic image of IGMN	133
53	AFM phase image and topographic image of IGEN	133
54	Overlay of DSC thermogram of IM: Imatinib mesylate, QS: Quillaja Saponin, SA: Bulk Steric acid, BSN: Blank solid lipid nanoparticles, ISN3: Imatinib mesylate loaded solid lipid nanoparticles.	135
55	Overlay of DSC thermogram of IM: Imatinib mesylate, QS: Quillaja Saponin, PA: Bulk Palmitic acid, BPN: Blank solid lipid nanoparticles, IPN3: Imatinib mesylate loaded solid lipid nanoparticles of palmitic acid.	135
56	Overlay of DSC thermogram of IM: Imatinib mesylate, QS: Quillaja Saponin, GPS: Bulk Glyceryl palmitostearate, BGPN: Blank solid lipid nanoparticles, IGPN: Imatinib mesylate loaded solid lipid nanoparticles of glyceryl palmitostearate.	136
57	<i>In vitro</i> release profile of IM from ISN in phosphate buffer saline pH 7.4. Values are expressed as mean \pm standard deviation (n=3).	137
58	<i>In vitro</i> release profile of IM from IPN in phosphate buffer saline pH 7.4. Values are expressed as mean \pm standard deviation (n=3).	138
59	<i>In vitro</i> release profile of IM from IGPN in phosphate buffer saline pH 7.4. Values are expressed as mean \pm standard deviation (n=3).	138
60	Comparative <i>in vitro</i> release profile of IM from ISN3, IPN3 and IGPN3 in phosphate buffer saline pH 7.4. Values are expressed as mean \pm standard deviation (n=3).	138
61	<i>In vitro</i> haemolysis assay performed in the presence of A) QS (50 μ g/ml solution in saline); B) and C) IM (10 μ g/ ml and 20 μ g/ ml in saline; D), E) and	141

Figure No	Title	Page No
	F) ISN3 (equivalent to IM concentration of 10 µg/ml, 20 µg/ml and 30 µg/ml and QS concentration of 150 µg/ml, 300 µg/ml and 450 µg/ml); G) and H) BLNs (equivalent to QS concentrations of 50 µg/ml and 150 µg/ml); I) Negative control- Saline; J) Positive control- Distilled water	
62	<i>In vitro</i> haemolysis assay performed in the presence of A) QS (50 µg/ml solution in saline); B) IM (10 µg/ml in saline); C) and D) IPN3 (equivalent to IM concentration of 10 µg/ml and 20 µg/ml and QS concentration of 150 µg/ml and 300 µg/ml); E) BSLNs (equivalent to QS concentrations of 150 µg/ml); F) B12-IPN3 (equivalent to IM concentration of 20 µg/ml and QS concentration of 300 µg/ml); G) HAC-IPN3 (equivalent to IM concentration of 20 µg/ml and QS concentration of 300 µg/ml) H) Negative control- Saline; I) Positive control- Distilled water	141
63	Graph showing cytotoxicity in MCF7 cells in the presence of IM, QS, ISN3, Blank ISN3, mixture of blank ISN3 + IM, B12- ISN3, HAJ- ISN3 and HAC- ISN3 as revealed by MTT assay. Values are expressed as mean ± standard deviation (n=3). * Quillaja saponin concentration is represented by µg/ml unit, whereas all other samples are represented in µM concentration.	143
64	Graph showing cytotoxicity in MCF7 cells in the presence of IM, IGPN3, Blank IGPN3, mixture of blank IGPN3 + IM, B12-IGPN3, HAJ-IGPN3 and HAC-IGPN3 as revealed by MTT assay. Values are expressed as mean ± standard deviation (n=3).	143
65	Graph showing viability in RAW 264.7 cells in the presence of IM, QS, ISN3, Blank ISN3, mixture of blank ISN3 + IM, B12- ISN3, HAJ- ISN3 and HAC- ISN3 as revealed by MTT assay. Values are expressed as mean ± standard deviation (n=3). * Quillaja saponin concentration is represented by µg/ml unit, whereas all other samples are represented in µM concentration.	144
66	Graph showing viability in RAW 264.7 cells in the presence of IM, IGPN3, Blank IGPN3, mixture of blank IGPN3 + IM, B12-IGPN3, HAJ-IGPN3 and	144

Figure No	Title	Page No
	HAC-IGPN3 as revealed by MTT assay. Values are expressed as mean \pm standard deviation (n=3).	
67	Propidium iodide staining of control (b), free IM (d), IGMN (f), HA-ILN treated (h) MCF7 cells showing dead cells in the later. Corresponding light microscopic images are shown above (a), (c), (e) and (f).	145
68	Sterility testing indicating absence of bacterial growth after 24 hours incubation with 1) ISN3, 2) B12-ISN, 3) HAC-ISN, 4) IGPN3, 5) HAC-IGPN and 6) IM in pH 7.4 PBS.	146
69	Sterility testing indicating absence of fungal growth after 14 days incubation with 1) ISN3, 2) B12-ISN, 3) HAC-ISN, 4) IGPN3, 5) HAC-IGPN and 6) IM in pH 7.4 PBS.	146
70	Plasma drug concentration profile after subcutaneous administration of IM, ISN3, B12-ISN and HA-ISN.	148
71	Plasma drug concentration profile after subcutaneous administration of IM, IGPN3 and HA-IGPN.	148
72	Lymph nodes in rat	149
73	Lymph node drug concentration profile after subcutaneous administration of IM, IGPN3 and HA-IGPN.	150

Introduction

1. INTRODUCTION

1.1 BREAST CANCER: MOTIVATION AND STATISTICS

Cancer is a disease characterized by uncontrolled growth of cells. Though herculean efforts have been put up by various researchers in understanding the dynamics of cancer, treatment still remains a distant solution. Breast cancer is the most common cause of cancer death among women (522 000 deaths in 2012), making it a major global health concern. In 2008, breast cancer caused 458,503 deaths worldwide (13.7% of cancer deaths in women) and in 2012 the number shot up to 522, 000 [1]. Since the 2008, the incidence of number of patients affected by breast cancer has increased by more than 20%, while mortality has increased by 14% which clearly indicates the dangers associated with it. Early diagnosis of cancer can be treated either by surgery or chemotherapy or local irradiation. But, unfortunately patients are diagnosed from breast cancer at a stage where the dissemination of cancerous cells to the adjacent lymph nodes has already begun by metastasis. Even after extended mastectomy, the tumour can recur due to metastasis of tumor cells to the sentinel lymph nodes [2].

1.2 METASTASIS OF BREAST CANCER AND THE ROLE OF LYMPHATICS IN ASSISTING THE SPREAD

Breast cancer originates in the lobular or ductal epithelial cells as a result of a series of genetic events which leads to inhibition of normal apoptotic responses and aberrant regulation of the cell cycle. Several genes and signalling pathways are involved in the development of breast cancer including the germ-line or somatic mutations in tumor-suppressor genes (e.g., p53, BRCA1, BRCA2, and PTEN), disturbance in the signalling pathways or estrogen receptors, and over expression of proto-oncogenes like HER2/neu. Additionally, breast cancer also promotes metastasis [3,4].

Metastasis is the spread of cancer from one organ or tissue to distant organ environments. More than 90% of the cancer deaths are as a result of metastatic spread [5]. When cancer is diagnosed at an early stage, before it has spread, it can often be treated by surgery or chemotherapy or local irradiation. But, when cancer is detected after it is known to have metastasized, treatments are much less successful. Also, in patients where metastasis is not observed in the initial diagnosis, it can occur at a later time.

Cancer cells escape from the primary tumour site to the secondary organs through the blood vessels and lymphatic vessels. For some cancers like breast, prostate, colon and lung, dissemination via lymphatics precedes dissemination through blood vessels. Generally metastasis starts within the regional lymph nodes and facilitates the migration of tumour cells to other organs of the body by lymphangiogenesis. Figure 1 represents the pathway for the metastatic dissemination of cancerous cells and the process of metastasis to different organs in the body [4]. Lymphangiogenesis is a process that generates new lymphatic vessels from the pre-existing lymphatics or lymphatic endothelial progenitors. Lymphatic vessels are comparatively more favourable for the transport of pre-metastatic cancerous cells than the blood vessels because of the following reasons:

- Discontinuous basement membrane and loose cell- cell junctions of the endothelial cells
- Lower flow rate of the lymph that increases survival by minimizing shear stress
- A 1000-fold high concentration of hyaluronic acid, a molecule with potent cell protecting and pro- survival properties [4]

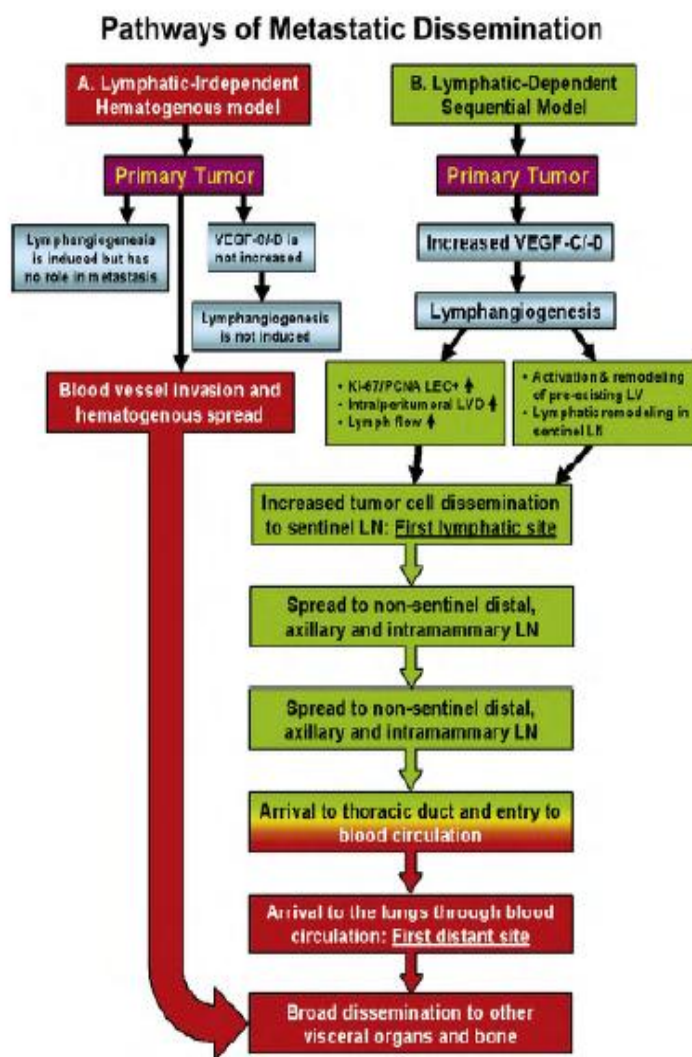


Figure 1. Metastatic dissemination of cancerous cells through the lymphatics

Figure 2 represents the metastasis of breast cancer to different organs. Thus, inhibiting lymph node metastases by targeting the anticancer drugs to the regional lymph nodes will not only reduce the tumour burden, but will also prevent the cancer metastasis through the lymphatics. This can ultimately lead to an improvement in the quality of patients' life and survivability [6]. Application of targeted delivery of anticancer nanotherapeutics to the cancer cells in the regional lymph nodes is a good option to inhibit metastases of breast cancer.

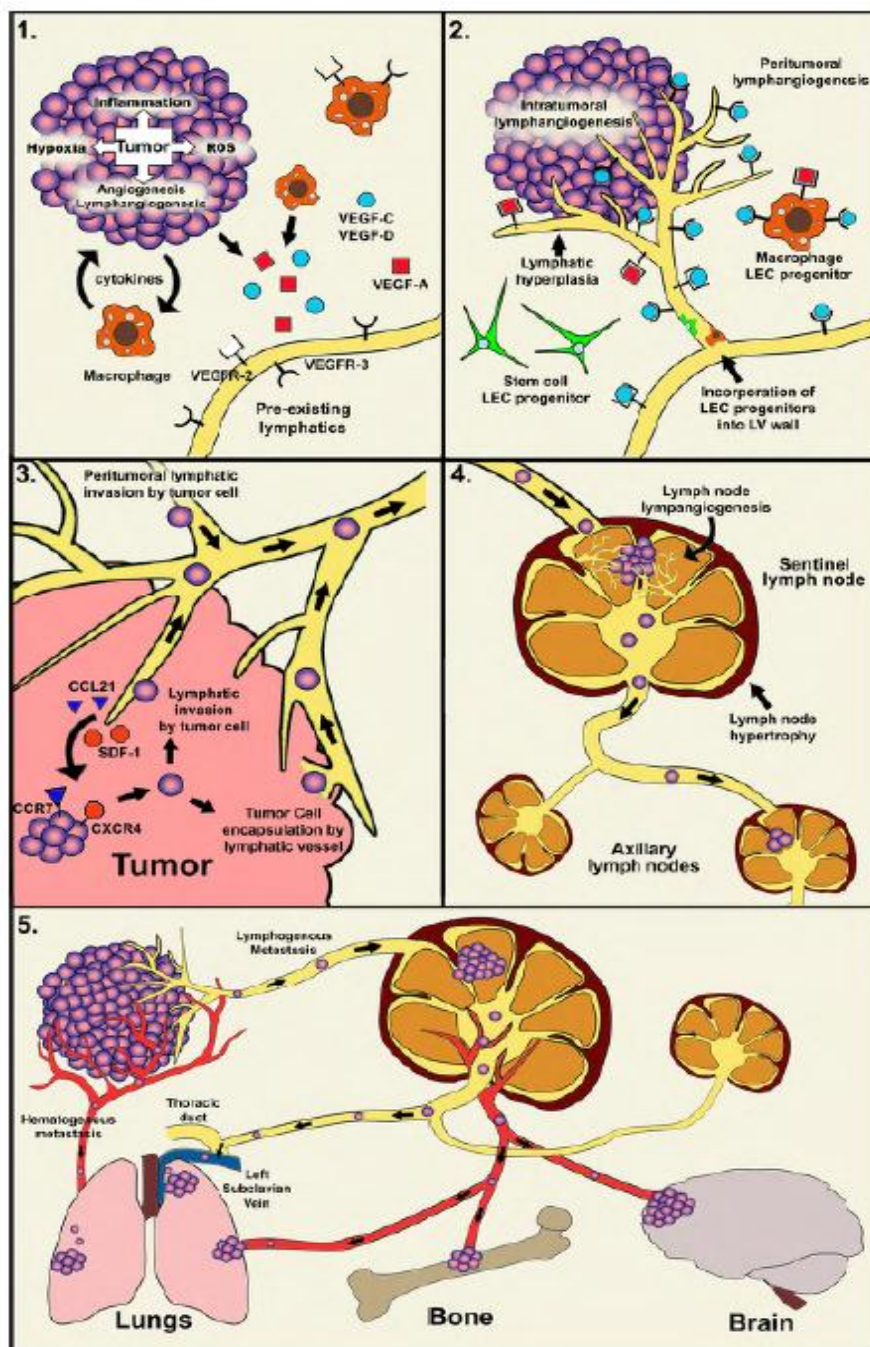


Figure 2. Diagrammatic steps representing the metastasis of breast cancer to different organs. 1) proliferation 2) lymphangiogenesis 20 migration and invasion 4) intravasation 5) metastasis to secondary sites

1.3 LYMPHATICS AND THEIR ROLE

The discovery, study and evolution of lymphatics have a great history, spinning across centuries. Initial description about lymphatics was first made by the ancient Greeks in 300 B.C and thereafter several theories and treaties have propped up. It was only in 1622 that the lymphatic system came into prominence through various works of Gasparo Aselli [7]. Then, only by 19th century a clear picture about lymphatics came into existence owing to the works of the Hunter brothers, William Hewson, William Cruikshank and Paolo Mascagni [7].

The lymphatic system, found in all tissues of the body, is a one- way transport system for the collection, filtration and returning of interstitial fluid and proteins to the blood circulation. Apart from maintaining the tissue fluid balance, it also plays a major role in the trafficking of immune cells and dissemination of tumour cells. The lymphatic system consists of circulating lymph, network of lymphatic pathways like lymphatic capillaries, collecting vessels, trunks and ducts and lymphatic organs like lymph nodes, thymus, bone marrow, spleen, tonsils, Peyer patches and mucosa associated lymphoid tissue (MALT) [8].

During the passage of blood through its vessels, plasma fluid and proteins come out to the interstitial spaces owing to the hydrostatic and pressure gradients. This exudate is termed as interstitial fluid and a part of this is reabsorbed into post capillary venules. The uptake of the remaining fraction occurs through the thin endothelium of the initial lymphatic capillaries through intracellular junctions, which is termed lymph. As lymph originates from the blood, the chemical composition, amount of lipids, enzyme activity and proteins composition is usually same as that of plasma, but vary only in terms of their concentration. Lymph from the initial lymphatic capillaries is drained into the lymphatic vessels and may possibly encounter lymph nodes which filter the lymph. Then, it enters into the lymphatic vessels and large lymphatic vessels through numerous

lymphatic trunks which collect lymph from different parts of the body. Finally, the lymph from the lymphatic ducts will be returned back to the blood circulation. During the course of passage of lymph through the lymphatic structure, lymph is encountered by lymph nodes. The lymph nodes act as mechanical filters by filtering the lymph and also act as immunological mediators by producing antibodies and proliferating lymphocytes [9]. Figure 3 represents an overview of the lymphatic system.

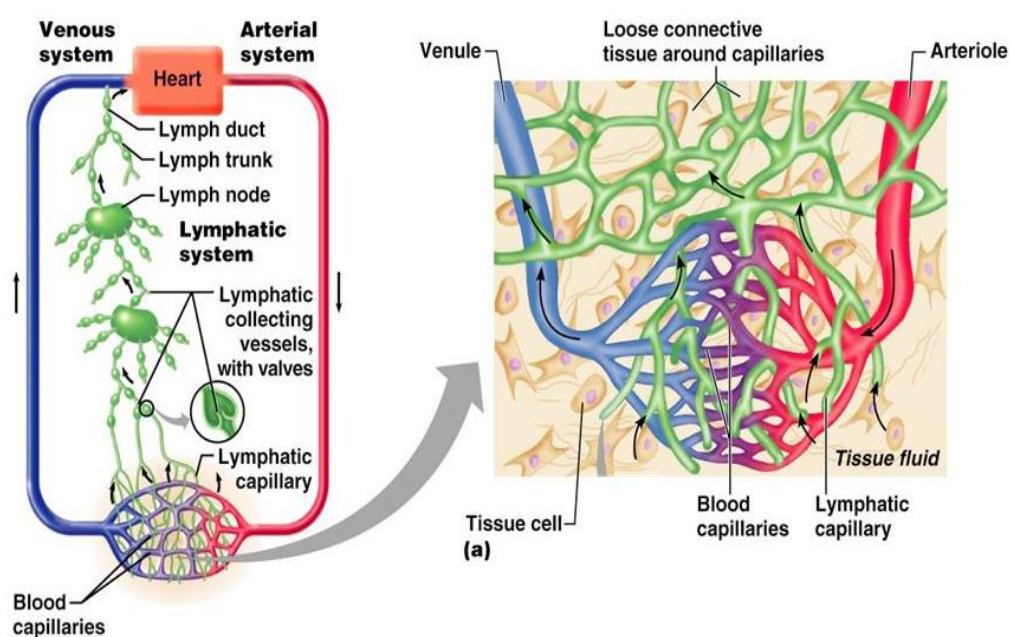


Figure 3. Overview of the lymphatic system

1.4 NANOTHERAPEUTICS FOR CANCER CHEMOTHERAPY

Nanotherapeutics involves application of nanotechnology in the field of medicine to aid treatment for diseases at the nanoscale, where majority of the biological molecules exist and function. Advances in nanotechnology are being applied in the development of novel therapeutics which can address a number of shortcomings of conventional drugs/ molecules. Additionally, using nanotherapeutics, problems of conventional anticancer drugs such as dose related

toxic effects (haemolytic a naemia, bone marrow toxicity, etc), nonselective killing of non tumor cells and drug resistance has been addressed. Recently, numerous investigations have been concentrated on biodegradable nanotherapeutics (using lipids and polymers) for the delivery of anticancer drugs to the desired target, which has great potential to revolutionize the future of cancer therapy [6,10,11]. Some of the complex issues solved using nanotherapeutics are, enhanced permeation across the complex blood brain barrier [12]; the ability of the multi drug resistant cancer cells to overcome the drug resistance for anticancer drugs and selective targeting of the nanotherapeutics to the cancerous cells [13]. Some of the nanotherapeutics approved by FDA in treating cancer like DaunoXome (Lipid based daunorubicin for Kaposis sacoma), Doxil (lipid based Doxorubicin for various cancers), Abraxane (Albumin bound paclitaxel for breast cancer and metastatic pancreatic cancer), etc have shown great potential and the window remains wide open for further development of nanotherapeutics for treating cancer and other ailments [14].

1.5 LIPID BASED NANOTHERAPEUTICS

Lipids are a chemically diverse group of compounds with high solubility in non polar solvents and poor solubility in water. They are chemically complex in nature and play a crucial role by forming the basic structural elements of the biological membranes, vitamins, hormones, intracellular messengers, enzyme cofactors, emulsifying agents in the digest tract, electron carriers, etc. Apart from being a major part of our diet, lipids form a major constituent of our body. This clearly indicates that lipids are biocompatible, non toxic to our body. Hence, if used wisely, lipids can form an excellent carrier for drug delivery in terms of acceptability to the body, safety and scalability [15–17] . Lipids are usually either fatty acids and/ or their derivatives, and substances related to these compounds. They are generally amphiphilic in nature because of the presence hydrophilic head

portion to which the lipophilic fatty acid(s) tail portion is esterified [14–19]. The melting point of lipids normally increases with an increase in its molecular weight (hydrocarbon chain length) and decreases with unsaturation (presence of double bonds) of the fatty acid. Each lipid is uniquely identified by their fatty acid composition, melting point, hydrophilic-lipophilic balance (HLB), and solubility in non-polar organic solvents. Over the past few decades there has been a surge in the application of lipids to cater the needs of drug delivery. Owing to the unique properties of lipids viz., their physiochemical diversity, affordability, biocompatibility, ease of metabolism, biodegradability and proven ability to enhance oral bioavailability of poorly water soluble have made them preferred candidates for various drug delivery applications [16,20–22].

1.6 VARIOUS KINDS OF LIPID BASED COLLOIDAL DRUG CARRIERS

Lipid-based colloidal drug carriers like liposomes, solid lipid nanoparticles, nanostructured lipid carriers, lipid based micelles, lipid polymer hybrids, lipid emulsions, lipid nanospheres, cubosomes, ethosomes, phytosomes, etc have been used to improve the therapeutic efficacy of drugs and plant extracts [16,20,23–28].

Liposomes are compact vesicles which are composed of one or more phospholipid bilayers enclosing an aqueous phase. They can be briefly classified as small unilamellar vesicles, large multilamellar vesicles, large unilamellar vesicles depending on the size and number of lipid bilayers present. They are excellent drug carriers and are capable of carrying hydrophilic drugs in their inner aqueous phase or hydrophobic drugs in their hydrophobic lipid bilayers. As liposomes are composed of the biomembranes, they are biodegradable, non-toxic and widely used [29]. Liposomes can also evade phagocytosis against macrophages by imparting stealth character and consequently enhance the half life

of drugs. They can also increase the solubility and absorption of poorly water-soluble drugs. Although some group of researchers are of the view that liposomes are capable of protecting the drugs in the gastrointestinal tract against the hostile conditions, other group of researchers showed that the enzymatic activity in the duodenum and bile salts can destroy the lipid bilayers of the liposomes. But, liposomes which are prepared from phospholipids (with a phase transition temperature above 37°C) and cholesterol are most resistant to degradation [30,31].

Solid lipid nanoparticles (SLNs) are colloidal carriers consisting of a solid lipid core at room temperature, dispersed in an aqueous solution of stabilizers. They are produced by replacing the liquid lipid (oil) part of an emulsion with solid lipids which exist as solids at both room and body temperature. The minute size of SLNs (20- 500 nm) enables efficient uptake of drugs into the intestine via the lymphatic route [32]. The main advantages offered by SLNs are, controlled release of drugs, improved stability of drugs, good drug loading, ability to entrap both hydrophilic and lipophilic drugs. These solid lipid nanoparticles, after being converted to powder by freeze drying can be filled in hard gelatin capsules or can also be incorporated as a suspended form in PEG and filled into soft gelatin capsules. The spray-dried or lyophilized powders can even be filled into sachets [19,30,33–36].

Nanostructured lipid carriers (NLCs) are similar to SLNs, but additionally contain liquid oil component (mostly unsaturated fatty acids) along with solid lipid component. They have been introduced to overcome the limitations of SLNs i.e., limited drug loading capacity and drug expulsion during storage. It is an established fact that longer fatty acid triglycerides require higher energy (i.e., the higher the temperature) for melting. The oil inside the NLC system will provide a uniform heating medium in melting the lipid and will result in an efficient emulsification. Their size varies from 100- 500 nm and has been frequently used for enhancing bioavailability and drug targeting purposes also [37–42].

Lipid--polymer hybrid nanoparticles contain a hydrophobic polymeric core along with the drug, a lipid monolayer and an outer layer made of PEG eg. PEG-DSPE. This polymer-drug mixture is encapsulated in a lipid layer (lecithin), which is further covalently conjugated to DSPE-PEG. Lipid--polymer hybrids have found applications in cancer therapeutics. They offer good promise owing to their biodegradability, biocompatibility, sustained drug-release profile, stealth nature and excellent stability in blood [43,44].

Lipid based micelles are formed by self-assembly of amphiphilic block copolymers. When dispersed in water, the amphiphilic block copolymers assemble into 30- 50 nm spheres with a core-shell structure. The hydrophobic segments form the core and the hydrophilic segments protrude into the aqueous medium. Lipids micelles are formed by adding surfactants (like phospholipids or PEG-phosphatidylethanolamine) at a concentration above the critical micellar concentration. They are easy to prepare and offer good stability [45,46].

Lipid emulsions are parenteral products containing vegetable oils which are emulsified with lecithin. The droplet size of the lipid emulsion varies from 200 to 300 nm. Apart from using lipid nanoemulsions for nutraceutical purpose, they are used for drug delivery purpose due to the ability of oils to solubilise low water soluble drugs and to reduce toxicity of intravenously administered drugs. Generally, medium chain triglycerides and long chain triglycerides are used in the preparation of lipid emulsions [47].

Lipid nanospheres are based on the logical selection of individual lipid components and ratios of drug and lipids using a complex formulation composition. They are generally less toxic with small particle size. These formulation factors allow better interaction with lipids for hydrolysis and favours rapid *in vivo* drug release [48].

Cubosomes are discrete, sub-micron or nanostructured particles formed from fragmentation and steric stabilization of inverse bi-continuous cubic phases of lipids. Cubosomes have high internal surface area along with cubic crystalline structures. The cubic phases possess a very high solid like viscosity, which is a unique property because of their intriguing bicontinuous structures which enclose two distinct regions separated by the bilayer. They exhibit different internal cubic structure and composition with different drug loading modalities [49,50].

1.7 LIPID BASED NANOTHERAPEUTICS FOR PREVENTION OF CANCER METASTASIS BY TARGETING THE LYMPHATICS

Recently, numerous investigations have been concentrated on the development of lipid based nanotherapeutics for the delivery of anti-cancer drugs to the desired target which has great potential to revolutionize the future of cancer therapy. It is a rapidly progressing field which can solve several limitations of conventional drug delivery. Herculean efforts have also been made to target various compounds to specific regions like brain, eye, breast, lungs, liver, colon etc. But attempts to target or deliver a specific compound to the lymphatics are comparatively less and this might owe to the simple fact that the lymphatics are present throughout the body and the medium is dynamic. Though the problems associated with targeting compounds to the lymphatics are challenging, the advent of nanotechnology has made the complex science appear simpler. In order to reach the lymphatics, the size of the particles should be in the range of 10- 100 nm, the uptake rate into the lymphatics should be high and the route of delivery route should be appropriate [9]. Extensive literature survey suggests that solid lipid based nanoparticles can be selectively absorbed into the lymphatic system when administered subcutaneously [51,52].

1.8 SOLID LIPID NANOPARTICLES

Solid lipid nanoparticles (SLNs) are a relatively new class of spherical drug carriers which are of submicron size (10 to 1000 nm) [19]. They are made from physiological lipids (lipid acids, mono, di, or triglycerides, glyceride mixtures or waxes) that remain in a solid state at room and body temperature. Usually cytotoxic drugs show poor specificity, high toxicity and multi drug resistance. But, SLNs can solve these problems by enhanced permeability and retention effect (EPR) and by imparting specific targeting property to the cancerous cells [53]. Also, stealth character can be imparted to the SLNs by coating with non ionic surfactants to evade macrophage uptake and enhance their circulation time in the body [51,52]. Further, SLNs show controlled release, better stability and low drug leakage compared to other nanocarriers upon long term storage. Recently, researchers have also worked on specifically targeting solid lipid nanoparticles of lopinavir [54], methotrexate [55], etc to the lymphatics using SLNs. Their results have been promising which showed higher amounts of drug enter the lymphatics after administration through SLNs.

In order to reduce the toxic effect of anticancer drugs to the healthy cells and to impart targeting nature to the cancer cells, the surface of the SLNs has been modified (by conjugation or adsorption) using ligands like transferrin (an iron-binding glycoprotein that binds to the transferrin receptors present on breast cancer cells) [12], folic acid [56,57], hyaluronic acid (it binds specifically to CD44 receptors, an extracellular protein on cell membranes that is over expressed only in tumors) [58]. Finally, the industrial scale up of solid lipid nanoparticles is very feasible and has been successfully attempted to scale up from laboratory to industrial level [19,59].

1.9 ADVANTAGES OF SLNs

SLNs combine the advantages of nanoparticles prepared using polymers and also avoid their disadvantages [14,19,37]. The numerous advantages of SLNs are:

- SLNs in the range of below 200 nm (or sometimes 100 nm) are not taken up by the cells of Reticulo Endothelial System (RES) and thus evade liver and spleen filtration [21,60].
- Controlled release of the loaded drug can be achieved for several weeks [61].
- Drug targeting to specific cells/organs can be achieved [7,62].
- SLNs are stable for longer time when compared to other colloidal drug delivery systems [63].
- SLNs prepared by high pressure homogenization are highly reproducible and economically inexpensive [19].
- SLNs formulations have the feasibility of incorporating both hydrophilic and hydrophobic drugs [60].
- The lipid carriers are biodegradable and safe [64].
- Organic solvents are avoided in the SLN preparation.
- Large scale production and sterilization are feasible [65].

1.10 TOXICITY AND REGULATORY STATUS OF LIPID EXCIPIENTS

The Food and Drug Administration (FDA) has published listings in the Code of Federal Regulations (CFR) for generally regarded safe (GRAS) category substances and a separate list entitled Inactive Ingredient Guide (IIG) for excipients was approved and incorporated in the marketed products. As excipients play an integral part in the formulation, it is necessary to have a proper system to obtain regulatory clearance before using them in the formulation. This is very true for lipid excipients in view of their distinct physicochemical properties and potential complex interactions with other ingredients or physiological environment that may occur *in vivo*.

In the past, excipients like diluents, fillers, binders, lubricants, coatings, solvents, and dyes, were considered inert without any interactions with the drug, packaging material and biological environment. Off late, great deal of excipient research has delivered several novel excipients with some toxicities and interactions. Thus, it is necessary to evaluate the toxicity and interaction profile of the excipients.

Toxicity and the status of excipients safety are some of the major issues for the development and usage of a product. One can have an excellent delivery system, but if the excipients are toxic, it is not possible to introduce them into the clinic setup. Fortunately, as lipids are present in the body and in all the foods which we take, the problem of safety owing to lipids will generally not arise and majority of the lipids are GRAS. But the final safety of the formulation may vary due to the usage of surfactants or co-surfactants which may be toxic (like Cremophor). Thus, for the preparation of various lipid formulations, surfactants of GRAS status must be used [33,66–68].

The status of excipients of lipids has to be discussed as a function of the administration routes. Usage of lipids for topical and oral administration of solid lipid nanoparticles, nanostructured lipid carriers, etc is absolutely safe with respect to lipids. Almost all the lipids can be used in the formulation of topical pharmaceutical and cosmetic products. Additionally, lipids from the food industry can also be used in the pharmaceutical industry after getting the due clearance from the regulatory bodies. Usage of a specific lipid in the food industry does not allow its direct usage for the preparation of pharmaceutical products. But, the toxicity data of a new lipid used in the food sector can be used for getting clearance from the pharmaceutical regulatory bodies [69–71].

For parenteral purpose, the category of lipids used for drug delivery applications change with respect to the type of lipid based formulation. Liposomes

have been traditionally administered by parenteral route for treating various ailments without any problem. Although SLNs and NLCs have been deemed safe on paper without any toxicity issues, they have not been the preferred carrier for administration of drugs via parenteral route. A good tolerability (without any changes to liver and spleen) was also observed even after administration of 6 bolus injections of lipid (cetyl palmitate) at a dose of 1.33 g lipid/kg body weight. Surprisingly, there are also no products available in the market for parenteral purpose. But, glycerides which are composed of fatty acids as in oils of have been used for parenteral fat emulsions for nutraceutical purpose [33,46].

Lipids also commonly reduce the toxicity of several anticancer drugs by making them less toxic to the body and thereby protecting the healthy cells. In a nut shell, lipids are totally biocompatible without any toxicity owing to its natural origin.

1.11 METHODS OF PREPARATION OF SOLID LIPID NANOPARTICLES

Preparation of solid lipid nanoparticles can be broadly categorised into hot melt and cold melt methods based on whether the lipid is melted by application of heat energy. Various methods of preparations of solid lipid nanoparticles have been proposed to meet different objectives [72]. The following are the general methods used for the preparation of SLNs.

1.11.1 High pressure homogenization technique:

This technique was first developed by Muller and Lucks. High pressure homogenization technique can be employed for both hot and cold homogenization processes where the initial common step involves dispersing or dissolving the drug in a melted lipid phase [65].

Hot High Pressure Homogenization:

Initially the lipid is melted approximately above 5°C its melting point followed by dispersing or dissolving the drug in the melted lipid to produce an oil phase. Simultaneously, a suitable surfactant is dissolved in water to produce an aqueous phase which is also heated to maintain at a temperature similar to the oil phase. Then the melted lipid phase is dispersed by the addition of aqueous phase using a high speed stirrer to form a pre emulsion. This pre emulsion is passed through a high pressure homogenizer with optimized conditions of pressure and cycles to obtain a dispersion of SLNs.

Cold High Pressure Homogenization:

Similar to the hot homogenization method, initially the lipid is melted approximately above 5°C its melting point, followed by dispersing or dissolving the drug in the melted lipid to produce a clear and homogeneous oil phase followed by cooling the melt using dry ice or liquid nitrogen to form a solid drug dispersed lipid matrix. A high cooling rate will provide dispersion where the drug is uniformly distributed in the matrix. Then the solidified lipid matrix is reduced to microparticles by ball or mortar milling. This dispersion of lipid microparticles is dispersed in a cold aqueous surfactant solution and is allowed to pass through a high pressure homogenizer to form a suspension containing SLNs [19].

For substances which are thermo labile, cold high speed homogenization is the preferred method as the time of exposure to the heat is less when compared to the hot high speed homogenization method. Another advantage which the cold high speed homogenization method possesses is that it is better suitable for the loading of hydrophilic drugs as there won't be any partitioning of the drug from the lipid phase to the aqueous phase. This technique can also be used when the lipid matrix consists of lipids with high melting point. This technique is less effective in dispersing the lipids as the solid lipid matrix remains in the solid state

during homogenisation. Hence, the homogenization needs to be carried out slightly below the melting point of the lipid. This can soften the lipid during the homogenization process and facilitate dispersion of lipid leading to production of SLNs with smaller particle size [35].

1.11.2 Microemulsion technique:

This technique was developed by Gasco. Initially, the lipid material is melted to form an oil phase. Simultaneously, an o/w surfactant/ co-surfactant is added to the aqueous phase and is heated at the same temperature as that of the oil phase. The melted lipid and aqueous phases are mixed in such a ratio (1:2 to 1:100) so that a microemulsion is formed. A special thermostatic syringe can be used for the purpose of preparing microemulsion. Once the size of the microemulsion region in the phase diagram is fixed, the system needs to be kept at elevated temperatures during the production process to avoid conversion to a different system. This hot microemulsion is then diluted into excess of cold water to convert the microemulsion to an ultrafine nanoemulsion, thereby facilitating the internal lipid to re-crystallize. One main disadvantage is dilution of the suspension with large volume of water, which produces final product with concentrations below 1% particle content. Another disadvantage associated with this technique is the removal of large quantities of water in the final stage of processing. Also, the addition of high concentrations of surfactants and co-surfactants during the formulation may cause toxicity [71].

1.11.3 Solvent emulsification- evaporation technique:

This technique was initially developed by Sjostrom and Bergenstahl in 1992. The lipid material is initially dissolved in water-immiscible organic solvents like cyclohexane or dichloromethane or chloroform or methylene chloride, followed by the addition of drug to it. An aqueous phase containing surfactant is prepared and added to the organic phase containing lipid to form an emulsion. The organic phase evaporated under mechanical stirring at high speeds or reduced

pressure to obtain an o/w emulsion consisting of a dispersion of SLNs. The solvent evaporation step must be quick for the formation of smaller particles without any aggregation. This technique can be best applied for the incorporation of hydrophilic molecules such as proteins and peptides [19,73].

1.11.4. Solvent Displacement Technique:

The solvent displacement technique was first described by Fessi et al. for the production of polymeric nanoparticles and recently this technique has also been used to prepare SLNs. In this process, the lipid material is dissolved in a partially water- miscible solvent such as ethanol, acetone, or methanol followed by the addition of the drug to this organic phase. The aqueous phase is prepared by dissolving the o/w surfactant in water. The organic phase is carefully injected into the aqueous phase as a fine jet under high speed stirring. Droplets of solvent of nanometre size are formed from the o/w interface. The presence of surfactant stabilizes the droplets and finally the lipid nanoparticles are formed after complete evaporation of the water miscible organic solvent [48].

1.11.5. Emulsification- Diffusion Technique:

The emulsification- diffusion techniques patented by Quintanar- Gerrero and Fessi is generally used to produce polymeric nanoparticles. Initially, to maintain thermodynamic equilibrium, a saturated solvent system of partially water- soluble solvents like benzyl alcohol or tetrahydrofuran is prepared by adding sufficient water. Then the lipid of choice and drug are dissolved in the saturated solvent to produce an organic phase. This organic phase is then emulsified under rapid agitation by addition of an aqueous solution containing a stabilizer. Finally, the lipid starts precipitating by the diffusion of solvent to the external phase to obtain an o/w emulsion of SLNs. The organic solvent is then eliminated by suitable method after which an aqueous dispersion of lipid nanoparticles of 100 nm and good size distributions is formed [74].

1.11.6. Ultrasonication:

High shear homogenization and ultrasonication are the earliest dispersing techniques used for the production of SLNs and they can be either used in combination or separately. Initially the lipid is melted at a temperature 5°C above its melting point. Simultaneously, surfactant is added to the aqueous solution and heated to the same temperature of the lipid phase. The surfactant solution is dispersed in the lipid phase and homogenized using a high shear homogenizer for a predetermined time. Finally, the obtained pre emulsion is homogenised using a probe sonicator to obtain SLNs [61].

1.12 SCALE UP FEASIBILITY

For the success of a technology or a product, the ease of scale up at large industrial scale is very important. Fortunately, lipid based formulations are very easy to scale up because of the simplicity of the preparation methods and availability of equipments (like high pressure homogenisers) which can cater the need at industrial level. Using high pressure homogenisers, a GMP unit for large scale clinical batch production of solid lipid nanoparticles has already been developed and validated for batch sizes between 2 and 10 kg. Additionally, a large scale production setup for solid lipid nanoparticles has also been designed with a capacity as large as 50–150 kg per hour by placing two homogenisers in series. Thus, large scale production of SLNs is possible by discontinuous or continuous fashion [33,66,67,75–77].

1.13 STABILITY OF SOLID LIPID NANOPARTICLES

Formulations of nanoparticles in an aqueous medium results in poor stability and hinder the clinical use of the formulation. The physical and chemical instability of the nanoparticles arising due to the leakage of drug from the matrix and aggregation among the particles are the main obstacles encountered in the nanoparticles formulation. To overcome this difficulty, the water component has

to be removed and thus freeze drying technique comes into play. Freeze-drying (lyophilisation) is a process which removes water from a frozen material by sublimation and desorption under vacuum. However, the high stress involved in freeze drying and desiccation needs to be avoided and so, cryoprotectants such as aerosol, trehalose and mannitol are incorporated [78].

Freeze drying is an efficient way to boost the chemical and physical stability for a long duration. Freeze drying may be requisite to accomplish long term stability for a product containing hydrolysable molecules or a suitable product for per-oral delivery. Conversion into the solid state would prevent Oswald ripening and avoids hydrolytic reactions. Spray-drying is an alternative method to lyophilisation. But the compounds can be destabilized due to the elevated temperatures and high shear forces. Additionally, partial melting of the lipid phase during spraying can result in particle growth.

1.14 TARGETING LIGAND AND THEIR RECEPTORS

Research efforts have been recently shifting from cytotoxic nonspecific chemotherapies to molecularly targeted rationally designed drugs. Targeted chemotherapies offer a great potential advantage due to their ability to enhance specificity to deliver high doses directly to the target site. Anyway, this requires the identification of the relevant biomarkers or receptors that are over-expressed specifically by diseased cells but not in healthy tissue, so as to attain such selective targeted delivery. Information pertaining to the receptors used in the current research work has been described below:

1.14.1 Vitamin B12 and Transcobalamin II Receptors

Vitamin B12 (cyanocobalamin) is an essential nutrient in the mammals with very poor bioavailability [79,80]. The recommended dietary allowance is 1-5 µg per day and deficiency can lead to a number of diseases, including weakness, fatigue, constipation, and on a more serious scale, megaloblastic anaemia,

pernicious anaemia, and neurological malfunctions. Cyanocobalamin is the largest and most complex vitamin of all and it can be produced only by certain bacteria and archaea; hence, it is accessible in mammals only through diet. Vitamin B 12 in the bloodstream is transported and taken up in the liver and other tissues by transcobalamin II (TCII). The TCII-B12 complex (holo- TCII) is transported into the plasma of the tissues by TCII receptor-mediated endocytosis operated by the transmembrane proteins. The internalized holo-TCII complex enters the lysosomes and dissociates into free cobalamin by lysosomal proteases. Vitamin B12 in cells is converted into its biologically-active cofactors, methylcobalamin and adenosylcobalamin. As rapidly dividing tumor cells require higher amounts of methionine and energy for cell proliferation, they show preferential accumulation of vitamin B12 compared with the healthy cells. Thus vitamin B12 helps in targeting cancer cells. Moreover, it shows additional features that make it suitable for possible therapeutic applications: it is water soluble, has no known toxicity and, as an indispensable vitamin for sustaining life, it is unlikely that a mutational arrest of vitamin B12 uptake (with concomitant failure of vitamin-mediated therapy) could occur. In testis, breast, ovarian, thyroid, uterine and brain tumors, there is a greater demand for vitamin B12 along with over expression of TC II receptors. Thus vitamin B12 conjugated nanocarriers can be used for targeting drugs or imaging agents directly to the tumor site [79].

1.14.2 Hyaluronic Acid (HA)

HA is an extracellular matrix component composing of polyanionic glycoaminoglycan with repetitive disaccharide units of D-glucuronic acid and D-N-acetylglucosamine. It can be used as a targeting ligand in nanomedicine for selectively identifying, binding and killing tumors over-expressing CD44 receptors [58,81]. As CD44 receptors are over expressed in multiple human cancer cells with increasing density over progression of different stages of cancers, HA can be efficiently targeted to the cancer cells. Additionally, HA is

widely available, economic and biocompatible. CD44 receptors functions as a bioactive signalling transmitter and plays a role in the invasion and metastasis of different tumours including breast carcinomas. CD44 is a ubiquitous multistructural and multifunctional cell surface adhesion molecule involved in cell-cell and cell-matrix interactions. CD44 also has a role in a variety of responses, including lymphocyte homing, hematopoiesis, angiogenesis, inflammation and tumorigenesis. Thus, attaching HA to the nanocarriers containing anticancer drugs can improve its targeting ability to the tumour cells [81,82].

1.15 QUILLAJA SAPONIN (QS) AND ITS ROLE AS A SURFACTANT

QS is a non-ionic amphiphilic surfactant extracted from the bark of *Quillaja saponaria* (Soap bark tree). QS is a glycoside with a lipophilic backbone of Quillaic acid and gypsogenic acid (a triterpene aglycone), to which hydrophilic polysaccharide moieties like rhamnose, xylose, arabinose, galactose, fucose and glucuronic acid are attached [83]. Thus, QS can perform the role of a surfactant by adsorbing at the oil and water interface to form an emulsion [84]. Despite the characterisation of the micellar properties of QS as early as 1800 AD and approval by the US Food and Drug Administration (FDA) [85], its application has not gained prominence in the pharmaceutical sector so far. In addition to its emulsifying property, QS also possesses many bioactivities (larvicidal, antitumor, antimicrobial etc.) and is used as a natural foaming agent in cosmetic products, and as an adjuvant in vaccine delivery [86][87][88]. Furthermore, a product based on the *Quillaja saponaria* bark extract is marketed under the trade name Q-Naturale and approved by FDA for use as emulsifier in beverages.

Thus, in the current research work, HA/ vitamin B12 surface modified SLNs of Imatinib mesylate (IM) were prepared to target the metastatic breast cancer cells in the lymphatics. Additionally, the efficiency of QS to form SLNs was also evaluated.

Aim & Objective

2. AIM AND OBJECTIVES

In order to reach the lymphatics of the breast, the uptake of nanoparticles into the lymphatics should be high and the route of delivery should be appropriate. The current doctoral research work has been planned to develop and evaluate ligand conjugated SLNs of Imatinib mesylate (IM) which can specifically target and kill the tumor cells in the lymphatics. Additionally, the role of lipids in solubilising IM and the utility of QS, a natural surfactant obtained from the bark of *Quillaja saponaria*, in the preparation of SLNs has also been evaluated for the first time.

The specific objectives of the work include:

Specific objective 1:

To predict the solubility of IM in the lipids and to study the various properties of lipids which affect its solubilisation.

Specific objective 2:

To develop and optimize SLNs of IM conjugated with ligands (like HA and vitamin B12) to facilitate targeting to the cancerous cells in the lymph nodes.

Specific objective 3:

To evaluate the utility of QS, a novel and unexplored natural surfactant with anticancer activity, in the preparation of SLNs.

Specific objective 4:

To characterize and evaluate the optimized SLNs for size, surface charge, morphology, conjugation efficiency, entrapment efficiency, physical state of the entrapped drug and *in vitro* release studies.

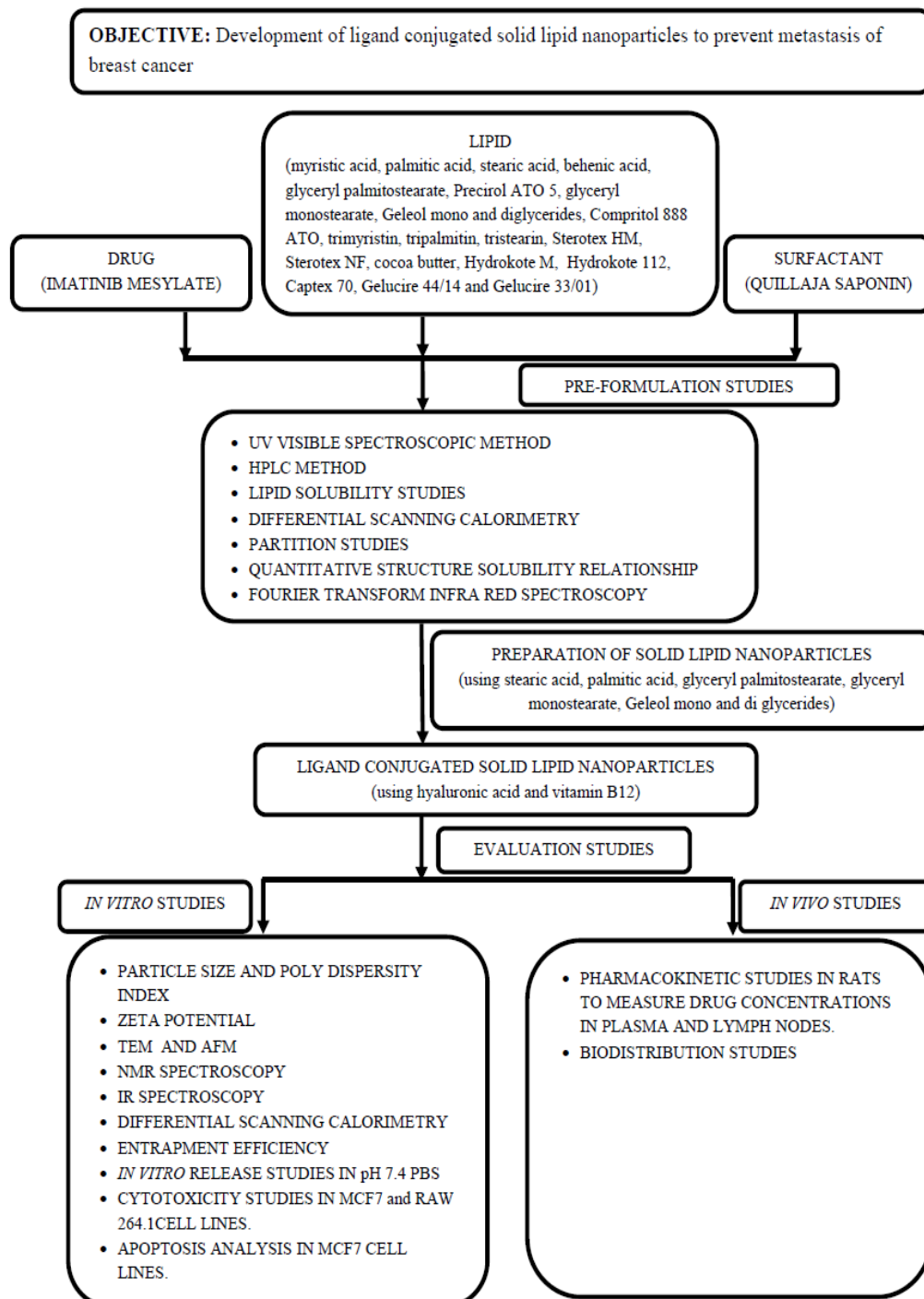
Specific objective 5:

To assess the cytotoxicity of the SLNs using *in vitro* cancerous and non cancerous cell lines.

Specific objective 6:

To evaluate the concentration of IM in blood and sentinel lymph nodes in female Wistar rats after subcutaneous administration of the developed SLNs.

Scheme of the work



Review of Literature

3. REVIEW OF LITERATURE

3.1. METASTASIS OF BREAST CANCER

Ran et al., 2010 elaborately described on lymphangiogenesis and lymphatic metastasis of breast cancer. They stated that metastasis of cancer through the lymphatics is the main prognostic factor for survival of patients with breast cancer and associated malignancies, which is facilitated by lymphangiogenesis. Major proteins which induce lymphangiogenesis have been mentioned in detail. The changes which are observed during different stages of breast cancer metastasis have also been mentioned. They also summarized the newer concepts related to lymphatic metastasis of breast cancer and its lymphangiogenesis by addressing some controversial questions [4].

Tayyeb et al., 2014 described the pathogenesis of breast cancer to brain. They mentioned the reasons breast cancer, its metastasis and the basic pathophysiology behind it in a molecular basis. Additionally, they have also described various novel approaches for designing targeted based therapies for its treatment [89].

Perret et al., 2008 summarised various pharmacological strategies to prevent metastasis of cancer. The lack of proper treatment for metastatic breast cancer was discussed and information on the available targets has been mentioned. Among them, the metastasis suppressor genes seem to be the most promising. In spite of this, during recent years, a dozen of molecules, which fulfil the definition of a specific metastatic drug that inhibits the metastases without altering the growth of the primary tumour (which can be eradicated by surgery), have been identified and assessed for the proof of the concept. The continuation of this effort would benefit in terms of efficiency, if the objectives were defined more precisely. It is particularly important to distinguish molecules that prevent spread of the

metastatic cells of the early-stage primary tumour from the ones which induce a regression of the established metastases or to inhibit the transition from disseminated occult tumour cells to dormant micrometastasis. This second goal is a more relevant in the current clinical setting where the detection of early metastatic spread is very difficult, and therefore would call for greater effort on the part of the scientific community [90].

3.2 Lymphatic targeting of drugs using nanoparticles

Cho et al., 2014 discussed the importance of targeting various kinds of nanoparticles to the lymphatics. They highlighted that targeting anticancer, immunotherapeutic drugs and lymphoid contrast agents, to both tumors and the lymphatics, has several advantages such as reduced systemic side effects and increased efficacy. The mechanism, efficiency and challenges of different nanoparticles like polymeric nanoparticles, liposomes, and lipid-based vehicles for lymphatic targeting and their clinical perspectives has been discussed [91].

Liu et al., 2013 developed paclitaxel expansile nanoparticles for lymph node targeting to prevent the metastasis of breast cancer. *In vitro* showed a dose-dependent cytotoxicity and decreased the growth of cancerous cells *in vivo* against human triple negative breast cancer murine models. It also decreased the metastasis of nanoparticles from the lymph nodes [92].

Reddy et al., 2007 tested in detail whether nanoparticles loaded with vaccines can be targeted to the dendritic cells of the lymph nodes and consequently activate them to obtain better response. They observed that after intradermal injection of the nanovaccines, the interstitial flow assisted in transporting them efficiently into the lymphatic capillaries and lymph nodes, (dendritic cells) in a size dependent manner. They used a model antigen ovalbumin, and successfully obtained higher levels of humoral and cellular immunity in mice [93].

Oussoren et al., 2001 developed liposomes to target the lymphatics by subcutaneous administration. They described that the size and anatomical site of injection usually influence the lymphatic absorption and lymph node uptake of subcutaneously administered. They also demonstrated that phagocytosis by macrophages is the major important mechanism for uptake of liposomes to the lymph nodes. This is a major finding with respect to targeting nanoparticles to the lymphatics [51].

Qin et al., 2013 developed polymeric micelles to enhance its concentrations in the lymphatics for treating metastasis of cancers. They prepared micelles using polyethylene glycol-phosphatidylethanolamine (PEG-PE) of size 14.5 nm using doxorubicin and vinorelbine. Their results showed migration of PEG-PE micelles into the interstitial tissue of the lymphatic vessels and finally accumulated in the lymph nodes. *In vivo* whole body imaging in rats showed reduction in the metastasis rate in murine breast cancer model. They also observed enhanced antitumor activity of primary tumors and prevented its metastases to the lungs [6].

Hawley et al., 1995 provided vast information on targeting of colloids to lymph nodes and described the influence of lymphatic physiology and characteristics of colloids. The influence of route of administration to the regional lymph nodes was also described [94].

Feng et al., 2010 described the roles of dextrans for improving lymphatic drainage using liposomes. They developed novel liposomes containing dextrans to reduce undesirable retention of antineoplastic agents and to reduce the damage at the local tissue. The liposomes reduced the local retention and enhanced the drainage to the lymphatics. Pharmacokinetic studies showed the enhanced drainage of liposomes through lymphatics and reversal to systemic circulation. Dextrans, efficiently enhanced the drainage of liposomes into the lymphatics and can be used as adjuvants with liposomes [95].

Mortimer et al., 2014 studied the influence of different kinds of plasma proteins on opsonisation of nanoparticles and elaborated in detail. They showed that plasma proteins (majorly albumin) can form a hard corona around the nanoparticles, which is the main criterion for recognition by the mononuclear phagocyte system [96].

Mueller et al., 2015 attempted to target antigen to the lymph nodes using PRINT hydrogels. They developed a platform for the delivery of vaccines using hydroxy-poly (ethylene glycol). The developed cylindrical nanoparticles measured 80×180 nm and showed good uptake by antigen presenting cells and also stimulated proliferation of CD4+ helper T cells. These PRINT hydrogels can be used to target other drugs to the lymphatics [97].

Kaminskas et al., 2009 showed that PEGylated polylysine dendrimers improved the absorption and lymphatic targeting following subcutaneous administration in rats. The impact of PEGylation on the absorption and lymphatic transport of the dendrimers modified by different molecular weights of PEG or 4-benzene sulphonate after subcutaneous or intravenous administration was studied. PEGylation using PEG 200 rapidly and completely absorbed into the blood after SC administration. Increasing the chain length of PEG decreased its absorption into the blood and consequently enhanced lymphatic uptake [98].

3.3 DIFFERENT TYPES OF NANOPARTICLES

Chang et al., 2012 discussed various liposome-based drugs and their therapeutic efficacy. They discussed and compared the therapeutic effect of clinically approved liposome based drugs and the free drugs. They also determined the clinical effect with relationship to the lipid content. Crucial preclinical and clinical information about the principal liposomal formulations were also discussed [99].

Geng et al., 2007 studied the effect of filaments shaped nanoparticles (filomicelles) versus spherical particles with respect to drug delivery, transport and trafficking. The filomicelles remained in the circulation for nearly 1 week after intravenous injection, which is nearly ten times longer than the spherical shaped nanoparticles [100].

Liu et al., 2016 tried to improve the oral bioavailability of Sorafenib using “Spring” and “Parachute” molecular interactions. They noticed that the solubility of sorafenib could be increased by 50-fold with the co-existence of poly vinyl pyrrolidone-vinyl acetate and sodium lauryl sulphate (SLS), due to the formation of complexes at a low critical aggregation concentration. The ability of poly vinylpyrrolidone-vinyl acetate to keep the drug in solution (parachute) was impaired by SLS. They concluded that poly vinyl pyrrolidone-vinyl acetate enhanced the solubility and super saturation of sorafenib due to the molecular interactions between them. *In vitro* dissolution and dog pharmacokinetic *in vivo* evaluation showed good *in vitro-in vivo* correlation [101].

Karanam et al., 2014 developed poly (ϵ -caprolactone) nanoparticles of carboplatin and performed characterization and *in vitro* cytotoxicity studies in U-87 MG cell lines. Nanoparticles below 100 nm were efficiently taken up by U-87 MG cells and exhibited significantly higher cytotoxicity than free drug. Carboplatin in the form of nanoparticles did not induce haemolysis in rat red blood cells [60].

Joshi et al., 2006 formulated and evaluated topical gel based on nanostructured lipid carrier of Valdecoxib. The NLCs was suitably gelled and characterized with respect to drug content, pH, spreadibility, rheology, and *in vitro* release. The developed gel showed faster onset and also prolonged the activity for 24 hours [102].

Kasongo et al., 2011 worked on the selection and characterization of lipid excipients for the manufacture of Didanosine loaded SLNs and NLCs. They evaluated the suitability of lipids for the manufacture of solid lipid nanoparticles SLNs and NLCs. The crystalline nature and polymorphism of lipids was tested using differential scanning calorimetry and wide-angle X-ray scattering. Precirol ATO 5 and Transcutol HP showed the good solubilizing potential for the drug. DSC and WAXS profiles of DDI/bulk lipids mixture obtained before and after exposure to heat showed no interactions between the drug and the lipids [103].

Geng et al., 2005 developed Poly (ethylene oxide)-block-Polycaprolactone (PEG-PCL) giant and flexible worm micelles for the first time. These worm micelles immediately generate spherical micelles due to hydrolysis of polycaprolactone hydrolysis. The mechanism behind the hydrolysis and the kinetics was described in detail [104].

Levchenko et al., 2002 studied the effect of surface charge and polymer coating on the biodistribution and clearance of liposomes. Phosphatidylcholine (PC)/ cholesterol liposomes were prepared using stearylamine/ phosphatidic acid/ phosphatidyl serine/ polyethylene glycol of different molecular weights. The chemical nature of the charged lipid is important *in vivo*. They found out that short PEG (750) and longer PEG (5000) inhibited the clearance of positively charged, whereas, only longer PEG (5000) inhibited the clearance of negatively charged. They also highlighted that opsonins of different molecular size are possibly involved in the clearance of differently charged liposomes [105].

Sanna et al., 2014 discussed on target based cancer therapy using nanoparticles. They stressed the need for nanotechnology in cancer treatment and highlighted the progress made by nanoparticles in other fields of science. Different nanoparticles used for treating cancers have been discussed in detail with a special focus on increasing the specificity. They also discussed on the clearance mechanisms for the nanoparticles and elaborated on various nanoformulations which are in phase II clinical trials [106].

Kamaly et al., 2012 described target based polymeric therapeutic nanoparticles with a special focus on its design, development and clinical translation. Various polymeric materials ranging from orthopaedic implants, resorbable sutures, macroscale and microscale drug delivery systems such as microparticles and wafers, multifunctional nanoparticles were discussed in detail. The safety, efficacy, solubility, metabolism, plasma binding, biodistribution, target tissue accumulation were detailed in depth. Additional information with respect to the design and development of target based polymeric nanoparticles and the challenges associated with development were discussed [107].

Li et al., 2008 described the pharmacokinetics and bio-distribution of nanoparticles. They stated that nanoparticles can be promising for improving the efficacy of drugs. The chemical and physical properties of the nanoparticles like particles size, zeta potential, surface chemistry and morphology, are major factors that determine their pharmacokinetic and bio-distribution. The fate of the nanoparticles after cellular internalization and the various strategies for overcoming the numerous barriers for intracellular delivery and drug release were also discussed with a focus of the future directions [108].

Weissig et al., 2014 discussed elaborately on various nanopharmaceuticals which are in the current market. They highlighted the importance offered by some internationally acclaimed research bodies who have paved way for the development of nanopharmaceuticals. They have detailed the growth of the nanopharmaceuticals which are in the market. They provided elaborate information on 43 approved nanopharmaceuticals with a special focus on its clinical outcomes [109].

Joshi et al., 2008 developed nanostructured lipid carrier gel for topical application. The gel was assessed for *in vitro* release and *in vitro* skin permeation using rat skin. The efficacy of the NLC gel was also tested in aerosil-induced rat paw edema model. The NLC gel of celecoxib showed faster onset of action and also prolonged the activity for 24 h [110].

3.4 APPLICATION OF LIPIDS IN LYMPHATIC DELIVERY

Siram et al., 2014 worked to target and increase its retention time of diethylcarbamazine citrate (DEC). The influence of various excipients on the size, shape, texture, surface charge, physical nature of the entrapped drug, entrapment efficiency and *in vitro* drug release of SLNs was also studied in detail. Additionally, *in vivo* animal studies were also performed to estimate the drug concentration in blood and lymph after oral administration. The results indicated an average size in the range of 27.25 ± 3.43 nm to 179 ± 3.08 nm among all the batches of the formulations. *In vivo* studies in rats showed a 4 fold enhancement in the amount of DEC that has reached the lymphatics after oral administration by SLNs [60].

Mishra et al., 2015 prepared solid lipid nanoparticles of Praziquantel for targeting the intestinal lymphatics and also tested them by performing suitable *in vivo* studies. The SLNs were prepared by hot homogenization followed by ultrasonication using triglycerides, lecithin and different surfactants. *In vivo* results in rats indicated a 6 fold increase in $AUC_{0-\infty}$ after intraduodenal administration of SLNs loaded with Praziquantel in rats when compared to Praziquantel in saline. Absorption of Praziquantel through the intestinal lymphatics was confirmed using cycloheximide [61].

Mu et al., 2013 discussed on the lipid based formulations used in oral delivery of lipophilic drugs (poorly water soluble drugs). They also described various lipid based products available in the market. They gave information about the different types of lipids which vary by their physiochemical properties and chemical structures. They also gave an overview on the digestion and absorption of lipids *in vivo* [111].

Porter et al., 2001 provided elaborate information on the intestinal lymphatic drug transport. They provided information on the mechanism of access of drugs to the intestinal lymph and described the role of lipid in the digestion and absorption. The ability of various lipid carriers to stimulate lymphatic drug transport was discussed with respect to the class, chain length and degree of saturation of the lipids. They gave future directions for performing intestinal lymphatic transport studies in cell culture model and genetically modified animals [112].

Khan et al., 2013 reviewed lipid based nanoformulations for lymphatic delivery. They mentioned the lymphatic system and the complexities involved in targeting the drugs to it. Lipid based formulations like solid lipid nanoparticles and nanostructured lipid carriers, were described with a special focus to deliver drugs to the lymphatics. Important factors like particle size, surface charge, types of lipid and concentration of the emulsifier molecular weight, and hydrophobicity were discussed in detail. Various *in vitro* and *in vivo* models for studying the drug transport in the lymphatic system were also mentioned [14].

Shah et al., 2013 prepared SLNs of carvedilol for lymphatic targeting. Carvedilol SLNs were prepared using Compritol 888 ATO and Poloxamer 188 as the lipid carrier and surfactant by hot homogenisation method. *In vitro* cell line studies using Caco-2 cell line exhibited a higher uptake for carvedilol SLNs when compared to its free form. These results indicated higher uptake to the intestinal lymphatics [113].

Driscoll et al., 2002 discussed on the various lipid-based formulations for the delivery of drugs to the intestinal lymphatics. Impact of various lipid based vehicles and their components used for preparing them, various physicochemical properties of the drugs, different animal models and experimental techniques have been described in detail. This review also described the success and limitations of lipid-based vehicles for lymphatic targeting and showcased potential areas of future research [114].

Shete et al., 2013 developed long chain lipid based NLCs for tamoxifen to target them to the lymphatics and lymph nodes. They performed systematic preformulation studies, formulated them and characterization them. Solubility of the drug was screened in the oils, surfactants and co-surfactants to identify suitable components. NLCs of the drug showed a good dissolution profile when compared to its free form [115].

Cai et al., 2011 reviewed lymphatic drug delivery using solid lipid nanoparticles and liposomes. Various routes of delivery like subcutaneous, intestinal, and pulmonary routes has been described and their applications to improve lymphatic penetration and retention of drug molecules has been mentioned in detail. They also briefed the recent advances in the field of imaging and drug delivery using solid lipid nanoparticles and liposomes [64].

Nakamura et al., 2012 prepared PEGylated liposomes by different techniques and also compared their characteristics. Their results showed that a higher stealth nature in the blood with low degradation of PEG can be inhibited by post-modification method. They concluded by stating that post modification method is advantageous in all the aspects [116].

Kim et al., 1994 attempted to target methotrexate loaded differently charged liposomes to the lymphatics after intramuscular injection to rats. Their results indicated entry of liposomes injected by intramuscular route to the lymphatics. The concentration of the drug was 100-350 folds higher in the lymph when compared to the plasma concentration. Positively charged liposomes localized more in lymph nodes when compared to the neutral and negatively charged counterparts [117].

Kaur et al., 2008 targeted surface-engineered zidovudine liposomes to the lymphatics. The surface charge of the liposomes was modified by incorporating stearylamine and dicetyl phosphate as charge modifier and mannose was tagged to the surface to enhance localization to lymphatics. The tissue distribution pattern of mannose modified liposomes showed a significant reduction of the free zidovudine concentration in serum. Fluorescent microscopy and tissue distribution studies showed higher concentration of the surface modified liposomes in the lymph nodes and spleen [11].

Kinman et al., 2006 developed lipid based Indinavir nanoparticles for targeting the lymphatics of HIV-infected macaques. After subcutaneous administration, these nanoparticles enhanced the concentrations of drug by 250-270% higher than the plasma indinavir concentrations in both visceral and peripheral lymph nodes. Enhancement in anti-HIV activity was also observed in the animals. The results indicate that indinavir lipid nanoparticles are efficient for targeting to the lymphatics [44].

Nune et al., 2011 mentioned the various trends and advances in the field of lymphatic targeting using diagnostic and drug delivery agents. They described the necessity of targeting various agents (dyes and drugs) to the lymphatics and are of the opinion that the existing tools are not up to the mark. They provided information on the application of novel nanocarriers like quantum dots, carbon nanotubes and other polymeric nanoparticles to improve the current scenario in delivering dyes and drugs to the lymphatics [118].

Paliwal et al., 2009 studied the effect of lipid core material on characteristics of SLNs meant for lymphatic delivery. They hypothesized that the composition of SLNs alters the absorption of drugs to and through lymphatic route. They prepared SLNs using Compritol 888 ATO, glycerol monostearate, stearic acid and tristearin. *In vivo* studies were also performed to evaluate the

lymphatic uptake and bioavailability. Their results showed a good lymphatic uptake and bioavailability with the use of Compritol 888 ATO, a mixture of different derivatives of behenic acid [55].

Nishioka et al., 2001 briefed on targeting lymphatic using various colloidal carriers. They have discussed on the recent progress with regard to emulsions, nanocapsules, nanospheres and liposomes for lymphatic targeting. They highlighted the importance of targeting anticancer drugs to the regional lymph nodes through subcutaneous administration. Information about the delivery of diagnostic agents to the regional lymph nodes was also provided [119].

Makwana et al., 2015 prepared SLNs of Efavirenz (EFV) to target the lymphatics and also elucidated its mechanism of uptake by blocking the flow of chylomicron. They prepared SLNs of EFV using Gelucire 44/14, Lipoid S 75, Compritol 888 ATO and Poloxamer 188 by hot homogenization technique and ultrasonication method. Their results of tissue distribution and lymphatic transport indicated that a significant amount of EFV had by-passed the hepatic portal system and entered the lymphatics. Thus it enhanced the oral bioavailability of EFV [120].

3.5 SOLID LIPID NANOPARTICLES AND THEIR APPLICATION IN LYMPHATIC TARGETING

Chauhan et al., 2005 prepared solid dispersions of etoricoxib using different lipid carriers by spray drying technique and evaluated their properties using diffuse reflectance infrared fourier transform spectroscopy, differential scanning calorimetry, hot stage microscopy, radiograph powder diffraction, and dissolution studies. The absence of etoricoxib peaks in radiograph powder diffraction profiles of solid dispersions suggested presence of etoricoxib in an amorphous state. The solid dispersions showed a better *in vitro* dissolution profile when compared with pure etoricoxib, physical mixtures of drug with lipid carriers, and spray-dried etoricoxib [121].

Fahy et al., 2011 wrote a detailed review on the classification of the lipids based on their structures and different tools. They provided information on Lipid Metabolites and Pathways Strategy (MAPS) consortium which is involved in the detection, quantitation and pathway reconstruction of lipids. They also discussed various developments by the Lipid MAPS over a period of time [122].

Wang et al., 2006 studied the ability of stealth SLNs in situ to evade phagocytic uptake by mouse peritoneal macrophages. Fluorescent SLNs were prepared using rhodamine B as the marker and polyoxyethylene stearate as stealth agent. At all time points, phagocytic uptake of SLNs was better than stealth SLNs [123].

Mehnert et al., 2012 published a very elaborate review on the production, characterization and applications of SLNs. Information pertaining to the selection of the ingredients, different ways to manufacture and stabilise them have been mentioned. Various routes of administration and their *in vivo* fate has been discussed [18].

Rohit et al., 2013 worked on a technique to prepare SLNs of hydrophilic drugs with high entrapment efficiencies. They changed the composition of the lipid matrix by mixing different ratios of glyceryl monostearate, Compritol 888 ATO and stearic acid to achieve high entrapment efficiencies for hydrophilic drugs. Their results showed high entrapment efficiencies when stearic acid was combined with Compritol 888 ATO in the ratio of 1:4 [124].

Muller et al., 2000 provided detailed information on solid lipid nanoparticles right from its origin. They stated that SLNs has the advantages of other nanoparticulate carriers and at the same time, does not possess their major disadvantages. They provided information on the current state of the art regarding production techniques for SLN, drug incorporation, loading capacity and drug release, especially focusing on drug release mechanisms. The regulatory status of

excipients, toxicity information, different routes of administration, sterilization techniques for SLNs and information pertaining to their long-term stability studies and industrial scale up are also discussed in detail [19].

3.6 IMATINIB MESYLATE

Bende et al., 2010 developed and validated a HPLC method for the estimation of imatinib mesylate plasma and tissue sample of rats. They used a Zorbax Extend (5 μ m, 4.6 \times 250 mm) double end-capped C18 column with a mobile phase consisting of methanol and aqueous triethyl amine (60:40, v/v) of pH 10.5 at a flow rate of 1 ml/min. A good recovery was observed and their developed method demonstrated a good linearity from 25 to 1600 ng/ml with a regression coefficient of 0.9995. Their method was suitable for performing *in vivo* pharmacokinetic studies [125].

Marslin et al., 2015 proved that imatinib mesylate loaded poly(lactide-co-glycolide) nanoparticles improved its anticancer activity and reduced cardiotoxicity. Methylthiazolyldiphenyl-tetrazolium bromide assay showed that poly(lactide-co-glycolide) nanoparticles of Imatinib mesylate were more cytotoxic to MCF-7 breast cancer cells when compared to the equivalent concentration of unencapsulated imatinib mesylate. There were no signs of cardiotoxicity in Wistar rats after orally administration of poly (lactide-co-glycolide) nanoparticles of Imatinb mesylate for 28 days. Histological sections of the hearts of Wistar rats also did not show any significant cardiotoxic symptoms [126].

Guetens et al., 2003 quantified the Imatinib mesylate in erythrocytes and plasma by sediment technology and liquid chromatography–mass spectrometry. Imatinib mesylate and the internal standard were eluted on a Waters C18 column (50 \times 2.1 mm I.D) using a mixture of methanol and ammonium acetate. Their developed method can be used for the quantification of Imatinib mesylate in plasma [127].

Zhou et al., 2015 studied whether administration of imatinib and dasatinib influenced pharmacokinetic parameters in rats. They orally administered imatinib, dasatinib and a combination to rats and measured various pharmacokinetic parameters. These results indicated that dasatinib slightly influenced the pharmacokinetic profile of imatinib in rats and can lead to drug-drug interactions if administered simultaneously [128].

Gupta et al., 2015 developed and optimized nanostructured lipid carriers (NLCs) of imatinib base to improve their anticancer and pharmacokinetic properties. NLCs were prepared by hot homogenization method and optimized using Plackett-Burman design and central composite design. An *in vivo* pharmacokinetic study was conducted in rats after both oral and intravenous administration. The *in vitro* cytotoxicity was evaluated by MTT assay on NCI-H727 cell-lines. The optimized NLC showed a particle size of 148.80 ± 1.37 nm and zeta potential of -23.0 ± 1.5 mV and showed higher bioavailability after oral administration [129].

3.7 QUILLAJA SAPONIN

Maier et al., 2015 studied on new phenylpropanoid sucrose esters from the inner bark of *Quillaja saponaria*, quillajasides A and B. The phenolic composition of aqueous extracts of the inner bark of *Quillaja saponaria* was compared with commercially available *Quillaja* extracts. Piscidic acid (+) and several p-coumaroyl sucrose esters are the major phenolics in both extracts. The antioxidant activity and their applicability in enzymatic browning reactions were also tested [88].

Kralova et al., 2012 discussed on the different surfactants used in food industry. They focussed on the formation, structures, and properties of different emulsions in food. The importance of the major end points described in the Organisation for Economic Co-operation and Development guidelines for the

hazard assessment of food chemicals were described and the main parameters such acute toxicity, reproductive toxicity, sub-acute repeated studies, long-term studies, allergy, and mutagenicity tests were measured. They mainly focussed on monoglycerides, lecithins, glycolipids, fatty alcohols and fatty acids [130].

Martin et al., 1999 briefed about different kind of saponins and their industrial uses. Their structures, molecular weights and properties along with this uses have been described in detail [85].

Yang et al., 2013 studied the stability of emulsions of food products using Quillaja saponin as a surfactant. They studied the suitability of this surfactant with Tween 80. They also studied the effect of homogenization pressure, number of passes, and concentration of the emulsifier on the particle size. Their results highlighted the applicability of Quillaja saponin in food and beverage industry over a long run [131].

Francis et al., 2002 reviewed the biological action of saponins in animals. They discussed the anticarcinogenic, antioxidant, immunostimulant, membrane-rupturing, hypocholesterolaemic, antifungal and antiviral properties of saponins. They also significantly affected the growth and reproduction in animals. They stated that the haemolytic action of saponins is due to affinity of aglycone moiety [132].

Guclu-Ustundag et al., 2013 described the properties, applications and processing of saponins. Biological activities of saponins like anticancer and anticholesterol activity and their applications in food, cosmetics, and pharmaceutical industries has been described. They also described the effect of processing on the properties and structure of saponin [83].

3.8 IMPORTANCE OF DRUG SOLUBILISATION IN THE LIPIDS

Bergstrom et al., 2016 discussed various computational tools for prediction of intestinal drug absorption, models for prediction of the suitable formulation strategies for B-r-o-5 compounds and models to understand the interplay between the drug, formulation and physiological environment. For B-r-o-5 compounds, non-traditional delivery strategies are required to achieve adequate exposure after oral administration. Molecular interaction patterns between the drugs and excipients, molecular dynamics simulations were discussed. Computational biopharmaceutical profiling can be used to identify formulateability during the lead optimization and early development stages [133].

Silva et al., 2016 prepared lipid based formulations of carvedilol by testing its compatibility with different lipid excipients to enhance its bioavailability. They checked for the presence physical and chemical interactions between the drug and excipients using differential thermal analysis, thermogravimetric analysis, fourier transform infrared spectroscopy and isothermal stress testing. The results indicated the lipids which are incompatible with the drugs which also did not reduce the drug content over long term storage. Lipids like stearic acid, palmitic acid, glyceryl behenate, tribehenin-PEG, polyglyceryl- 6-isostearate and diethylene glycol monoethyl ether were suitable for developing lipid based formulations. They stressed the necessity of performing preliminary studies for proper selection of drugs [134].

Umamatheswari et al., 2010 applied QSAR for the synthesis, and antimicrobial evaluation of novel piperidin derivatives. Their synthesized compounds were screened against different bacterial and fungal strains by serial dilution method. The results of QSAR studies indicated that increase in the weakly polar component of the solvent accessible surface area favoured the antibacterial activity, whereas an increased polarizability and decreased ionisation potential and hydrogen bond donor favoured antifungal activity [135].

Zheng et al., 2012 worked to identify different approaches for enhancing the oral bioavailability of poorly water-soluble drugs in the drug discovery stage. LCQ789, preclinical BCS Class II compound was used and to enhance bioavailability existing techniques like reduction in particle size, solid dispersions, lipid based formulations and co-crystals were used. High throughput screening and Gastroplus were used to reduce the amount of drug used. Amongst the various techniques used, solid dispersions and lipid based formulation showed highest bioavailability [136].

Warren et al., 2013 explored the microstructures of lipid based formulations and studied their dispersion patterns in the gastrointestinal tract at molecular level using molecular dynamics. Their formulations contained glycerides derivatives as lipids and drugs like (danazol, acyclovir, ketoprofen, hydrocortisone, or progesterone) were used. As the water content increased, the lipid microstructures gradually changed from a continuous phase to a reverse micellar solution and consequently to lamellar lipids under the influence of hydrogen bonds. They stated that application molecular dynamics simulations is a good option to view changes of lipid based formulations at molecular levels and advised usage of these *in silico* tools during formulations [137].

Yang et al., 2013 showcased the importance of Van der Waals dispersion forces that contribute to molecular recognition of the solutes in the solution. They stated that properties that lead to self-assembly and molecular recognition are due to non-covalent interactions. In this work they have used synthetic molecular balances to measure interactions between apolar alkyl chains. They observed that solvent-solvent interactions lead to apolar association in the solution [138].

Jensen et al., 2010 showed that the solubility of corticosteroids in the lipids and their release from the matrix is dependent on the polarity of the lipids. The effect of composition of the lipids on their ability to solubilise and release

betamethasone-17-valerate (BMV) was estimated by varying the content of lipid monoglyceride content and the chain length of the fatty acids. The effect of physicochemical properties of the drug was determined by studying 5 different corticosteroid derivatives which differ in their lipophilicity. The results highlighted that the solubility of corticosteroids in the lipid phase and their release was greatly influenced by the distribution of drugs in the lipid matrix [139].

Jorgenson et al., 2000 predicted the solubility of 150 drugs in water using Monte Carlo Simulations. Their results showed that descriptors like the solvent accessible surface area, numbers of hydrogen bonds and indices for cohesive interactions in solids correlated with the pharmacologically important properties like octanol/water partition coefficient and aqueous solubility [140].

Sacchetti et al., 2012 tried to predict the solubility of drugs in the lipids and established a relationship of drug solubility in lipid mixtures. In their study, they tested the solubility of four drugs in eighteen different lipids. The results indicated that solubility of the drugs in the lipid mixtures can be quantified as an average of its solubility in the individual lipids [141].

Li et al., 2006 screened and characterized various lipid carriers and drug-polymer-lipids for their interactions, which will be helpful in the rational designing of polymer-lipid nanoparticles. The solubility parameters of Verapamil HCl (VRP), Verapamil HCl-dextran complex (VRP-DS), and various lipids were calculated. Additionally, partition coefficients of VRP and VRP-DS in lipids were also determined. The thermodynamics behind the binding of VRP to DS was determined by isothermal titration calorimetry. The solid state properties and the interactions among them were characterized using differential scanning calorimetry and powder X-ray diffraction. They stated that the drug loading efficiency and drug loading capacity of a lipid matrix depends on the binding and the interactions of the VRP-DS complex with the lipid [142].

Ortwine et al., 2013 studied on various physicochemical and DMPK *in silico* models to ease up the drug discovery and to simplify the selection of new drug molecules for future line of work. They have provided information on various physicochemical and DMPK properties, the problems associated during their calculation and different softwares available. The methods followed by the companies to communicate results were also discussed in detail [143].

Lipinski et al., 2012 performed several experiments and attempted to correlate with computationally predicted solubility and permeability of drugs in discovery and development. They predicted ‘the rule of 5’ which states that poor absorption or permeation is more likely if there are more than 5 H bond donors, 10 H-bond acceptors, if the molecular weight is greater than 500 and Log P is greater than 5. During the development setting, solubility calculations focused on the prediction of the exact value and are usually difficult due to polymorphism. Recent works on linear free energy relationships and Log P approaches were also discussed and they stated that predictions are possible for closely related analogous series of compounds when experimental thermodynamic solubility measurements are also simultaneously performed [144].

Golbraikh et al., 2002 highlighted the importance of q^2 during the validation while performing quantitative structure–activity relationship modelling. In general a high leave-one-out cross-validated R^2 (LOO q^2) i.e., $q^2 > 0.5$ is considered as an indicator for the high predictive ability. They highlighted the fact that a high value of LOO q^2 is necessary, but not mandatory for a model to possess high predictive power. They also stressed that external validation is the only method to establish a reliable QSAR model [145].

Greenhalgh et al., 1999 attempted to predict the miscibility in solid dispersions using solubility parameters. They reported the interactions and possible incompatibilities in solid dispersions of hydrophobic drugs in hydrophilic carriers (with solubility parameters employed as a means of interpreting results). They stated that calculation of Hildebrand parameters is a good tool to predict interactions and potential incompatibilities between the drug and lipid carriers [146].

Subashini et al., 2011 applied molecular dynamics for the simulation of uptake of three drugs, doxorubicin, silymarin and gliclazide in six polymers (alginic acid, sodium alginate, chitosan, Gantrez AN119 (methyl-vinyl- ether-co-malic acid based), Eudragit L100 and Eudragit RSPO). Molecular dynamics simulation of the drug in the vicinity of the polymer molecule in the presence of water molecules was performed using Gromacs-forcefield, (300 ps, 300 K) and the interaction energies between them were calculated. These energies were evaluated with respect to the electric-dipole, Van der Waals and hydrogen bond forces. The hydrophilic interaction between nanoparticles and water was inversely correlated with the uptake of the drug. The molecular dynamics simulation can be applied in developing polymer based drug delivery systems to obtain reasonable approximation of drug uptake [147].

Alskar et al., 2016 developed tools for the early prediction of drug solubility in lipids by studying more than 2,000 solubility measurements. Computational models were developed for *in silico* prediction of solubility, and drug loading capacity in the lipids. Drugs with a melting point below 150°C showed reasonable solubility in the glycerides. *In silico* models also showed good predictions of the loading capacity in the formulations without performing experimental studies (R^2 0.79) using thermal properties and molecular information descriptors of the crystalline drug [133].

Chen et al., 2012 gave their perspective on the various applications of lipid based formulations in drug discovery. They had an opinion that structure activity relationship and lead optimization of a new drug candidate with required physicochemical properties for lipid formulations, and a good design of *in vitro* and *in vivo* studies during drug discovery play an important role. These will help in establishing a good connection with the preclinical evaluation and clinical development goals, and can significantly reduce the time consumed in the development of formulations and also increase the development of a potentially viable clinical formulation [148].

Cheng et al., 2003 developed a rapid quantitative structure-property relationship model for the prediction of aqueous solubility from the molecular structures. Genetic algorithms and multiple linear regressions were used to develop the mathematical models for a diverse set of compounds including small, drug and drug-like molecules. Those models predicted the solubility of the training and test sets and those results correlated well with the experimental values. Using the 2-D structures as input, their model could compute solubility for 90 000-700 000 compounds/h on a SGI Origin 2000 workstation and can be used in data mining and screening of a vast set of molecules [149].

Patel et al., 2015 attempted to predict the solubility of drugs in lipidic solvent mixture using a modelling and thermodynamics. They applied the data gathered from the *in silico* modelling to develop self micro emulsifying drug delivery systems. They also investigated the usage of the thermodynamic model to study the solubility behaviour of the drugs (Clotrimazole and Fluconazole) in oils. Their results showed a good correlation between the predicted solubility and experimental solubility [150].

Persson et al., 2013 developed computational tools for the prediction of drug solubility in lipids and lipid based formulations. The solubility of 30 structurally diverse drug molecules was measured in soybean oil, Captex355, polysorbate 80 and PEG400 and were used as responses during the development of partial least squares model. Various molecular descriptors and melting point were used as variables for the development of the model and the results were validated with test sets. A strong correlation was observed between polysorbate80 and PEG400. They observed that the solubility of drugs in medium chain triglycerides and long chain triglycerides can be predicted by calculating the various molecular descriptors [151].

Chevillard et al., 2012 worked on *in silico* prediction of aqueous solubility by developing a multimodel protocol based on the similarity of chemical structure. They evaluated ten *in silico* models for prediction of aqueous solubility for several data sets to assess their reliability and proposed a new diverse data set for 150 molecules. Their “multimodel protocol”, allowed selection of the most accurate model for a compound and showed accurate results for prediction of solubility when compared with other individual models [152].

Benet et al., 2011 applied biopharmaceutics drug disposition classification system for 927 drugs. Among the 897 parent drugs, 78.8% (707) drugs are orally administered. The lowest percentage solubility and a dose number were recorded. Other parameters like percent drug excreted unchanged in urine, LogP, and LogD 7.4 were measured. Additionally, *in silico* parameters for polar surface area, predicted Log solubility in water, calculated LogP, and the number of hydrogen bond acceptors and hydrogen bond donors for the active moiety were estimated and a comparison was made with experimentally measured values and *in silico* values. They discussed the potential use of BDDCS to estimate the disposition characteristics of novel drugs in the early stages of development [153].

Ali et al., 2015 performed preformulation and physicochemical interaction studies for furosemide using different solid lipids like Compritol 888 ATO, Hydrokote C, Imwitor 491, Imwitor 372P, and Witepsol H12 using Fourier transform infrared, Raman, differential scanning calorimetry, X-ray diffraction, scanning electron microscopy. Compritol 888 ATO showed highest solubility for the drug. FTIR, Raman, DSC and XRD studies indicated no chemical interactions with the lipids used. *In vitro* drug release study showed the release of drug to follow either of Zero order release, Higuchi or Korsmeyer–Peppas model [154].

3.9 PREPARATION AND CHARACTERISATION OF SOLID LIPID NANOPARTICLES AND CONJUGATION USING VARIOUS LIGANDS

Chalikwar et al., 2012 formulated solid lipid nanoparticles of nimodipine and enhanced its oral bioavailability via lymphatic transport system. They used (2³) factorial design was employed to optimised the best formulation and to study the effect of various excipients on particle size, polydispersity index, zeta potential, drug entrapment efficiency, drug loading efficiency and *in vitro* drug release. Pharmacokinetic studies in male Albino Wistar rats showed 2.08-fold increase in the relative bioavailability for SLNs than the free drug [155].

Bailon et al., 2009 studied about PEG and PEGylation. They stated the necessity of PEGylation to improve clinically efficacy and pharmacokinetic profile than the existing drug molecules. They highlighted that PEGylation sustains the clinical response with a low dose. They also focussed different approaches and strategies for the development of PEGylated products [156].

Venishetty et al., 2013 prepared SLNs of docetaxel and ketoconazole to enhance the permeability of docetaxel across the blood brain barrier. Additionally, their surface was modified with folic acid. These SLNs were characterized for size, surface charge, *in vitro* release, cytotoxicity, and cellular uptake in brain endothelial cell line. The results of the plasma and brain pharmacokinetic studies showed an enhanced uptake across the brain for docetaxel [62].

Garg et al., 2007 attempted to prepare azidothymidine loaded galactosylated liposomes with enhanced cellular uptake, reduced hematopoietic toxicity, and altered pharmacokinetics. Galactosylated liposomes were prepared and characterized *in vitro* to target the lectin receptors present on the macrophages. Their formulation maintained a higher level of drugs in tissues rich in galactose specific receptors and enhanced the half-life of the drug [157].

Yuan et al., 2008 tested the cellular uptake and cytotoxicity of paclitaxel of solid lipid nanoparticles in A549 cancer cells. The order of cellular uptake ability of solid lipid nanoparticles prepared using various lipids decreased in the order of glycerol tristearate > monostearin > stearic acid > Compritol 888 ATO. Because of low drug entrapment efficiency of glycerol tristearate solid lipid nanoparticles, monostearin solid lipid nanoparticles were considered best to improve the cytotoxicity of paclitaxel. Additionally, polyethylene glycol monostearate and synthesized conjugate, folic acid–stearic acid were further introduced into the solid lipid nanoparticles. PEG and folate modified solid lipid nanoparticles enhanced the cellular uptake and cytotoxicity of the solid lipid nanoparticles [158].

Biswas et al., 2013 developed surface functionalized doxorubicin-loaded liposomes with octa-arginine to enhance the anticancer activity. They conjugated commercially available Doxil with a octa-arginine. The conjugated liposomes increased the intracellular and intratumoral delivery when compared to unmodified liposomes. It also improved the cytotoxic activity *in vitro* and *in vivo*. The results indicated improvement in the therapeutic window of PEGylated liposomes with lower non-specific toxicity [159].

Becker et al., 2015 prepared lipid based solid oral formulations by melt coating, melt granulation and melt extrusion using fluid bed coaters, spray dryers or extruders. They attempted to produce a bigger batch of lipid based products by

scaling up to pilot or production scale. They also mentioned the challenges, experiences and formulations which could help to efficiently choose the excipients [59].

3.10 PHARMACOKINETIC STUDIES

Edwards et al., 2001 provided information about various animal models for the study of the intestinal lymphatic drug transport. The advantages and disadvantages with respect to the usage of both small and large animal models and the various factors which have been found to influence the outcome of intestinal lymphatic drug transport studies with these models have also been discussed [160].

Feeney et al., 2016., discussed the origin, progress and future perspectives for oral lipid-based formulations. The various advantages of lipid-based formulations, general properties and classification over the past fifty years were briefed. The ability of lipid-based formulations to promote intestinal solubilisation, supersaturation and absorption and the various methods employed to assess formulation performance, various techniques to increase drug lipophilicity and lipid solubility were also elaborated in detail [161].

Wang et al., 2015 studied to investigate the effect of orally administered genistein and Imatinib on the pharmacokinetics in rats. A single dose of genistein had no effect on the pharmacokinetics of imatinib. The results showed that multiple doses of genistein induced the metabolism of imatinib, whereas single dose of genistein had no effect [162].

Boyd et al., 2001 provided a valuable protocol for the collection of lymph from cannulated lymphatic ducts in rats. They mentioned a step by step protocol on how to identify the thoracic and mesenteric lymphatic duct and a detailed surgical procedure to cannulate and collect lymph from them [163].

Gaur et al., 2014 tried to enhance the oral bioavailability of Efavirenz by encapsulating it in SLNs. The SLNs were prepared (using glyceryl monostearate as lipid carrier and tween 80 as surfactant) and analyzed for physical parameters, stability, and pharmacokinetic profile. The solid lipid nanoparticles showed a particle size and PDI of 124.5 ± 3.2 nm and 0.234 respectively. Pharmacokinetic studies showed a 5 fold increase in peak plasma concentration and 11 fold increase in AUC when comparison to free Efavirenz [164].

Scope & Plan of Work

4. SCOPE AND PLAN OF WORK

4.1 SCOPE

In the present scenario there are sufficient amount of anticancer drugs which can kill the tumor cells in the body. But, these drugs are equally toxic to the healthy cells of the body and cause several potential side effects, leading to reduced patient life and compliance. To avoid the possible side effects posed by the anticancer drugs, many people prefer surgical and radiation methods for the treatment. Though surgical removal of the tumor in breast cancer patients has been found to be beneficial, the incidence of recurrence of cancer to the other parts of the body (including breast) is very high and is attributed to metastasis of the cancer cells from the primary site through regional lymphatics. As metastasis of cancerous cells occurs in the regional lymphatics, it is essential for the drug to reach the regional lymphatics to arrest metastasis. In order to reach the lymphatics, the size of the particles should be in the range of 10- 100 nm, the uptake rate into the lymphatics should be high and the delivery route should be appropriate. SLNs can safely target and deliver anticancer drugs by subcutaneous administration to the regional lymphatics, the residing place of the metastatic cancer cells. Hence, the current doctoral research work has been planned to work on the development and evaluation of ligand conjugated SLNs of IM which can specifically target and kill the tumor cells in the lymphatics. The development of SLNs requires solubilisation of the drug in the lipid carrier to achieve good entrapment efficiencies and stability. There is no model to predict the solubility of drugs in lipids. Hence, examining the various properties of lipids which influence their ability to solubilise the drugs has also been examined and a model has been developed to predict the solubility of IM in lipids for the first time. The utility of QS, a natural surfactant obtained from the bark of *Quillaja saponaria*, in the preparation of SLNs has also been evaluated for the first time.

To achieve the above mentioned specific objectives the following research work has been followed.

4.2 PLAN OF WORK

• PREFORMULATION STUDIES

- Construction of calibration curve using UV spectroscopy
- Bioanalytical method development using high performance liquid chromatography
- Screening of lipids for IM solubility
- Solid state characterization using differential scanning calorimetry
- Quantification of Maximum Solubility
- Calculation of total solubility parameters, polarity of IM and lipids
- Identification of descriptors and development of QSSR Model
- Compatibility of IM with the lipids using FTIR
- Determination of partitioning coefficient of IM in different lipids and water

• CHEMICAL CONJUGATION OF STEARIC ACID AND LIGANDS

- Chemical conjugation of hyaluronic acid-stearic acid conjugate
- Chemical conjugation of vitamin B12-stearic acid conjugate

• PREPARATION OF SOLID LIPID NANOPARTICLES

- Formulation of SLNs of IM using stearic acid as lipid carrier
- Formulation of SLNs of IM using palmitic acid as lipid carrier
- Formulation of SLNs of IM using glyceryl palmitostearate as lipid carrier
- Formulation of SLNs of IM using glyceryl monostearate as lipid carrier
- Formulation of SLNs of IM using Geleol mono and di glycerides as lipid carrier

• SURFACE MODIFICATION OF SOLID LIPID NANOPARTICLES

- Surface modification of SLNs using hyaluronic acid

-
- **IN VITRO CHARACTERISATION OF SOLID LIPID NANOPARTICLES**
 - Confirmation of ligand- lipid conjugate by NMR spectroscopy
 - Determination of particle size and polydispersity index by Malvern Zeta Sizer
 - Determination of zeta potential by Malvern Zeta Sizer
 - Determination of particle shape and morphology by Transmission Electron Microscope
 - Determination of particle surface morphology using Atomic Force Microscope
 - Determination of entrapment efficiency and drug loading efficiency
 - *In vitro* release studies
 - *In vitro* haemolysis test

 - **IN VITRO CELL LINES STUDIES**
 - *In vitro* cytotoxicity studies
 - Apoptosis analysis using propidium iodide staining

 - **IN VIVO ANIMAL PHARMACOKINETIC STUDIES**
 - To estimate the pharmacokinetic parameters in blood
 - To estimate the pharmacokinetic parameters in lymph nodes

 - **STABILITY STUDIES**

Materials & Method

5. MATERIALS AND METHODS

5.1 MATERIALS

S. No	Name	Source
1	Imatinib mesylate	Natco Pharmaceuticals, India
2	Quillaja saponin	Sigma Aldrich, USA
3	Hyaluronic acid	Sigma Aldrich, India
4	Vitamin B12	Veer Chemie Organics, India
5	Myrisitic acid	Sigma Aldrich, India
6	Palmitic acid	Sigma Aldrich, India
7	Stearic acid	Sigma Aldrich, India
8	Behenic acid	Sigma Aldrich, India
9	Glyceryl monostearate	HiMedia, India
10	Glyceryl palmitostearate	Subhash Chemicals, India
11	Precirol ATO 5 [®]	Gattefosse, France
12	Geleol mono and di glycerides [®]	Gattefosse, France
13	Compritol 888 ATO [®]	Gattefosse, France
14	Trimyristin	SD fine chemicals, India
15	Tripalmitin	SD fine chemicals, India
16	Tristearin	SD fine chemicals, India
17	Gelucire 44/14 [®]	Gattefosse, France
18	Gelucire 33/01 [®]	Gattefosse, France
19	Captex 70 [®]	Gattefosse, France
20	Sterotex NF [®]	Abitec, USA

S. No	Name	Source
21	Sterotex HM [®]	Abitec, USA
22	Hydrokote 112 [®]	Abitec, USA
23	Hydrokote M [®]	Abitec, USA
24	Cocoa butter	MN Goodies Private limited, India
25	Pluronic F-127 [®]	Sigma Aldrich, USA
26	Potassium dihydrogen phosphate	Himedia, India
27	Acetonitrile-HPLC	Sigma Aldrich, USA
28	Tetra butyl methyl ether	Sigma Aldrich, USA
29	Ortho phosphoric acid	Sigma Aldrich, USA
30	Ammonium acetate	HiMedia, India
31	Acetone	HiMedia, India
32	Sodium hydroxide	Himedia, India
33	D-mannitol	SD Fine chemicals, India
34	Potassium bromide	Himedia, India
35	Sodium chloride	HiMedia, India
36	Potassium chloride	HiMedia, India
37	Disodium hydrogen phosphate	HiMedia Mumbai
38	Dialysis membrane (Mw.Wt-12,000-14,000 Daltons)	HiMedia, India
39	Dialysis membrane clips	HiMedia, India
40	Tri sodium citrate	HiMedia, India

5.2 INSTRUMENTS

S. No.	NAME OF THE INSTRUMENT	MANUFACTURER
1	High Speed homogenizer	Pro Scientific
2	Malvern Zeta Sizer ZS 90	Malvern instruments
3	Ultrasonic homogenizer	Sonics
4	Lyophilizer	Lyodel
5	Centrifuge	Eppendorf
6	Bath Sonicator	PCI, Mumbai
7	Inverted Phase Contrast Microscope	Nikon
8	Transmission Electron Microscope	JOEL TEM 2100
9	Atomic Force Microscope	NTMDT, NTEGRA Prima
10	Digital Weighing Balance	Shimadzu
11	Magnetic stirrer	Remi equipments Ltd., Mumbai
12	UV-Visible Spectrophotometer	UV-1650 PC Shimadzu
13	FTIR Spectrophotometer	8400 S Shimadzu
14	IR Hydraulic Pellet Press	M 15 Techno Search Instruments
15	Differential Scanning Calorimeter	TA instruments
16	High Pressure Liquid Chromatography	Waters

5.3 IMATINIB MESYLATE (IM)

Chemical name : Methanesulfonic acid;4-[(4-methylpiperazin-1-yl)methyl]-N-[4-methyl-3-[(4-pyridin-3-yl)pyrimidin-2-yl)amino]phenyl] benzamide

Empirical formula : C₃₀H₃₅N₇O₄S

Molecular weight : 589.715 g/mol

Structure : The structure of IM is shown in Figure 4.

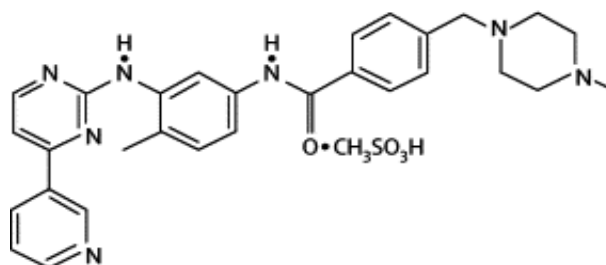


Figure 4. Structure of IM

Colour:

White to off white to brownish or yellowish tinged crystalline powder

Solubility:

Soluble in aqueous buffers \leq pH 5.5, but very slightly soluble in neutral to alkaline aqueous buffers; freely soluble to very soluble in dimethyl sulfoxide, methanol, and ethanol; insoluble in n-octanol, acetone, and acetonitrile.

Mechanism of action:

Imatinib is a 2-phenyl amino pyrimidine derivative which functions as a specific inhibitor of a group of tyrosine kinase enzymes present in the body. It occupies the tyrosine kinase active site, which leads to a decrease in the activity. Although there are a large number of tyrosine kinase enzymes in the body, Imatinib is specific for the tyrosine kinase domain in Abelson proto-oncogene

(abl), c-kit and platelet-derived growth factor receptor (PDGFR). In breast cancer, the fusion of abl with bcr (breakpoint cluster region), bcr-abl is observed. IM specifically decreases the bcr-abl activity and prevents progression of cancers. Imatinib does also inhibit other targets like c-kit and PDGF-R, ABL2, DDR1 and NQO2.

Bioavailability:

98%

Absorption:

Readily absorbed following oral administration.

C_{max}:

2-4 hours

Distribution:

Widely distributed throughout all body compartments, except adipose tissue

Peak serum concentration:

80 to 200 nanograms per ml after a single 50-mg dose.

Half life:

18 hours

Excretion:

Bile and feces

Dosage forms:

Tablets

Toxicity and side effects:

Usage of IM is associated with temporary elevations in serum aminotransferase levels and instances of severe acute liver injury which can be severe, which can lead to fatalities. Additionally, acute hepatitis and reactivation of an underlying hepatitis B is also observed.

5.4 QUILLAJA SAPONIN (QS)

Source	:	Inner bark of <i>Quillaja saponaria</i>
Synonyms	:	EINECS 215-731-2, HSDB 2171, soap bark saponin
Chemical name	:	soap bark saponin
Empirical formula	:	beta-D-Glucopyranosiduroni acid, (3 beta, 4 alpha, 16alpha)-17-carboxy-16-hydroxy-23-oxo-28 norolean-12-en-3-yl
Molecular weight	:	2284.406 g/mol
Structural formula	:	The structure of QS is shown in Figure 5.

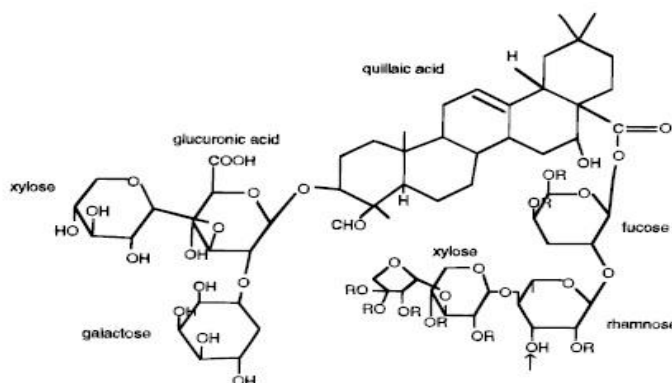


Figure 5. Structure of QS

Functional category:

Emulsifier, solubiliser, food applications

Melting point:

292°C

Solubility:

Soluble in water.

Stability and storage condition:

Slightly hygroscopic.

Safety:

Irritant to eyes and respiratory tract; haemolytic

Regulatory status:

GRAS listed and accepted for use as a food additive in Europe.

5.5 VITAMIN B12

Synonyms:

Cyanocobalamin

Chemical name:

Cyanocobalamin; Cobalamin; 68-19-9; Crystamine; Anacobin

Empirical formula:

Cobalt(3+);[(2R,3S,4R,5S)-5-(5,6-dimethylbenzimidazol-1-yl)-4-hydroxy-2-(hydroxymethyl)oxolan-3-yl][(2R)-1-[3-[(1R, 2R, 3R, 5Z, 7S, 10Z, 12S, 13S, 15Z, 17S, 18S, 19R) -2, 13,18-tris(2-amino-2-oxoethyl)-7,12,17-tris(3-amino-3-oxopropyl) -3,5, 8,8,13,15,18,19-octamethyl-2,7,12,17-tetrahydro-1H-corrin-24-id-3-yl]propanoylamino]propan-2-yl] phosphate;cyanide.

Chemical formula:

$C_{63}H_{88}CoN_{14}O_{14}P$

Molecular weight:

1355.388 g/mol

Structure: The structure of vitamin B 12 is mentioned in Figure 6.

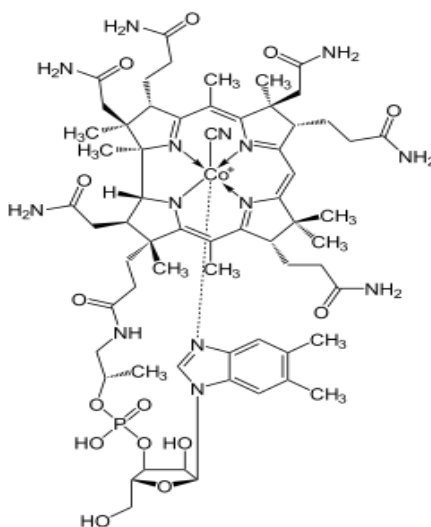


Figure 6. Structure of vitamin B12

Functional category:

Water soluble vitamin, treatment of pernicious anemia

Melting point: 300°C**Solubility:**

High water solubility (12500 mg/ml), soluble in alcohol; insoluble in acetone, chloroform and ether.

Stability and storage conditions:

Hydrated crystals are stable to air, max stability in pH range 4.5-5. Solutions of cyanocobalamin in water or 0.9% sodium chloride are stable and can be autoclaved for short periods of time (15-20 minutes) at 121°C.

Safety:

Cyanocobalamin injection is extremely safe when given by the intramuscular or deep subcutaneous route, but it should never be given intravenously. Rare occurrences of anaphylactic reaction (skin rash, itching, wheezing) may be observed after parenteral administration.

Regulatory status:

GRAS listed and FDA approved.

5.6 HYALURONIC ACID

- Chemical name** : Hyaluronate Tetrasaccharide; AC1MJ1T9;
CHEMBL1697748;
- Chemical formula** : $C_{28}H_{44}N_2O_{23}$
- Empirical formula** : (2S,3S,4S,5R,6R)-6-[(2S,3R,4R,5S,6R)-3-acetamido-2-[(2S,3S,4R,5R,6R)-6-[(2R,3R,4R,5S,6R)-3-acetamido-2,5-dihydroxy-6-(hydroxymethyl)oxan-4-yl]oxy-2-carboxy-4,5-dihydroxyoxan-3-yl]oxy-5-hydroxy-6-(hydroxymethyl)oxan-4-yl]oxy-3,4,5-trihydroxyoxane-2-carboxylic acid
- Molecular weight** : 776.651 g/mol
- Structural formula** : The structure of hyaluronic acid is mentioned in Figure 7.

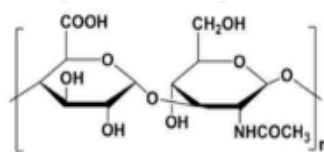


Figure 7. Structure of hyaluronic acid

Functional category:

Hyaluronic acid is a natural high-viscosity mucopolysaccharide with alternating beta (1-3) glucuronide and beta (1-4) glucosaminidic bonds. It is distributed widely throughout connective, epithelial, and neural tissues. It is used in treating osteoarthritis. It is also used as a dermatological agent, keratolytic, protectant, dermatological and wound care agent.

Melting point:

94°C

Solubility:

Easily soluble in cold water (46.6 mg/ ml). Insoluble in organic solvents.

Stability and storage conditions: Do not freeze; protect from light. Store at 2 to 25°C.

Safety:

Rare post market reports of immediate post injection reactions included extreme swelling of the lips and the whole face and symptoms of hypersensitivity such as anaphylactic shock.

Regulatory status:

GRAS and FDA approved.

5.7 PALMITIC ACID

Synonyms	:	Cetylic acid; Emersol 143; Edenor C16 98-100; 1-pentadecanecarboxylic acid; hexadecylic acid;
Chemical name	:	Hexadecanoic acid
Empirical formula	:	C ₁₆ H ₃₂ O ₂
Molecular weight	:	256.42 g/mol.
Structure	:	The structure of palmitic acid is mentioned in Figure 8.



Figure 8. Structure of palmitic acid

Functional category:

Emulsifying agent; skin penetrant; tablet and capsule lubricant.

Melting point:

63-64°C

Solubility:

Soluble in ethanol (95%); practically insoluble in water.

Stability and storage conditions:

The bulk material should be stored in a well-closed container in a cool, dry, place.

Safety:

Palmitic acid is used in oral and topical pharmaceutical formulations and is generally regarded as nontoxic and nonirritant at the levels employed as an excipient. However, palmitic acid is reported to be an eye and skin irritant at high levels and is poisonous by intravenous administration.

Regulatory status:

GRAS listed. Included in the FDA Inactive Ingredients Guide (oral tablets). Included in nonparenteral medicines licensed in the UK.

5.8 STEARIC ACID

Synonyms	:	Cetylacetic acid; Crodacid; E570; Edenor; Emersol; Hystrene; Industrene; Kortacid 1895; Pearl Steric; Pristerene; stereophonic acid; Tegostearic.
Chemical name	:	Octadecanoic acid
Empirical formula	:	$C_{18}H_{36}O_2$
Molecular weight	:	284.47 g/mol
Structural formula	:	The structure of stearic acid is mentioned in Figure 9.



Figure 9. Structure of stearic acid

Functional category:

Emulsifying agent; solubilizing agent; tablet and capsule lubricant.

Melting point:

54°C

Solubility:

Freely soluble in benzene, carbon tetrachloride, chloroform, and ether; soluble in ethanol (95%), hexane, and propylene glycol; practically insoluble in water.

Stability and storage:

Stearic acid is a stable material; an antioxidant may also be added to it. The bulk material should be stored in a well-closed container in a cool, dry place.

Safety:

Stearic acid is widely used in oral and topical pharmaceutical formulations; it is also used in cosmetics and food products. Stearic acid is generally regarded as a nontoxic and non-irritant material. However, consumption of excessive amounts may be harmful.

Regulatory status:

GRAS listed. Accepted as a food additive in Europe (fatty acids). Included in the FDA Inactive Ingredients Guide (sublingual tablets; oral capsules, solutions, suspensions, and tablets; topical and vaginal preparations). Included in nonparenteral medicines licensed in the UK. Included in the Canadian List of Acceptable Non-medicinal Ingredients.

5.9 GLYCERYL PALMITOSTEARATE

Synonyms:

Glycerin palmitostearate; glycerol palmitostearate; 2-[(1-oxohexadecyl)-oxy]-1,3-propanediyl dioctadecanoate and 1,2,3-propane triol.

Chemical name:

Octadecanoic acid, 2,3-dihydroxypropyl ester mixed with 3-hydroxy-2-[(1-oxohexadecyl)-oxy] propyl octadecanoate [8067-32-1]

Empirical formula:

Glyceryl palmitostearate is a mixture of mono-, di-, and triglycerides of C16 and C18 fatty acids.

Functional category:

Biodegradable material; coating agent; gelling agent; release modifying agent; sustained-release agent; tablet and capsule diluent; tablet and capsule lubricant; taste-masking agent.

Melting point:

52-55°C

Solubility:

Freely soluble in chloroform and dichloromethane; practically insoluble in ethanol (95%), mineral oil, and water.

Stability and storage:

Glyceryl palmitostearate should not be stored at temperatures above 358 °C. For storage for periods over 1 month, glyceryl palmitostearate should be stored at a temperature of 5–158 °C in an airtight container, protected from light and moisture.

Safety:

Glyceryl palmitostearate is used in oral pharmaceutical formulations and is generally regarded as an essentially nontoxic and nonirritant material.

Regulatory status:

GRAS listed. Included in the FDA Inactive Ingredients Guide (oral suspension, oral tablet). Included in nonparenteral preparations licensed in Europe. Included in the Canadian List of Acceptable Non-medicinal Ingredients.

5.10 GLYCERYL MONOSTEARATE

Synonyms:

Capmul GMS-50; Cutina GMS; 2,3-dihydroxypropyl octadecanoate; glycerine monostearate; glycerin monostearate; glycerol monostearate; glycerol stearate; glyceryl stearate; GMS; Imwitor 191; Imwitor 900; Kessco GMS; Lipo GMS 410; Lipo GMS 450; Lipo GMS 600; monoester with 1,2,3- propanetriol; monostearin; Myvaplex 600P; Myvatex; 1,2,3- propanetriol octadecanoate; Protachem GMS-450; Rita GMS; stearic acid, monoester with glycerol; stearic monoglyceride; Stepan GMS; Tegin; Tegin 503; Tegin 515; Tegin 4100; Tegin M; Unimate GMS.

Chemical name:

Octadecanoic acid, monoester with 1,2,3 propanetriol

Empirical formula:

$C_{21}H_{42}O_4$

Molecular weight:

358.6 g/mol

Structure:

The structure of glyceryl monostearate is mentioned in Figure 10.

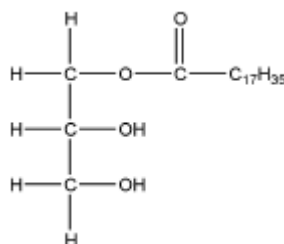


Figure 10. Structure of glyceryl monostearate

Functional category:

Emollient; emulsifying agent; solubilizing agent; stabilizing agent; sustained-release ingredient; tablet and capsule lubricant.

Melting point:

55-60°C

Solubility:

Soluble in hot ethanol, ether, chloroform, hot acetone, mineral oil, and fixed oils. Practically insoluble in water, but may be dispersed in water with the aid of a small amount of soap or other surfactant.

Stability and storage:

If stored at warm temperatures, glyceryl monostearate increases its acid value upon aging owing to the saponification of the ester with trace amounts of water. Effective antioxidants may be added, such as butylated hydroxytoluene and propyl gallate. Glyceryl monostearate should be stored in a tightly closed container in a cool, dry place, and protected from light.

Safety:

Glyceryl monostearate is widely used in cosmetics, foods, and oral and topical pharmaceutical formulations and is generally regarded as a nontoxic and nonirritant material.

Regulatory status:

It is included in the GRAS list. It is also included in the FDA Inactive Ingredients Guide (oral capsules and tablets; ophthalmic, otic, rectal, topical, transdermal, and vaginal preparations). Included in nonparenteral medicines licensed in the UK. Included in the Canadian List of Acceptable Non-medicinal Ingredients. If glyceryl monostearate is produced from animal fats (tallow), there may be additional regulatory requirements that the source be free of contamination from bovine spongiform encephalopathy.

5.11 GELEOL MONO AND DI GLYCERIDES

Synonyms:

Mono- and di- glyceride mixtures of stearic acid and palmitic acid; glyceryl mono and di stearate.

Chemical name:

Mixtures of mono- and di glycerides of stearic and palmitic acid.

Molecular weight:

414.9 g/mol

Functional category:

Coating agent; tablet binder; tablet and capsule lubricant; thickening agent; washing & cleaning products, lubricants and greases, adhesives and sealants, polishes and waxes, fertilisers, coating products and air care products.

Melting point:

65-77°C

Solubility:

Soluble when heated in chloroform and dichloromethane and in many organic solvents; slightly soluble in hot ethanol (96%); practically insoluble in cold ethanol (95%), hexane, mineral oil, and water.

Stability and storage condition:

It should be stored in a tightly stored container, at a temperature less than 35°C.

Safety:

It is used in cosmetics, foods and oral pharmaceutical formulations, and is generally regarded as a relatively non-irritant and nontoxic material. The US Cosmetic Ingredients Review Expert Panel evaluated glyceryl behenate and concluded that it is safe for use in cosmetic formulations in present practices of use and concentration.

Regulatory status:

GRAS listed and it is accepted for use as a food additive in Europe. It is included in the FDA Inactive Ingredients Database (oral capsules, tablets and suspensions).

5.12 DETERMINATION OF LAMBDA MAX (λ_{\max}) FOR IM USING UV SPECTROPHOTOMETER

Five mg of pure IM was weighed accurately and transferred carefully to a 50 ml standard flask. Sufficient volume of pH 7.4 phosphate buffer was added to the standard flask to obtain a stock solution of IM with a concentration 100 $\mu\text{g/ml}$. A suitable amount of this stock solution was transferred into a quartz cuvette and scanned from the wavelength of 200 to 400 nm using UV spectrophotometer. The wavelength at which maximum absorbance occurred was observed and noted down as the lambda max.

5.13 CONSTRUCTION OF CALIBRATION CURVE FOR IM USING UV SPECTROPHOTOMETER AT 256 nm

Five mg of pure of IM was weighed accurately and transferred carefully to a 50 ml standard flask. Sufficient volume of pH 7.4 phosphate buffer was added to the standard flask to obtain a stock solution of IM with a concentration 100 $\mu\text{g/ml}$. From this stock solution, 0.2 ml, 0.4 ml, 0.6 ml, 0.8 ml, 1 ml, 1.2 ml, 1.4 ml, 1.6 ml, 1.8 ml and 2 ml were accurately withdrawn into a 10 ml standard flask and made up to 10 ml using pH 7.4 phosphate buffer to produce different solutions of IM with concentrations of 2, 4, 6, 8, 10, 12, 14, 16, 18 and 20 $\mu\text{g/ml}$ respectively. The absorbance of the prepared solutions was determined by UV spectrophotometer at 256 nm. A standard curve of absorbance vs concentration was obtained and the r^2 value was determined.

5.14 DEVELOPMENT OF ANALYTICAL METHOD USING HIGH PERFORMANCE LIQUID CHROMATOGRAPHY

Quantitative and qualitative analysis of IM was carried out using reverse phase-high performance liquid chromatography (RP-HPLC).

5.14.1 Preparation of standard stock solutions

Ten mg of pure IM was weighed accurately and transferred carefully to a 10 ml standard flask. Sufficient volume of methanol was added to the standard flask to obtain a stock solution of IM with a concentration 1000 $\mu\text{g/ml}$ to form primary stock solution.

5.14.2 Selection of detection wavelength

Primary stock solution was scanned from the wavelength of 200 to 400 nm using UV spectrophotometer. The wavelength at which maximum absorbance occurred was observed and noted down as the lambda max.

5.14.3 Optimization of Chromatographic conditions

A RP-HPLC method was used because of its simplicity and suitability. Different types of columns, mobile phase, flow rate, and the influence of pH were examined during the development of a chromatographic method.

A Waters 515 HPLC along with a Sunfire C8 (4.6 x 150mm, 3.5 μ) column was used for the study and the mobile phase consisted of Acetonitrile: Water (0.1% formic acid) at a ratio of 30:70. The flow rate was maintained at 0.3 ml/ min and 20 μ l of the sample was injected using a rheodyne injector. An ultraviolet detector was used and the samples were analyzed at a wavelength of 265 nm. The method for estimation of IM was validated in terms of specificity, linearity and reproducibility.

5.14.4 Extraction of IM from plasma

Ninety microliters of drug-free plasma was spiked with 10 μ l of standard imatinib. The spiked sample was vortexed for 30 s followed by addition of 1 ml of methanol and re-vortexing for 3 min. The sample was centrifuged at 12, 000 rpm for 10 minutes at 4°C and an aliquot of 800 μ l from supernatant was evaporated in a turbovap for 20 min, it is then reconstituted with 200 μ l of cold acetonitrile. From this an aliquot of 20 μ l was injected into HPLC for quantification [125].

Extraction efficiency

Extraction efficiency from the rat plasma was determined by comparing the responses obtained from extracted sample spiked with known amount of IM with the extracted blank sample. The recovery was evaluated at three different concentrations of analyte quality control standards area and was compared against the mean area of respective un-extracted quality control standards area. The mean recovery for IM was calculated.

Recovery

The recoveries were assessed by comparing the peak area of IM extracted from QC samples to those of the same concentration of IM spiked into blank-plasma post-extracts were calculated.

5.14.5 Validation of the analytical method

The method was validated according to guidelines set on the International conference on Harmonization (ICH) for the validation of analytical procedure. The developed method was validated in terms of specificity, linearity, accuracy, precision, limit of detection and limit of quantification.

Specificity

Specificity is the ability of a method to discriminate between the intended analyte and other components in the sample. A method is said to be specific when it shows a peak corresponding to single analyte in the presence of the interferences. It was carried out by comparing the standard retention time spectra and the sample retention time spectra.

Linearity

A series of concentrations (5, 10, 20, 40, 60, 80, 100 µg/ml) were prepared from the stock solution and their respective peak areas were plotted. A standard curve of peak area vs concentration was obtained and the regression equations were calculated. For plasma studies, 90µl of blank plasma was spiked with 10µl of the standard stock solution to obtain concentrations in the range of 250 ng/ml-16 µg/ml.

Accuracy

Samples of concentrations 10, 20 and 40 µg/ml for analysis of aqueous samples and 250, 1000 and 2000 ng/ml for plasma studies were analyzed in 5-folds in three separate analytical runs for evaluation of accuracy and interday/intraday precision. The accuracy was calculated by dividing the observed concentration and the nominal concentration and multiplying by 100%.

$$\% \text{ Nominal} = (\text{measured concentration} / \text{Actual concentration}) \times 100$$

Precision

Precision was measured by interday (on three consecutive days) and intraday variation by analysing 6 replicates over 3 different concentrations of IM. The precision was obtained from response of each of these solutions and by calculating percentage relative standard deviation (% RSD).

$$\%RSD = (SD/ \text{mean}) \times 100$$

Limit of Detection and Limit of Quantification (LOD and LOQ)

LOD is the lowest amount of analyte in a sample that can be detected but not necessarily quantitated under the stated experimental conditions. On the other hand, LOQ is the lowest amount of analyte in a sample that may be determined with acceptable accuracy and precision. LOD and LOQ values were determined from the regression curve. The residual standard deviation of a regression line or the standard deviation of y-intercepts of regression lines were used as the standard deviation. Based on the standard deviation of the response and the slope LOD and LOQ are calculated.

$$LOD = 3.3 \sigma/s$$

$$LQD = 10 \sigma/s$$

Where σ is the standard deviation of response and s is the slope of the calibration curve [127].

5.14.6 Stability

Stability of IM was investigated under a variety of storage and process conditions viz., rat plasma and deproteinized rat plasma samples at room temperature, at -20°C and freeze thaw cycles [125].

5.15 SOLUBILITY OF IM IN VARIOUS LIPIDS

The lipids used in the present study were myristic acid, palmitic acid, stearic acid, behenic acid, glyceryl palmitostearate, Precirol ATO 5[®], glyceryl monostearate, Geleol mono and diglycerides[®], Compritol 888 ATO[®], trimyristin, tripalmitin, tristearin, Sterotex HM[®], Sterotex NF[®], cocoa butter, Hydrokote M[®], Hydrokote 112[®], Captex 70[®], Gelucire 44/14[®] and Gelucire 33/01[®]. To test the solubility of IM in these lipids, 5 mg of IM was added to 1 g of lipid and heated to a temperature above 10°C of its melting point in a test tube. To check the maximum amount of IM that could be solubilised in 1 gm of lipid, IM was slowly added in increments of 1 mg until no more IM could be dissolved [115].

To confirm the solubility of IM in various lipids, the endothermic melting temperature of IM, bulk lipids and mixture of IM and lipids was measured in a differential scanning calorimeter (Universal V4.7A TA instruments). Briefly, 10 mg of the sample was placed on an aluminium pan and scanned between 25°C and 300°C at a range of 5°C/ min under nitrogen gas [165].

5.16 CALCULATION OF TOTAL SOLUBILITY PARAMETERS, POLARITY OF IM AND LIPIDS

Total solubility parameter (δ_{total}) and polarity of a substance (X_p) for IM and lipids were calculated using equation 1 and equation 2 respectively [113,146].

$$\delta_{total}^2 = \delta_d^2 + \delta_p^2 + \delta_h^2 \text{ ----- Equation (1)}$$

$$X_p = 1 - \frac{\delta_d^2}{\delta_{total}^2} \text{ ----- Equation (2)}$$

where,

δ_{total} = total solubility parameter,

δ_d = contribution from dispersion forces ($\delta_d = \frac{\sum F_{di}}{V}$),

δ_p = contribution from polar force ($\delta_p = \frac{\sqrt{\sum F_{pi}^2}}{V}$),

δ_h = contribution of hydrogen bonding ($\delta_h = \sqrt{\frac{\sum E_{hi}}{V}}$),

F_{di} = molar attraction constant due to dispersion component,

F_{pi} = molar attraction constant due to polar component,

E_{hi} = hydrogen bonding energy,

V = molar volume,

X_p = polarity.

5.17 IDENTIFICATION OF DESCRIPTORS AND DEVELOPMENT OF QUANTITATIVE STRUCTURE SOLUBILITY RELATIONSHIP (QSSR) MODEL

Various descriptors (molecular and physicochemical) of the lipids and their statistical relationship with respect to solubilisation of IM were obtained using QikProp, Schrodinger [135][166]. Initially, the structures of the individual lipids were sketched and cleaned up in Maestro by providing the SDF files of the lipids as input. The structures were processed using LigPrep to obtain three dimensional structures and their energy was minimised using OPLS-2005. The descriptors of the lipids were generated using QikProp, Schrodinger. Due to small data sets, multiple linear regression (MLR) was used over PCA (principal component analysis) and PLS (partial least square) to build a statistical model which enabled the prediction of solubility of IM using these descriptors. For the development of the model, the lipids were initially divided into a training set containing 6 lipids (67% of the dataset) and a test set of 3 lipids (33 % of the dataset). The training set of lipids were used initially to develop an MLR model (Strike module, Schrodinger) to examine and correlate the influence of the descriptors to solubilise IM. The descriptors which lowered the the R^2 (squared correlation coefficient) and Q^2 (cross validated R^2) were removed. The solubility of IM in lipid as % w/w was used as response and three separate MLR models were constructed by varying the number of subsets. The ability of these models to predict the solubility of IM was then verified using the test set of lipids. The solubility equations generated for

each model were also validated for their robustness using leave one out model (LOO). Statistically important parameters like R^2 ; RMSE (root mean square error); F (Fisher's value); P (Probability); Q^2 ; R^2_m (multiple correlation coefficient); R^2_{pred} (predictive correlation coefficient) were calculated to validate the models.

5.18 DETERMINATION OF PARTITIONING COEFFICIENT OF IMATINIB MESYLATE IN DIFFERENT LIPIDS AND WATER

In a typical partition experiment, 10 mg of IM was dispersed in a mixture of 1 ml of double distilled water and 1 g of molten lipid (maintained at a temperature 10°C above the melting point of the lipid). The mixture was shaken for 60 min at the same temperature and then kept at room temperature for 45 min to allow partitioning to reach equilibrium. The aqueous phase was separated and the amount of IM in the aqueous solution was quantified in a UV spectrophotometer at 256 nm. Partition coefficient was estimated by calculating the ratio between the amount of IM in lipid and amount of IM in the aqueous phase [142].

5.19 INFRARED (IR) ABSORPTION SPECTROSCOPY

The purity of the drug was determined by subjecting IM for IR analysis using Fourier Transform Infrared Spectroscopy (FT/IR 8400S CE) Shimadzu spectrophotometer). The samples were prepared as KBr pellet method. Drug and potassium bromide are mixed in the ratio of 1:100 and a pellet is formed by compressing at 8 ton/mm^2 pressure. The wavelength range was selected from $400 - 2000\text{ cm}^{-1}$ in Shimadzu FT-IR spectrophotometer. The IR spectrum of pure IM was compared with spectrum obtained from Indian Pharmacopoeia 2007.

Similarly IR spectrum was obtained for each individual lipid (stearic acid, palmitic acid, glyceryl palmitostearate, glyceryl monostearate and Geleol mono and di glycerides), QS and the physical mixture of IM and lipids [167].

5.20 CHEMICAL CONJUGATION OF LIPID WITH LIGANDS

The ligands (hyaluronic acid and vitamin B12) were chemically conjugated to stearic acid or stearyl amine using carbodiimide chemistry. Initially, 20 mg of stearic acid (or stearyl amine) and 30 mg 1-Ethyl-3-(3-dimethylaminopropyl) carbodiimide (EDC) was added to 5 ml of dimethyl formamide and allowed to react at room temperature for 1 hour. To this mixture, 30 mg of ligand (hyaluronic acid and vitamin B 12) and 0.5 ml pyridine were added and reacted overnight. Twenty ml of distilled water was added to the reaction mixture to precipitate the stearic acid-ligand conjugates like hyaluronic acid-stearic acid (HA-SA) and vitamin B12-stearic acid (B12-SA). The precipitate was dialysed against distilled water for 3 days using cellulose membrane (8000 molecular weight cut off) to remove the unreacted chemicals. Finally, the product was filtered using a 0.45 μm millipore filter and lyophilized [158,168].

5.21 PREPARATION OF IM LOADED SOLID LIPID NANOPARTICLES (SLNs)

IM loaded SLNs were prepared *via* a hot homogenisation method followed by ultrasonication. Briefly, the lipid was melted at a temperature above 5°C its melting point in a water bath. IM was added to the melted lipid to form a clear, homogeneous lipid phase. Simultaneously, an aqueous solution (10 ml) of QS preheated to as that of the lipid phase was dispersed in the lipid phase using a high shear homogeniser (Pro SC- 250). This pre-emulsion was sonicated in an ultrasonic homogeniser (Vibra cell, Sonics) at 40% amplitude and cooled in an ice bath to form IM loaded SLNs. Different batches of SLNs were prepared by changing the lipids, amount of QS, parameters of high speed homogenisation and probe sonication [60,169].

5.22 PREPARATION OF SLNs ADSORBED WITH HYALURONIC ACID

Hyaluronic acid adsorbed SLNs were prepared by electrostatic attraction. Briefly, 1 ml of the dispersion was slowly added under vigorous stirring at 5,000 rpm to a hyaluronic acid solution at a concentration of 0.05%, 0.10%, 0.15% or 0.20% w/v. The concentration of hyaluronic acid, the mass ratio of hyaluronic acid to SLNs, the adding rate and the stirring rate were investigated to obtain the optimum formulation [58,82].

5.23 PREPARATION OF SLNs CONJUGATED WITH LIGANDS

For the preparation of SLNs conjugated with ligands like hyaluronic acid and vitamin B 12, 50 mg the corresponding conjugates of stearic acid, HAJ-SA and B12-SA were added to the lipid phase during the preparation of SLNs.

5.24 FREEZE DRYING

The formulations were freeze-dried using Lyodel freeze drier at a temperature and pressure of -30 °C and -1 mbar, respectively, until the product was dried [78,170]. The freeze-dried powder was used for differential scanning measurements and nuclear magnetic resonance (NMR) spectroscopy.

5.25 NMR SPECTROSCOPY

¹H NMR spectrum was used to analyze the synthesized stearic acid- ligand conjugates. The samples were measured at 298K with about CDCl₃ solution using a NMR Spectrometer (AC-80, Bruker Biospin, Germany) [171].

5.26 DETERMINATION OF PARTICLE SIZE AND POLY DISPERSITY INDEX (PDI)

The average particle size and PDI of the SLNs was measured by photon correlation spectroscopy using Malvern Zetasizer (Nano ZS90, Malvern Instruments) at 25°C [42,172].

5.27 DETERMINATION OF ZETA POTENTIAL

The zeta potential of the formulations was measured using Malvern Zetasizer (Nano ZS90, Malvern Instruments). The samples were placed in a glass cuvette (at 25°C) and a Zeta dip cell was used to find out the potential. The samples were diluted suitably using deionised water [173].

5.28 TRANSMISSION ELECTRON MICROSCOPY

The sample was cast on top of a carbon coated copper grid and the grid was air dried at room temperature. The particle shape and morphology were visualized at a voltage of 80 kV. The images were observed at a magnification value of 50,000 X [174].

5.29 ATOMIC FORCE MICROSCOPY

The sample was adsorbed on the surface of silicon wafer and allowed to dry at room temperature. The samples were examined using Multimode Scanning probe microscope (NTMDT, NTEGRA prima, Russia) in semi-contact mode with a force constant range of 0.35- 6.06 N/m and a resonating frequency range of 47-150 KHz. The phase image and topology image were used to determine the morphology of SLN [175].

5.30 ENTRAPMENT EFFICIENCY

To calculate encapsulation efficiency, 2 ml of the formulation was centrifuged at 20,000 rpm for 45 min at 10 °C and the supernatant was analysed for free drug concentration using HPLC [176]. Blank SLNs were used as a control. Encapsulation efficiency was calculated using the following equation:

$$\text{Encapsulation efficiency (\%)} = \frac{\text{Amount of drug added during preparation} - \text{Amount of free drug in the supernatant} \times 100}{\text{Amount of drug added during preparation}}$$

5.31 *IN VITRO* DRUG RELEASE

In vitro drug release profiles of the unconjugated and conjugated SLNs and IM solubilised in phosphate buffered saline (PBS) pH 7.4 was studied by dialysis bag method. Briefly, 1 ml sample was loaded into a dialysis bag with a molecular weight cut off of 12,000- 14,000 Daltons and both its ends were sealed with clips. The dialysis bag was then placed in a beaker containing 50 ml of PBS maintained at $37\pm 1^{\circ}\text{C}$ under stirring at 50 rpm using a magnetic stirrer. At various time points, 2 ml of PBS was withdrawn from the beaker. Each withdrawal was compensated by addition of 2 ml of fresh PBS to the beaker. The drug content of the collected samples was determined by a suitable analytical method [177].

5.32 *IN VITRO* HAEMOLYSIS TEST

The *in vitro* haemolytic potential of QS, IM, unconjugated and conjugated SLNs was studied. Distilled water and normal saline served as positive and negative controls respectively. Rat blood was freshly collected in a microcentrifuge tube containing 50 μl of trisodium citrate and centrifuged at 1500 rpm for 15 min. After removing the supernatant containing plasma and cell debris, the pellet containing RBCs (red blood cells) was washed three times with normal saline. After the final wash, RBCs were collected by centrifugation at 1500 rpm. Purified RBCs were resuspended in normal saline to reach 2% (v/v) final concentration. The test samples were then added to test tubes containing 2.5 ml of 2% RBC suspension and incubated for 4 h at 37°C . After incubation, the samples were centrifuged at 2500 rpm for 10 min and the supernatants were observed for any indication of haemolysis [178].

5.33 *IN VITRO* CYTOTOXICITY STUDIES

In vitro cytotoxicity of IM, QS, unconjugated and conjugated SLNs against human breast cancer cells (MCF7) and its effect on the viability of murine macrophage cells (RAW 264.7) were tested by 3-[4,5-dimethylthiazol-2-yl]- 2,5-

diphenyl-tetrazoliumbromide (MTT) assay. Cell cultures were maintained in flasks containing Dulbecco's modified Eagle's medium supplemented with fetal bovine serum (FBS, 10%), glutamine (2 mM), streptomycin (200 µg/ml), gentamycin (400 µg/ml), penicillin (250 units/ml) and insulin (1 mg/ml) in a carbon dioxide incubator at 37°C with 5% CO₂.

Prior to the experiment, 5000 cells/well were seeded in 96 well plates and incubated overnight for their attachment. Then, the medium was replaced with fresh medium containing various concentrations of the samples. After 48 h of incubation, 10 µl of 5 mg/ml MTT stock was added to each well and incubated for 4 h. Then, 100 µl of DMSO was added to each well and the optical density was determined at 570 nm by a microplate reader. Cytotoxicity and cell viability in the presence of the samples (ISN3, B12-ISN, HAC-ISN, IGPN3, HAC-IGPN and IM) were compared with untreated control cells [174,179].

5.34 APOPTOSIS ANALYSIS

Apoptosis was measured by propidium iodide (PI) staining using MCF7 cell line. At > 90% confluence, cells (1×10^5 cells/ml) were seeded in six-well plates and incubated with free IM, IGPN3, and HA-IGPN with an equivalent concentration of IM of 10 µg/ml for 24 hours. Cells incubated with PBS served as control. The cells were washed with PBS fixed in methanol: acetic acid (3:1,v/v) for 10 min and stained with 50 µg/ml PI for 10 min. Finally, the nuclear morphology of apoptotic cells with fragmented/ condensed was examined under laser scanning confocal microscope (Nikon Ti series; Nikon Corporation, Tokyo, Japan) [180].

5.35 STERILITY TESTING

Sterility testing was performed against bacteria and fungi on ISN3, B12-ISN, HAC-ISN, IGPN3, HAC-IGPN and IM in pH 7.4 PBS using incubation method. A positive control containing the particular stain and negative control without addition of samples or strain were used also used. Thioglycollate

resazurine broth was used as the medium for the detection of bacteria and tripcase soy broth was used as medium for the detection of yeasts and fungi. *Staphylococcus aureus*, and *Aspergillus Niger* were used as the bacterial and fungal strains respectively. The respective samples (1 ml) were incubated for 14 days at $32.5 \pm 2.5^\circ\text{C}$ (thioglycollate resazurine medium) or at $22.5 \pm 2.5^\circ\text{C}$ (tripcase medium). The turbidity of the media was then observed over a basic period of 14 days in comparison to positive controls. The experiment was done two times.

5.36 *IN VIVO* PHARMACOKINETIC STUDIES

In vivo animal studies were carried out to estimate the amount of drug that has reached the systemic circulation and to find out the uptake of the drug into the lymphatic vessels. The studies were carried out according to the guidelines of the Council for the Purpose of Control and Supervision of Experiments on Animals, Ministry of Social Justice and Empowerment, Government of India and the study protocol was carried out after obtaining the consent from PSG Institutional Animal Ethical Committee with registration No: 158/99/CPCSEA. Female Wistar rats weighing 280 - 310 gms have been used for the study and were categorized into 6 groups with 5 rats in each group. The rats were fed ad libitum with rodents chow allowing free access to drinking water. Prior to the study the animals were kept for overnight fasting but were allowed free access to water.

5.36.1 Determination of pharmacokinetic parameters of Imatinib Mesylate in blood:

The formulations were administered subcutaneously and the blood was collected from the retro-orbital venous plexus puncture of the rat with the aid of capillary tubes at 0.5, 1, 2, 4, 8, 12, 24, 36 and 72 hours post dosing. The samples were collected in a microcentrifuge tube containing 50 μl of tri sodium citrate and centrifuged at 2,500 rpm for 10 minutes. The plasma is collected and stored at -20°C for further analysis [41].

Group 1, Group 2, Group 3, Group 4, Group 5 and Group 6 consisted of animals used for the estimation of pharmacokinetic parameters in blood which were administered with ISN3, B12-ISN, HAC-ISN, IGPN3, HAC-IGPN and IM in pH 7.4 PBS (IM-PBS) respectively. A dose equivalent to 15 mg/ kg was administered subcutaneously at the mammary tissue and the blood (0.3 ml) was collected by retro-orbital venous plexus puncture with the aid of capillary tube at 0.5, 1, 2, 4, 8, 12, 24, 36, 48, 60 and 72 hours post dose. The samples were collected in a microcentrifuge tube containing 50 µl of tri sodium citrate and centrifuged at 2,500 rpm for 10 minutes. The plasma samples were collected and stored at -80°C for quantitative analysis using HPLC.

5.36.2 Determination of drug concentration of Imatinib Mesylate in sentinel lymph nodes:

For the estimation of IM in the sentinel lymph nodes, three additional groups of rats containing 21 rats in each group were used. A dose equivalent to 15 mg/ kg of IM was administered subcutaneously at the mammary tissue and at each sampling point (2, 4, 8, 12, 24, 48 and 72 hrs), three rats from each group were euthanized. Thereafter, two superficial lymph nodes, namely subiliac lymph node lying in the fold of thigh musculature adjacent to the ileac artery and popliteal lymph node lying near biceps femoris in the hind limb were located and harvested. The selection of lymph nodes was decided on the basis of their anatomical vicinity to the site of formulation administration. Lymph nodes collected at each time point were pooled separately, weighed, dipped in PBS and homogenised. IM was extracted from the lymph homogenate and quantified via HPLC. The pharmacokinetic parameters were calculated using WinNonlin (6.1; Phrsight, Mountain View, CA) [181].

5.37 STABILITY STUDIES AS PER ICH GUIDELINES

Stability of formulations during storage conditions includes preservation of the initial particle size, prevention of degradation reactions and prevention of drug leakage from the lipid matrix.

Stability studies were performed for the formulations, ISN3, HAC-ISN, B12-ISN, IGPN3, HAC-IGPN and B12-IGPN. The study was carried out as per the ICH guidelines, where in which, the samples were stored in room temperature (25 to 27°C) and in refrigerator (3 to 5°C) over a period of 12 months. The appearance of the formulation, particle size, zeta potential and entrapment efficiency were measured for every 3 months [164].

5.38 STATISTICAL ANALYSIS

Statistical analysis was carried out with the help of GraphPad Prism (version 5). Results are expressed as mean \pm standard deviation (three independent values of the same formulation). Statistical significance was determined for *in vitro* release data by two-way analysis of variance (ANOVA). Bonferroni posttest was also used to compare the p values of each column at various individual time points. Student's t-test was used to carry out the statistical analysis for *in vivo* animal studies and for finding out a significant relationship between concentration of lipid and size. In all cases, p value <0.05 was considered to be statistically significant.

Results & Analysis

6. RESULTS AND ANALYSIS

6.1 DETERMINATION OF LAMBDA MAX (λ_{\max}) OF IMATINIB MESYLATE USING UV SPECTROPHOTOMETER

The wavelength at which maximum amount of radiation absorbs is called λ_{\max} of the compound and for IM maximum absorption was observed at 256 nm as shown in Figure 11.

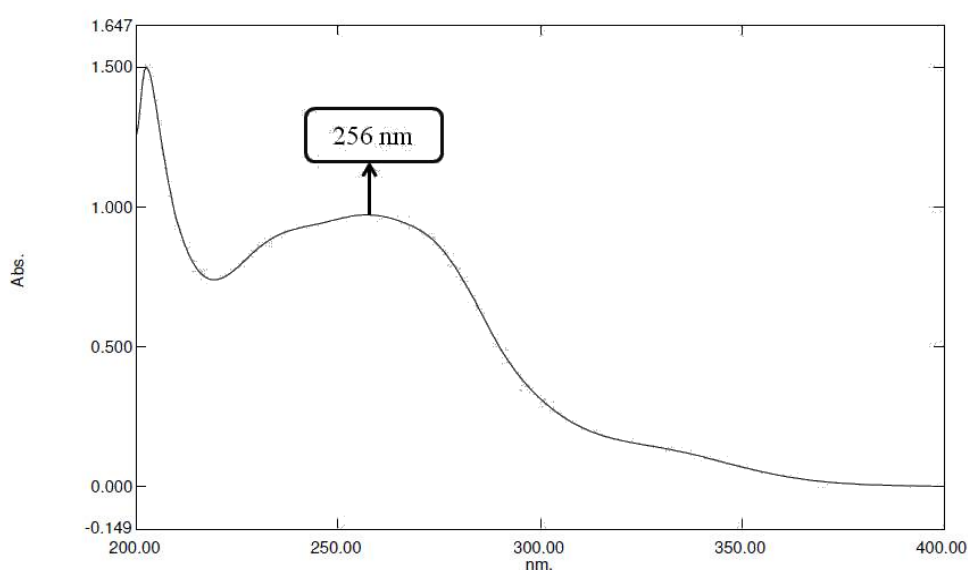


Figure 11. Wavelength of maximum absorbance for IM using UV spectrophotometer

6.2 CONSTRUCTION OF CALIBRATION CURVE FOR IMATINIB MESYLATE USING UV SPECTROPHOTOMETER AT 256 nm

Standard curve of IM was plotted using UV spectrophotometer and the corresponding absorbance at 256 nm was determined for various concentrations ranging from 4 to 18 mcg/ml. The absorbance values corresponding to the concentrations are shown in Table 1 and the graph obtained by plotting absorbance vs. concentration is shown in Figure 12.

Table 1. Calibration curve data for IM by UV spectroscopy

S No	CONCENTRATION (mcg/ml)	ABSORBANCE (256 nm)
1	0	0.000
2	4	0.233
3	6	0.336
4	8	0.430
5	10	0.559
6	12	0.660
7	16	0.871
8	18	0.980

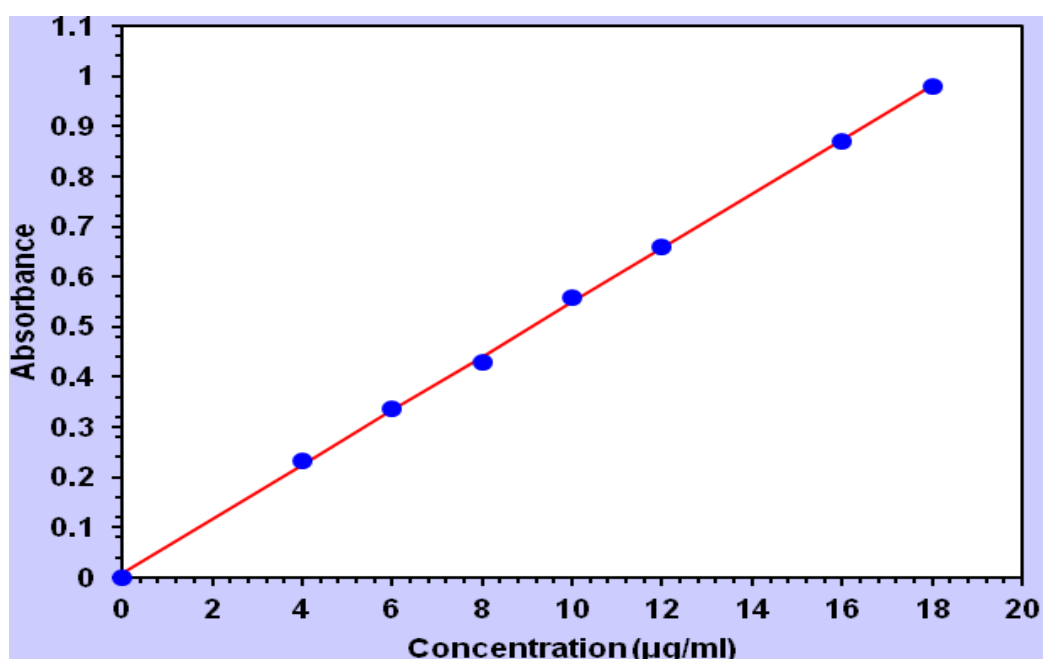


Figure 12. Calibration curve for the estimation of IM by UV spectroscopy

6.3 ANALYTICAL METHOD DEVELOPMENT

6.3.1 Optimisation of process parameters

A RP-HPLC method was developed for the estimation of IM in aqueous and plasma samples using a UV detector. The wavelength selected for the detection of IM was 256 nm. The chromatographic conditions were optimized to provide excellent performance for the assay of IM within a short time using a

simple mobile phase and appropriate flow rate. The selection of mobile phase was based upon the polarity of the drug. Different trails were performed by changing the columns, mobile phase composition, pH, flow rate and the chromatographic conditions were fixed. The conditions mentioned in Table 2 were optimised for the estimation of IM.

Table 2. Optimised chromatographic conditions for HPLC

PARAMETER	FIXED CONDITION
Stationary phase	Sunfire C8 (4.6 x 150mm, 3.5 μ
Mobile phase	Acetonitrile: Water (0.1 % formic acid) pH- 3.4
Mobile phase ratio	Gradient run, (30:70 v/v)
Detection wavelength	256 nm
Flow rate	0.3 ml/min
Sample volume	20 μ l
Needle wash	Water HPLC grade
Column temp	25°C

The method was validated as per ICH guidelines by using various parameters to ensure the accomplishment of its application.

6.3.2 Method validation

The optimized method was validated of in terms of specificity, linearity, accuracy, precision, specificity, limit of detection, limit of quantification as per ICH guidelines.

Specificity

A good specificity was observed for the developed method where a good separation was observed without any additional peaks. The representative chromatograms of pure sample of IM, IM estimated in aqueous and IM in rat plasma is mentioned in Figure 13.

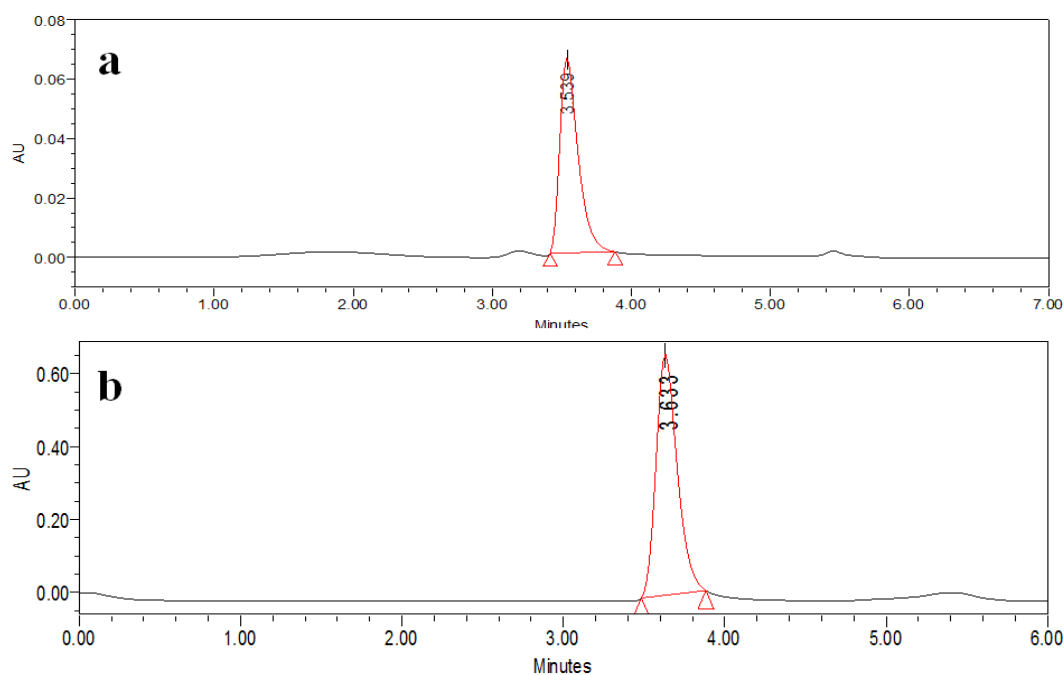


Figure 13. Representative chromatogram of IM in aqueous sample (a) and rat plasma (b)

The calibration curve for IM in the aqueous and plasma samples was constructed by plotting a graph between peak area versus concentration and the corresponding regression equations were also calculated. The corresponding peak areas for different concentrations for aqueous and plasma samples were shown in Table 3 and Table 4 respectively. The calibration curve obtained by plotting peak area vs. concentration in aqueous and plasma samples was shown in Figure 14 and Figure 15 respectively. A correlation coefficient (r^2) of 0.9998 and 0.9992 was observed for the calibration curves plotted in aqueous and plasma samples respectively.

Table 3. Calibration curve data for IM in aqueous samples

S No	Nominal concentration (mcg)	Peak area
1.	5.000	821637.57
2.	10.000	1612348.54
3.	20.000	3217510.85
4.	40.000	6116660.56
5.	60.000	9091352.13
6.	80.000	12155547.29
7.	100.000	14954444.83

Table 4. Calibration curve data for IM in plasma samples

S No	Nominal concentration (ng/ml)	Peak area
1.	250	15922.190
2.	500	19788.850
3.	1000	29600.888
4.	2000	52821.869
5.	4000	90336.032
6.	8000	171643.672
7.	16000	315960.481

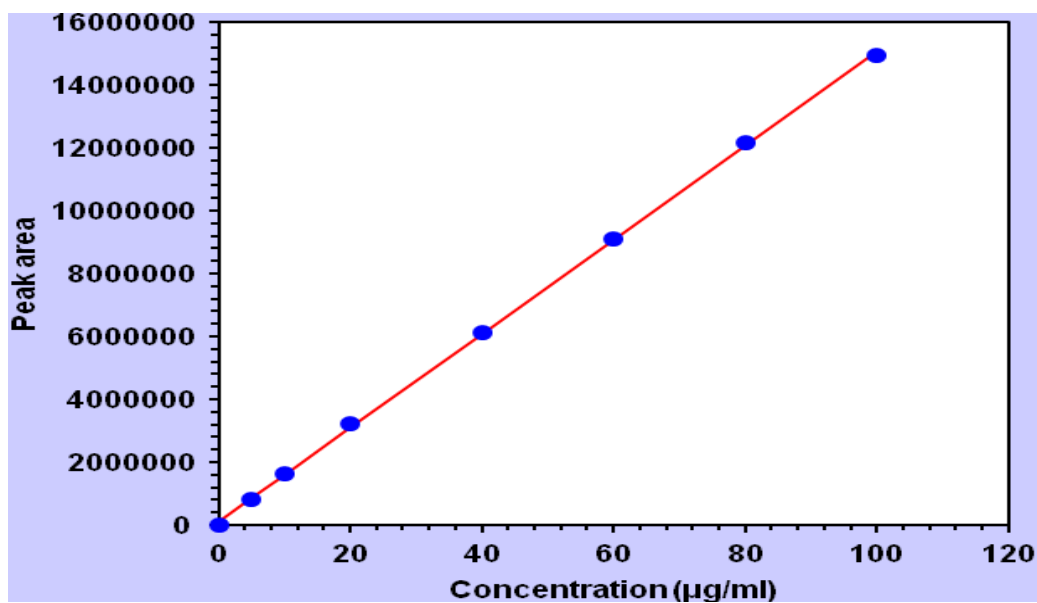


Figure 14. Calibration curve of IM in aqueous samples

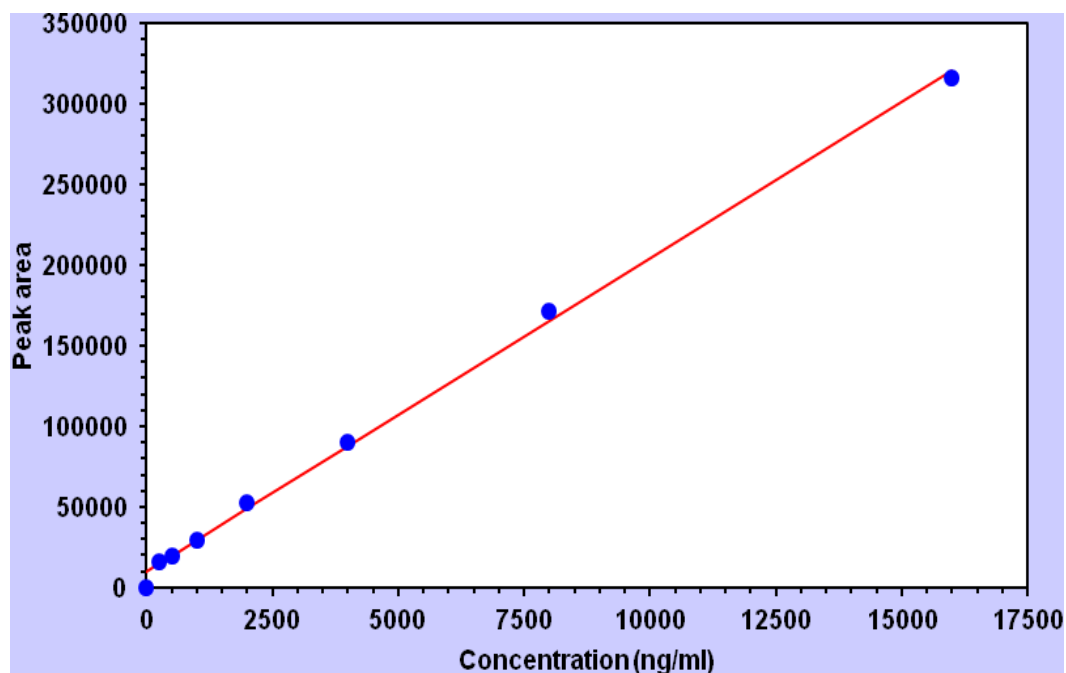


Figure 15. Calibration curve of IM in rat plasma.

Accuracy

The accuracy of the proposed method for IM in aqueous and plasma samples are mentioned in Table 5 and Table 6. A good accuracy was observed for the samples.

Table 5. Accuracy of IM in aqueous samples

Spiked concentration (µg/ml)	LQC		HQC	
	10		40	
S.NO	Calculated concentration (µg/ml)	Accuracy %	Calculated concentration (µg/mL)	Accuracy %
1	9.78	97.8	38.92	97.3
2	9.63	96.3	39.21	98.02
3	9.58	95.8	39.68	99.2
4	9.8.7	98.7	39.98	99.5
5	10.15	101.4	40.14	100.35
Mean	-	97.5	-	98.96
SD		2		1.28

Table 6. Accuracy of IM in plasma samples

S. No	Spiked concentration (ng/ml)	Measured concentration (ng/ml)	Accuracy (%) \pm SD
1.	250	251.8	100 \pm 2
2.	1000	1002.8	100.28 \pm 1.84
3.	2000	2012.4	100.29 \pm 0.92

Precision

To check the repeatability, different concentrations of IM were used. The response of each of these solutions was measured and percentage relative standard deviation (% RSD) was calculated. In aqueous samples, for intraday precision, three different concentrations were prepared (10, 20 and 40 μ g/ml) with five replicates of each, and their peak area was measured on the same day. Similarly, for interday precision, three different concentrations were prepared (25, 50 and 75 μ g/ml) with three replicates of each, and their corresponding peak area was measured on three subsequent days. The results were reported in terms of the relative standard deviation (RSD). The interday and intraday precision values are represented in Table 7. In plasma samples, for intra and interday precision 250, 1000 and 2000 μ g/ml concentrations were used and their corresponding peak areas were measured. The results were reported in terms of the relative standard deviation (RSD) in Table 7.

Table 7. Interday and intraday precision of IM in aqueous and plasma samples

IM	Aqueous		Plasma	
	Concentration (μ g/ml)	% RSD	Concentration (μ g/ml)	% RSD
Interday	10	2	250	1.60
	20	1.64	1000	1.84
	40	1.61	2000	0.92
Intraday	10	2	250	2.0
	20	1.91	1000	1.84
	40	1.29	2000	0.67

LOD and LOQ

The LOD and LOQ of the developed method for estimating IM in aqueous and plasma samples were established by injecting the low concentration of the standard solution using the developed RP-HPLC method. The LOD and LOQ in aqueous and plasma samples were found to be 14.5 ng/ml and 43.93 ng/ml respectively.

6.3.3 Stability

The results of stability studies of IM in rat plasma in different conditions are represented in Table 8. The results indicated that IM was stable at room temperature at least 24 h and in refrigerated conditions $\pm 4^{\circ}\text{C}$. Additionally, IM was also stable in deproteinized plasma, after freeze-thaw cycles and after storage at -20°C for 6 months.

Table 8. Stability of IM at different temperatures and after freeze thaw test

Duration	Samples	Concentration(ng/ml)			
		250		1000	
		%accuracy	%cv	%accuracy	%cv
24 hrs	Plasma $\pm 4^{\circ}\text{C}$	94.49	1.84	97.16	0.56
	Deproteinized samples	99.54	0.73	99.38	1.30
48 hrs	Plasma $\pm 4^{\circ}\text{C}$	95.23	2.12	96.55	3.14
6 months	At -20°C	97.32	2.46	98.64	1.22
	Samples from freeze-thaw testing	98.51	3.38	98.76	2.04

6.4 SCREENING OF LIPIDS FOR IM SOLUBILITY

The results of solubility study (Table 9) indicated that IM was soluble in only some of the lipids tested in the study. Formation of a clear lipid phase in the mixture of IM and the corresponding lipid indicate solubilisation of IM in the lipid. A clear lipid phase was observed when IM was dissolved in myristic acid, palmitic acid, stearic acid, glyceryl palmitostearate, Precirol 5 ATO, glyceryl

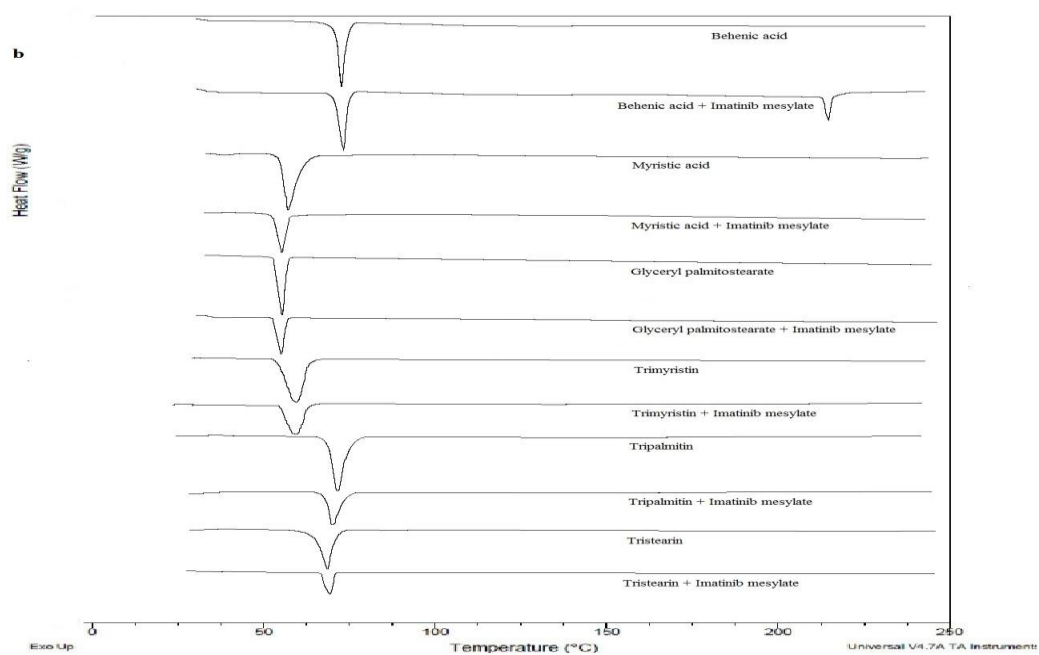
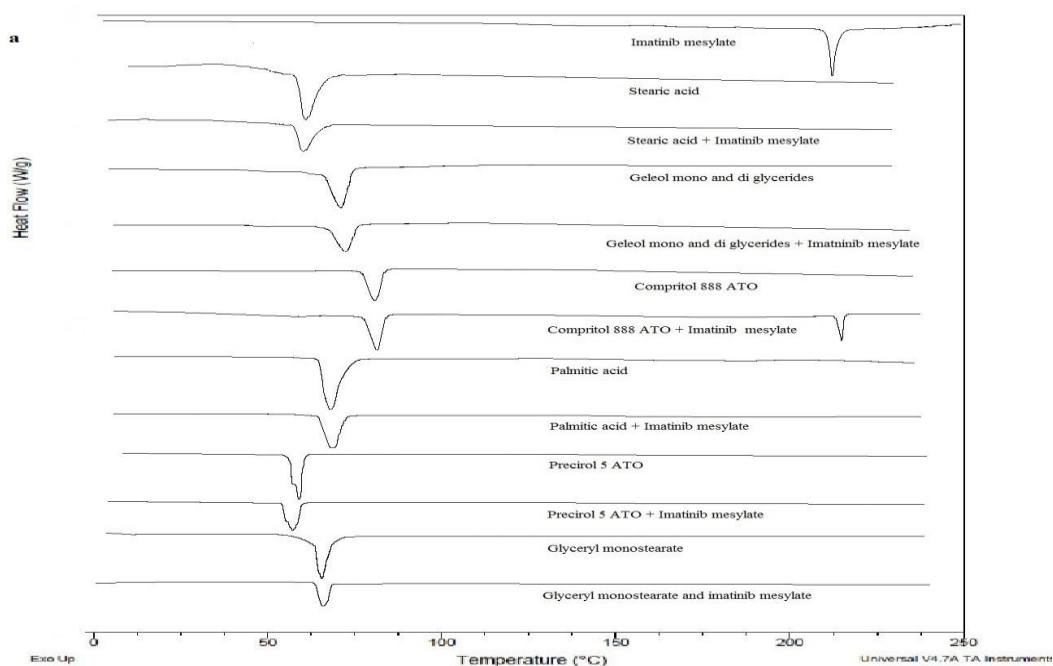
monostearate, Geleol mono and di glycerides, trimyristin, tripalmitin and tristearin. But, when behenic acid, Compritol 888 ATO, Sterotex HM, Sterotex NF, cocoa butter, Hydrokote M, Hydrokote 112, Captex 70, Gelucire 44/14 and Gelucire 33/01 were used to solubilise IM, a clear lipid phase was not observed which indicated the inability of those lipids to solubilise IM.

Table 9. Assessment of solubility of IM in various lipids

S No.	Name of the lipid	Solubility of IM
1	Myristic acid	Soluble
2	Palmitic acid	Soluble
3	Stearic acid	Soluble
4	Behenic acid	Soluble
5	Glyceryl palmitostearate	Soluble
6	Precirol ATO 5 [®]	Soluble
7	Glyceryl monostearate	Soluble
8	Geleol mono and di glycerides [®]	Soluble
9	Compritol 888 ATO [®]	Insoluble
10	Trimyristin	Soluble
11	Tripalmitin	Soluble
12	Tristearin	Soluble
13	Serotex HM [®] (hydrogenated soya bean seed oil)	Insoluble
14	Serotex NF [®] (hydrogenated cotton seed oil)	Insoluble
15	Cocoa butter	Insoluble
16	Hydrokote M [®] (hydrogenated palm kernel oil)	Insoluble
17	Hydrokote 112 [®] (hydrogenated palm kernel oil)	Insoluble
18	Captex 70 [®] (mixture of 70% medium chain triglycerides)	Insoluble
19	Gelucire 44/14 [®] (mixture of lauroyl macrogol-32 glycerides and lauroyl polyoxyl-32 glycerides)	Insoluble
20	Gelucire 33/01 [®] (mixture of glycerides and esters of fatty acids and poly ethylene glycol)	Insoluble

6.5 SOLID STATE CHARACTERISATION USING DIFFERENTIAL SCANNING CALORIMETRY

The results of the DSC were concomitant with the results obtained from the solubility studies. DSC thermogram of IM indicated a melting peak at 227.83°C corresponding to its melting point (Figure 16). When myristic acid, palmitic acid, stearic acid, glyceryl palmitostearate, Precirol 5 ATO[®], glyceryl monostearate, Geleol mono and di glycerides[®], trimyristin, tripalmitin and tristearin were used as the lipids carriers to solubilise IM, their corresponding DSC thermograms showed a melting peak corresponding only to the melting point of the lipid, but did not show the melting peak corresponding to IM at 227.83°C. This absence of melting peak of IM confirmed the ability of the above lipids to solubilise IM. However, thermograms of other lipids such as Compritol 888 ATO[®] in Figure 16 (a), behenic acid in Figure 16 (b), and, Sterotex HM[®], Sterotex NF[®], cocoa butter, Hydrokote M[®], Hydrokote 112[®], Captex 70[®], Gelucire 44/14[®] and Gelucire 33/01[®] in Figure 16 (c) showed the corresponding melting peaks of the lipids as well as IM confirming the inability of these lipids to solubilise IM. The melting points of the lipids used were mentioned in Table 10.



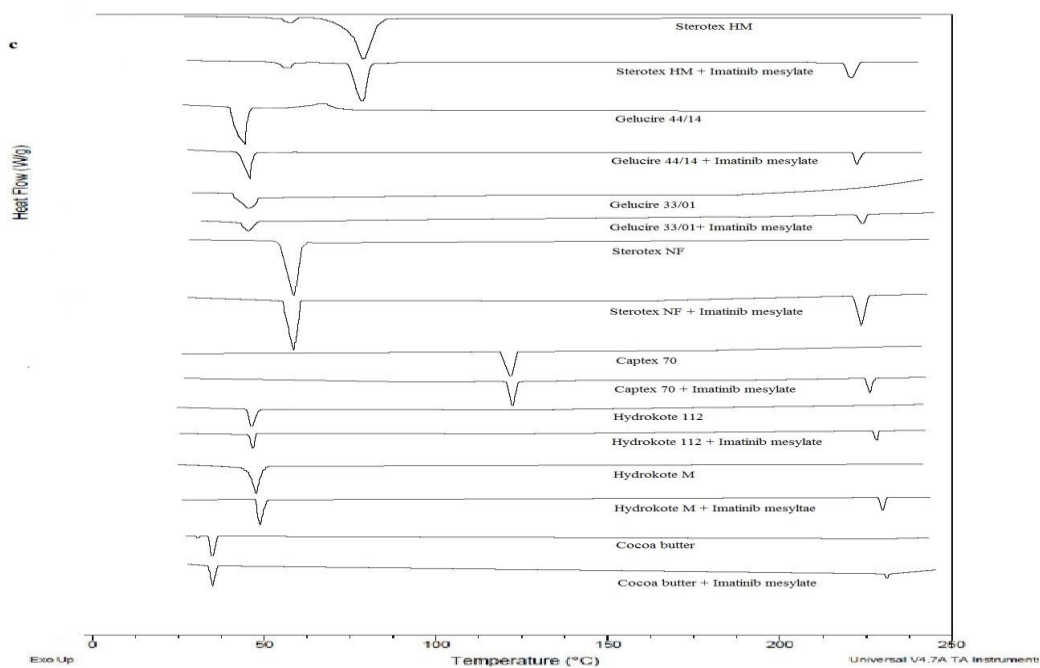


Figure 16. DSC thermograms of IM, bulk lipids and mixture of IM and lipid (a, b and c).

Table 10. Quantitative solubility of IM in the lipids and their melting points

S No.	Name of the lipid	Solubility (% w/w)	Melting point (°C)
1	Myristic acid	2.76 ± 0.11	57.8
2	Palmitic acid	2.10 ± 0.23	62.3
3	Stearic acid	1.94 ± 0.08	57.5
4	Behenic acid	0.01 ± 0.01	80.9
5	Glyceryl palmitostearate	2.93 ± 0.15	50.2
6	Precirol ATO 5	3.17 ± 0.19	51.5
7	Glyceryl monostearate	6.19 ± 0.22	63.7
8	Geleol mono and di glycerides	3.31 ± 0.27	67.5
9	Compritol 888 ATO	-	74.5
10	Trimyristin	0.97 ± 0.08	59.8
11	Tripalmitin	0.64 ± 0.12	68
12	Tristearin	0.45 ± 0.04	64.2
13	Sterotex HM (hydrogenated soya bean seed oil)	-	69.1
14	Sterotex NF (hydrogenated cotton seed oil)	-	66.2
15	Cocoa butter	-	38.7
16	Hydrokote M (hydrogenated palm kernel oil)	-	43.2
17	Hydrokote 112 (hydrogenated palm kernel oil)	-	44.4
18	Captex 70	-	126.5
19	Gelucire 44/14	-	43.6
20	Gelucire 33/01	-	54.7

6.6 QUANTIFICATION OF SOLUBILITY OF IMATINIB MESYLATE IN THE LIPIDS

The maximum solubility of IM in various lipids tested in the present study is listed in Table 10. Among the lipids used, glyceryl monostearate was the most efficient to solubilise IM (6.19 ± 0.22 %). On the other hand, tristearin showed the lowest ability to solubilise IM (0.45 ± 0.04 %). The decreasing order of the lipids with respect to solubilisation of IM is as follows, glyceryl monostearate > Geleol mono and di glycerides > Precerol ATO5 > glyceryl palmitostearate > myristic acid > palmitic acid > stearic acid > trimyristin > tripalmitin > tristearin > behenic acid.

6.7 ESTIMATION OF TOTAL SOLUBILITY PARAMETERS, POLARITY OF IMATINIB MESYLATE AND LIPIDS

The results of calculated solubility parameters and polarities of IM and the lipids are shown in Table 11. The solubility parameters of the tested lipids were found to be in the range of 17.34 to 23.06 MP. Amongst the lipids used, glyceryl palmitostearate and behenic acid were found to have the highest and lowest values respectively. The solubility parameter for IM was found to be 32.52 MPa^{1/2}. As Compritol 888 ATO, Sterotex HM, Sterotex NF, cocoa butter, Hydrokote M, Hydrokote 112, Captex 70, Gelucire 44/14 and Gelucire 33/01 are mixtures of mono, di and triglyceride derivatives of fatty acids and hydrogenated mixtures of fatty acids their solubility parameters were not estimated.

Table 11. Solubility parameter and polarity of IM and lipids along with their difference in solubility parameters.

S. No.	Name of the compound	δ_d	δ_p	δ_h	Solubility Parameter (MPa ^{1/2})	Difference of solubility parameter with IM (MPa ^{1/2})	Polarity
1	IM	26.14	13.46	13.86	32.52	-	0.35
2	Myristic acid	16.42	1.64	6.26	17.65	14.87	0.13
3	Palmitic acid	16.46	1.46	5.90	17.55	14.97	0.12
4	Stearic acid	16.49	1.31	5.59	17.46	15.06	0.11
5	Behenic acid	16.54	1.09	5.10	17.34	15.18	0.09
6	Glyceryl palmitostearate	17.52	2.82	13.87	23.06	9.46	0.32
7	Precirol ATO 5 [®]	--	--	--	--	--	--
8	Glyceryl monostearate	16.4	4.3	8.8	20.36	12.15	0.35
9	Geleol mono and di glycerides [®]	--	--	--	--	--	--
10	Compritol 888 ATO [®]	16.4	4.3	11.3	21.42	11.10	0.18
11	Trimyristin	16.69	1.11	5.24	17.53	14.99	0.09
12	Tripalmitin	16.70	0.98	4.94	17.44	15.08	0.08
13	Tristearin	16.70	0.88	4.68	17.37	15.15	0.08

6.8 IDENTIFICATION OF DESCRIPTORS AND DEVELOPMENT OF QUANTITATIVE STRUCTURE SOLUBILITY RELATIONSHIP MODEL

Figure 17 shows the three dimensional structures of the lipids that were developed using LigPrep. Although QikProp module of Schrodinger provided information pertaining to 51 different descriptors of the lipids used in the study, only those descriptors which showed good correlation with the solubility of IM ($r^2 > 0.6$) were used for the development of model (data not shown). Additionally, non-significant descriptors were removed to avoid distortions and to improve the efficiency of the model. Three separate models were constructed to identify the important descriptors which influenced the solubility of IM in the lipids viz., model 1, model 2 and model 3 by choosing one, two and three subsets respectively (Table 12). Among those, descriptors of the lipids which relate to its polar properties like the index of cohesive interaction in solids ($AC \times DN^{0.5}/SA$), estimated number of hydrogen bonds that would be accepted by the solute from water molecules in an aqueous solution (accptHB), estimated number of hydrogen bonds that would be donated by the solute to water molecules in an aqueous solution (donorHB) and solvent accessible surface area (SASA) were used for the model development and their corresponding descriptor values for the various lipids used in the study are mentioned in Table 13. The equations generated by the 3 models (viz., model 1, model 2 and model 3) using MLR are mentioned as equations 3, equation 4 and equation 5 respectively.

$$\%solubility\ of\ IM = 3.1163e^{-01} + 6.4972e^{+02} \frac{AC \times \sqrt{DN}}{SA} \quad \text{----- equation 3}$$

$$\%solubility\ of\ IM = 7.868e^{-01} + 1.707e^{+03} \frac{AC \times \sqrt{DN}}{SA} - 2.299e^{00} donorHB \quad \text{---- equation 4}$$

$$\%solubility\ of\ IM = 7.434e^{00} + 3.485e^{+03} \frac{AC \times \sqrt{DN}}{SA} - 1.2709e^{00} donorHB - 1.127e^{00} accptHB \quad \text{-----equation 5}$$

These equations can predict the solubility of IM in lipids and additionally describe the major descriptors which influenced the solubilisation of IM in the lipids. The statistical values pertaining to the model development is mentioned in Table 14.

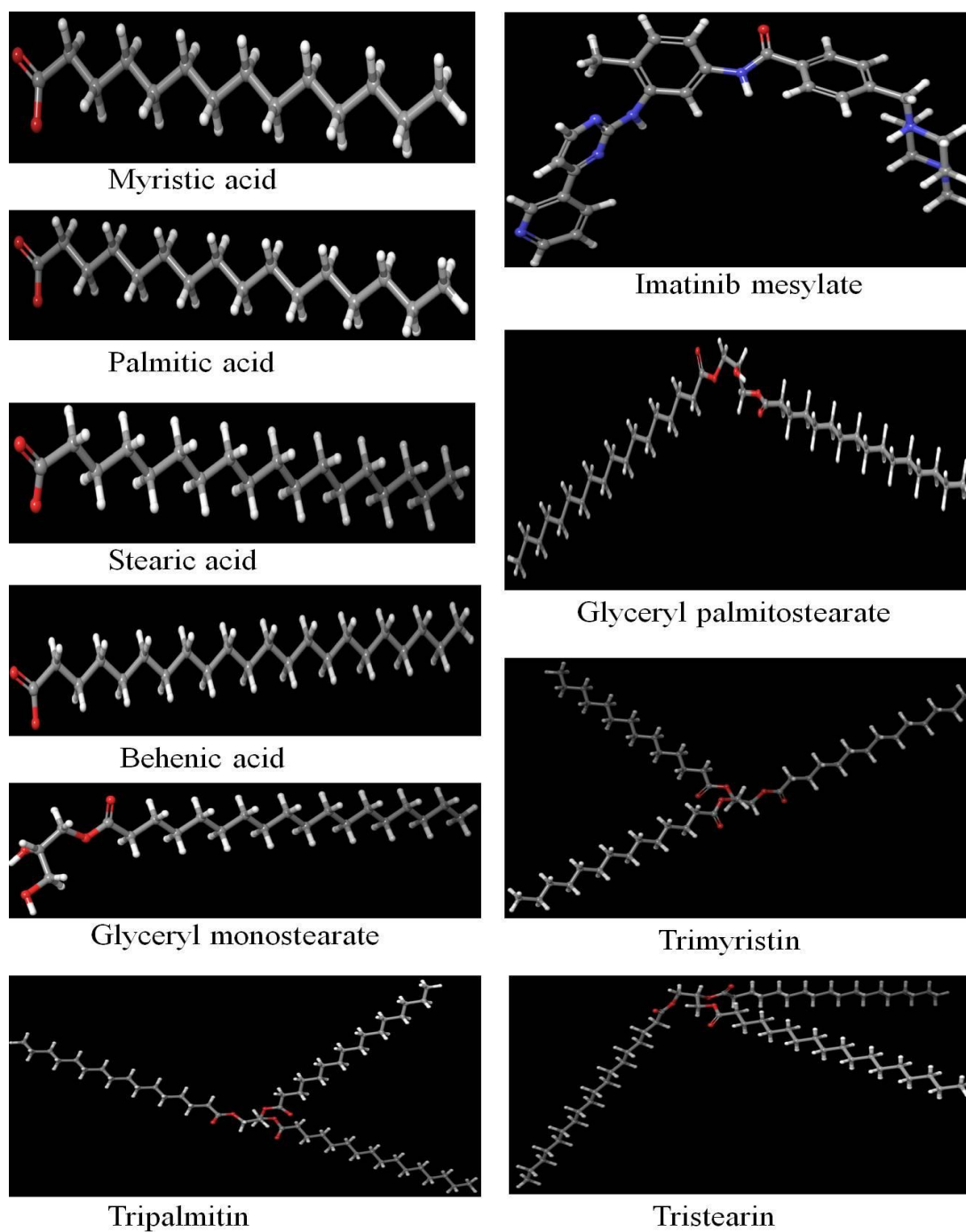


Figure 17. Three dimensional molecular structures of IM and lipids.

Table 12. Details of the three MLR models developed

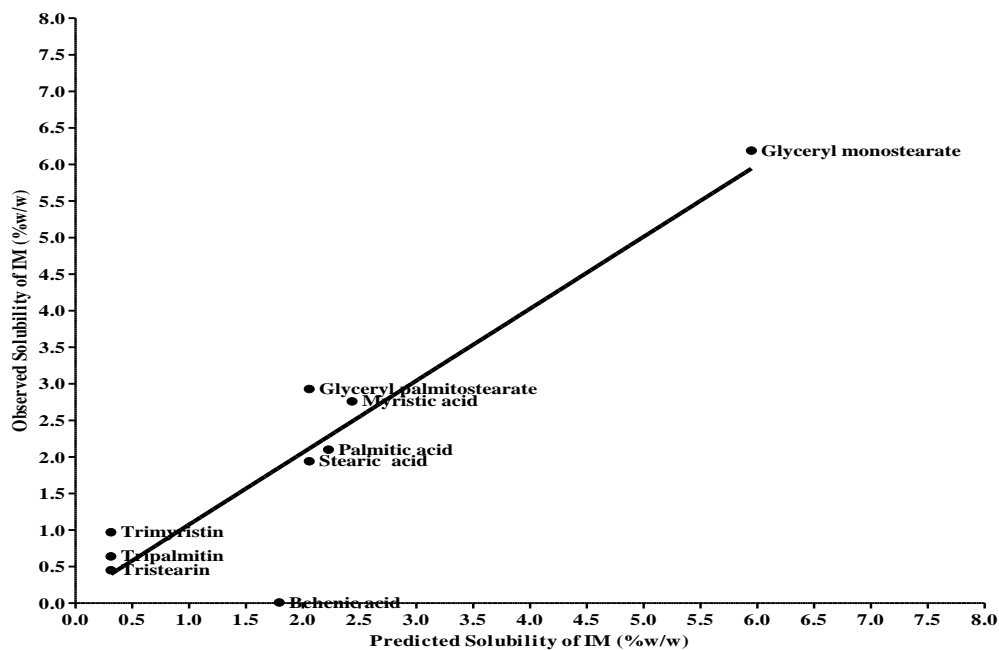
Model	Number of sub sets	Used descriptors	Observed descriptors
Model 1	1	AC×DN ^{0.5} /SA, accptHB, donorHB and SASA	AC×DN ^{0.5} /SA
Model 2	2	AC×DN ^{0.5} /SA, accptHB, donorHB and SASA	AC×DN ^{0.5} /SA and donorHB
Model 3	3	AC×DN ^{0.5} /SA, accptHB, donorHB and SASA	AC×DN ^{0.5} /SA, donorHB and accptHB

Table 13. Molecular and physicochemical descriptors of the lipids

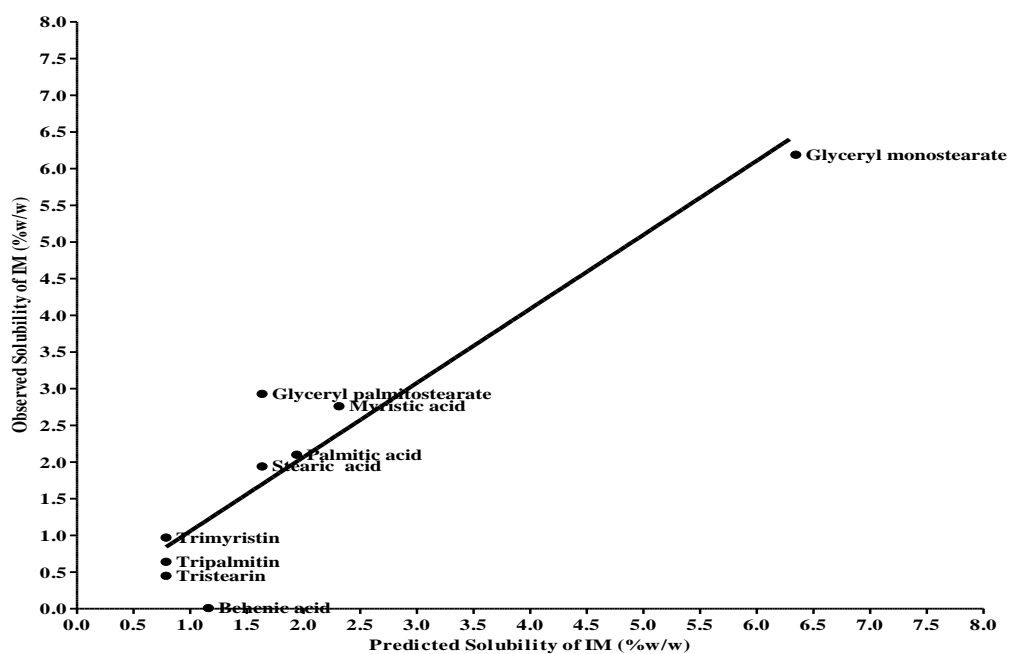
S No	Name of the lipid	AC×DN ^{0.5} /SA	accptHB	donorHB	SASA
1	Myristic acid	0.0032753	2	1	610.633
2	Palmitic acid	0.0029556	2	1	676.678
3	Stearic acid	0.0026928	2	1	742.716
4	Behenic acid	0.0022862	2	1	874.804
5	Glyceryl palmitostearate	0.0026928	2	1	742.716
6	Glyceryl monostearate	0.0086735	5.4	2	880.467
7	Trimyristin	0	6	0	1692.1
8	Tripalmitin	0	6	0	1889.22
9	Tristearin	0	6	0	2087.11

Table 14. Statistical results of the three QSSR models developed to predict solubility of IM

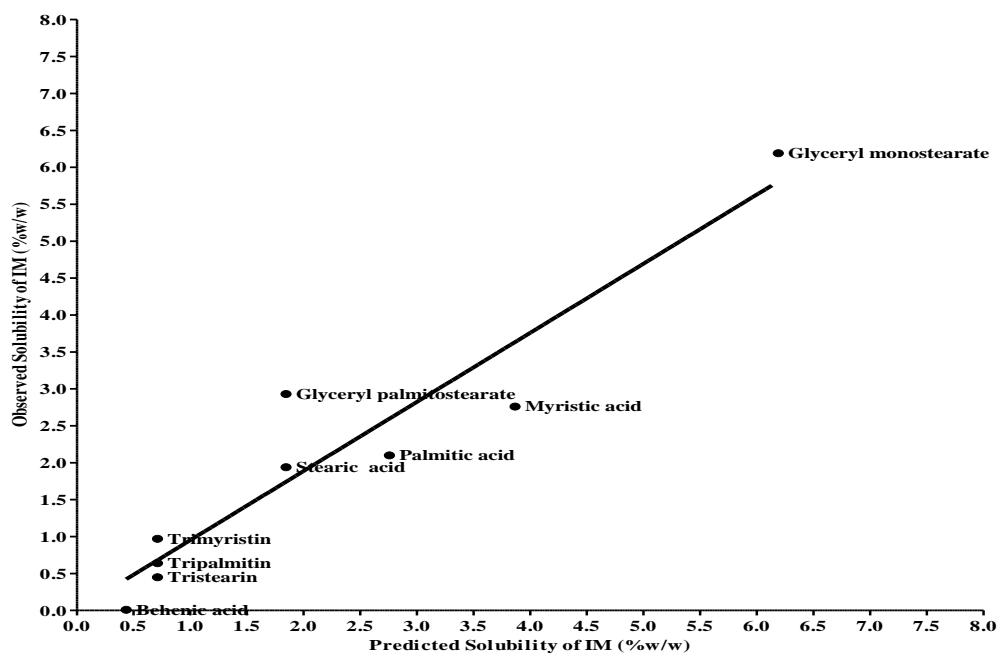
Factors	TRAINING SET					TEST SET			
	R ²	RMSE	F	P	Q ²	R ²	R ² M	R ² pred	RMSE
1	0.826	0.863	19.1	1.202e-02	0.65	0.949	0.936	0.912	0.275
2	0.876	0.730	10.6	4.369e-02	0.74	0.995	0.948	0.878	0.324
3	0.925	0.566	8.3	1.098e-01	0.63	0.917	0.895	0.525	0.642



(i)



(ii)



(iii)

Figure 18. Experimentally determined plot representing solubility of IM in lipids against predicted solubility of IM in lipids as observed in (i) model 1, (ii) model 2 and (iii) model 3.

6.9 DETERMINATION OF PARTITIONING COEFFICIENT OF IMATINIB MESYLATE IN DIFFERENT LIPIDS AND WATER

The highest partition for IM was observed towards glyceryl palmitostearate (0.39 ± 0.08). The order of partition of IM in the lipids was found to be descending as follows; glyceryl palmitostearate (0.39 ± 0.08) > Precirol ATO 5 (0.28 ± 0.03) > Geleol mono and di glycerides (0.26 ± 0.02) > glyceryl monostearate (0.33 ± 0.01) > stearic acid (0.22 ± 0.02) > palmitic acid (0.16 ± 0.01) > myristic acid (0.12 ± 0.01).

6.10 INFRARED (IR) ABSORPTION SPECTROSCOPY

The IR spectrum of pure IM in Figure 19 represents characteristic wave numbers at 1177 cm^{-1} , 1418 cm^{-1} , 1447 cm^{-1} , 1525 cm^{-1} , 2111 cm^{-1} and 3445 cm^{-1} . These wave numbers are compared with the IR obtained from standard pharmacopeia. The IR spectrum of QS was shown in Figure 20. It showed specific wave numbers at 1728 cm^{-1} and 3389 cm^{-1} corresponding to the ketone group and alcoholic $-\text{OH}$ groups present in the saponin. Additionally, strong bands were observed in the region of $1340\text{--}1450\text{ cm}^{-1}$ and 2940 cm^{-1} , which corresponds to the ketone and carboxylic acid groups present in the saponin. The IR spectrum corresponding to the lipids stearic acid, palmitic acid, glyceryl palmitostearate, glyceryl monostearate and geleol mono and diglycerides was shown in Figure 21, Figure 22, Figure 23, Figure 24 and Figure 25 respectively. The IR spectrum of stearic acid and palmitic acid prominently showed wave numbers in the regions of $2500\text{--}3000\text{ cm}^{-1}$ which correspond to carboxylic acid groups present in the fatty acids. The IR spectrum of glyceryl palmitostearate and glycerylmonostearate showed wave numbers in the regions of 1200 cm^{-1} and 1700 cm^{-1} representing the acetate and ester functional groups present in the monoglyceride derivatives.

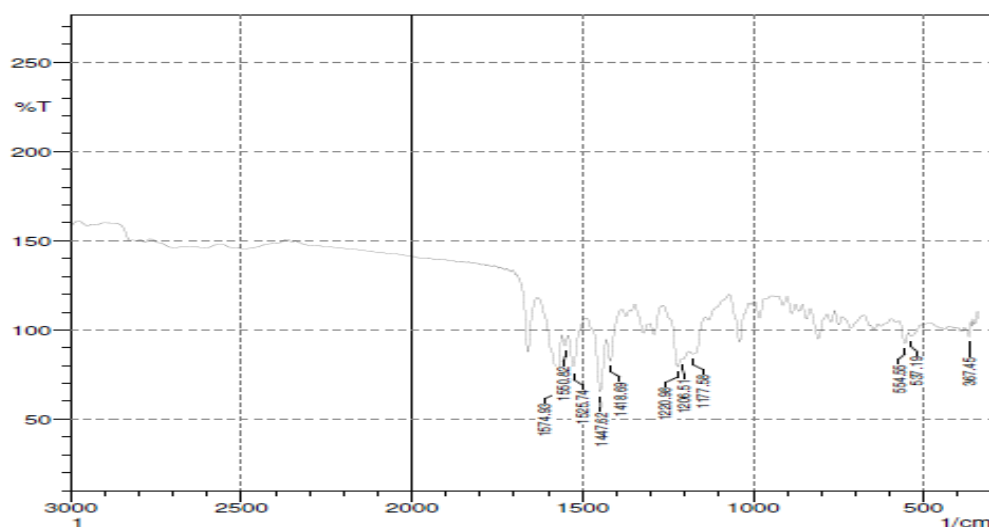


Figure 19. IR spectrum of IM: pure sample

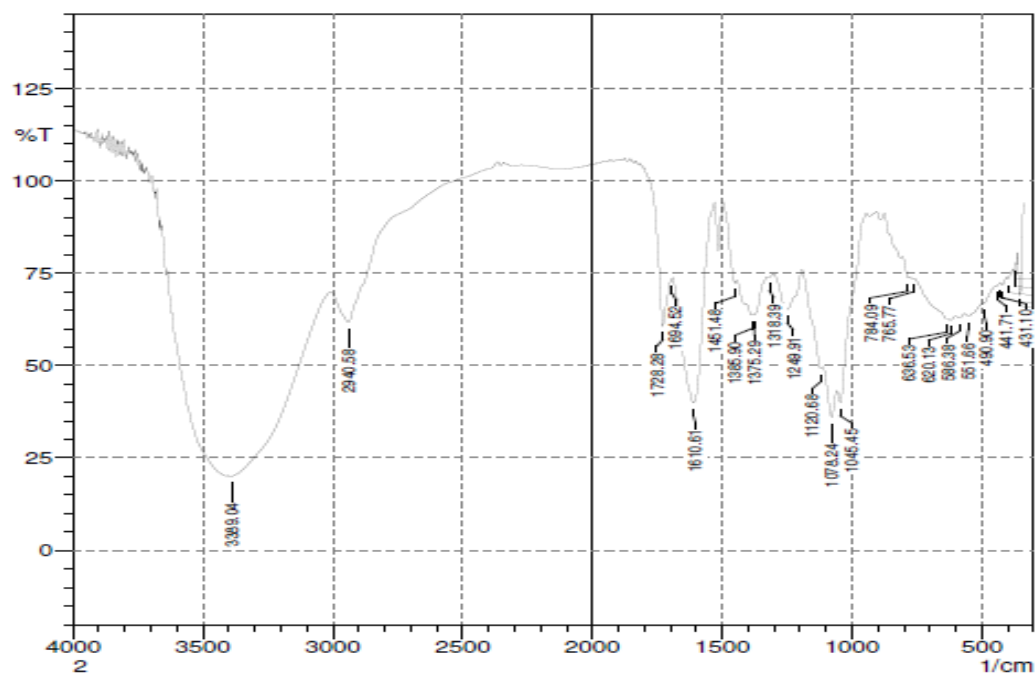


Figure 20. IR spectrum of QS: pure sample

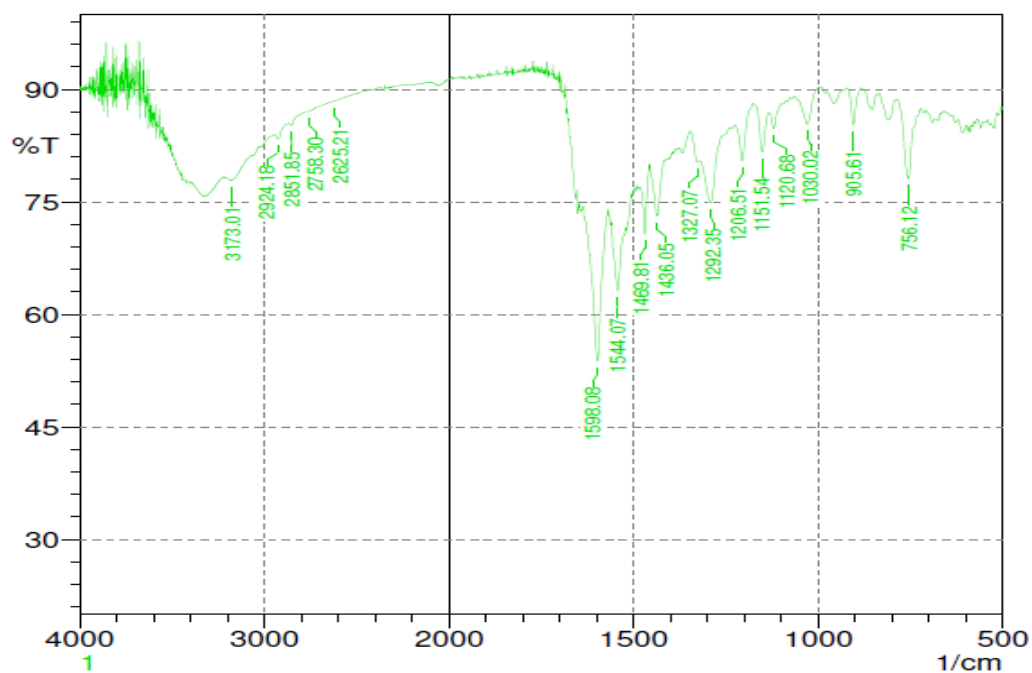


Figure 21. IR spectrum of stearic acid: pure sample

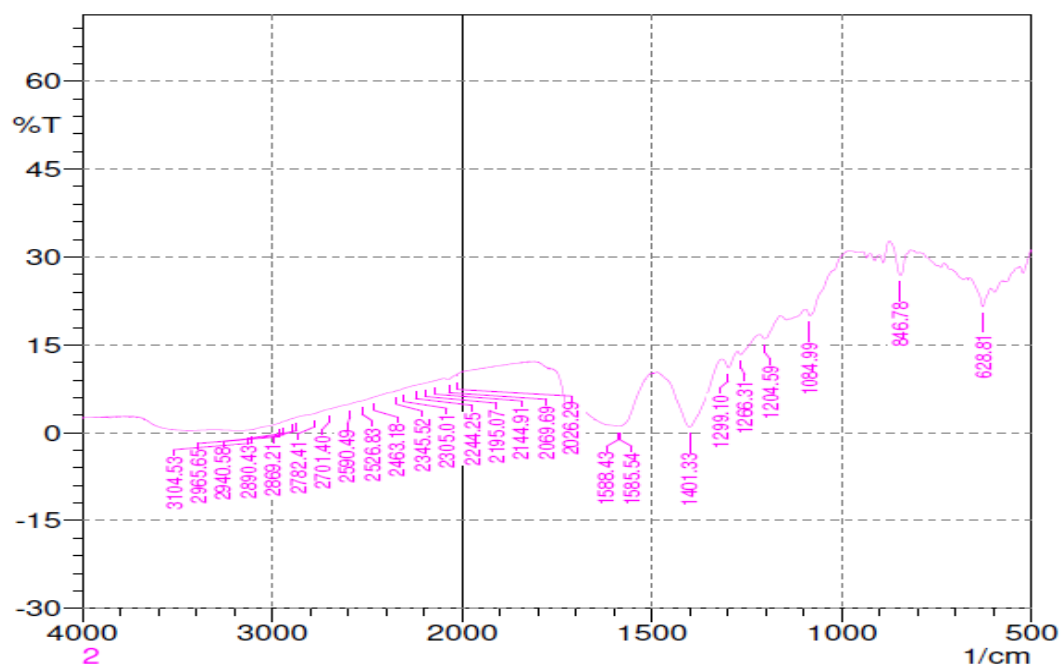


Figure 22. IR spectrum of palmitic acid: pure sample

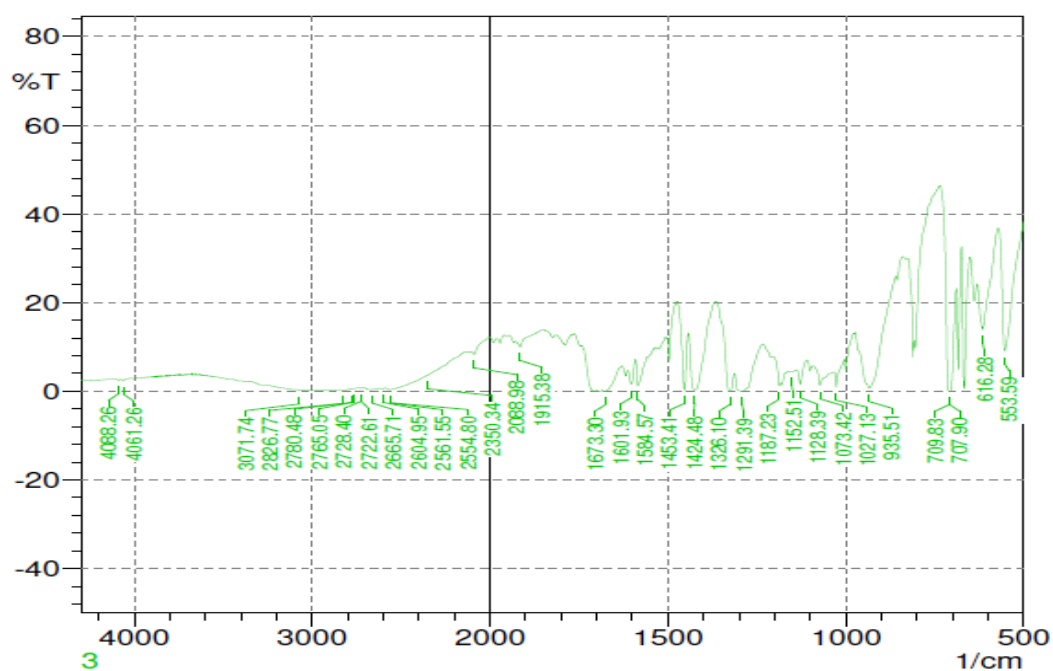


Figure 23. IR spectrum of glyceryl palmitostearate: pure sample

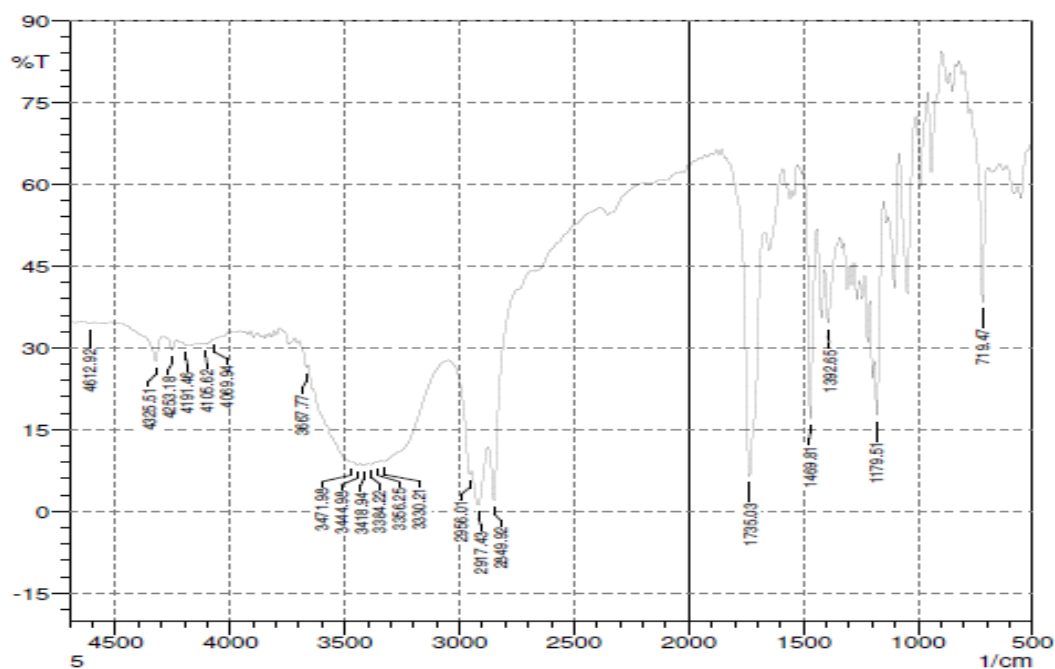


Figure 24. IR spectrum of glyceryl monostearate: pure sample

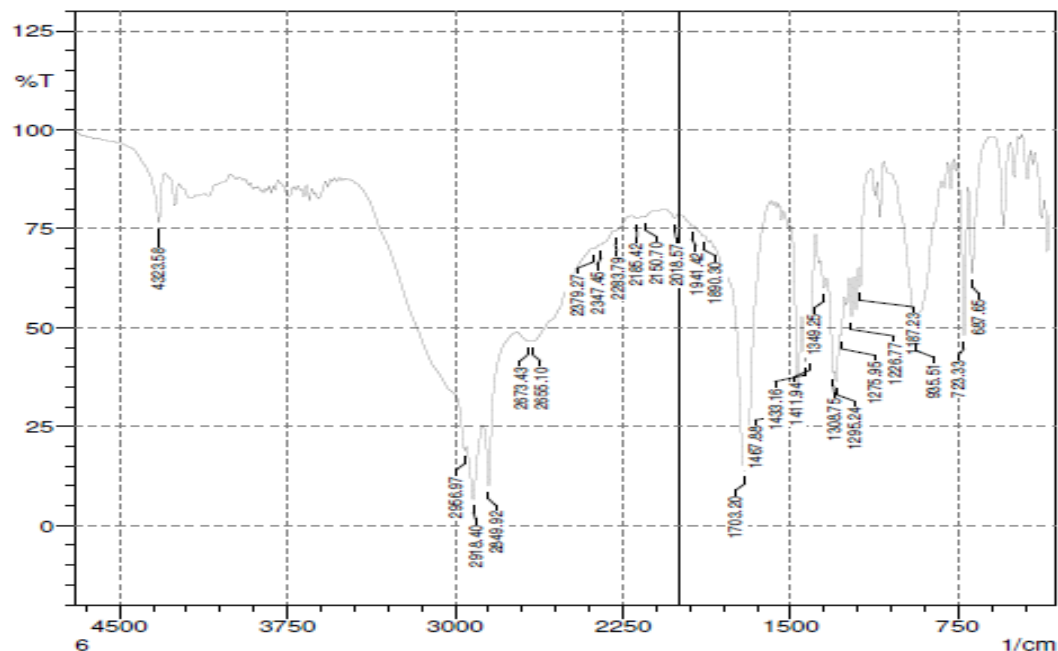


Figure 25. IR spectrum of Geleol mono and di glycerides: pure sample

IR SPECTRA OF THE PHYSICAL MIXTURES OF IMATINIB MESYLATE AND LIPIDS

The IR spectra of the physical mixtures of IM and corresponding lipids are shown in Figure 26 to Figure 30. Table 15 mentions the various functional groups pertaining to IM, lipids and their corresponding mixtures.

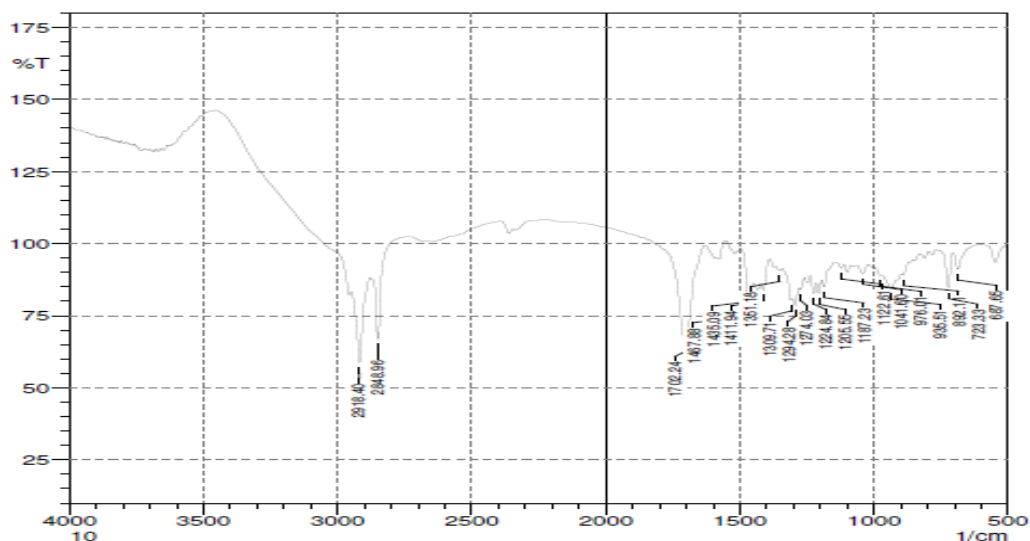


Figure 26. IR spectrum of physical mixture: IM, QS and stearic acid

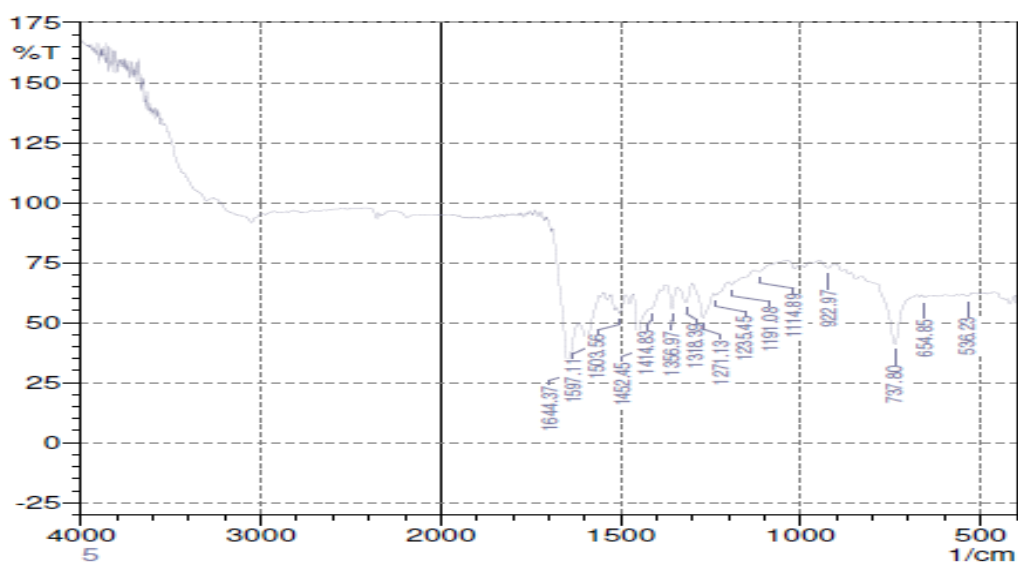


Figure 27. IR spectrum of physical mixture: IM, QS and palmitic acid.

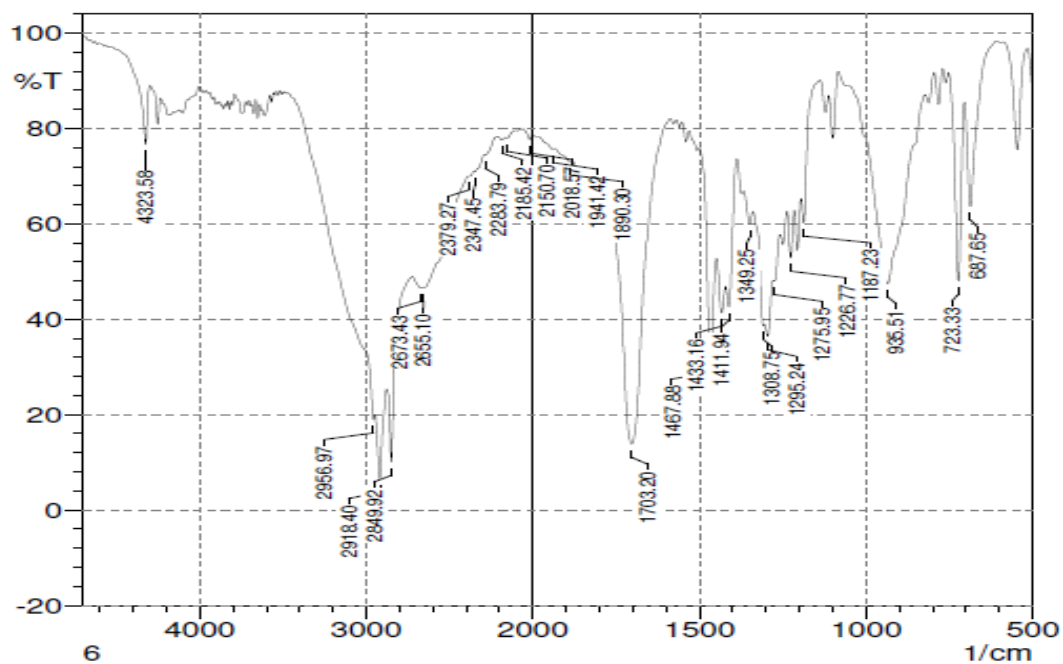


Figure 28. IR spectrum of physical mixture: IM, QS and glyceryl palmitostearate

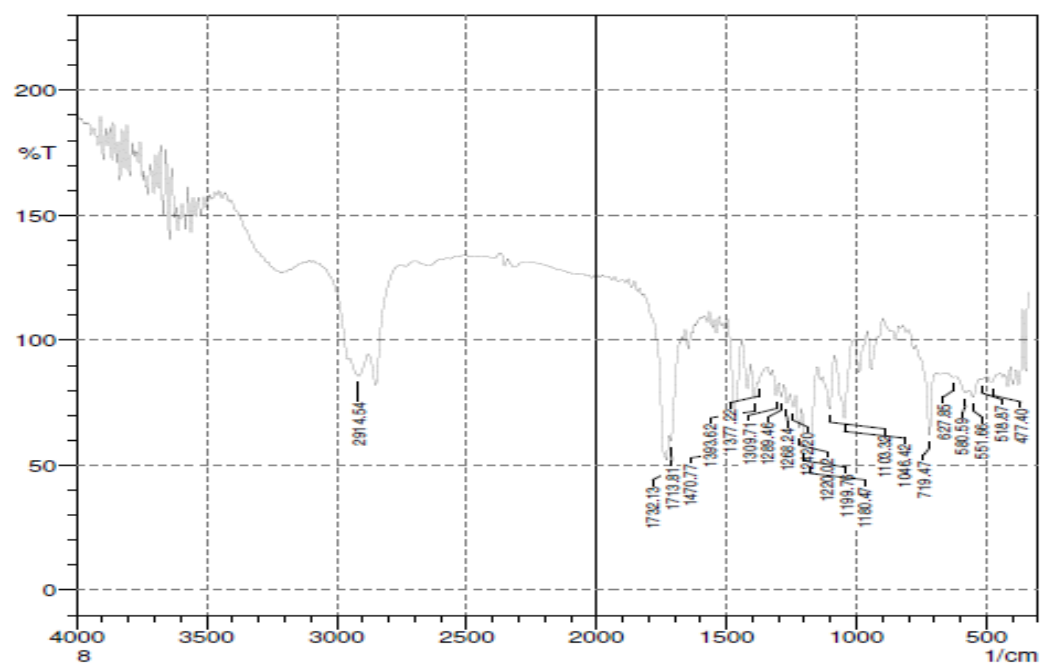


Figure 29. IR spectrum of physical mixture: IM, QS and glyceryl mono stearate

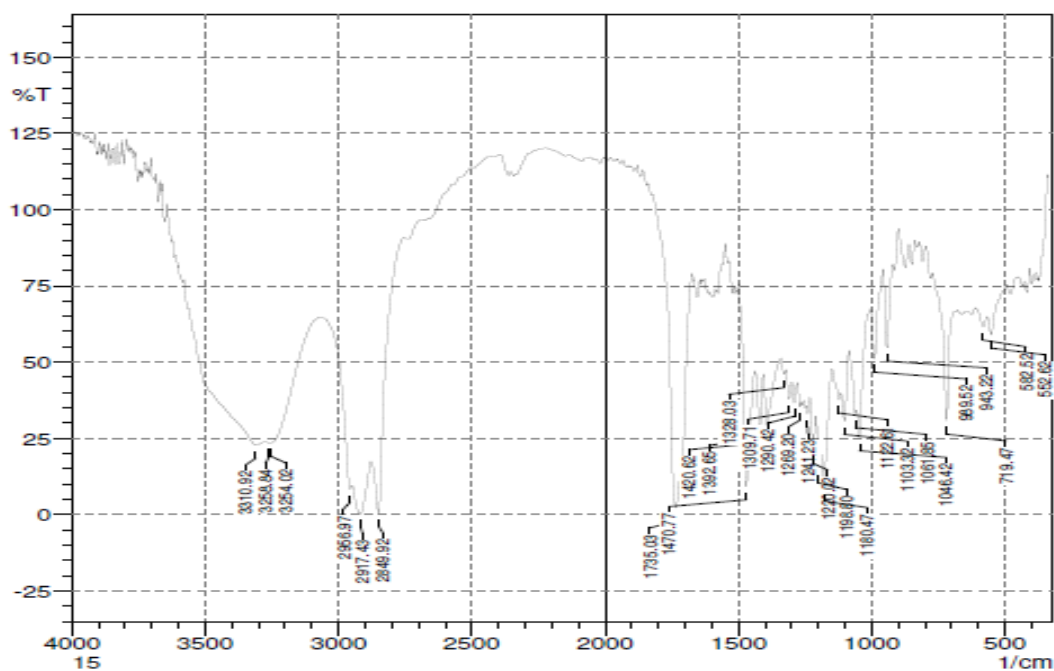


Figure 30. IR spectrum of physical mixture: IM, QS and Geleol mono and diglycerides

Table 15. Functional groups corresponding to IM, lipids and physical mixture as observed in FT-IR spectroscopy.

Functional groups	Peak wave number (cm ⁻¹)		
	IM	Lipid	Physical mixture
C=O stretch	1177	-	1178
Amide	1418	-	1418
Aromatic C=C stretching	1525	-	1525
Alkynyl C-H& C=C stretching	2111	1662	1662
Aromatic amine (NH ₂)	3445	1605	1605 and 3445

6.11 CHEMICAL CONJUGATION OF STEARIC ACID WITH LIGANDS

The formation of hylauronic acid conjugated stearyl amine (HAJ-SA) and vitamin B12 conjugated stearic acid (B12-SA) was confirmed using IR and NMR spectroscopy. The NMR spectrum of stearic acid, HAJ-SA and B12-SA is shown in Figure 31, Figure 32 and Figure 33 respectively. Conjugation of stearic acid with vitamin B12 was confirmed by the formation of amide linkage between COOH groups of stearic acid and NH₂ group of vitamin B12. Whereas conjugation of HA to stearyl amine was confirmed by the formation of amide linkage between COOH groups of HA and NH₂ groups of stearyl amine. The IR spectrum of both the conjugates in Figure 34 and Figure 35 showed peaks at 1647 cm⁻¹, 1552 cm⁻¹ and 1658 cm⁻¹ corresponding to the formation of amide bond stretching and NH bending. After lyophilisation, 14.1 mg of HA-SA and 12.3 mg of B12-SA were obtained.

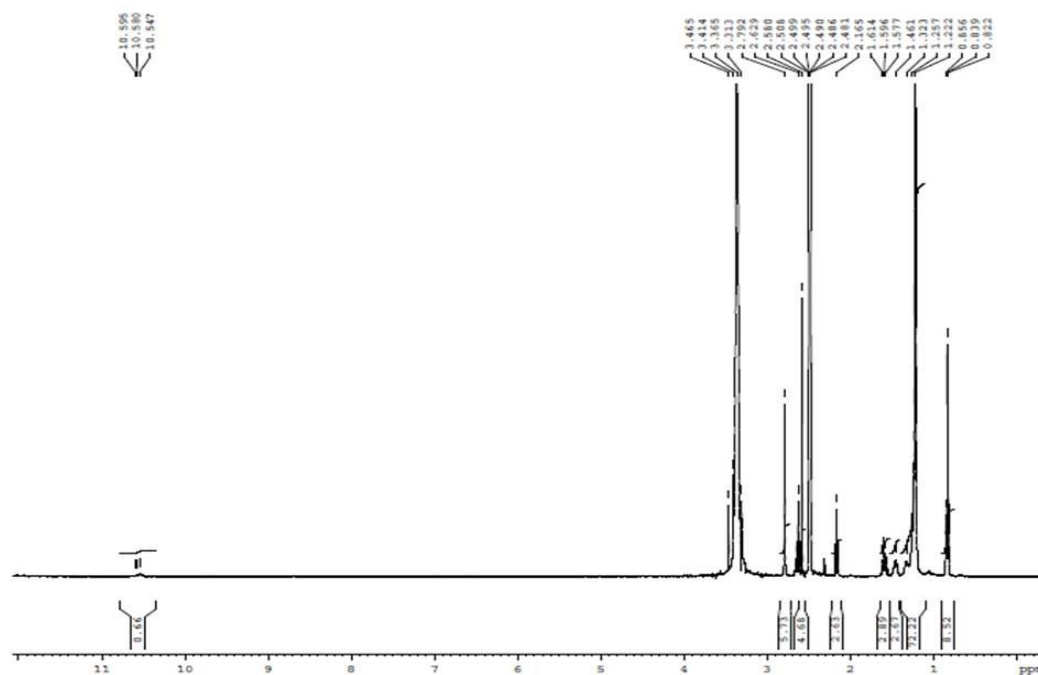


Figure 31. NMR spectra of stearic acid

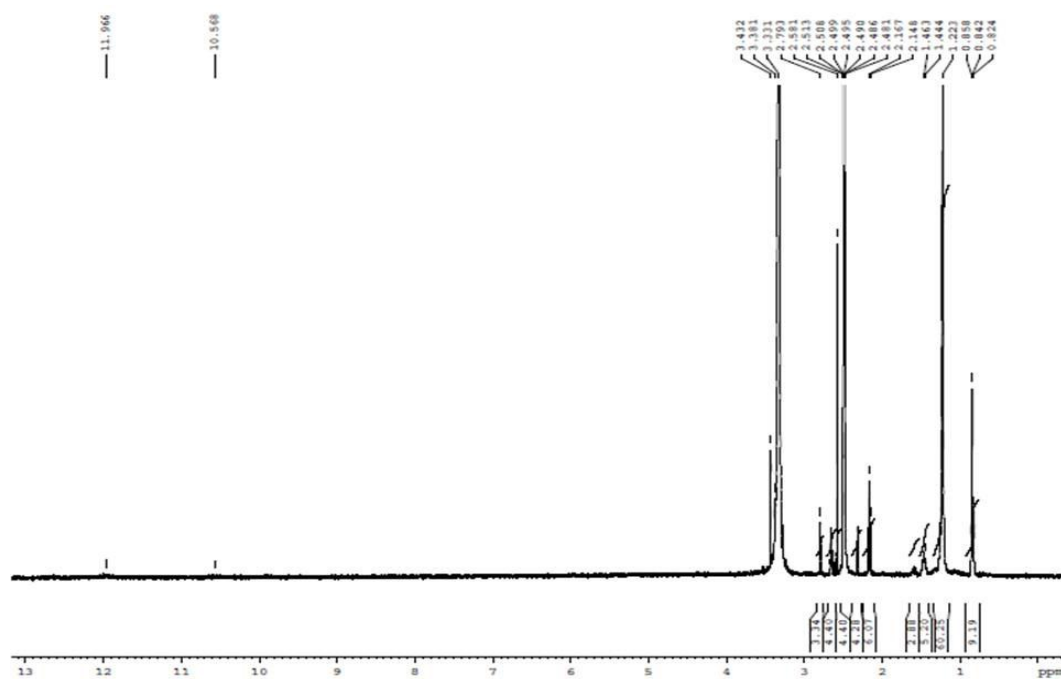


Figure 32. NMR spectra of the conjugate: HAJ-SA

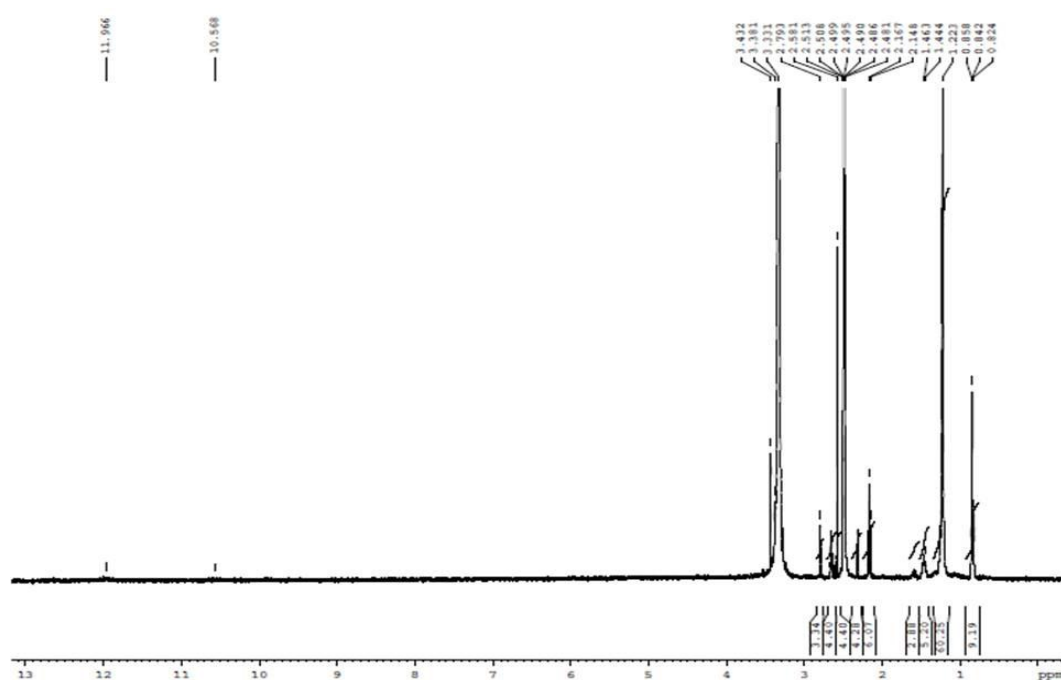


Figure 33. NMR spectra of the conjugate: B12-SA

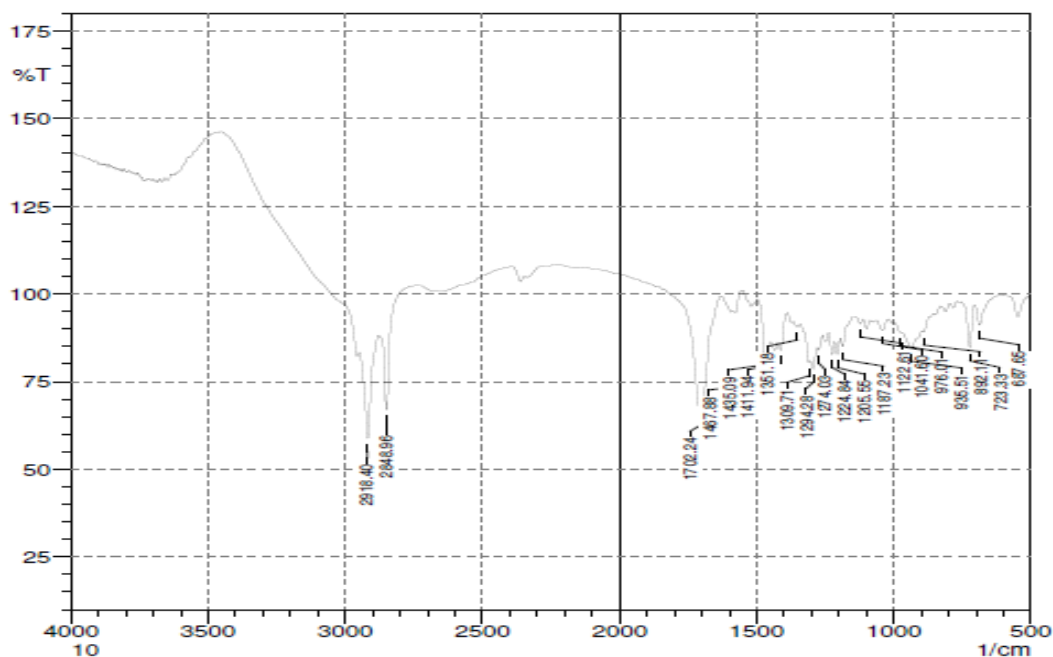


Figure 34. FT-IR spectra of the conjugate: HAJ-SA

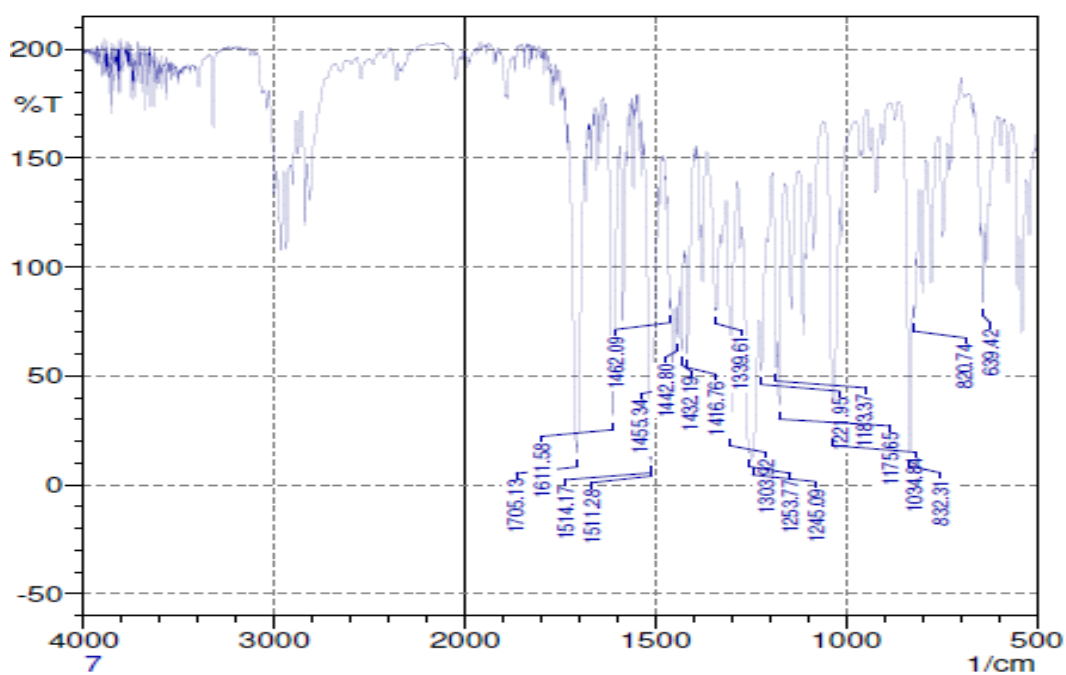


Figure 35. FT-IR spectra of the conjugate: B12-SA

6.12 PREPARATION OF IM LOADED SOLID LIPID NANOPARTICLES (SLNs)

SLNs of IM were prepared using different lipid carriers like stearic acid, palmitic acid, glyceryl palmitostearate, glyceryl monostearate and geleol mono and diglycerides as lipid carriers and QS, a non-ionic amphiphilic surfactant extracted from the bark of *Quillaja saponaria* was used as a surfactant for the preparation of SLNs of IM. A hot melt homogenisation method using high shear homogenisation and probe sonication was employed for the preparation. As each lipid has a characteristic composition which influences the formation of SLNs, the same set of parameters with respect to speed and time of homogenisation and time of sonication may not be suitable for all the lipids. High speeds may result in the formation of froth and cream, whereas low speed may not be suitable for the formation of nanoparticles. Table 16 represents the optimised conditions for each lipid during the preparation of SLNs. The compositions of various batches of SLNs prepared were mentioned in Table 17.

Table 16. Optimised conditions for the formation of SLNs

S No	Lipid used	Temperature maintained during formulation	Homogenization speed and time	Sonication time	Code
1	Stearic acid	75 °C	13, 000 rpm; 4 min	2 min	ISN
2	Palmitic acid	68 °C	14,000 rpm; 4 min	4 min	IPN
3	Glyceryl palmitostearate	60 °C	14, 000 rpm; 6 min	6 min	IGPN
4	Glyceryl monostearate	65 °C	15, 000 rpm; 4 min	4 min	IGMN
5	Geleol mono and di glycerides	67 °C	15,000 rpm; 2 min	6 min	IGEN

Table 17. Composition of different batches of SLNs

Code	IM (mg)	Lipid (%)	QS (%)
STEARIC ACID BASED SLNs			
ISN1	20	4	0.5
ISN2	20	4	1
ISN3	20	4	1.5
ISN4	20	8	0.5
ISN5	20	8	1
ISN6	20	8	1.5
ISN7	20	12	0.5
ISN8	20	12	1
ISN9	20	12	1.5
B12-ISN	20	4	1.5
HAJ-ISN	20	4	1.5
HAC-ISN	20	4	1.5
PALMITIC ACID BASED SLNs			
IPN1	20	4	0.5
IPN2	20	4	1
IPN3	20	4	1.5
IPN4	20	8	0.5
IPN5	20	8	1
IPN6	20	8	1.5
IPN7	20	12	0.5
IPN8	20	12	1
IPN9	20	12	1.5
GLYCERYL PALMITOSTEARATE BASED SLNs			
IGPN1	20	4	0.5
IGPN2	20	4	1
IGPN3	20	4	1.5
IGPN4	20	8	0.5
IGPN5	20	8	1
IGPN6	20	8	1.5
IGPN7	20	12	0.5
IGPN8	20	12	1
IGPN9	20	12	1.5
B12-IGPN	20	4	1.5
HAJ-IGPN	20	4	1.5
HAC-IGPN	20	4	1.5

Code	IM (mg)	Lipid (%)	QS (%)
GLYCERYL MONOSTEARATE BASED SLNs			
IGMN1	20	4	0.5
IGMN2	20	4	1
IGMN3	20	4	1.5
IGMN4	20	8	0.5
IGMN5	20	8	1
IGMN6	20	8	1.5
IGMN7	20	12	0.5
IGMN8	20	12	1
IGMN9	20	12	1.5
GELEOL MONO AND DIGLYCERIDES BASED SLNs			
IGEN1	20	4	0.5
IGEN2	20	4	1
IGEN3	20	4	1.5
IGEN4	20	8	0.5
IGEN5	20	8	1
IGEN6	20	8	1.5
IGEN7	20	12	0.5
IGEN8	20	12	1
IGEN9	20	12	1.5

6.13 PHYSICAL ADSORPTION WITH HYALURONIC ACID

HA was coated onto the surface of the nanoparticles by electrostatic attraction. Different concentrations of HA (0.05%, 0.10%, 0.15% or 0.20% w/v) were used for the coating of SLNs. After coating with HA the particle size of the formulations reduced. Various concentrations have been tried in order to obtain a formulation without any aggregation among the particles.

6.14 FREEZE DRYING

Freeze dried powders of the samples were used only for performing differential scanning calorimetric studies. The freeze dried powdered samples is shown in Figure 36.

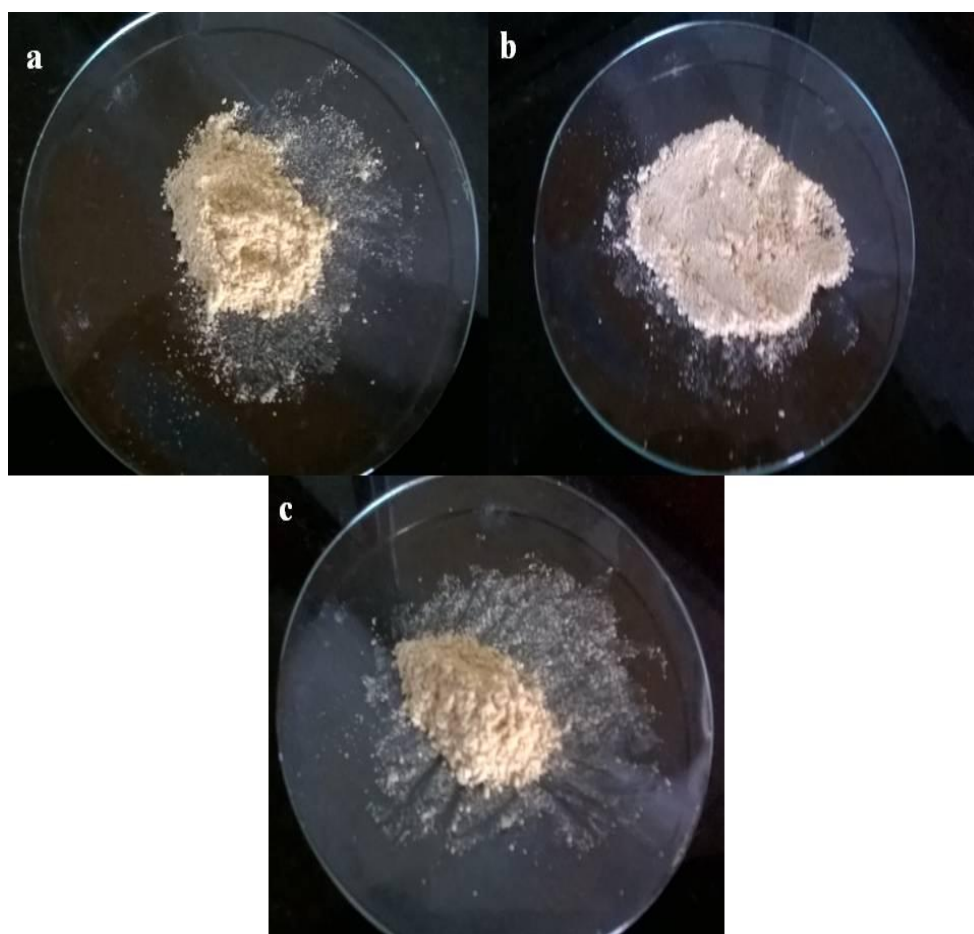


Figure 36. Freeze dried powder samples of ISN (a), IPN (b) and IGPN (c).

6.15 DETERMINATION OF PARTICLE SIZE AND POLY DISPERSITY

INDEX

The particle size of the SLNs of stearic acid containing IM is shown in Table 18. The average particle size of the different batches of ISN ranged from 143.5 ± 3.5 nm to 641.9 ± 4.2 nm. A highest particle size was obtained for formulation ISN7 containing 12% stearic acid and 0.5% QS. A least particle size was observed for formulation ISN6 containing 8% stearic acid and 1.5% QS. The

particle size of the ISN was influenced by the amount of stearic acid and QS. The PDI of the formulations was found to be below 0.25, which indicates that the nanoparticles are partially monodisperse. Addition of conjugates like vitamin B12-stearic acid (B12-ISN) and HA-stearic acid (HAJ-ISN) during the preparation of SLNs showed a mild increase in the particle size from 159.5 ± 4.7 nm to 169.1 ± 3.16 nm and 173.1 ± 4.5 nm respectively. But, coating of ISN3 with HA (HAC-ISN3) decreased the particle size to 87.3 ± 5.9 nm.

Table 18: Particle size, polydispersity index, zeta potential and entrapment efficiency of the formulations

Code	Average Size (nm \pm SD)	Polydispersity index (\pm SD)	Zeta potential (mV \pm SD)	Entrapment efficiency (% \pm SD)
STEARIC ACID BASED SLNs				
ISN1	457.8 ± 3.8	0.183 ± 0.03	0.20 ± 1.1	66.2 ± 1.2
ISN2	320.5 ± 2.5	0.155 ± 0.03	0.62 ± 0.1	62.7 ± 1.5
ISN3	159.5 ± 4.7	0.127 ± 0.01	0.95 ± 0.5	61.3 ± 1.1
ISN4	423.4 ± 3.2	0.186 ± 0.01	-0.78 ± 0.8	59.5 ± 0.9
ISN5	269.7 ± 3.7	0.165 ± 0.01	-1.97 ± 0.1	57.0 ± 1.7
ISN6	143.5 ± 3.5	0.128 ± 0.01	-0.42 ± 1.2	54.1 ± 1.9
ISN7	641.9 ± 4.2	0.206 ± 0.03	-1.83 ± 0.2	44.1 ± 1.9
ISN8	447.5 ± 8.7	0.237 ± 0.03	-2.43 ± 0.4	45.0 ± 1.4
ISN9	400.9 ± 6.2	0.162 ± 0.02	-2.23 ± 0.2	41.0 ± 1.0
B12-ISN	169.1 ± 3.2	0.205 ± 0.01	10.2 ± 1.2	56.9 ± 1.4
HAI-ISN	173.1 ± 4.5	0.228 ± 0.02	-6.4 ± 0.7	50.6 ± 1.5
HAC-ISN	87.3 ± 5.9	0.162 ± 0.01	-12.8 ± 1.7	47.8 ± 2.1
PALMITIC ACID BASED SLNs				
IPN1	395.2 ± 5.5	0.203 ± 0.03	-1.08 ± 0.2	57.1 ± 0.3
IPN2	310.3 ± 9.5	0.185 ± 0.01	-1.70 ± 0.6	55.6 ± 0.5
IPN3	133.1 ± 8.4	0.128 ± 0.01	-4.29 ± 0.6	53.1 ± 0.9
IPN4	517.8 ± 7.4	0.172 ± 0.03	-1.29 ± 0.5	48.5 ± 0.6

Code	Average Size (nm \pm SD)	Polydispersity index (\pm SD)	Zeta potential (mV \pm SD)	Entrapment efficiency (% \pm SD)
IPN5	301.2 \pm 9.3	0.227 \pm 0.02	-1.77 \pm 0.9	44.4 \pm 1.1
IPN6	267.6 \pm 5.9	0.262 \pm 0.03	-2.73 \pm 0.5	39.8 \pm 0.6
IPN7	611.0 \pm 4.1	0.234 \pm 0.05	-3.91 \pm 0.8	44.1 \pm 0.3
IPN8	309.9 \pm 5.3	0.236 \pm 0.02	-2.09 \pm 0.2	47.4 \pm 0.7
IPN9	283.5 \pm 7.1	0.279 \pm 0.02	-1.83 \pm 0.3	50.4 \pm 0.8
GLYCERYL PALMITOSTEARATE BASED SLNs				
IGPN1	218.0 \pm 3.2	0.247 \pm 0.02	1.21 \pm 0.7	51.3 \pm 0.9
IGPN2	145.3 \pm 4.5	0.211 \pm 0.01	0.56 \pm 0.3	56.7 \pm 0.8
IGPN3	106.4 \pm 4.7	0.08 \pm 0.01	1.03 \pm 0.14	55.1 \pm 1.1
IGPN4	269.8 \pm 2.3	0.203 \pm 0.01	3.37 \pm 0.1	55.2 \pm 1.5
IGPN5	174.9 \pm 4.3	0.172 \pm 0.09	2.79 \pm 0.4	58.0 \pm 0.7
IGPN6	122.8 \pm 2.9	0.166 \pm 0.01	2.49 \pm 0.3	59.4 \pm 1.3
IGPN7	430.7 \pm 2.2	0.131 \pm 0.02	3.72 \pm 0.2	61.7 \pm 0.9
IGPN8	326.7 \pm 4.8	0.227 \pm 0.02	3.37 \pm 0.3	63.6 \pm 0.7
IGPN9	206.9 \pm 4.1	0.125 \pm 0.01	2.51 \pm 0.4	65.9 \pm 0.6
B12-IGPN	118.7 \pm 3.9	0.194 \pm 0.02	1.63 \pm 0.5	51.5 \pm 1.2
HAI-IGPN	130.6 \pm 2.7	0.212 \pm 0.02	-2.3 \pm 0.6	49.9 \pm 2.1
HAC-IGPN	92.1 \pm 2.41	0.08 \pm 0.01	-10.67 \pm 1.32	43.4 \pm 0.7
GLYCERYL MONOSTEARATE BASED SLNs				
IGMN1	740.9 \pm 15.6	0.155 \pm 0.01	4.07 \pm 0.2	54.1 \pm 0.6
IGMN2	538.0 \pm 15.70	0.182 \pm 0.01	3.17 \pm 0.5	50.4 \pm 1.0
IGMN3	422.6 \pm 8.2	0.134 \pm 0.01	-2.92 \pm 0.3	47.1 \pm 0.7
IGMN4	430.1 \pm 9.1	0.347 \pm 0.02	-13.78 \pm 2.3	-
IGMN5	296.4 \pm 8.4	0.309 \pm 0.01	-7.05 \pm 0.8	44.1 \pm 0.5
IGMN6	168.5 \pm 7.5	0.175 \pm 0.01	-3.56 \pm 0.2	41.9 \pm 1.1
IGMN7	360.6 \pm 7.5	0.371 \pm 0.03	-14.96 \pm 0.8	-
IGMN8	245.3 \pm 9.	0.328 \pm 0.01	-6.14 \pm 0.3	47.2 \pm 1.1
IGMN9	126.6 \pm 6.1	0.250 \pm 0.02	-3.36 \pm 0.5	48.9 \pm 0.6

Code	Average Size (nm \pm SD)	Polydispersity index (\pm SD)	Zeta potential (mV \pm SD)	Entrapment efficiency (% \pm SD)
GELEOL MONO AND DI GLYCERIDE BASED SLNs				
IGEN1	354.8 \pm 7.9	0.183 \pm 0.01	-2.45 \pm 0.1	57.5 \pm 1.2
IGEN2	224.7 \pm 8.4	0.163 \pm 0.01	-2.52 \pm 0.3	56.6 \pm 0.9
IGEN3	118.4 \pm 5.1	0.135 \pm 0.02	-2.01 \pm 0.1	59.0 \pm 0.3
IGEN4	376.7 \pm 6.7	0.460 \pm 0.02	-11.18 \pm 1.7	60.7 \pm 1.2
IGEN5	260.3 \pm 10.5	0.354 \pm 0.02	-4.47 \pm 0.7	55.4 \pm 1.3
IGEN6	155.2 \pm 7.4	0.232 \pm 0.01	-2.32 \pm 0.1	47.0 \pm 1.2
IGEN7	653.9 \pm 8.4	0.384 \pm 0.01	-12.03 \pm 2.7	66.5 \pm 1.3
IGEN8	443.7 \pm 9.7	0.264 \pm 0.01	-6.44 \pm 0.6	55.3 \pm 1.0
IGEN9	321.2 \pm 11.7	0.180 \pm 0.01	-3.25 \pm 0.3	51.5 \pm 0.7

The particle size of the SLNs of IM prepared using palmitic acid (IPN) ranged from 133.1 \pm 8.4 nm to 611.0 \pm 4.1 nm. Highest particle size was obtained for formulation IPN7 containing 12% stearic acid and 0.5% QS. Least particle size was obtained for IPN3 containing 4% stearic acid and 1.5% QS. The polydispersity index of the IPN ranged from 0.128 \pm 0.01 to 0.279 \pm 0.02. The particle size and polydispersity index of the formulations prepared using palmitic acid were also influenced by the amount of lipid carrier and surfactant used.

When glyceryl palmitostearate was used as lipid carrier the particle of the IGPN was in the range of 430.7 \pm 2.2 nm to 92.1 \pm 2.41 nm. Least particle size was obtained for formulation IGPN3 containing 4% glyceryl palmitostearate and 1.5% QS. Highest particle size of 430.7 \pm 2.2 nm was obtained for formulation IGPLN7 containing 12% glyceryl palmitostearate and 0.5% QS. The particle size of the SLNs prepared after addition of B12-SA and HA-SA showed an increase in particle size to 118.7 \pm 3.9 nm and 130.6 \pm 2.7 nm respectively. But coating with HA reduced the particle size to 92.1 \pm 2.41 nm. Table 18 represents the particle

size of the formulations prepared using glyceryl palmitostearate as the lipid carrier. The particle size distribution data and polydispersity index data obtained for HAC-IGPN3 using Malvern particle size analyser is represented in Figure 37.

SLNs of IM prepared using glyceryl monostearate as the lipid carrier showed particle size ranging from 126.6 ± 6.1 nm to 740.9 ± 15.6 nm. The polydispersity index of the formulations ranged from 0.182 ± 0.01 to 0.371 ± 0.03 . The particle size and polydispersity index of the different batches of formulations was mentioned in Table 18.

Geleol mono and diglycerides was also used as a lipid carrier to prepare SLNs loaded with IM. The particle size range of the different batches of formulations varied from 118.4 ± 5.06 nm to 653.9 ± 8.4 nm. A highest particle size was obtained for formulation IGEN7 containing 12% geleol mono and diglycerides and 0.5% QS. Least particle was obtained for IGEN3 containing 4% geleol mono and diglycerides and 1.5% QS.

Results

	Size (d.nm):	% Intensity:	St Dev (d.n...
Z-Average (d.nm): 92.06	Peak 1: 109.2	97.6	51.32
Pdl: 0.069	Peak 2: 4415	2.4	914.9
Intercept: 0.680	Peak 3: 0.000	0.0	0.000
Result quality : Good			

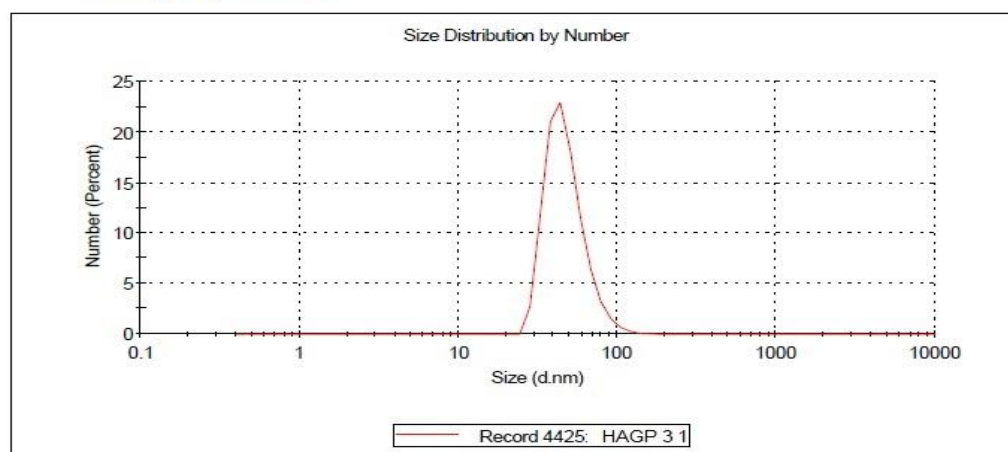


Figure 37. Particle size distribution and polydispersity index for HAC-IGPN3

6.16 DETERMINATION OF ZETA POTENTIAL

The zeta potential of all the formulations was found to be neutral (-10 mV to +10 mV). The zeta potential of the formulations however had a mild negative charge due to the ionisation of lipid carriers. After coating the surface of SLNs with HA, the surface charge increased to a slight negative magnitude. Whereas SLNs prepared by addition of B12-SA and HA-SA did not show a major change in the zeta potential. Table 18 mentions the zeta potential of all the formulations prepared using different lipid carriers. Figure 38 represents the zeta potential of HAC-IGPN3.

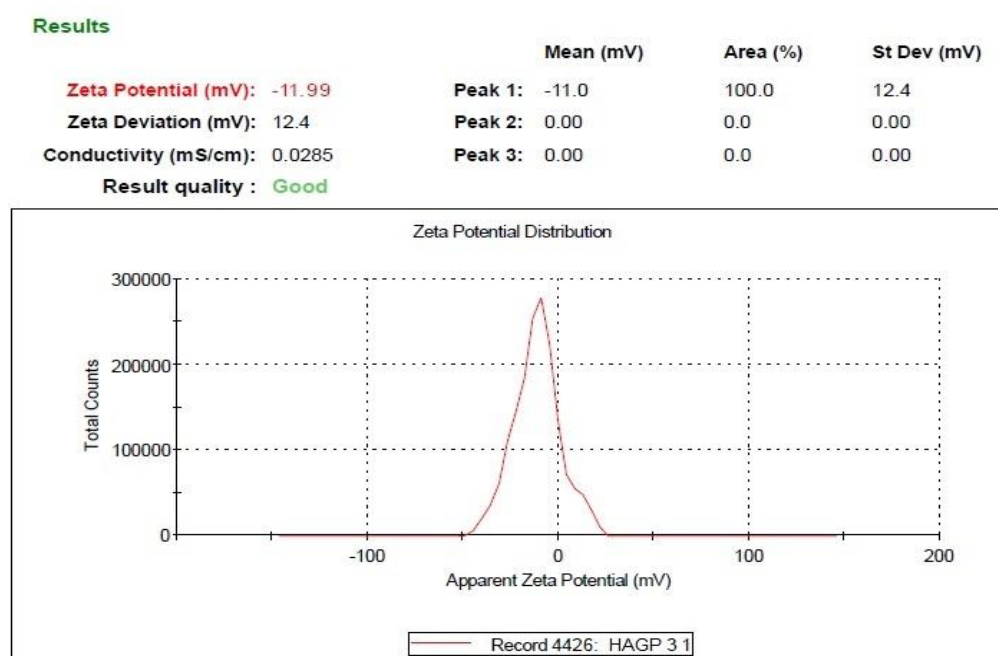


Figure 38. Zeta potential for HAC-IGPN3

6.17 TRANSMISSION ELECTRON MICROSCOPY

The micrographs obtained from TEM were used to visualise the morphology of the SLNs. ISN prepared solely with stearic acid showed quassi shaped nanoparticles Figure 39 ISN prepared after addition of vitaminB12-stearic acid conjugate and HA-stearic acid conjugate did not influence the shape of the SLNs.

But, additional coating of SLNs with HA showed spherical shaped nanoparticles (Figure 40). The TEM of ISN after conjugating with vitamin B12 is shown in Figure 41. Aggregation was not observed in any of the particles prepared using stearic acid as a lipid carrier. The morphology of the IPN showed spherical shaped nanoparticles with mild aggregations (Figure 42). IGPN prepared using glyceryl palmitostearate as lipid carrier were found to possess quasi shaped nanoparticles without any aggregations Figure 43. Addition of vitamin B12-stearic acid conjugate and HA-stearic acid conjugate did not influence the morphology of the nanoparticles (Figure 44). But, when IGPN were coated with HA, nests of spherical nanoparticles were observed Figure 45. These nests were found to be in the size range of 100 nm which embed nanoparticles of size less than 50 nm. Although these nests give an appearance of aggregation, however they are not actually aggregated as their individual surfaces are not destroyed. There is a possible reason for HA to withhold IM loaded SLNs. These nests of nanoparticles can play a role in staying for longer time in the lymphatics. IGMN showed aggregates of nanoparticles which are non spherical in shape Figure 46. IGEN showed particles spherical to cubical shaped structures Figure 47.

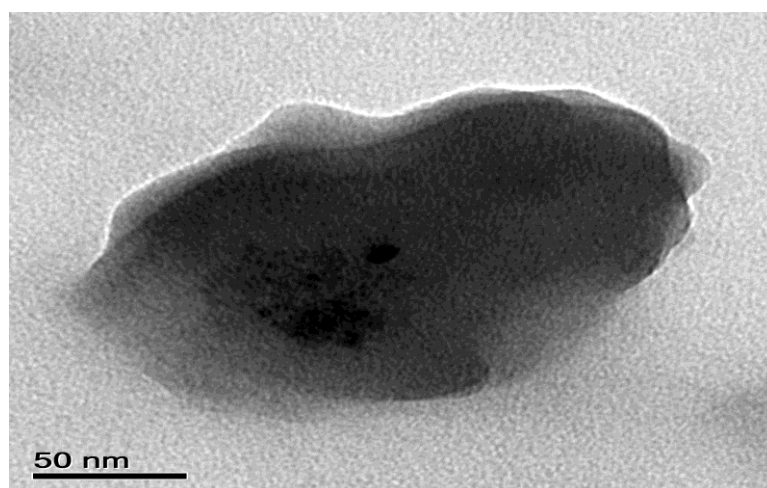


Figure 39. Transmission electron microscope image of ISN

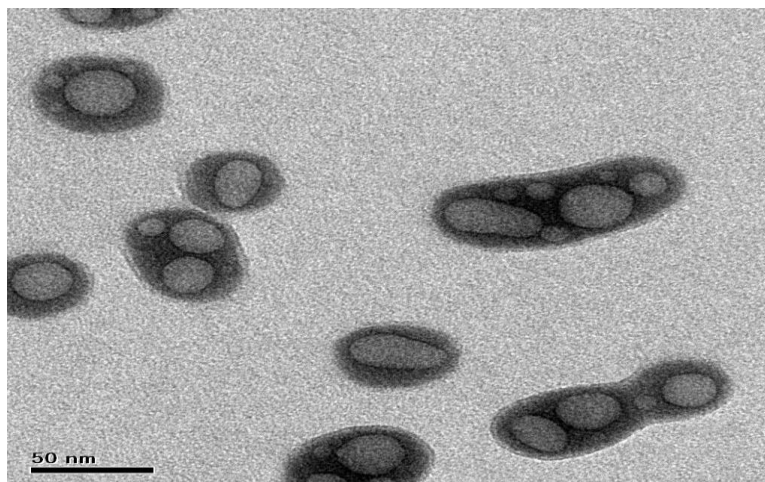


Figure 40. Transmission electron microscope image of HA-ISN

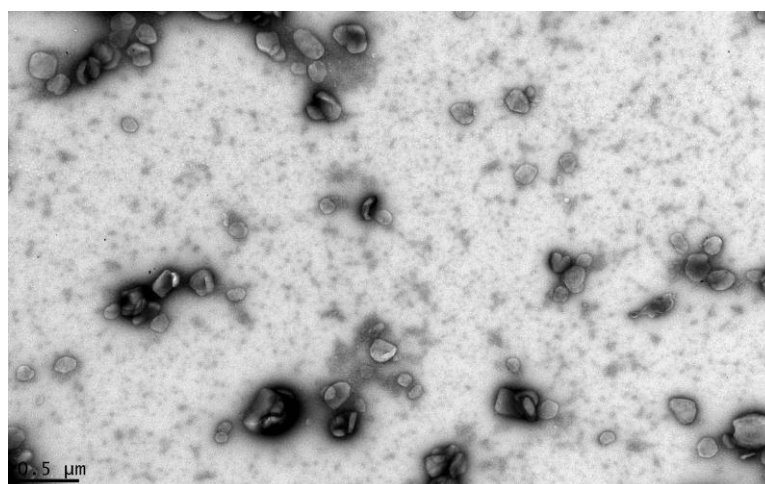


Figure 41. Transmission electron microscope image of B12-ISN

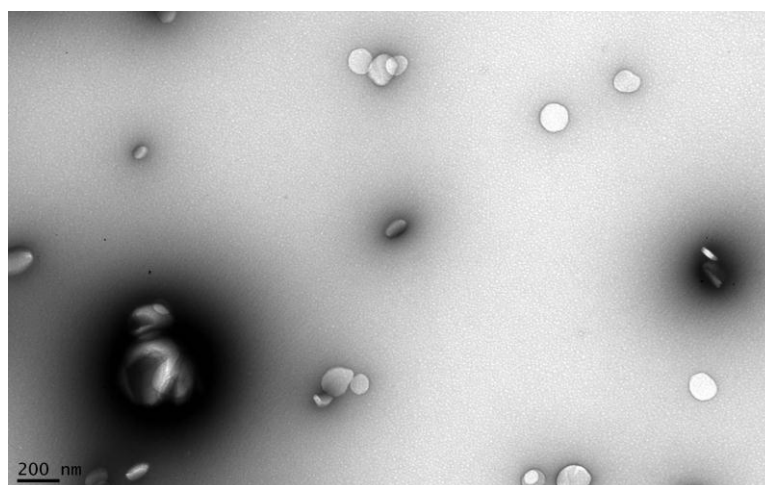


Figure 42. Transmission electron microscope image of IPN

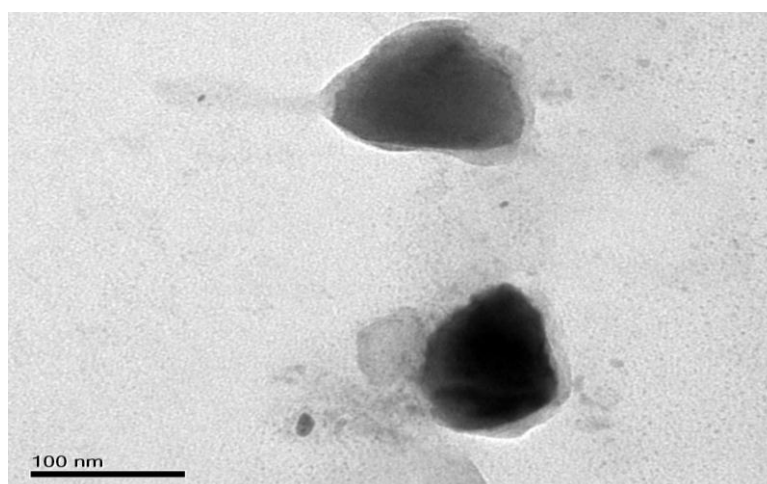


Figure 43. Transmission electron microscope image of IGPN

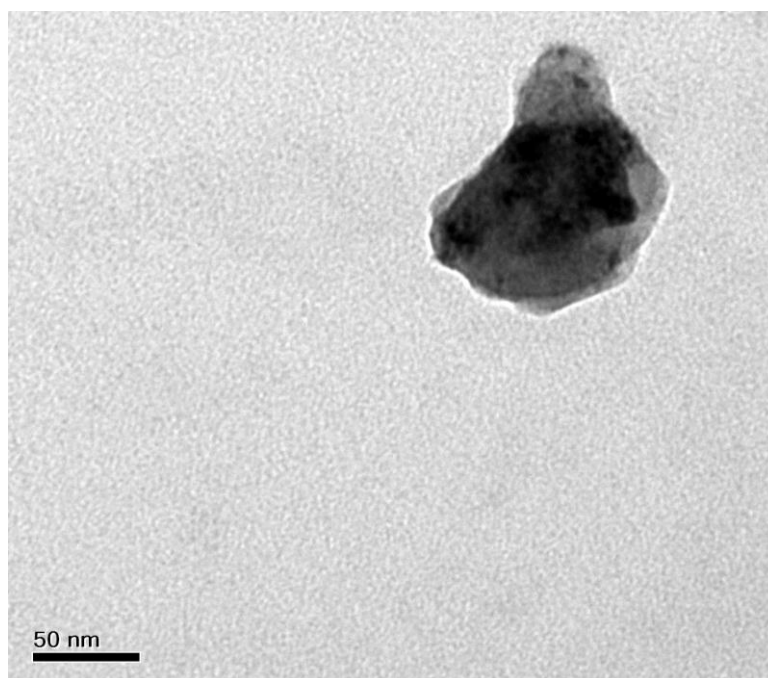


Figure 44. Transmission electron microscope image of B12-IGPN

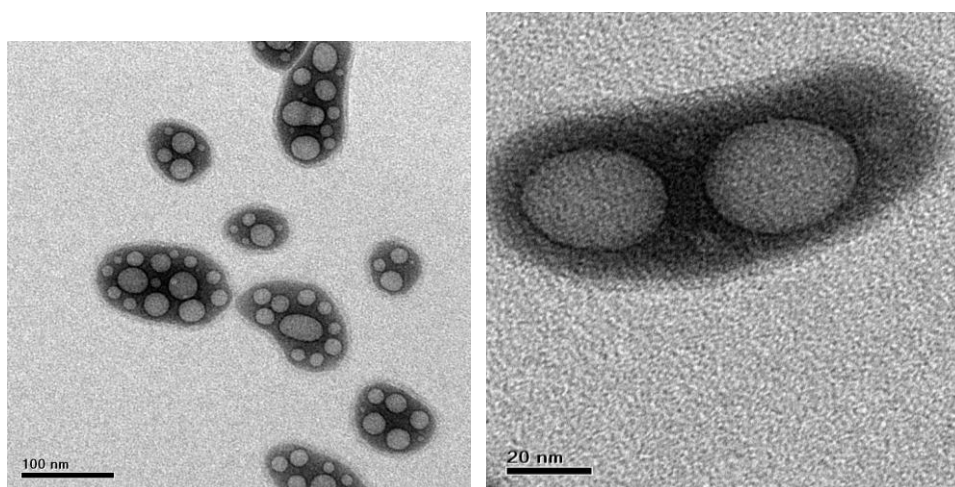


Figure 45. Transmission electron microscope image of IGPN-HA

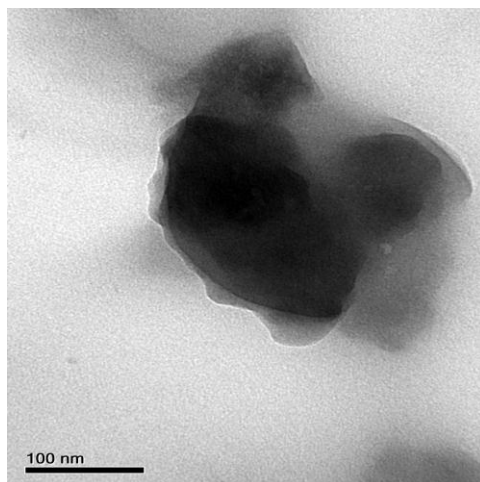


Figure 46. Transmission electron microscope image of IGMN

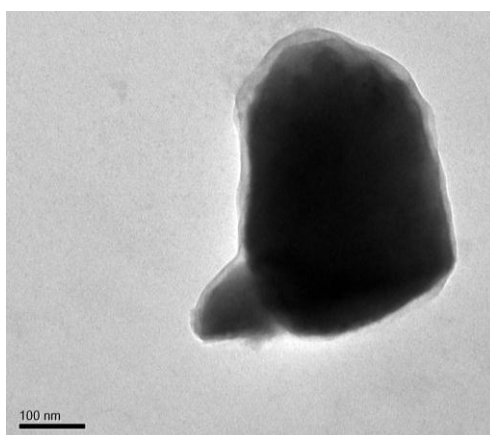


Figure 47. Transmission electron microscope image of IGEN

6.18 ATOMIC FORCE MICROSCOPY

Analysis of the morphology of ISN, IPN, IGPN, and HAC-IGPN from Figure 48, Figure 49, Figure 50 and Figure 51 respectively showed spherical shaped particles with a smooth topography and without any aggregations. But, AFM images of IGMN and IGEN in Figure 52 and Figure 53 respectively showed aggregated nanoparticles.

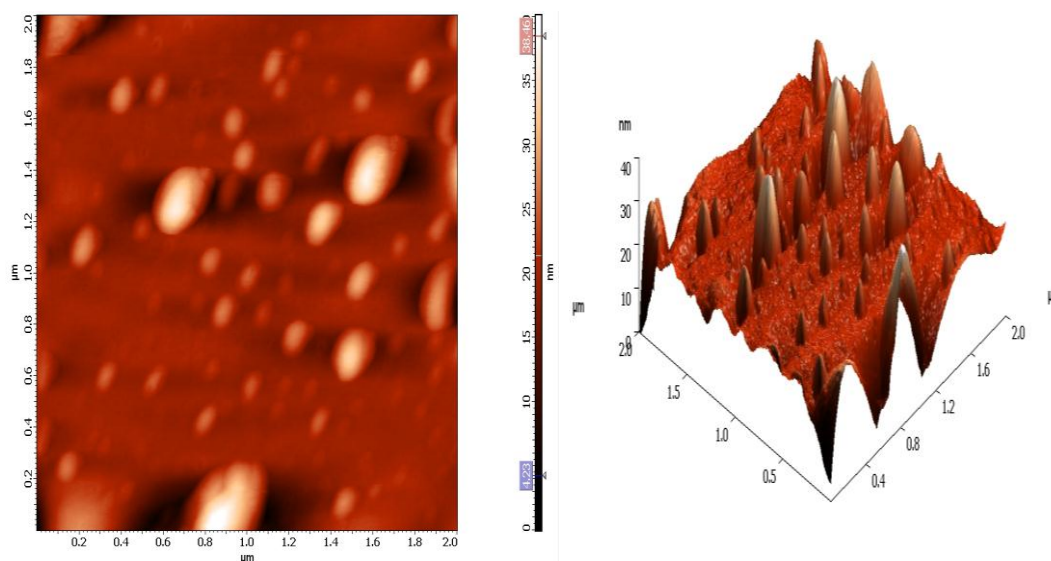


Figure 48. AFM phase image and topographic image of ISN

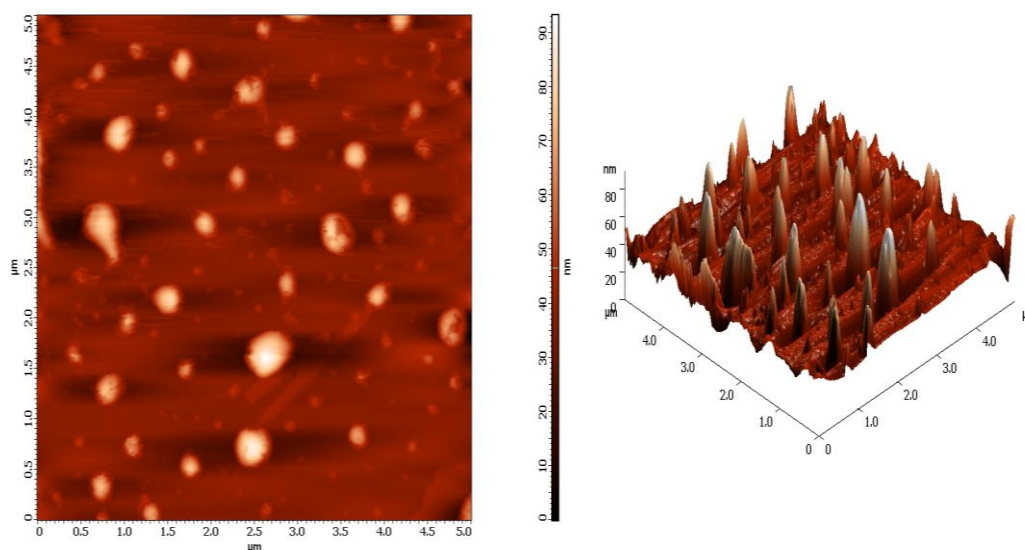


Figure 49. AFM phase image and topographic image of IPN

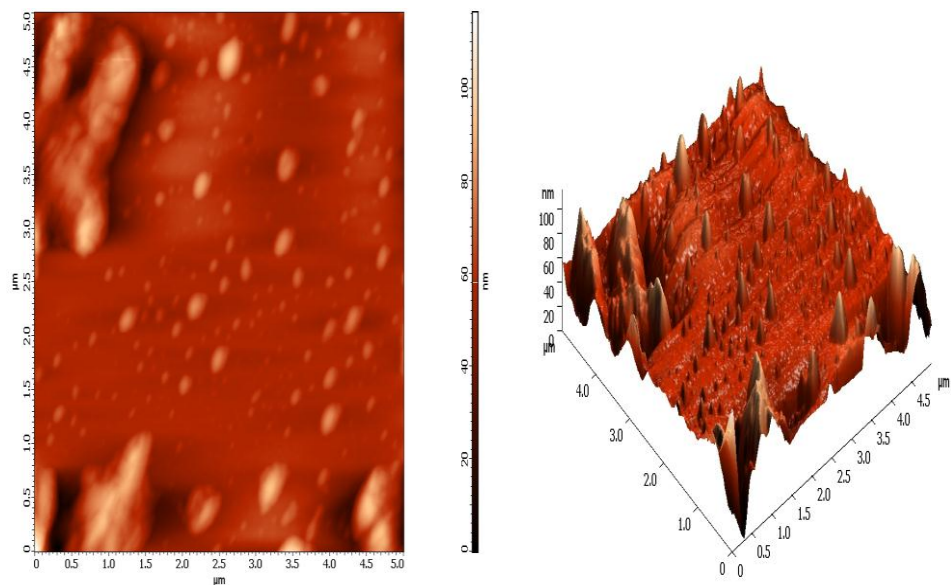


Figure 50. AFM phase image and topographic image of IGPN

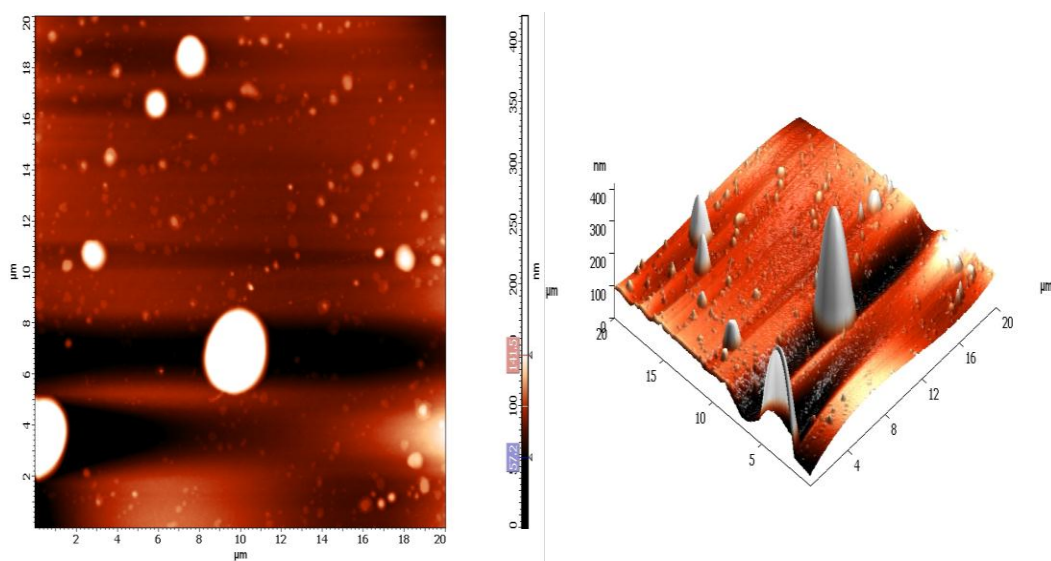


Figure 51. AFM phase image and topographic image of HAC-IGPN

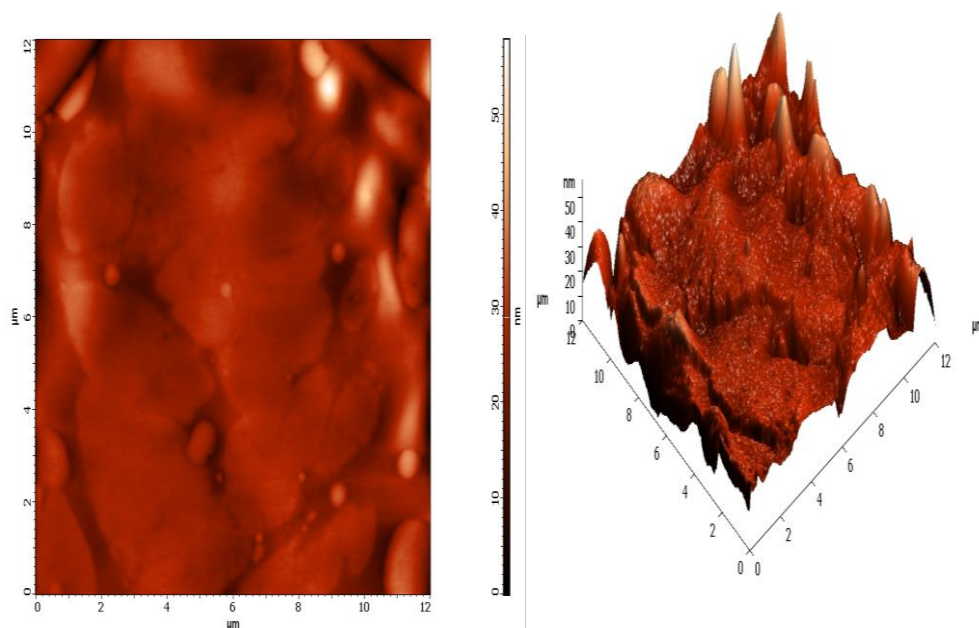


Figure 52. AFM phase image and topographic image of IGMN

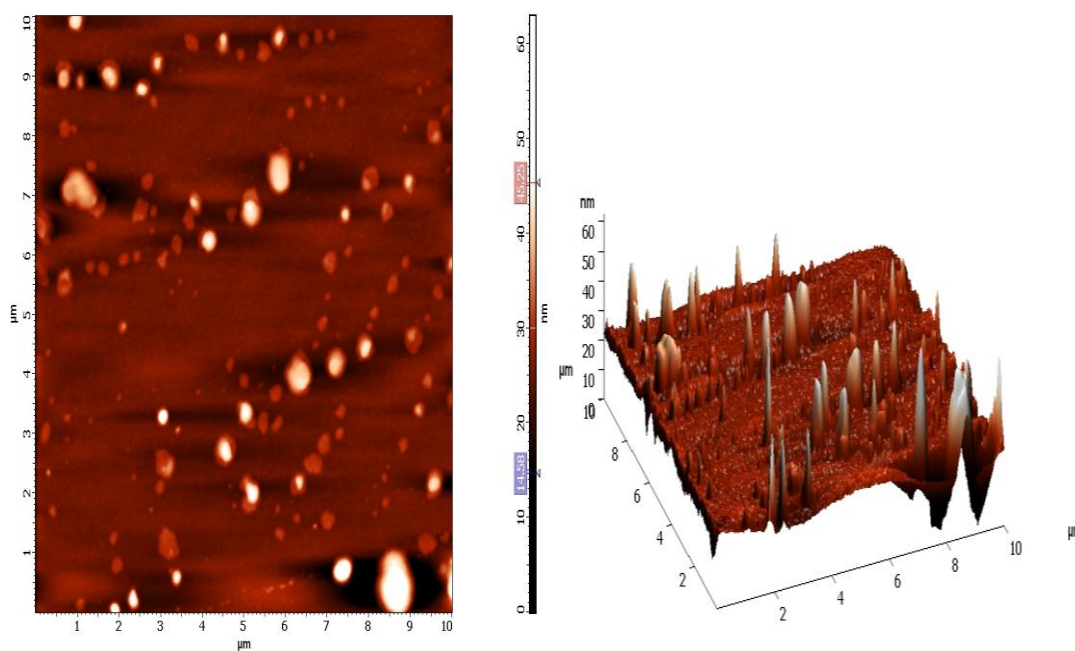


Figure 53. AFM phase image and topographic image of IGEN

6.19 MEASUREMENT OF ENTRAPMENT EFFICIENCY

The entrapment efficiency of the various formulations prepared using different lipids carriers was mentioned in Table 18. The overall entrapment efficiencies of the formulations were low. The entrapment efficiencies of the formulations prepared using stearic acid was found to be in the range of $66.2 \pm 1.2\%$ to $41.0 \pm 1.0\%$. When palmitic acid was used, the entrapment efficiencies of the formulations were in the range of $39.8 \pm 0.6\%$ to $57.1 \pm 0.3\%$. Formulations prepared using glyceryl palmitostearate were found to have entrapment efficiencies in the range of $65.9 \pm 0.6\%$ to $51.3 \pm 0.9\%$. Different batches of IGM prepared using glyceryl monostearate were found to have entrapment efficiencies in the range of $41.9 \pm 1.1\%$ to $54.1 \pm 0.6\%$. SLNs prepared using geleol mono and diglycerides as lipid carrier showed entrapment efficiencies ranging from $66.5 \pm 1.3\%$ to $47.0 \pm 1.2\%$.

6.20 DIFFERENTIAL SCANNING CALORIMETRY FOR FORMULATIONS

The thermogram of IM in Figure 53 indicated an endothermic melting point of $227.8\text{ }^{\circ}\text{C}$. The endothermic melting point of bulk stearic acid, palmitic acid and glyceryl palmitostearate was observed at 62.3°C , $57.5\text{ }^{\circ}\text{C}$ and 50°C respectively in Figure 54, Figure 55 and Figure 56. For QS an endothermic melting point was observed at 126.5°C . The thermograms of ISN, IPN and IGPN did not show any endothermic melting peak for IM as observed in Figure 54, Figure 55 and Figure 56.

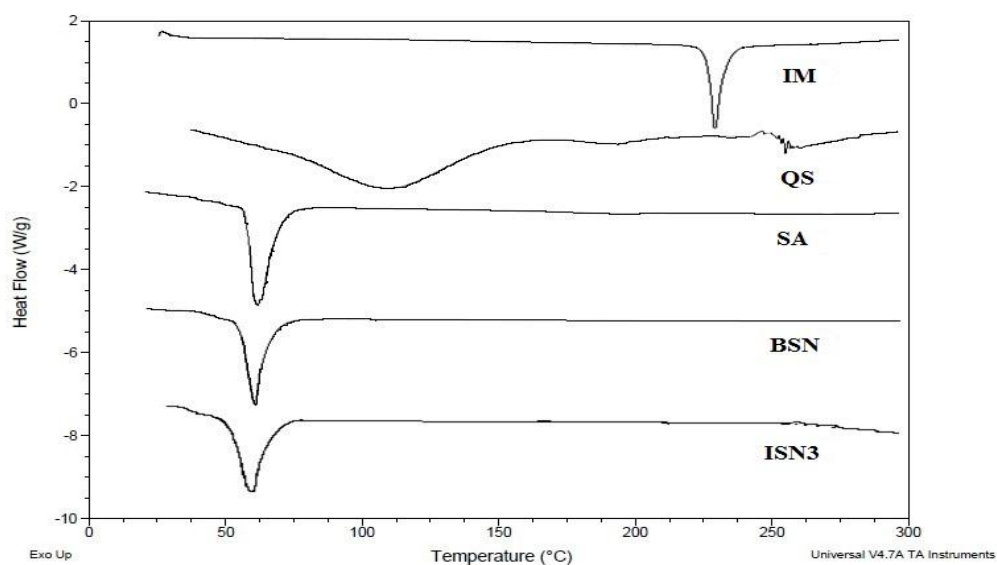


Figure 54. Overlay of DSC thermogram of IM: Imatinib mesylate, QS: quillaja saponin, SA: Bulk Stearic acid, BSN: Blank SLNs, ISN3: IM loaded SLNs

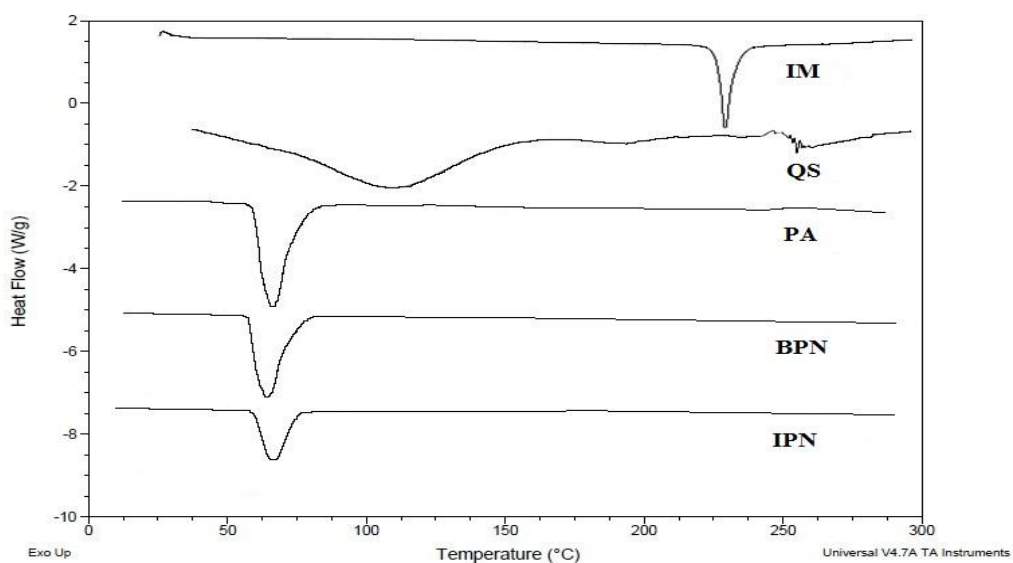


Figure 55. Overlay of DSC thermogram of IM: Imatinib mesylate, QS: quillaja saponin, PA: Bulk Palmitic acid, BPN: Blank SLNs, IPN3: IM loaded SLNs of palmitic acid

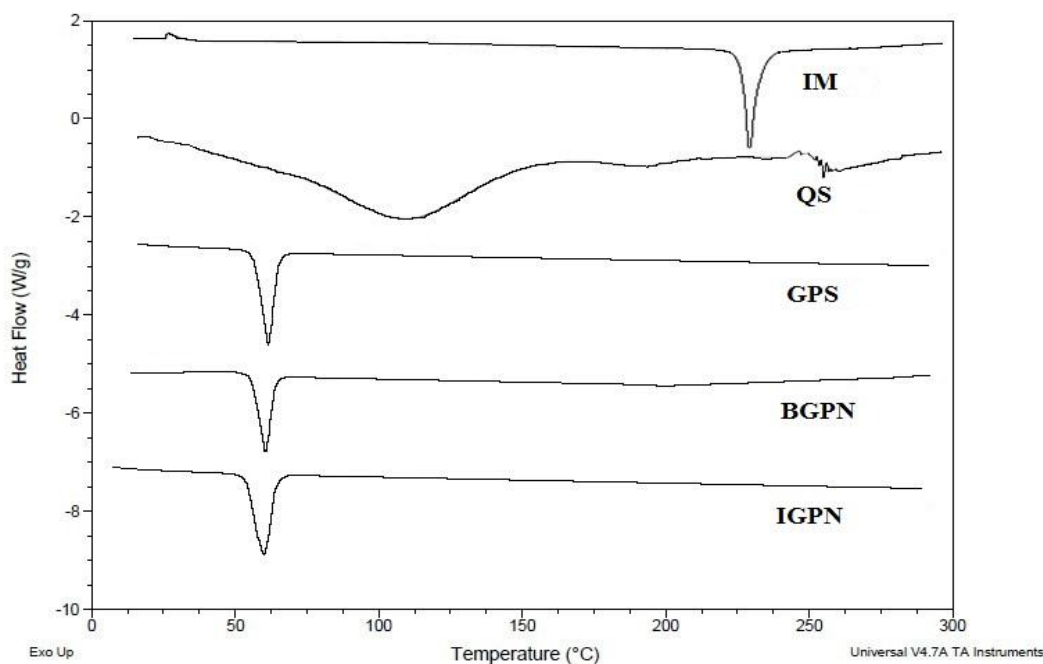


Figure 56. Overlay of DSC thermogram of IM: Imatinib mesylate, QS: quillaja saponin, GPS: bulk glyceryl palmitostearate, BGPN: Blank SLNs, IGPN: IM loaded SLNs of glyceryl palmitostearate

6.21 *IN VITRO* DRUG RELEASE

In vitro drug release patterns of ISN, IPN and IGPN in PBS pH 7.4 are shown in Figure 57, Figure 58 and Figure 59. In almost 12 hours, IM was completely released from all the SLNs prepared using different lipid carriers. Pure IM exhibited a rapid release across the dialysis membrane. Although long chain fatty acids like palmitic acid, stearic acid and glyceryl palmitostearate were used in the study, the release of IM from the lipid core was rapid due to the hydrophilic nature of IM. When conjugates of HAJ-SA and B12-SA were used in the preparation of SLNs, a comparatively sustained release profile was observed (Figure 57 and Figure 59). The comparative *in vitro* release profile using different lipids is shown in Figure 60.

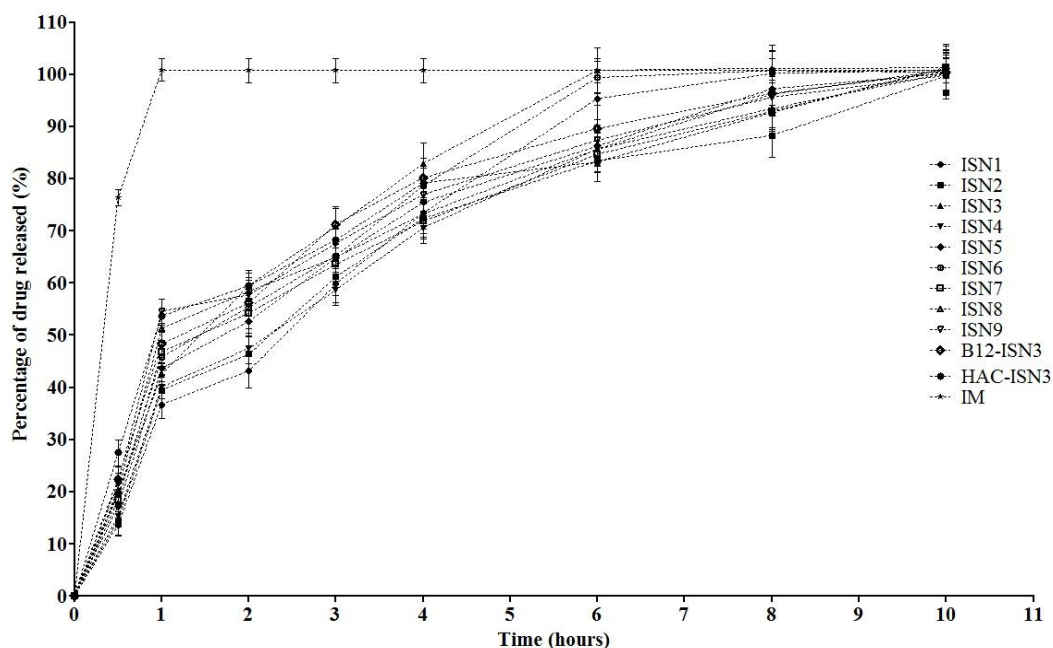


Figure 57. *In vitro* release profile of IM from ISN in phosphate buffer saline pH 7.4. Values are expressed as mean \pm standard deviation (n=3).

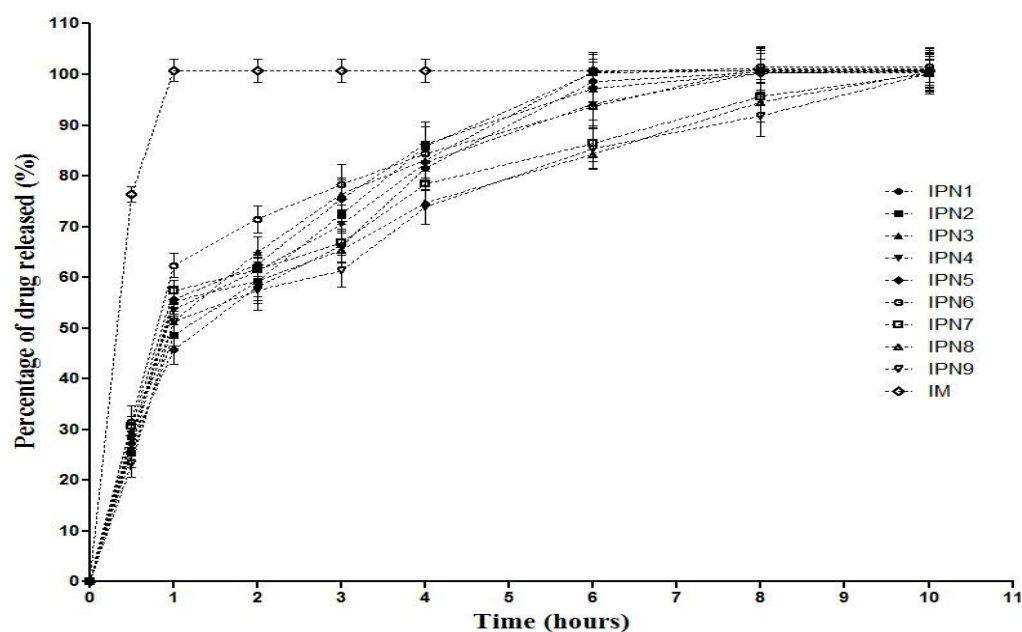


Figure 58. *In vitro* release profile of IM from IPN in phosphate buffer saline pH 7.4. Values are expressed as mean \pm standard deviation (n=3).

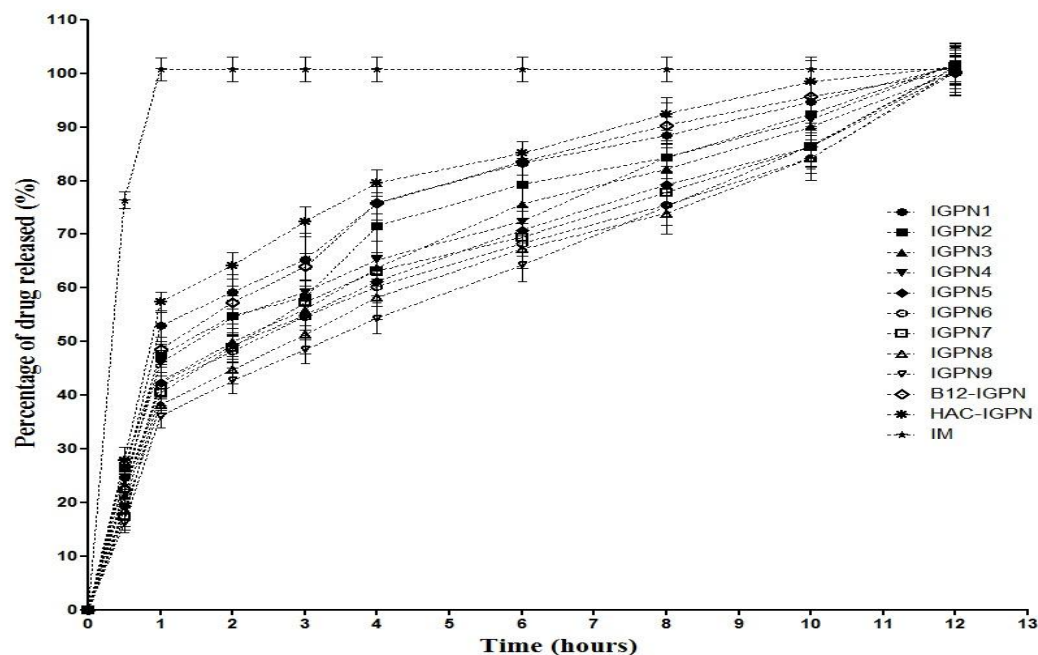


Figure 59. *In vitro* release profile of IM from IGPN in phosphate buffer saline pH 7.4. Values are expressed as mean \pm standard deviation (n=3).

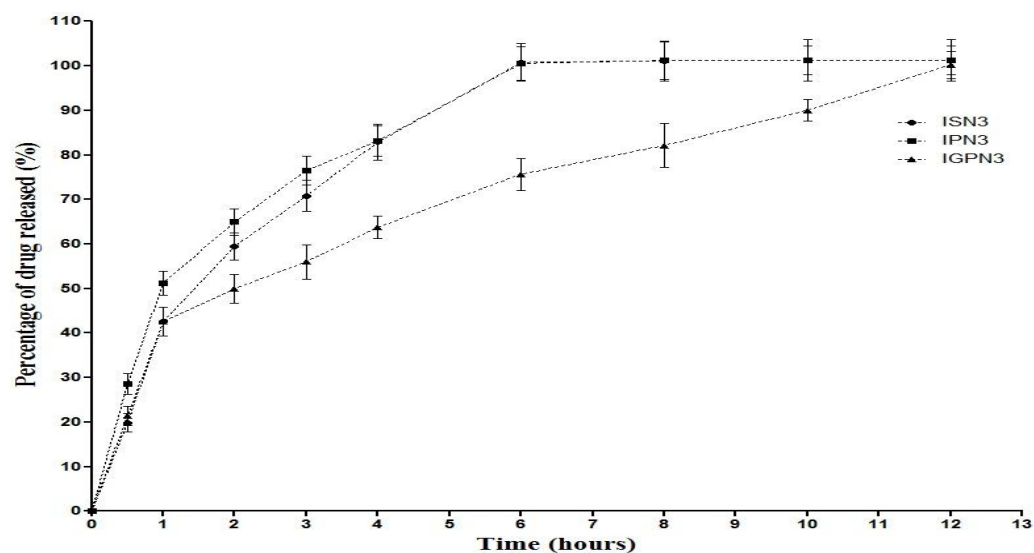


Figure 60. Comparative *in vitro* release profile of IM from ISN3, IPN3 and IGPN3 in phosphate buffer saline pH 7.4. Values are expressed as mean \pm standard deviation (n=3).

6.22 RELEASE KINETICS

The obtained release data was fitted into various kinetic models (zero order, first order, Higuchi and Korsmeyer-Peppas) to find out the mechanism of drug release from the SLNs. The results of the release kinetics was mentioned in Table 19,20 and 21.

Table 19. Mechanism of release of IM from ISN

Code	Zero order model (r ²)	First order model (r ²)	Higuchi model (r ²)	Korsmeyer-Peppas model	
				(r ²)	n
ISN1	0.7358	0.9778	0.9676	0.9518	0.517
ISN2	0.6588	0.9809	0.9751	0.9631	0.465
ISN3	0.5112	0.9894	0.9448	0.9330	0.412
ISN4	0.7005	0.9797	0.9830	0.9735	0.484
ISN5	0.5891	0.9810	0.9689	0.9619	0.434
ISN6	0.5466	0.9760	0.9520	0.9389	0.423
ISN7	0.5554	0.9630	0.9646	0.9626	0.417
ISN8	0.4484	0.9484	0.9397	0.9473	0.381
ISN9	0.3900	0.9483	0.9237	0.9367	0.365
B12-ISN	0.4380	0.9793	0.9422	0.9534	0.381
HAC-ISN	0.3071	0.9358	0.9124	0.9570	0.338
IM	-1.7513	0.9957	-0.0660	0.9631	0.465

Table 20. Mechanism of release of IM from IPN

Code	Zero order model (r ²)	First order model (r ²)	Higuchi model (r ²)	Korsmeyer- Peppas model	
				(r ²)	n
IPN1	0.4587	0.9756	0.9477	0.9561	0.387
IPN2	0.4016	0.9833	0.9281	0.9359	0.374
IPN3	0.2991	0.9821	0.9080	0.9413	0.344
IPN4	0.3121	0.9652	0.9160	0.9570	0.343
IPN5	0.2518	0.9744	0.8936	0.9359	0.331
IPN6	0.0681	0.9600	0.8344	0.9211	0.290
IPN7	0.2392	0.9207	0.8937	0.9564	0.321
IPN8	0.3435	0.9231	0.9187	0.9529	0.347
IPN9	0.4394	0.9382	0.9416	0.9562	0.375
IM	-1.7513	0.9957	-0.0660	0.9631	0.465

Table 21. Mechanism of release of IM from IGPN

Code	Zero order model (r ²)	First order model (r ²)	Higuchi model (r ²)	Korsmeyer- Peppas model	
				(r ²)	N
IGPN1	0.2374	0.9331	0.8905	0.9519	0.326
IGPN2	0.3681	0.9201	0.9323	0.9761	0.353
IGPN3	0.5205	0.9351	0.9666	0.9822	0.398
IGPN4	0.4302	0.9061	0.9438	0.9736	0.368
IGPN5	0.5398	0.9153	0.9628	0.9700	0.404
IGPN6	0.5121	0.8864	0.9556	0.9668	0.392
IGPN7	0.5550	0.9219	0.9618	0.9634	0.412
IGPN8	0.6322	0.9170	0.9749	0.9704	0.439
IGPN9	0.7272	0.9321	0.9829	0.9740	0.486
B12-IGPN	0.3313	0.9571	0.9185	0.9585	0.350
HAC-IGPN	0.0785	0.9404	0.8401	0.9387	0.294
IM	-2.1255	0.9958	-0.2663	0.9631	0.465

6.23 IN VITRO HAEMOLYSIS TEST

A comparative *in vitro* haemolytic analysis was performed for SLNs of IM (ISN, IPN and IGPN), QS, IM, and blank SLNs of palmitic acid, stearic acid and glyceryl palmitostearate. The results in Figure 61 and Figure 62 revealed that QS (50 µg/ml) showed haemolysis. But, SLNs of IM prepared using individual lipids like stearic acid and glyceryl palmitostearate, blank SLNs and IM did not induce haemolysis.

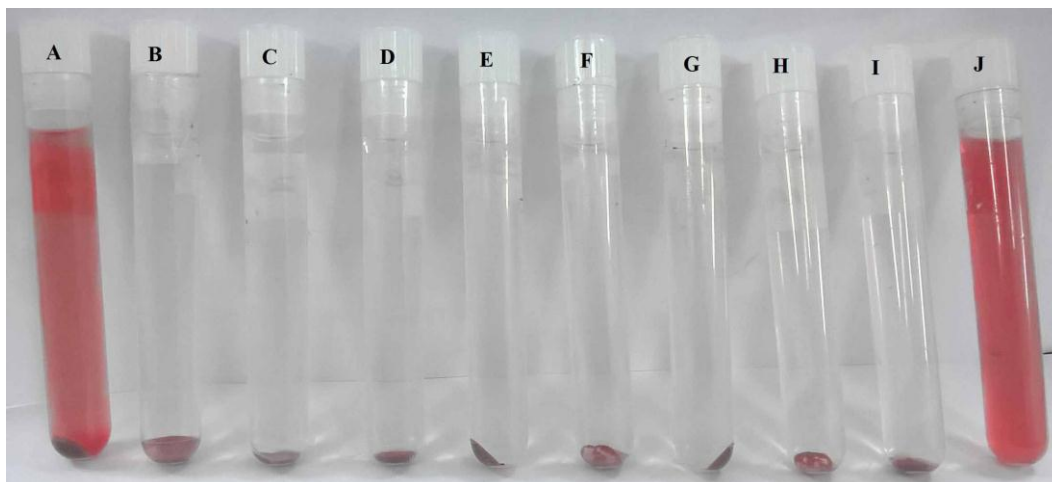


Figure 61. *In vitro* haemolysis assay performed in the presence of A) QS (50 $\mu\text{g/ml}$ solution in saline); B) and C) IM (10 $\mu\text{g/ml}$ and 20 $\mu\text{g/ml}$ in saline; D), E) and F) ISN3 (equivalent to IM concentration of 10 $\mu\text{g/ml}$, 20 $\mu\text{g/ml}$ and 30 $\mu\text{g/ml}$ and QS concentration of 150 $\mu\text{g/ml}$, 300 $\mu\text{g/ml}$ and 450 $\mu\text{g/ml}$); G) and H) BSNs (equivalent to QS concentrations of 50 $\mu\text{g/ml}$ and 150 $\mu\text{g/ml}$); I) Negative control- Saline; J) Positive control- Distilled water.

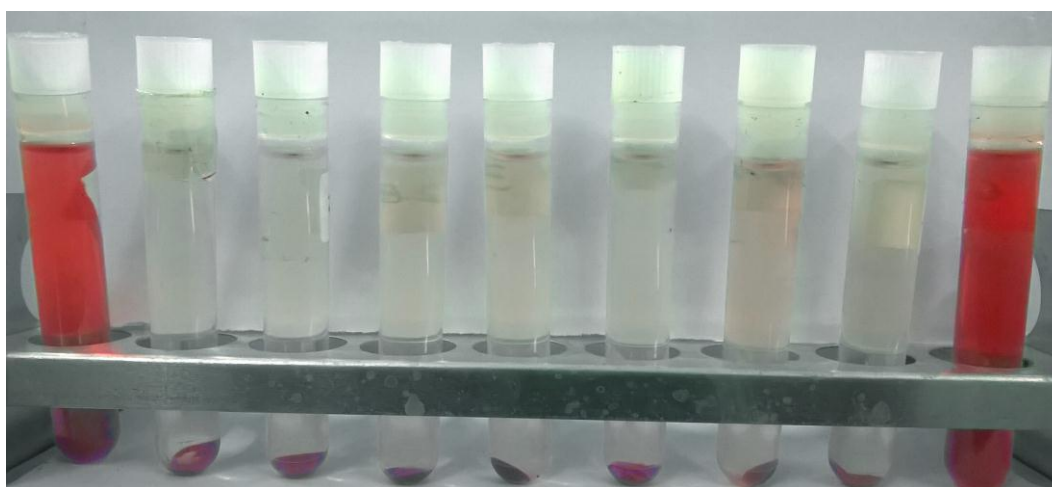


Figure 62. *In vitro* haemolysis assay performed in the presence of A) QS (50 $\mu\text{g/ml}$ solution in saline); B) IM (10 $\mu\text{g/ml}$ in saline); C) and D) IPN3 (equivalent to IM concentration of 10 $\mu\text{g/ml}$ and 20 $\mu\text{g/ml}$ and QS concentration of 150 $\mu\text{g/ml}$ and 300 $\mu\text{g/ml}$); E) BSLNs (equivalent to QS concentrations of 150 $\mu\text{g/ml}$); F) B12-IPN3 (equivalent to IM concentration of 20 $\mu\text{g/ml}$ and QS concentration of 300 $\mu\text{g/ml}$); G) HAC-IPN3 (equivalent to IM concentration of 20 $\mu\text{g/ml}$ and QS concentration of 300 $\mu\text{g/ml}$) H) Negative control- Saline; I) Positive control- Distilled water

6.24 IN VITRO CYTOTOXICITY STUDIES

In vitro cytotoxicity studies were performed for IM, QS, SLNs of IM (ISN and IGPN), their corresponding conjugated SLNs, blank SLNs of stearic acid and glyceryl palmitostearate) and blank SLNs (of stearic acid and glyceryl palmitostearate) and IM. Figure 63 represents the results of the cytotoxicity studies performed for IM, QS, ISN3, blank SLNs of stearic acid, blank SLNs of stearic acid and IM, B12-ISN3, HAJ-ISN3 and HAC-ISN3 in MCF7 cell line. Figure 64 represents the results of the cytotoxicity studies performed for IM, QS, IGPN3, blank SLNs of glyceryl palmitostearate, blank SLNs of glyceryl palmitostearate and IM, B12-IGPN3, HAJ-IGPN3 and HAC-IGPN3 in MCF7 cell line. The IC₅₀ values were mentioned in Table 22.

Correspondingly, the viability of the samples were also tested in RAW 264.7 cell line. Figure 65 and Figure 66 represents the results of the viability tests for the given samples. None of the samples were found to be toxic against RAW 264.7 cell line.

Table 22. IC₅₀ values of various samples

S No	Name of the sample	IC ₅₀ value *
1	IM	7.39
2	QS	8.17
3	ISN3	1.23
4	Blank ISN3	6.91
5	Blank ISN3 + IM	3.11
6	B12-ISN3	1.03
7	HAI-ISN3	1.17
8	HAC-ISN3	0.76
9	IGPN3	1.80
10	Blank IGPN3	6.31
11	Blank IGPN3 + IM	2.21
12	B12-IGPN3	1.45
13	HAI-IGPN3	1.25
14	HAC-IGPN3	0.91

* QS concentration is represented by µg/ml unit, whereas all other samples are represented in µM concentration.

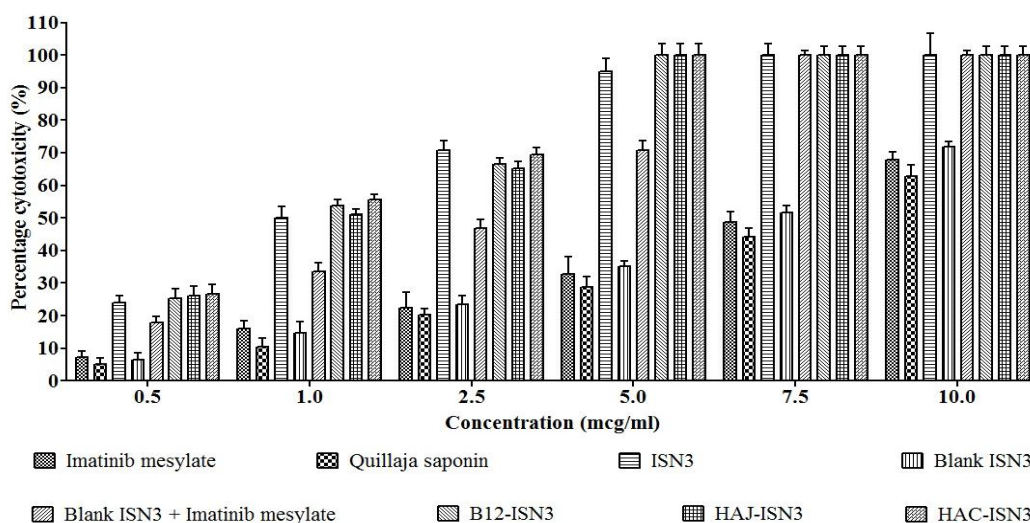


Figure 63. Graph showing cytotoxicity in MCF7 cells in the presence of IM, QS, ISN3, Blank ISN3, mixture of blank ISN3 + IM, B12- ISN3, HAJ- ISN3 and HAC- ISN3 as revealed by MTT assay. Values are expressed as mean \pm standard deviation (n=3). * QS concentration is represented by $\mu\text{g/ml}$ unit, whereas all other samples are represented in μM concentration.

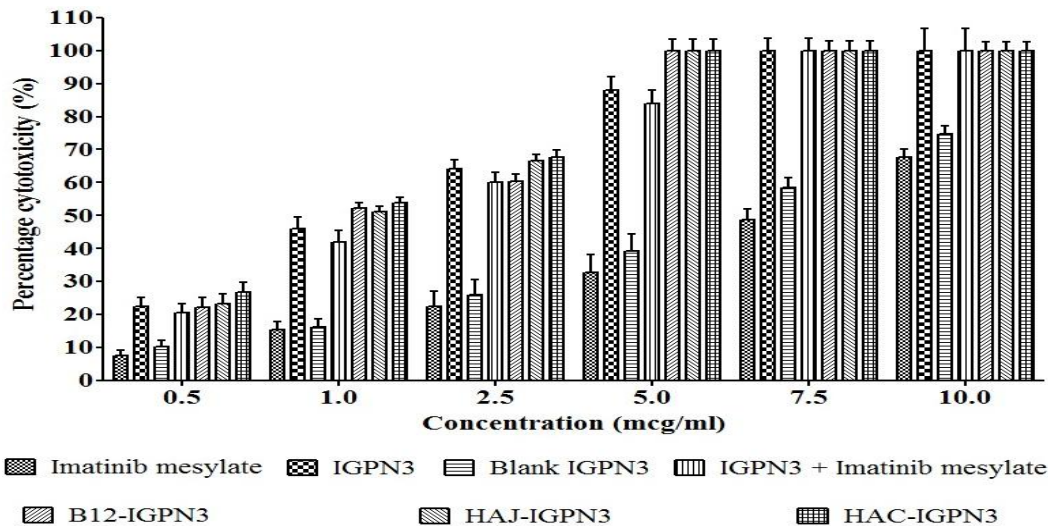


Figure 64. Graph showing cytotoxicity in MCF7 cells in the presence of IM, IGPN3, Blank IGPN3, mixture of blank IGPN3 + IM, B12-IGPN3, HAJ-IGPN3 and HAC-IGPN3 as revealed by MTT assay. Values are expressed as mean \pm standard deviation (n=3).

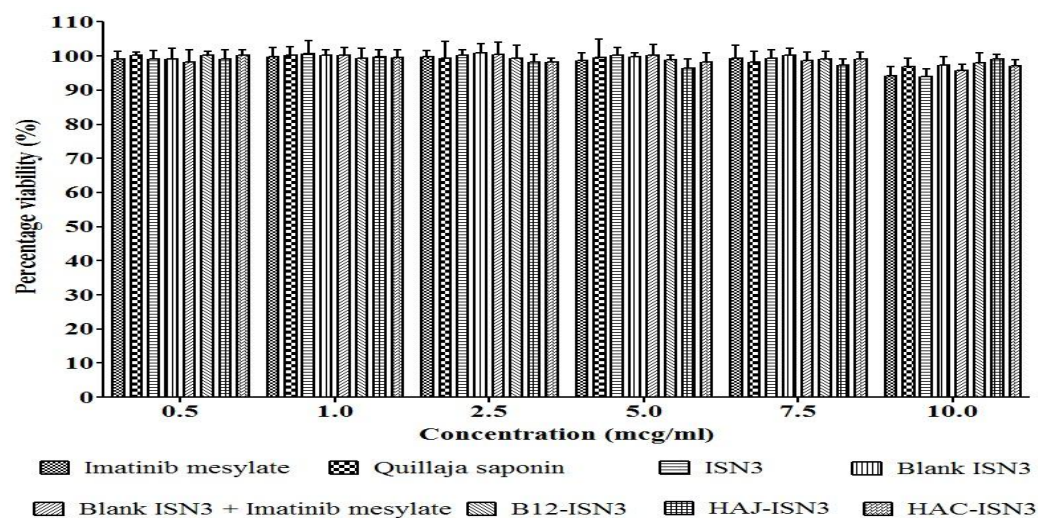


Figure 65. Graph showing viability in RAW 264.7 cells in the presence of IM, QS, ISN3, Blank ISN3, mixture of blank ISN3 + IM, B12- ISN3, HAJ- ISN3 and HAC- ISN3 as revealed by MTT assay. Values are expressed as mean \pm standard deviation (n=3). * QS concentration is represented by $\mu\text{g/ml}$ unit, whereas all other samples are represented in μM concentration.

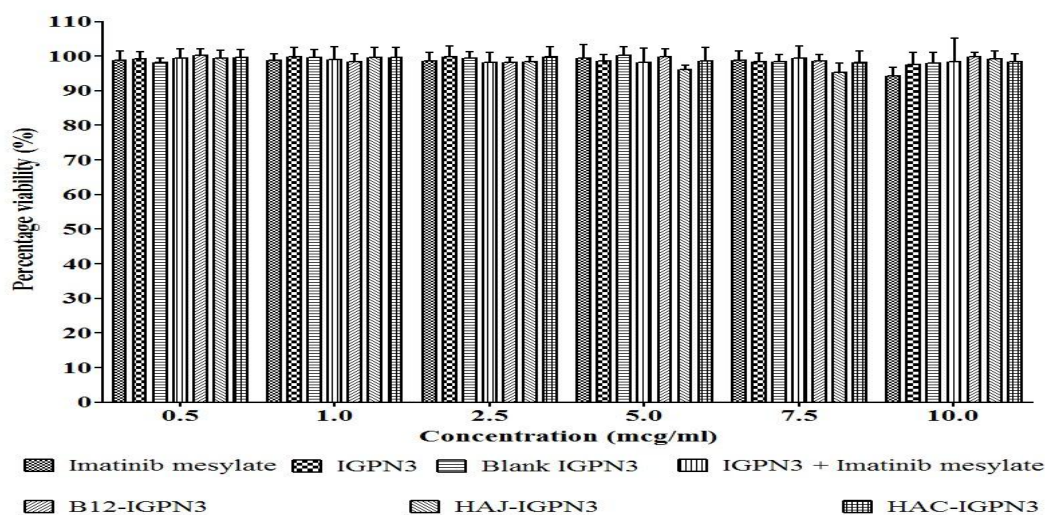


Figure 66. Graph showing viability in RAW 264.7 cells in the presence of IM, IGPN3, Blank IGPN3, mixture of blank IGPN3 + IM, B12-IGPN3, HAJ-IGPN3 and HAC-IGPN3 as revealed by MTT assay. Values are expressed as mean \pm standard deviation (n=3).

6.25 APOPTOSIS ANALYSIS

MCF 7 cell line treated with free IM, IGPN3 and HA-IGPN3 were stained with propidium iodide and observed for the DNA damage. The results of the study after treatment with control and IM (and nanoparticles) were represented in Figure 67. Figure 67 (b), (d), (f) and (h) represents the fluorescence images of MCF7 cells after treatment with control, free IM, IGMN, HA-ILN treated MCF7 cells. Their corresponding light microscopic images are shown in Figure 67 (a), (c), (e), and (g).

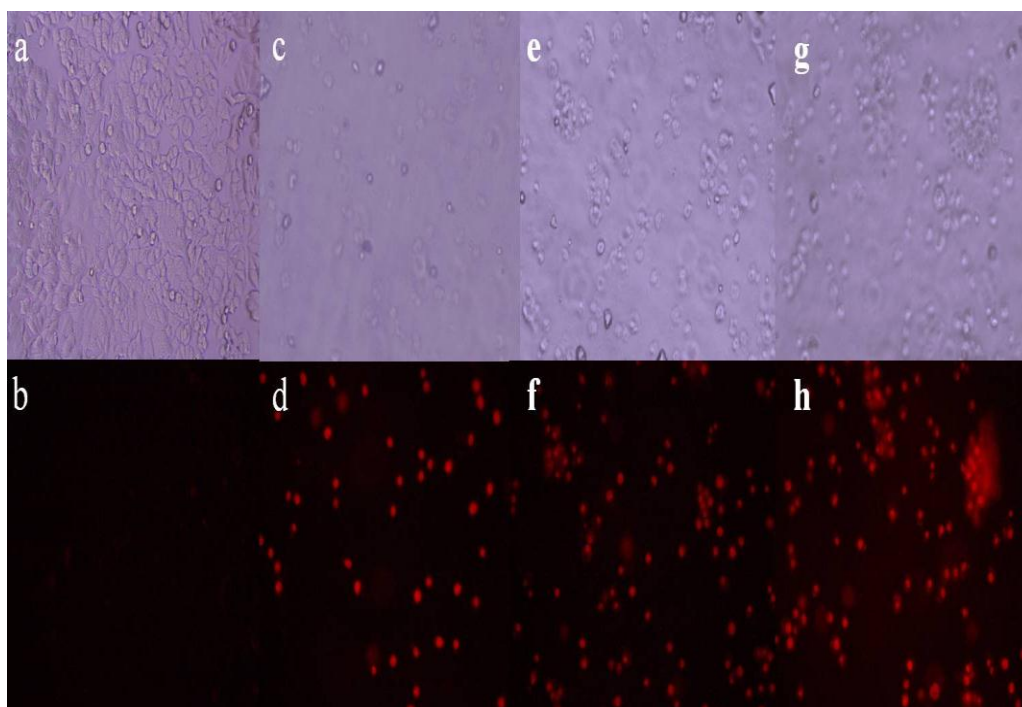


Figure 67. Propidium iodide staining of control (b), free IM (d), IGMN (f), HA-ILN treated (h) MCF7 cells showing dead cells in the later. Corresponding light microscopic images are shown above (a), (c), (e) and (g).

6.26 STERILITY TESTING

In order to ensure the sterility of ISN3, B12-ISN, HAC-ISN, IGPN3, HAC-IGPN and IM in pH 7.4 PBS, the samples were tested for sterility according to pharmacopoeial requirements. Sterility was evaluated by the observation of the media containing the respective samples for the proliferation of bacteria or fungi during the incubation period. These results demonstrated in Figure 68 and Figure 69 did not show any visible bacterial or fungal growth for all the batches of nanoparticles tested. But, the positive controls showed substantial increase of turbidity indicating bacterial or fungal growth. These results suggest that the prepared SLNs are sterile.



Figure 68. Sterility testing indicating absence of bacterial growth after 24 hours incubation with 1) ISN3, 2) B12-ISN, 3) HAC-ISN, 4) IGPN3, 5) HAC-IGPN and 6) IM in pH 7.4 PBS



Figure 69. Sterility testing indicating absence of fungal growth after 14 days incubation with 1) ISN3, 2) B12-ISN, 3) HAC-ISN, 4) IGPN3, 5) HAC-IGPN and 6) IM in pH 7.4 PBS

6.27 IN VIVO PHARMACOKINETIC STUDIES

Pharmacokinetic parameters of IM in blood:

Pharmacokinetic studies were performed in female wistar rats after subcutaneous administration to quantify the amount of drug present in the blood at different time points. Various pharmacokinetic parameters like C_{max} , T_{max} , $T_{1/2}$, MRT, AUC_{0-t} , $AUC_{0-\infty}$, $AUMC_{0-t}$, $AUMC_{0-\infty}$ and clearance were calculated using Winonlin 5.3 and the values are represented in Table 23. Figure 70 and Figure 71 represents the plasma concentration profiles of different samples at different time intervals.

Table 23. Pharmacokinetic parameters of IM in blood

Pharmacokinetic parameter	IM	IGPN3	HA-IGPN	ISN3	B12-ISN	HA-ISN
$T_{1/2}$ (h)	18.331 ± 0.5	21.7 ± 4.1	49.01 ± 4	20.3 ± 5.5	25.8 ± 0.5	40.8 ± 3.7
T_{max} (h)	4	12	12	8	12	12
C_{max} (µg/ml)	1947.7 ± 38.9	1475.3 ± 87.3	1377.7 ± 41.3	1615.3 ± 79.1	1842.7 ± 45.6	1290 ± 37.987
AUC_{0-t} (µg/ml*h)	34483.8 ± 2608.7	66796.1 ± 4135.7	79321.6 ± 1322.3	60167.5 ± 1468.7	71557.2 ± 530.9	64319.5 ± 1371.9
$AUC_{0-\infty}$ (µg/ml*h)	36979.2 ± 2534.9	73523.51 ± 5733.6	133356 ± 4617.6	67347.8 ± 2521.6	84451.4 ± 877.8	97178.8 ± 5992.9
$MRT_{0-\infty}$ (h)	20.4 ± 0.2	30.4 ± 0.2	35.2 ± 0.6	27.9 ± 0.6	28.5 ± 0.2	33.1 ± 0.4
Cl_{obs}	410.0 ± 31.1.0	204.9 ± 16.1	112.6 ± 4.0	222.9 ± 8.5	177.6 ± 1.9	154.8 ± 9.9

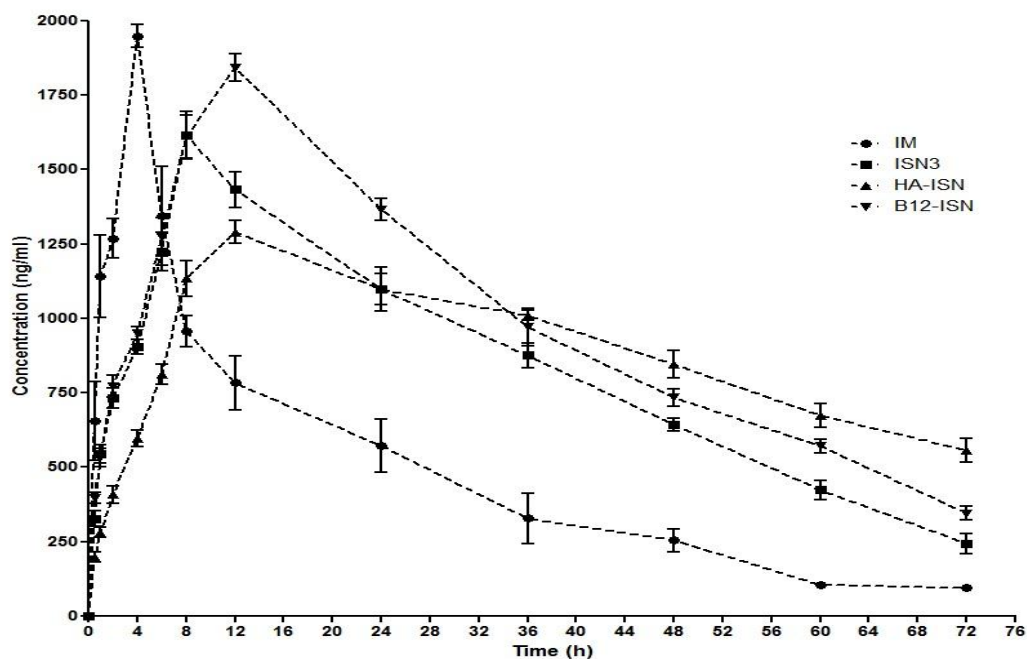


Figure 70. Plasma drug concentration profile after subcutaneous administration of IM, ISN3, B12-ISN and HA-ISN.

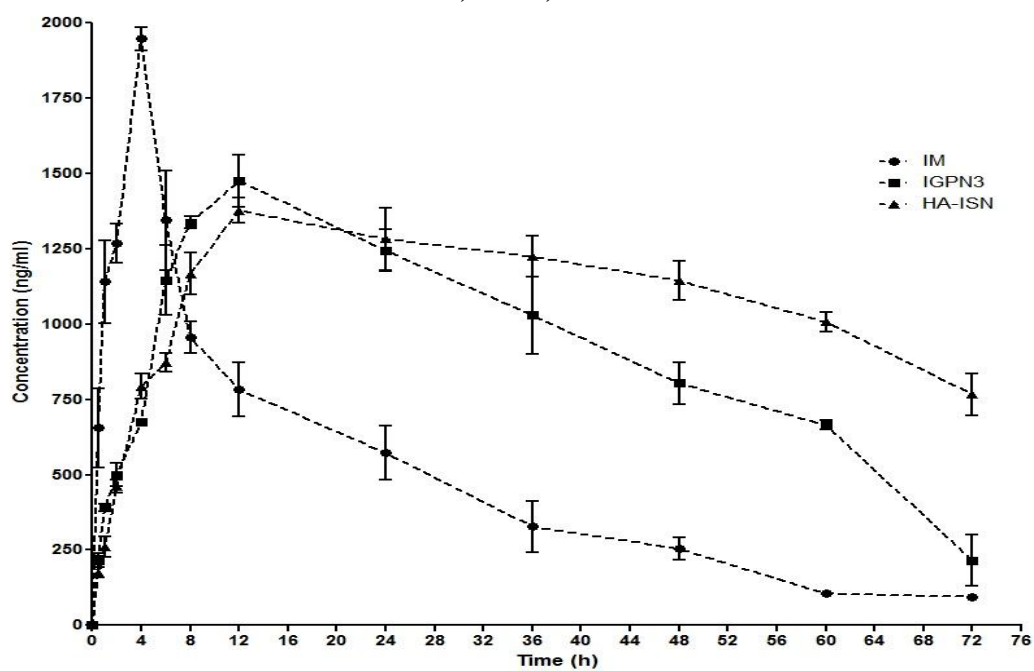


Figure 71. Plasma drug concentration profile after subcutaneous administration of IM, IGPN3 and HA-IGPN.

The lymph nodes were isolated to quantify the amount of IM that has reached after subcutaneous administration (Figure 72). Table 24 represents the pharmacokinetic parameters of IM in the lymph nodes. Figure 73 represents the lymph node drug concentration profile after subcutaneous administration of IM, IGPN3 and HA-IGPN.

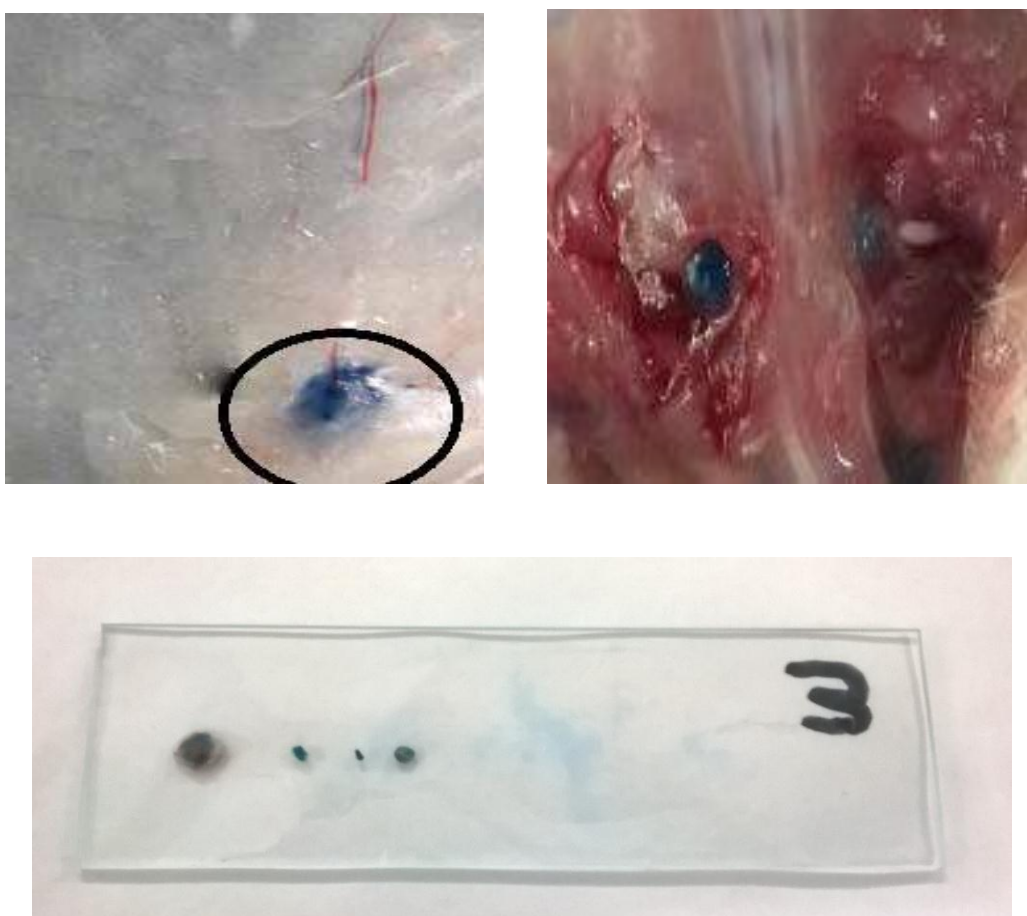


Figure 72. Lymph nodes in rat

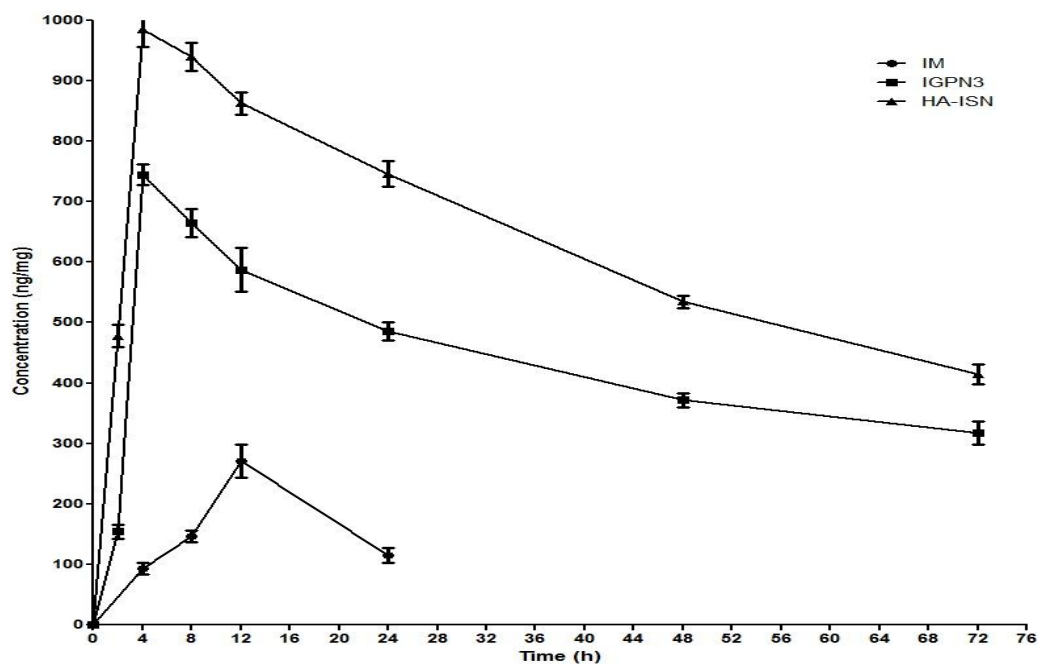


Figure 73. Lymph node drug concentration profile after subcutaneous administration of IM, IGPN3 and HA-IGPN.

Table 24. Pharmacokinetic parameters of IM in lymph nodes

Pharmacokinetic parameter	IM	IGPN	HA-IGPN
$T_{1/2}$ (h)	-	68.24 ± 4.1	53.84 ± 4
T_{max} (h)	12	4	4
C_{max} ($\mu\text{g/ml}$)	270.7 ± 38.9	744 ± 87.3	984.3 ± 41.3
AUC_{0-t} ($\mu\text{g/ml}\cdot\text{h}$)	3809.3 ± 2608.7	31364 ± 4135.7	45783 ± 1322.3
$AUC_{0-\infty}$ ($\mu\text{g/ml}\cdot\text{h}$)	-	62607.1 ± 5733.6	77971.4 ± 4617.6
$MRT_{0-\infty}$ (h)	-	101.1 ± 0.2	80.2 ± 0.6

6.28 STABILITY STUDIES

Stability studies were carried out ISN3, HAC-ISN, B12-ISN, IGPN3, HAC-IGPN and B12-IGPN at room temperature (20 - 25°C) and refrigerated conditions (3 to 5°C) over a period of 12 months. The stability of the formulations were evaluated for every 3 months by checking the appearance of the formulations, particle size, polydispersity index, zeta potential and entrapment efficiency. The results over a period of 12 months are mentioned from Table 25 to Table 28. The results indicate that the formulations are comparatively stable for 12 months in refrigerated conditions.

Table 25. Particle size of the formulations over a period of 12 months

Stability Condition	Formulation code	Average Particle size (nm)					
		Month					
		0	1	3	6	9	12
Room temperature (25 °C)	ISN3	159.5 ± 4.7	189.2 ± 9.3	304.8 ± 13.8	1132.4 ± 45.2	--	--
Refrigerated temperature (3 to 5 °C)		159.5 ± 4.7	161.3 ± 3.6	163.1 ± 4.1	167.6 ± 5.3	172.3 ± 5.8	189.3 ± 8.2
Room temperature (25 °C)	B12-ISN	169.1 ± 3.2	194.5 ± 5.9	347.7 ± 17.4	1094.3 ± 36.2	1489.5 ± 78.2	--
Refrigerated temperature (3 to 5 °C)		169.1 ± 3.2	170.2 ± 2.8	171.4 ± 3.9	184.6 ± 4.5	195.1 ± 6.1	208.4 ± 7.2
Room temperature (25 °C)	HAC-ISN	87.3 ± 5.9	203.4 ± 25.6	610.8 ± 65.3	--	--	--
Refrigerated temperature (3 to 5 °C)		87.3 ± 5.9	92.4 ± 3.8	95.7 ± 4.5	103.7 ± 5.8	117.3 ± 6.5	124.6 ± 7.4
Room temperature (25 °C)	IGPN3	106.4 ± 4.7	126.3 ± 5.3	178.2 ± 7.2	589.3 ± 16.8	1285.0 ± 104.5	--
Refrigerated temperature (3 to 5 °C)		106.4 ± 4.7	107.1 ± 5.3	110.5 ± 5.2	116.8 ± 6.3	121.9 ± 8.1	136.2 ± 12.7

Stability Condition	Formulation code	Average Particle size (nm)					
		Month					
		0	1	3	6	9	12
Room temperature (25 °C)	B12-IGPN	118.7 ± 3.9	156.8 ± 4.5	654.8 ± 35.8	1436.2 ± 102.4	--	--
Refrigerated temperature (3 to 5 °C)		118.7 ± 3.9	120.4 ± 2.7	124.6 ± 3.5	131.3 ± 4.6	149.7 ± 5.1	152.2 ± 6.4
Room temperature (25 °C)	HAC-IGPN	92.1 ± 2.4	179.2 ± 4.9	534.9 ± 39.2	--	--	--
Refrigerated temperature (3 to 5 °C)		92.1 ± 2.4	94.3 ± 3.3	96.7 ± 4.4	98.5 ± 5.7	101.8 ± 5.3	105.1 ± 6.1

Table 26. Polydispersity index of the formulations over a period of 12 months

Stability Condition	Formulation code	Polydispersity index (nm)					
		Month					
		0	1	3	6	9	12
Room temperature (25 °C)	ISN3	0.127 ± 0.01	0.248 ± 0.09	0.843 ± 0.101	1 ± 0.0	--	--
Refrigerated temperature (3 to 5 °C)		0.127 ± 0.01	0.124 ± 0.02	0.135 ± 0.08	0.132 ± 0.06	0.154 ± 0.04	0.205 ± 0.06
Room temperature (25 °C)	B12-ISN	0.205 ± 0.01	0.294 ± 0.08	0.348 ± 0.113	1.0 ± 0.0	1.0 ± 0.0	--
Refrigerated temperature (3 to 5 °C)		0.205 ± 0.01	0.212 ± 0.01	0.235 ± 0.05	0.242 ± 0.05	0.278 ± 0.07	0.285 ± 0.08
Room temperature (25 °C)	HAC-ISN	0.162 ± 0.01	0.348 ± 0.123	1.0 ± 0.0	--	--	--
Refrigerated temperature (3 to 5 °C)		0.162 ± 0.01	0.159 ± 0.02	0.173 ± 0.02	0.178 ± 0.05	0.241 ± 0.06	0.256 ± 0.07
Room temperature (25 °C)	IGPN3	0.08 ± 0.01	0.213 ± 0.05	0.893 ± 0.101	1.0 ± 0.0	--	--

Stability Condition	Formulation code	Polydispersity index (nm)					
		Month					
		0	1	3	6	9	12
Refrigerated temperature (3 to 5 °C)		0.08 ± 0.01	0.102 ± 0.02	0.113 ± 0.02	0.128 ± 0.06	0.132 ± 0.05	0.241 ± 0.103
Room temperature (25 °C)	B12-IGPN	0.194 ± 0.02	0.231 ± 0.05	0.764 ± 0.178	1.0 ± 0.0	--	--
Refrigerated temperature (3 to 5 °C)		0.194 ± 0.02	0.195 ± 0.01	0.203 ± 0.05	0.214 ± 0.08	0.262 ± 0.10	0.281 ± 0.12
Room temperature (25 °C)	HAC-IGPN	0.08 ± 0.01	0.342 ± 0.11	1.0 ± 0.0	--	--	--
Refrigerated temperature (3 to 5 °C)		0.08 ± 0.01	0.07 ± 0.01	0.105 ± 0.03	0.112 ± 0.04	0.172 ± 0.09	0.268 ± 0.102

Table 27. Zeta potential of the formulations over a period of 12 months

Stability Condition	Formulation code	Average Particle size (nm)					
		Month					
		0	1	3	6	9	12
Room temperature (25 °C)	ISN3	0.95 ± 0.5	-1.36 ± 0.7	-15.7 ± 3.6	-19.2 ± 7.2	--	--
Refrigerated temperature (3 to 5 °C)		0.95 ± 0.5	0.65 ± 0.3	-1.26 ± 0.5	-2.27 ± 0.4	-2.17 ± 0.6	-3.06 ± 0.7
Room temperature (25 °C)	B12-ISN	10.2 ± 1.2	14.7 ± 3.5	17.8 ± 4.2	18.4 ± 3.7	19.3 ± 5.4	--
Refrigerated temperature (3 to 5 °C)		10.2 ± 1.2	8.3 ± 0.9	6.4 ± 2.4	9.4 ± 2.7	11.3 ± 3.2	14.3 ± 5.1
Room temperature (25 °C)	HAC-ISN	-12.8 ± 1.7	-18.2 ± 3.7	-21.3 ± 4.5	--	--	--
Refrigerated temperature (3 to 5 °C)		-12.8 ± 1.7	-11.5 ± 4.1	-14.3 ± 6.3	-11.7 ± 5.8	-15.8 ± 3.7	-16.2 ± 4.5

Stability Condition	Formulation code	Average Particle size (nm)					
		Month					
		0	1	3	6	9	12
Room temperature (25 °C)	IGPN3	-1.03 ± 0.14	-21.3 ± 2.6	-15.8 ± 6.1	-13.2 ± 5.9	-17.6 ± 4.2	--
Refrigerated temperature (3 to 5 °C)		-1.03 ± 0.14	-2.4 ± 0.8	-4.6 ± 1.0	-3.1 ± 1.2	-5.3 ± 1.4	-5.8 ± 0.7
Room temperature (25 °C)	B12-IGPN	1.63 ± 0.5	8.4 ± 2.7	15.2 ± 3.9	17.3 ± 4.0	--	--
Refrigerated temperature (3 to 5 °C)		1.63 ± 0.5	2.3 ± 0.4	2.8 ± 1.2	1.89 ± 0.3	3.4 ± 0.5	4.2 ± 1.3
Room temperature (25 °C)	HAC-IGPN	-10.67 ± 1.32	-14.7 ± 2.0	-16.2 ± 4.3	--	--	--
Refrigerated temperature (3 to 5 °C)		-10.67 ± 1.32	-7.3 ± 1.4	-8.5 ± 2.7	-12.3 ± 4.9	-11.7 ± 3.0	-12.0 ± 2.1

Table 28. Entrapment efficiency of formulations over a period of 12 months

Stability Condition	Formulation code	Entrapment efficiency (%)					
		Month					
		0	1	3	6	9	12
Room temperature (25 °C)	ISN3	61.3 ± 1.1	64.7 ± 3.2	62.9 ± 5.6	58.6 ± 4.5	--	--
Refrigerated temperature (3 to 5 °C)		61.3 ± 1.1	61.5 ± 1.4	59.1 ± 2.5	57.3 ± 3.6	55.2 ± 3.8	53.2 ± 4.9
Room temperature (25 °C)	B12-ISN	56.9 ± 1.4	58.2 ± 3.5	54.8 ± 4.3	54.1 ± 3.1	48.2 ± 5.3	--
Refrigerated temperature (3 to 5 °C)		56.9 ± 1.4	57.2 ± 2.3	55.2 ± 2.6	53.2 ± 1.2	52.6 ± 2.8	48.3 ± 3.7

Stability Condition	Formulation code	Entrapment efficiency (%)					
		Month					
		0	1	3	6	9	12
Room temperature (25 °C)	HAC-ISN	47.8 ± 2.1	45.2 ± 2.5	38.3 ± 5.3	--	--	--
Refrigerated temperature (3 to 5 °C)		47.8 ± 2.1	46.2 ± 1.7	45.5 ± 3.5	43.6 ± 2.7	43.1 ± 3.9	42.6 ± 2.6
Room temperature (25 °C)	IGPN3	55.1 ± 1.1	53.7 ± 2.1	52.1 ± 2.8	45.7 ± 2.5	36.8 ± 2.7	--
Refrigerated temperature (3 to 5 °C)		55.1 ± 1.1	54.6 ± 2.4	53.2 ± 1.7	52.4 ± 2.2	52.7 ± 2.6	51.3 ± 3.1
Room temperature (25 °C)	B12-IGPN	65.9 ± 0.6	60.5 ± 1.4	51.2 ± 2.3	43.1 ± 2.7	--	--
Refrigerated temperature (3 to 5 °C)		65.9 ± 0.6	64.1 ± 1.6	63.2 ± 2.5	61.6 ± 3.1	60.3 ± 1.6	58.3 ± 1.4
Room temperature (25 °C)	HAC-IGPN	43.4 ± 0.7	40.6 ± 1.3	38.3 ± 2.4	--	--	--
Refrigerated temperature (3 to 5 °C)		43.4 ± 0.7	42.6 ± 2.1	41.5 ± 1.4	41.8 ± 1.9	40.5 ± 1.7	39.1 ± 2.2

Discussion

7. DISCUSSION

7.1 PREFORMULATION AND ANALYTICAL STUDIES

7.1.1 UV Spectroscopy:

The wavelength at which maximum amount of radiation is absorbed is called λ_{\max} and it is specific for every compound. In this study, the maximum absorption for Imatinib mesylate (IM) was observed at 256 nm, which was fixed as the λ_{\max} . A calibration curve was plotted with different concentrations of IM against its corresponding absorbance values. The calibration curve Figure 12. indicated a linear increase of absorbance when its corresponding concentrations values increased. The r^2 value (regression coefficient) was found to be 0.9995.

7.1.2 High Pressure Liquid Chromatography:

An analytical method was additionally developed using high pressure liquid chromatography to estimate the concentrations of IM in different pharmaceutical and biological samples. Different chromatographic variables i.e., columns, composition and ratio of the mobile phase, pH of the mobile phase and peak modifiers in mobile phase were varied and their influence on the elution of IM was studied. The effects of various parameters for the development of an optimised method were studied as follows:

Effect of mobile phase ratio:

Initially, different ratios of acetonitrile and water viz., 50:50, 40:60, 30:70 at pH 2.8 adjusted with formic acid were used as mobile phase. At 50:50 ratio, IM was eluted at 4.6 minutes with fronting. When the ratio was changed to 40:60 ratio, the elution time was reduced to 4 minutes with mild fronting. Finally, when 30:70 ratio was used, IM eluted at 3.5 minutes. Hence, mobile phase containing 30% acetonitrile and 70% water was selected as mobile phase.

Effect of pH:

Initially, when the pH was adjusted using orthophosphoric acid, an additional peak along with the peak of IM was observed. Later, when the pH was adjusted to 3.4 using 0.1% formic acid, the extra peak disappeared. Hence, the pH of the mobile phase was adjusted to 3.4 using 0.1% formic acid.

Effect of nature of stationary phase:

Different stationary phases like Phenomenex Luna C18 [(150 x 4.6mm), 5 μ], Sunfire C18 [(150 x 4.6mm), 3.5 μ], Sunfire C8 [(150 x 4.6mm), 3.5 μ] were used as columns. When Phenomenex Luna C18 was used, the drug did not elute and the peaks corresponding to IM were not observed. When Sunfire C18 was used, IM eluted at 1.1 min along with void volume. Various attempts to improve the retention time and peak symmetry using different ratios of mobile phase have been futile. Finally, when Sunfire C8 column was used, IM eluted at 4.6 minutes without any tailing and fronting. Hence for the present study, Sunfire C8 was used as the column.

Effect of flow rate:

At different flow rates of 0.2 ml/ min, 0.3 ml/ min and 0.5 ml/ min, the retention time of IM was 4.6 min, 3.5 min, and 1.1 min respectively. When the flow rate was maintained at 0.3 ml/ min a symmetric and well defined peak was observed. Hence, for the present study, a flow rate of 0.3 ml/ min was selected.

Thus, finally a Sunfire C8 [(4.6 x 150 mm), 3.5 μ] column with a mobile phase consisting of 30:70 of acetonitrile: water at pH 3.4 (0.1 % formic acid) with a flow rate of 0.3 ml/ min were optimised to estimate IM in pharmaceutical and biological samples. Using these conditions, a calibration curve for estimation of IM in pharmaceutical samples was plotted with the

obtained peak area for each concentration and the regression equations were calculated. A correlation coefficient of 0.9998 was observed Figure 14. Similarly, for the quantification of IM in plasma, a calibration curve against the peak area for each concentration was plotted and correlation co-efficient (r^2) was found to be of 0.9992 (Figure 15). The results of the validation studies indicated that the developed method was accurate, precise with good LOD and LOQ values. There were no changes in the concentration of IM during interday and intraday testing and sample degradation was not observed. Additionally, the developed method showed good limit of detection (LOD) and limit of quantification (LOQ). The test for specificity indicated that the peak of IM was pure without any interference. Thus the developed method was specific for IM. The results of the stability studies of IM in rat plasma indicated good stability at room temperature (25°C) and refrigerated temperatures (4°C) for 24 h. Additionally, IM was also stable in deproteinized plasma and in freeze-thaw cycles when stored at -20 C° for 6 months.

7.1.3 SCREENING FOR THE PRESENCE OF INTERACTIONS USING INFRA RED SPECTROSCOPY

IR spectroscopic studies were performed to rule out for the presence of any interactions between IM and the excipients (lipids and surfactant) used in the study. Major wave numbers at for pure IM like 1177 cm^{-1} , 1418 cm^{-1} , 2111 cm^{-1} and 3445 cm^{-1} which correspond to the ester group, amide groups, alkynyl stretching and aromatic amine respectively were observed. The IR spectrum of quillaja saponin (QS) showed specific wave numbers at 1728 cm^{-1} and 3389 cm^{-1} corresponding to the ketone group and alcoholic -OH groups present in the saponin. Additionally, strong bands were observed in the region of 1340- 1450 cm^{-1} and 2940 cm^{-1} , which corresponded to the ketone and carboxylic acid groups present in the saponin. The IR spectrum of stearic acid

and palmitic acid prominently showed wave numbers in the regions of 2500-3000 cm^{-1} which correspond to carboxylic acid groups present in the fatty acids. The IR spectrum of glyceryl palmitostearate and glycerylmonostearate showed wave numbers in the regions of 1200 cm^{-1} and 1700 cm^{-1} representing the acetate and ester functional groups present in the monoglyceride derivatives. In the physical mixture of IM and corresponding lipids (stearic acid, palmitic acid, glyceryl monostearate, glyceryl palmitostearate and geleol mono and diglycerides) the wave numbers corresponding to IM were present. Additionally, these wave numbers were also present in the physical mixtures of IM, QS and corresponding lipid. These results clearly indicate the stability of IM in the lipid melts and physical mixtures and rule out the presence of interactions between the drug and excipients used. The above mentioned lipids and surfactant can be used for the preparation of solid lipid nanoparticles.

7.2 SOLUBILITY OF IMATINIB MESYLTE IN LIPIDS: INFLUENCE OF MOLECULAR, CHEMICAL AND PHYSICOCHEMICAL PROPERTIES AND DEVELOPMENT OF A PREDICTORY MODEL

During the preparation of LBFs, solubilisation of drugs in the lipids is a crucial step to achieve good encapsulation efficiency and stability. Although lipophilic drugs can be solubilised in the lipids, finding a lipid that can solubilise hydrophilic drugs is a challenge [103]. Predicting the solubility of drugs in lipids is challenging unlike predicting their solubility in water. Water exists with a simple chemical structure, H₂O and with an established set of physicochemical properties. Thus, examining the influence of the various physicochemical properties of the drugs on solubility in water can easily be performed as compared to lipids. Lipids represent a broad term encompassing different categories like fatty acids, partial glycerides (mono, di and triglycerides), mixtures of fatty acids and partial glycerides, etc [122]. Each of these categories additionally has several lipids which vary in their chemical structure and physicochemical properties. Thus, screening or prediction of drug solubility in lipids includes examining the influence of the chemical structures and physicochemical properties of both drugs and lipids. Although some models have been developed to predict the solubility of the drugs in the lipids, they examined the molecular descriptors of the drugs which influence their solubilisation in the lipid excipients [133,150,165]. However, the influence of the molecular and physicochemical descriptors of various lipids affecting the solubility of drug have not been reported yet to the best of our knowledge. In this study, the influence of various molecular and physicochemical descriptors of the lipids on the solubility of IM was evaluated and a statistical correlation was developed among them using MLR to theoretically quantify the amount of IM that could be solubilised.

Various categories of lipids like fatty acids (myristic acid, palmitic acid, stearic acid, behenic acid), their mono, di and triglyceride derivatives (glyceryl palmitostearate, glyceryl monostearate, trimyristin, tripalmitin, tristearin, cocoa butter and Captex 70[®]), their lipid blends and derivatives (Precirol ATO 5[®], Geleol mono and diglycerides, Compritol 888 ATO[®]), hydrogenated derivatives of vegetable oils (Sterotex HM[®], Sterotex NF[®], Hydrokote M[®] and Hydrokote 112[®]) and polyethylene glycol derivatives (Gelucire 44/14[®] and Gelucire 33/01[®]) were used to evaluate the solubility profile of IM. As IM is a hydrophilic compound, it is essential to identify and use those lipids which can entrap higher amounts of IM during the preparation of LBFs. The solubility pattern of IM in the lipids (Table 10) was examined by considering the chemical structure, composition, total solubility parameters and physicochemical descriptors of the lipids.

7.2.1 Influence of structure, composition and polarity of lipids

Solubility of IM in the lipids showed a negative correlation with respect to the chain length of fatty acids. Additionally, the chain length also influenced the polarity of the lipids. Long chain fatty acids like myristic acid (C14), palmitic acid (C16) and stearic acid (C18) stearic acid were able to solubilise IM. On the other hand, an increase in the chain length to C22 (behenic acid) showed least solubility for IM. Amongst the fatty acids used in the study, myristic acid showed a high solubility of 2.76 ± 0.11 % w/w followed by palmitic acid, stearic acid and behenic acid with a solubility of 2.21 ± 0.23 % w/w, 1.94 ± 0.08 % w/w and 0.01 ± 0.01 % w/w respectively. The reduction in the polarity values upon increase in the carbon chain length from 0.13 (myristic acid) to 0.09 (behenic acid) suggested that an increase in the number of alkyl groups like $-\text{CH}_3$ and $-\text{CH}_2-$ will decrease the polarity of the lipids. Hence, IM was soluble in myristic acid in higher amounts than in palmitic acid and stearic acid and least soluble in behenic acid. Thus, to

solubilise hydrophilic drugs, fatty acids with a comparatively shorter carbon chain and which are comparatively polar in nature (i.e. hydrophilic polar lipids) may be the preferred choice.

Lipids like glyceryl monostearate and glyceryl palmitostearate are mono glyceride derivatives of long chain fatty acids, stearic acid and palmitic acid respectively and contain free hydrophilic functional groups like –OH and –COOH. These functional groups impart polar nature to the fatty acids and enable formation of a stronger hydrogen bonding with the drugs. Amongst the lipids used, a highest polarity value was observed for glyceryl monostearate, which could have been also been a factor for solubilisation of highest amount of IM. Additionally, the surface active nature of glyceryl monostearate could be attributed to solubilise highest amount of IM in the lipid matrix. Similarly, high solubilisation capacity for glyceryl monostearate was observed while testing the solubility of tamoxifen in various lipids by Shete et al 2013 [115]. They reported that formation of hydrogen bonds between the two hydrogen bond donor groups of glycerides in glyceryl monostearate and hydrogen bond acceptor group of tamoxifen could form a molecular complex which tends to further enhance the solubility of tamoxifen. When Geleol mono and diglycerides was used as a lipid carrier to solubilise IM, the monoglyceride (40-55%) and diglyceride (30-45%) derivatives of stearic acid in the lipid could have possibly helped in solubilising IM. But, comparatively lesser amount of drug was solubilised in Geleol mono and diglycerides than glyceryl monostearate. This suggested that the monoglyceride derivatives of stearic acid (glyceryl monostearate) are more efficient in solubilising IM than a lipid mixture containing mono and diglycerides of stearic acid (Geleol mono and diglycerides). Due to unavailability of diglycerides, we could not use them for our work even though it is an established fact that monoglycerides are more polar than diglycerides [182].

The respective triglyceride derivatives of myristic acid, palmitic acid and stearic acid like trimyristin, tripalmitin and tristearin do not contain free –OH and –COOH groups and are comparatively less hydrophilic than the fatty acids as suggested by their low polarity values. Their polarity values in Table 11 illustrate that the polarity of the triglycerides decrease in the order of trimyristin, tripalmitin and tristearin. Furthermore, due to the domination of the dispersive forces (alkyl groups), the polarity values for the triglycerides are relatively less when compared to the polarity values for monoglycerides and fatty acids. Thus, the triglycerides such as trimyristin, tripalmitin and tristearin could only solubilise low amounts of IM.

Precirol ATO (blend of glyceryl distearate and glyceryl palmitostearate), a mixture containing monoglycerides, diglycerides and triglycerides of palmitic acid and stearic acid, facilitated solubilisation of $3.17 \pm 0.19\%$ w/w of IM, which is more than the solubility of IM in palmitic acid and stearic acid. However, as behenic acid could not solubilise IM, Compritol 888 ATO[®] (glyceryl dibehenate and glyceryl behenate), a lipid mixture of mono, di and triglycerides of behenic acid could not solubilise IM either.

Captex 70[®], a mixture of 70% medium chain triglycerides (mostly caprylic acid and capric acid) could not solubilise IM. Sterotex HM[®] and Sterotex NF[®] are hydrogenated derivatives of soya bean seed oil and cotton seed oil respectively which offers the lipid a high lipophilic nature. Thus, they could not solubilise IM. Similarly, Hydrokote 112[®] and Hydrokote M[®], which are hydrogenated derivatives of palm kernel oil, could not solubilise IM in their matrix. Although cocoa butter is a mixture of triglycerides of stearic and palmitic acid, it could not solubilise IM. Gelucire 44/14[®] (mixture of lauroyl macrogol-32 glycerides and lauroyl polyoxyl-32 glycerides) and Gelucire 33/01[®] are mixture of glycerides and esters of fatty acids and poly ethylene

glycol (polyoxylglycerides) and could not solubilise IM. Thus, the lipids derived from polyethylene glycol may not be favourable to solubilise a hydrophilic drug like IM. Owing to the hydrophilic nature of IM, lipids which are comparatively more hydrophilic in nature were able to solubilise the drug.

7.2.2 Influence of solubility parameters on the ability of lipid to solubilise Imatinib Mesylate

In general, a similar magnitude of total solubility parameters for the drug and lipid suggests a greater miscibility between them. Hence, a least difference between the solubility parameters of drug and lipid could be a favourable choice to use. In the present study amongst the lipids used, lowest difference ($9.46 \text{ MPa}^{1/2}$) of total solubility parameters was observed with IM for glyceryl palmitostearate (Table 11). A comparison of the difference of the solubility parameters of IM with fatty acids and triglycerides do not indicate much difference, but, IM was comparatively more soluble in fatty acids. Among the fatty acids, with an increase in the carbon chain length, the values of the solubility parameter decreased and the corresponding difference with IM has increased. Although the dispersive forces increased with an increase in $-\text{CH}_2-$ groups, the decrease in the solubility parameters of the fatty acids correspond to the decrease in the polar forces and hydrogen bond forces (Table 11). Whereas in triglycerides, lower polar and hydrogen forces were observed than their fatty acids due to the domination of alkyl groups, which decreased their ability to solubilise hydrophilic drugs. The corresponding solubility values for IM also predicted lower solubility for triglycerides than their corresponding fatty acids (Table 10). A highest difference of $15.18 \text{ MPa}^{1/2}$ was observed for behenic acid, which showed least solubility for IM. Although Compritol 888 ATO[®] possess a low difference (11.10), it could not solubilise IM possibly due to the presence of low polar and hydrogen bonding

forces. Although the application of solubility parameters as a tool to evaluate the solubility of a drug yielded good results previously [113], in the current work it did not yield consistent results. This indicates that calculation of solubility parameters may not always yield useful results.

7.2.3 Influence of molecular and physicochemical descriptors on the ability of lipid to solubilise Imatinib Mesylate

Although 20 lipids were used to screen the solubility of IM, lipids which could only solubilise IM were selected to develop and validate a QSSR model. Figure 18 represents the graph obtained by plotting experimentally determined solubility of IM in lipids against predicted solubility of IM in lipids. Among the three models (i.e., model 1, model 2 and model 3) developed using the test set of lipids, only those descriptors which improved the efficacy and statistical significance were used. A good correlation among the training set of lipids was observed for model 1 ($R^2= 0.826$), model 2 ($R^2= 0.876$) model 3 ($R^2= 0.925$) with respect to the solubility of IM in the lipids. Also, these models showed good prediction in the test set of lipids with good robustness (Table 14). These models reflected the influence of descriptors of lipids like $AC \times DN^{0.5}/SA$, $accptHB$ and $donorHB$ and solvent accessible surface area (SASA) to solubilise IM. All these descriptors are related to the polar properties of the compounds. As IM is a hydrophilic drug, we presume the polar properties of the lipids to play a decision role in the solubilisation of IM. Although all the 3 models were statistically robust, model 1 developed taking one subset was a better one with a highest predictive correlation coefficient R^2_{pred} of 0.912. This model highlighted the role of the descriptor, $AC \times DN^{0.5}/SA$, to solubilise IM in the lipids. Additionally, all the three models had the descriptor $AC \times DN^{0.5}/SA$ in common. The descriptor $AC \times DN^{0.5}/SA$ represents effective cohesive index and is a measure of index of cohesive

interaction in the solids and directly relates to the intermolecular hydrogen bonding between the solute and solvent which is represented as $[\text{accptHB} \times \sqrt{\text{donorHB}}] / [\text{SA}]$. [149] It also signifies that there should be a good balance between the number of hydrogen bond acceptors and hydrogen bond donors sites in the solvent accessible surface area to solubilise the solute. [140] As observed by the values of $\text{AC} \times \text{DN}^{0.5} / \text{SA}$ in Table 13, highest value was observed for glyceryl monostearate. Glyceryl monostearate also had the highest number of accHB (5.4) and donorHB (2) which could have helped in solubilising highest amount of IM (with 10 acceptor hydrogen bond and 3 donor hydrogen bonds). The triglycerides trimyristin, tristearin and tripalmitin, used in the study had highest number of accptHB (6) each. But, they could solubilise only a substantial amount of IM as they do not have any donorHB. Although all the lipids belonging to the category of fatty acids had same number of accptHB (2) and donorHB (1), lowest solubilisation capacity of IM was observed for behenic acid. This could be possibly due to an increase in the number of alkyl chains which could have additionally increased the solvent accessible surface area. This increase in SASA could have decreased the $\text{AC} \times \text{DN}^{0.5} / \text{SA}$ leading to reduced solubilisation of IM in behenic acid. Although stearic acid and glyceryl palmitistearate had surprisingly similar values of $\text{AC} \times \text{DN}^{0.5} / \text{SA}$, accptHB and donorHB and SASA, highest solubilisation for IM was observed in glyceryl palmitostearate. The presence of a higher total polar surface area for glyceryl palmitostearate (135 A^2) when compared to stearic acid (37.3 A^2) could have enhanced its ability to solubilise IM.

In addition to $\text{AC} \times \text{DN}^{0.5} / \text{SA}$, other descriptors like accptHB and donorHB were also correlated with the solubility of IM as observed in equation 4 and equation 5. As mentioned previously, accptHB and donorHB

represent the number of hydrogen bonds that would be accepted by the solute from solvent molecules and donated by the solute to solvent molecules. These values are averages taken over a number of configurations, hence they can exist as non-integer. The values of *accptHB* and *donorHB* are directly related with $AC \times DN^{0.5} / SA$. Hence, IM with 10.5 *accptHB* and 2 *donorHB* could have been efficiently solubilised in lipids with a good ratio of *accptHB* and *donorHB* like glyceryl monostearate and glyceryl palmitostearate. All the three models developed were found to be statistically robust with a good power of prediction (Table 14).

7.2.4 Partitioning of drug between aqueous phase and lipid phase

During the preparation of LBFs like solid lipid nanoparticles, nanostructured lipid carriers, etc., aqueous phase (water) is usually added to the lipid phase containing drug. Even if the drug shows good solubility in the lipids phase, there are high chances for the drug to leak into the aqueous phase during this phase. Additionally, during cooling, the lipids crystallize, which lead to expulsion of drug from the lipid matrix. Hence it is beneficial to perform partitioning studies to finalise the lipid of choice. The results of the partitioning studies with all the lipids indicated highest partitioning for IM towards water [56]. Amongst all the lipids used in the study, IM showed highest partitioning towards glyceryl palmitostearate. Although the solubility studies showed IM to be highly soluble in glyceryl monostearate, partition studies did not show highest affinity for IM towards glyceryl monostearate. The surface active properties of glyceryl monostearate could have facilitated formation of micelles and improved the solubility of IM in the aqueous phase leading to poor retention of IM in the matrix of glyceryl monostearate. Lowest partition for IM was observed for myristic acid. Thus, for the preparation of LBFs of IM, usage of glyceryl palmitostearate as lipid carrier may yield high entrapment efficiency.

7.3 FORMATION OF LIGAND- LIPID CONJUGATES

Ligand-lipid conjugates of HAJ-SA and B12-SA were prepared by carbodiimide chemistry. Stearyl amine and stearic acid were conjugated to hyaluronic acid and vitamin B12 to form hyaluronic acid-stearic acid (HAJ-SA) and vitamin B12-stearic acid (B12-SA) conjugates respectively. The –COOH group present in the stearic acid reacted with the –NH₂ groups of vitamin B12 to form B12-SA moiety by amide linkage. Similarly, for the formation HAJ-SA moiety, the –COOH group of the hyaluronic acid reacted with the –NH₂ group present in stearyl amine by amide linkage.

The formation of B12-stearic acid and HA-stearic acid in both the cases was confirmed using NMR spectrum and IR spectrums. The NMR spectrum in Figure 32 and Figure 33 shows peak at 8 ppm which indicates the formation of amide. Similarly, the IR spectrum in Figure 34 and Figure 35 showed wave number at 1705 cm⁻¹, 1611 cm⁻¹ and 3100 cm⁻¹ which correspond to the amide stretching and NH bending of the formed conjugates. Wave numbers corresponding to the acid functional groups of either stearic acid or hyaluronic acid and amine functional groups of stearyl amine or vitamin B12 are absent in the regions of 1730 cm⁻¹ and 3330 cm⁻¹. These results indicate formation of ligand-lipid conjugates, HA-SA and B12-SA (Figure 34 and Figure 35).

7.4 SOLID LIPID NANOPARTICLES OF IMATINIB MESYLATE PREPARED USING STEARIC ACID AS LIPID CARRIER

Initial attempts to prepare a stable emulsion by hot homogenisation method using 4% stearic acid as a lipid core and 0.1- 0.4% of QS as an emulsifier have been unsuccessful due to phase separation and improper coverage of QS around the stearic acid. Although the critical micelle concentration of QS has been reported to be 0.01% [131], a minimum of 0.5% QS was required to cover the stearic acid core to produce SLNs. To form a good stable emulsion QS should be distributed properly on the surface of stearic acid when heating, thereby reducing the interfacial tension and facilitating the formation of small droplets during homogenisation. Moreover, QS present around the lipid surface should prevent aggregation among the nanoparticles upon cooling or upon long-term storage. Gelling was not observed in the formulations upon cooling indicating that the particle size did not increase and the surfactant concentration was sufficient to cover the outer lipid layer and thereby prevent aggregation upon cooling, when structural rearrangement of the lipid structures occurs.

For the preparation of ligand conjugated solid lipid nanoparticles, previously synthesised conjugates, HAJ-SA or B12-SA were added along with stearic acid during the preparation of solid lipid nanoparticles. Vitamin B12 conjugated solid lipid nanoparticles of IM using stearic acid (B12-ISN) were prepared by adding B12-SA (50 mg) along with stearic acid during the preparation of solid lipid nanoparticles. Similarly, for the preparation of hyaluronic acid conjugated solid lipid nanoparticles of IM using stearic acid (HAJ-ISN), HAJ-SA (50 mg) was added to stearic acid during the preparation of ISN. HA coated IM loaded solid lipid nanoparticles of stearic acid (HAC-ISN) were prepared by dispersing ISN3 in different concentrations of hyaluronic acid and probe sonicating for 5 minutes.

Both stearic acid and QS affected the size of ISNs. Table 17 shows the compositions of 9 batches of ISNs prepared by changing the amounts of stearic acid and QS. The size of ISNs from various batches ranged between 143.53 ± 3.47 nm to 641.87 ± 4.16 nm (Table 18). Surface conjugated ISNs, B12-ISN and HAJ-ISN showed a mild increase in the particle size from 159.5 ± 4.7 nm to 169.1 ± 3.2 nm and 173.1 ± 4.5 nm respectively. HAC-ISN showed a reduction in the particle size from 159.5 ± 4.7 nm to 87.3 ± 5.9 nm. The polysaccharide nature of hyaluronic acid could have reduced the surface tension of the system leading to reduction in the particle size. Additionally, sonication of ISN3 could have provided additional energy for a significant reduction in the particle size of the solid lipid nanoparticles. A particle size below 100 nm is a prerequisite for lymphatic targeting. Hence, HAC-ISN with a particle size of 87.3 ± 5.9 nm can be beneficial to target the lymphatics. Hyaluronic acid with a concentration of 0.1% was found to be optimum for coating around ISN3.

The particle size of the ISN was dependent on the amount of stearic acid and QS. When the concentration of stearic acid was maintained constant, the particle size was reduced with an increasing QS concentration, reflecting the role of QS as a surfactant. Probably, the increased QS concentration reduced the interfacial tension by adsorbing at the interface of the melted lipid phase and water, which might have facilitated the formation of smaller stable ISNs. On the other hand, when the concentration of QS was maintained constant, increase in stearic acid levels (e.g. 4%, 8% and 12%) variously affected the particle size. Compared to the particles present in the 4% stearic acid, smaller and larger particles were respectively found in 8% and 12% stearic acid formulations. The reduction in particle size of ISNs when the stearic acid concentration was increased from 4% to 8% can be attributed to the increased surface-active properties of stearic acid due to the presence of a

polar head and nonpolar chain. Whereas, the increase in particle size at 12% stearic acid might be due to the increased viscosity of the dispersed phase. Thus, use of 8% stearic acid was found to be optimum to obtain particles with smaller size in the present study. A comparison of the emulsifying properties of QS, lecithin and tween 80 showed that QS was able to form smaller particles at low concentration because of its lower molecular weight and higher proportion of non-polar to polar groups [69,183]. The polydispersity index of the formulations (Table 18) were in the range 0.127 to 0.237 indicating that they are moderately polydisperse, which could be attributed to the use of high speed homogenisation and ultrasonication methods for the preparation of nanoparticles. Thus, QS can be foreseen as a promising emulsifier for the formation of solid lipid nanoparticles.

TEM and AFM analysis of ISN3 showed quasi-spherical shaped nanoparticles (Figure 39). The central black core in the TEM image represents the drug entrapped in the surrounding lipid carrier. The outer corona observed as a bright light pattern represents the surfactant coat around the nanoparticle. The AFM images (Figure 48) show a smooth surface and non-aggregated particles. The nanoparticles of B12-ISN and HAJ-ISN did not show any change in their morphology. But, coating with hyaluronic acid changed the morphology of the nanoparticles to nests of spherical shaped nanoparticles (Figure 40). These nests showed nanoparticles below 50 nm. Although these nanoparticles seemed to be aggregated, they can't be deemed as aggregates because their surface still remains undamaged. These nests can be efficiently retained in the lymphatics by evading opsonisation and phagocytosis.

The zeta potential for the formulations was found to be neutral in the range of -2.43 ± 0.41 to 0.95 ± 0.54 mV (Table 18). Due to its non-ionic nature and attachment of hydrophilic sugar moieties to the lipophilic

backbone, QS would provide hydrophilicity and neutral charge to the particle surface. In spite of the neutral zeta potential of the formulations, aggregation among the particles was not observed because of the osmotic force created by the surfactant coating on the surface of nanoparticles. This net neutral charge can provide covertness to the particles against macrophages and thereby help in extending the half-life of drugs. B12-ISN showed a mild positive zeta potential of 10.2 ± 1.2 mV, which may be due to the ionisation of vitamin B12. But, the zeta potential of HAJ-ISN and HAC-ISN showed a negative zeta potential of -6.4 ± 0.7 mV and -12.8 ± 1.7 mV respectively. The change in the zeta potential of HAC-ISN from 0.95 ± 0.5 mV to -12.8 ± 1.7 mV confirmed coating of ISN by hyaluronic acid. Hyaluronic acid could have adsorbed on the surface of ISN by electrostatic attraction between the hyaluronic acid and the stabiliser coat present on the surface of SLNs.

As the surfactant shell can suppress the transition of the drug from one state to another state, the effect of QS on the polymorphic transition of SLNs and the physical form of IM in the lipid matrix using DSC was checked. The thermograms of IM, QS, stearic acid, BSNs and ISNs were shown in Figure 54. Endothermic peaks at 227.8 °C, 126.5 °C, and 59.8 °C were observed, respectively, for IM, QS and stearic acid. The absence of the melting peak of IM in the thermogram of the ISNs indicates that the IM entrapped in the lipid core was in an amorphous state. Further, the broadened peak and decreased melting point of stearic acid indicates loading of the drug in the lipid lattice structures. The decrease in the melting point of stearic acid from 60.8 °C in bulk stearic acid to 58.6 °C (BSLNs) and 57.7 °C (ISNs) respectively reveals a decrease in the particle size to colloidal range and increased number of lattice defects in the β' structured stearic acid. DSC thermograms were not obtained for the surface conjugated ISNs because the composition remained the same, with an exception of addition of conjugated stearic acid.

The entrapment efficiency of the formulations ranged between 41 % (ISN9) and 66 % (ISN1). Surface modified ISN showed a reduction in the entrapment efficiency from $61.3 \pm 1.1\%$ (ISN3) to $56.9 \pm 1.4\%$ (B12-ISN), $50.6 \pm 1.5\%$ (HAJ-ISN) and $47.8 \pm 2.1\%$ (HAC-ISN) respectively. For B12-ISN and HAJ-ISN the addition of conjugate to the lipid matrix could have reduced the entrapment efficiency. For HAC-ISN, additional homogenisation could have lead to repacking of the lipid matrix which could have reduced the entrapment efficiency. A negative trend with increasing stearic acid and QS concentrations was observed. High surfactant concentration could have enhanced the solubility of IM resulting in the partitioning of the drug into the aqueous medium, thereby leading to low entrapment efficiencies in the lipid core. IM also shows enhanced solubility in solutions with pH less than 5.5 [153]. Thus, 0.5% and 1.5% QS solutions with pH 4.5 and 4.3 respectively could have additionally enhanced the solubility leading to the partitioning of IM from the lipid phase to the aqueous QS solution.

In vitro drug release patterns of ISNs in PBS pH 7.4 are shown in Figure 57. A biphasic release pattern with an initial burst release of about 1 h, followed by a sustained release of IM from the lipid core for 10 h was observed. The initial burst release could be due to the free and surface adsorbed IM as reported in a recent study with IM nanoparticles [126]. Even though a long-chain fatty acid (stearic acid) was used as the lipid core, the release of the drug from ISN was not sustained for a longer duration due to the hydrophilic nature of IM. The coating of hyaluronic acid could have hindered the release of IM. More rapid release of the drug was observed in the formulations containing 1.5% of QS. HAC-ILN showed a comparatively sustained release profile of IM from its matrix. The r^2 (regression coefficient) values indicated a first order release pattern of IM from the lipid matrix.

It should be noted that saponins in general have an innate potential to cause lysis of RBCs due to their membrane lytic action, which might have restricted the use of QS as a surfactant in the pharmaceutical industry. A comparative *in vitro* haemolytic analysis of ISNs, QS, IM, and BSNs revealed that ISNs, BSNs and IM did not induce haemolysis Figure 61. Although QS induced haemolysis even at a low concentration (50 µg/ml) when presented singly, the ISNs and BSNs prepared using QS did not show haemolysis even at a much higher QS equivalent concentration (450 µg/ml). This is probably due to the fact that the lipophilic aglycone group of QS which is responsible for haemolysis [132] was adhered to the lipid matrix of the SLNs, exposing the non-haemolytic hydrophilic polysaccharide groups to the outer aqueous medium. In line with our observation, absence of haemolysis for anticancer drugs in nanoparticulate form has been previously reported [178]. When ISNs were tested for haemolytic activity at concentrations several folds higher (e.g., 10, 20 and 30 µg/ml) than its original C_{max} concentration (approximately 1 µg/ml) [184], we did not observe any haemolysis indicating that SLNs prepared using QS as a surfactant and IM as the drug is safe for intravenous administration.

Particle size and entrapment efficiency are two parameters which significantly affect the drug delivery and treatment efficacy of drug loaded nanoparticles. Small particles have good access into tumor cells by penetration through the cell membranes [185]. Equally, good entrapment efficiency is also desired to reduce the quantity of material for administration. So, it is desirable for the formulations to have smaller sized particles with good entrapment efficiency. Although formulation ISN6 possessed least particle size among all the formulations, its entrapment efficiency was low. Hence the formulation with the next lowest particle size and higher entrapment efficiency (ISN3) was selected for further investigations. As revealed by MTT assay (Figure 63),

HAC-ISN3 was the most cytotoxic against MCF7 cells among the formulations tested (IM, QS, ISN3, BSNs, BSNs- IM mixture, B12-ISN3, HAJ-ISN3 and HAC-ISN3). The IC_{50} (minimum inhibitory concentration) value of the samples (Table 22) decreased in the following order HAC-ISN3 ($0.76 \mu\text{M}$) < B12-ISN3 ($1.03 \mu\text{M}$) < HAJ-ISN3 ($1.17 \mu\text{M}$) < ISN3 ($1.226 \mu\text{M}$) < BSNs- IM mixture ($3.114 \mu\text{M}$) < BSNs ($6.91 \mu\text{M}$) < IM ($7.395 \mu\text{M}$). The results signify that IM encapsulated in solid lipid nanoparticles and surface modified with hyaluronic acid was more efficient in killing cancer cells than the free IM and ISN. Probably, this is due to the enhanced cellular uptake of lipid nanoparticles and/or a synergistic effect between QS (IC_{50} value = $8.167 \mu\text{g/ml}$) and IM present in the ISN3 and the presence of conjugating agent which could have enhanced its toxicity. The anticancer property of QS might be the reason for the higher cytotoxic potentials of BSNs and BSNs-IM mixture against MCF7 cells compared to IM.

On the other hand, when the RAW 264.7 cells (macrophages) were treated with the samples (IM, QS, ISN3, BSNs, BSNs- IM mixture, B12-ISN3, HAJ-ISN3 and HAC-ISN3), more than 90% cells were viable indicating that normal cells were not affected by any formulation including IM and QS (Figure 65) which indicates that IM and QS specifically target cancer cells. Cytotoxic effect of saponins against MCF7 cells and its protective effect against RAW 264.7 cells have been reported [186]. Although the mechanism behind the specificity of QS to cancer cells is unknown, as IM, (a tyrosine kinase inhibitor which specifically targets cancer cells expressing tyrosine kinase genes) was used, RAW 264.7 cells which do not this tyrosine kinase inhibitor could have been spared [126]. In agreement, conjugation of aptamer with doxorubicin enhanced the viability of RAW 264.7 cells without affecting the cytotoxic effect of doxorubicin to MCF cells [187]. The results indicate that HAC-ISNs are more efficient in killing the cancerous cells.

7.5 SOLID LIPID NANOPARTICLES OF IMATINIB MESYLATE PREPARED USING PALMITIC ACID AS LIPID CARRIER

Solid lipid nanoparticles of IM using palmitic acid (IPN) as a lipid carrier and QS as the surfactant were prepared by hot homogenisation technique using high shear homogeniser and probe sonicator. Initially, preliminary trial formulations of IPA were prepared by varying the parameters like the speed of high shear homogenization (10, 000- 15, 000 rpm), time of high shear homogenization (2- 10 minutes) and duration of probe sonication (2- 10 minutes) to obtain a stable formulation. Based on the preliminary trials conducted, a comparatively good stability was obtained after homogenising the mixture of water and lipid phases at 14, 000 rpm for 4 minutes and probe sonication for 4 minutes. Trails at conditions other than the optimised process parameters showed either an increase in the particle size of the formulations or frothing or phase separation. At high speeds, the surfactant coating on the surface of solid lipid nanoparticles (SLNs) could have been damaged or eroded, there by promoting aggregation and increase in the particle size.

Nine batches of formulations were prepared by changing the amount of palmitic acid (PA) and QS. The particle size of the formulations was in the range of 133.1 ± 8.4 nm to 611.0 ± 4.1 nm (Table 18). The influence of particle size of IPN on the amount of PA and QS was studied. When the amount of QS was increased from 0.5% to 1.5%, the particle size of the solid lipid nanoparticles reduced. Increased levels of QS could have reduced the surface tension and facilitated efficient dispersion of the lipid phase in the aqueous medium, thereby producing smaller sized IPNs. When the amount of palmitic acid was increased from 4% to 12%, the particle size of IPNs increased. Higher amounts of palmitic acid could have increased the viscosity and resistance for the lipid phase to disperse in the aqueous medium, which

leads to production of particles with a bigger size. Hence, higher amounts of palmitic acid could have increased the particle size of the IPNs. Thus, in order to obtain, IPNs of smaller size, it is preferable to use lower amounts of palmitic acid (4%) and higher amounts of QS (1.5%).

Due to the usage of QS, a non ionic surface stabilizer, in the preparation of IPNs, the zeta potential of the formulations was neutral and ranged from -1.08 ± 0.2 mV to -4.29 ± 0.6 mV. Although, the zeta potential is neutral, it will not cause any instability during storage for long time as QS is a surface stabiliser and provides osmotic force which prevents aggregation. This neutral charge can additionally impart stealth nature to the IPNs by preventing opsonisation and phagocytosis against macrophages. The mild negative charge could have been due to the ionisation of acid groups of palmitic acid [155].

Analysis of the morphology of the nanoparticles using TEM and AFM showed homogeneous, spherical shaped smooth nanoparticles with mild aggregations (Figure 42 and Figure 49). The particle size of the IPNs corroborated with that of the particle size results obtained from dynamic light scattering analysis i.e., less than 200 nm. Cracks or pin holes on the surface of nanoparticles were not seen.

DSC studies were performed to check the physical state of IM in IPN. The thermograms of IM, QS, bulk PA, BPN and IPN was represented in Figure 55. In the thermogram corresponding to IPN, endothermic peak of IM was absent. This indicated that IM was encapsulated in the lipid matrix in an amorphous form.

The ability of PA to entrap IM in its lipid matrix was low as evidenced by the low entrapment efficiencies. The entrapment efficiencies of the formulations were in the range of $39.8 \pm 0.6\%$ to $57.1 \pm 0.3\%$. As IM is

hydrophilic in nature, its entrapment in the lipophilic matrix of palmitic acid could have been poor, justifying the low entrapment efficiencies. The entrapment efficiencies of IPNs were influenced by the amount of PA and QS. The entrapment efficiency of the formulations showed a significant decrease when the amount of QS was increased from 0.5% to 1.5%. Higher amounts of QS could have enhanced the solubility of IM in the aqueous phase, thereby facilitating the partitioning of IM into the aqueous medium. The entrapment efficiency also decreased with an increase in the amount of PA from 4% to 12%. Higher amount of palmitic acid did not improve in the amount of IM entrapped in its matrix. *In vitro* release studies in pH 7.4 phosphate buffer saline showed a biphasic release pattern for IM from the IPA. The total amount of drug entrapped in the lipid matrix was released in almost 6-8 hours. In the initial hour, nearly 50% of the drug was released in all the formulations. This represents the burst release phase and corresponds to the free and surface adsorbed drug. In the remaining 4-6 hours, a comparatively sustained release profile was obtained. During this phase, the amount of IM released corresponded to the drug entrapped in the lipid matrix. Although a long chain fatty acid was used in the study, the release was not sustained possibly due to the small size of nanoparticles, hydrophilic nature of the drug and poor entrapment efficiencies. Low entrapment efficiencies for hydrophilic drugs encapsulated in SLNs have also been reported elsewhere [31,60]. The release pattern of IM from the lipid matrix of IPN showed a first order release.

Considering the high particle size and low entrapment efficiencies for IPA, solid lipid nanoparticles with the addition of lipid-ligand conjugates like B12-SA and HA-SA were not performed. Hence, additional evaluation studies like *in vitro* cytotoxicity assay and cell internalisation studies in cell lines, *in vivo* pharmacokinetic studies were not performed.

7.6 SOLID LIPID NANOPARTICLES OF IMATINIB MESYLATE PREPARED USING GLYCERYL PALMITOSTEARATE AS LIPID CARRIER

Partitioning studies showed highest partitioning for IM using glyceryl palmitostearate as the lipid carrier. IM loaded solid lipid nanoparticles using glyceryl palmitostearate (IGPN) as lipid carrier were prepared by hot homogenisation technique using high shear homogenisation and probe sonication. During the preliminary trials, 12% glyceryl palmitostearate and 0.5% QS were used to check for their ability to form o/w emulsion. Then, trials were performed at different homogenisation parameters like speed (10, 000- 15, 000 rpm) and duration of high shear homogenisation (2- 10 minutes) and duration of probe sonication (2- 10 minutes). Based on the stability, high shear homogenisation at 14, 000 rpm for 6 minutes and probe sonication for 6 minutes were selected as optimum parameters for preparing different batches IGPN. When different parameters were used, instability due to an increase in particle size or frothing was observed. Homogenising the emulsion at high speeds and longer duration could have damaged the surfactant coating around the particle surface. This damaged surface will induce aggregation among the nanoparticles and leads to an increase in the particle size [167]. Hence, choosing optimum conditions for the preparation of solid lipid nanoparticles is very important.

Different batches of IGPNs were prepared by varying the amount of the lipid, glyceryl palmitostearate and surfactant, QS. B12-IGPN and HAJ-IGPN were prepared by addition of HAJ-SA and B12-SA to the lipid, glyceryl palmitostearate during the process of preparation of IGPNs. Hyaluronic acid coated IGPN (HAC-IGPN) were prepared by dispersing IGPN in solution of hyaluronic acid of various concentrations. The cytotoxicity and apoptosis assay of the IGPNs was tested against MCF 7 cell line. Finally, pharmacokinetic studies were performed in female Wistar rats.

The average particle size of the formulations was found to be in the range of 92.1 ± 2.41 nm to 430.7 ± 2.2 nm (Table 18). The influence of the amount of glyceryl palmitostearate and QS on the particle size was studied. When the amount of glyceryl palmitostearate increased, the particle size of the nanoparticles significantly decreased ($p < 0.05$). Higher amounts of glyceryl palmitostearate could have enhanced the surface tension, thereby leading to the generation of solid lipid nanoparticles with reduced particle size. Among the various batches of SLNs prepared using different lipids (stearic acid, palmitic acid, glyceryl palmitostearate, glyceryl monostearate and Geleol mono and di glycerides), SLNs prepared using glyceryl palmitostearate were found to be of smaller size. High polarity of the lipids due to the presence of glyceryl groups in the lipid and better solubility of the drug in the lipid could have allowed the lipid to disperse well during the preparation of nanoparticles [188]. Additionally, usage of higher homogenisation speeds could have led to the generation of smaller sized nanoparticles amongst all the lipids. When the amount of QS was increased, the particle size of the IGPNs also increased. As QS is a surfactant, usage of higher amounts of QS during the preparation of solid lipid nanoparticles reduced the surface tension [131,189]. This reduced surface tension could have allowed the particles to disperse well during homogenisation, leading to the formation of particles with smaller size. Hence, for the preparation of smaller size of IGPN, it is favourable to use low level of glyceryl palmitostearate (4%) and high level of QS (1.5%). Ligand conjugated nanoparticles prepared using B12-SA and HA-SA increased the particle size of the nanoparticles to 118.7 ± 3.9 nm and 130.6 ± 2.7 nm respectively. Hyaluronic acid (HA) was coated on the surface of IGPNs by surface adsorption to form HAC-IGPN. The size of the nanoparticles reduced from 106.4 ± 4.7 nm to 92.1 ± 2.4 nm after coating with HA. As HA is a polysaccharide, it could have lowered the surface tension by acting as a

surfactant [82,130,190]. This reduced surface tension could have enhanced the ability of the particles to disperse well during homogenisation, leading to production of nanoparticles with smaller size. During the process of coating of HA, optimisation was carried out to identify the favourable concentration of HA required for coating with respect to size and stability. Among the different trials performed, 0.1 % was found to be optimum for the preparation of HAC-IGPN. Higher concentrations of hyaluronic acid increased the particle size of the SLNs due to aggregation. Aggregation due to higher concentration of hyaluronic acid have been reported in previous instances [58,82].

The morphology of the solid lipid particles of IGPN was observed using TEM and AFM. TEM images (Figure 43) of IGPN showed near spherical shaped particles without any aggregation. B12-IGPN showed spherical shaped particles without aggregations. HAC-IGPNs showed nests of nanoparticles coated by hyaluronic acid, as observed by a dark outer coating containing nanoparticles (Figure 45). Each nest measured below 100 nm and contained 2-3 particles with a size below 50 nm. Although these nests showed particles which are held together by hyaluronic acid, their surfaces are not aggregated. These nanoparticles would be ideal to enter and reside in the lymphatics for longer duration. Nanoparticles which are smaller than 100 nm are difficult to retain in the lymphatics as they are escaped out through the interstitial walls of the lymphatic capillaries. But, coating with hyaluronic acid favoured particle pseudo aggregation among the particles without damaging their surface. These nests with a size greater than 100 nm can remain in the lymphatics for longer duration by evading opsonisation. The topographic images obtained using semi-contact mode of AFM showed homogenous lateral and vertical particles (Figure 50 and Figure 51).

The zeta potential of the formulations was in the range of 1.63 ± 0.5 mV to 10.67 ± 1.32 mV. As QS is a non ionic surfactant, the zeta potential of

the formulations were neutral. The mild negative charge was due to the ionisation of fatty acid chains. Although the zeta potential of the formulations was neutral, aggregation may not be observed over long term storage because of the usage of a stearic stabilizer (QS) which can create an osmotic force and prevent aggregation among the nanoparticles [60,173,189]. The zeta potential of B12-IGPNs shifted to a mild positive charge (1.63 ± 0.5 mV) possibly due to modification of the surface of IGPN by B12-SA. Coating with hyaluronic acid reduced the zeta potential of the IGPN from -1.03 ± 0.14 mV to -10.67 ± 1.32 mV confirming the coating of hyaluronic acid on the surface of solid lipid nanoparticles [58,82].

The physical state of IM entrapped in IGPN was confirmed using DSC. The thermograms of IM, QS, glyceryl palmitostearate, BGPNS and IGPNs are shown in Figure 56. The endothermic peaks corresponding to IM, QS and glyceryl palmitostearate were observed at 227.8 °C, 126.5 °C, and 50.8 °C respectively. The absence of endothermic peak of IM in the thermogram of the IGPNs indicated that IM entrapped in the lipid core was in an amorphous state [191,192]. Additionally, the broadened peak and decreased melting point of glyceryl palmitostearate indicated loading of IM in the lipid lattice structures. The decrease in the melting point of glyceryl palmitostearate from 50.8 °C in bulk glyceryl palmitostearate to 49.2 °C (BGPNS) and 48.7 °C (IGPNs) respectively reveals a decrease in the particle size to colloidal range and increased number of lattice defects in the β' form of glyceryl palmitostearate. The entrapment efficiencies of the formulations were low which ranged from 43.4 ± 0.7 - $65.9 \pm 0.6\%$. The hydrophilic nature of IM, usage of high temperatures during the preparation and high solubility of IM in the aqueous phase could have lead to poor entrapment efficiencies. Among the different lipids used for the preparation of solid lipid nanoparticles, highest entrapment efficiency was observed for glyceryl palmitostearate. High solubility and high

partition of IM in glyceryl palmitostearate could have been the reason for high entrapment efficiency in glyceryl palmitostearate. The entrapment efficiency decreased for HAC-IGPNs. Sonication of the solid lipid nanoparticles after addition of IGPN could have caused a structural rearrangement of the SLNs, which could have promoted expulsion of IM from the lipid matrix. Additionally, the surface active nature of hyaluronic acid could have enhanced the solubility of IM in the aqueous phase. *In vitro* release studies of IM from IGPNs in pH 7.4 phosphate buffer saline showed a biphasic release pattern (Figure 59). In 12 hours almost all the drug entrapped in the lipid matrix was released. A burst release amounting to 50% of the free and surface adsorbed drug was observed in the first hour [167]. A sustained second phase was observed during which the remaining amount of drug was released. HAC-IGPNs showed a more sustained profile possibly due to the coating of hyaluronic acid which could have hindered the release of IM from the lipid matrix.

Saponins are potent haemolytic agents as their membrane lytic action can lyse the RBCs [132]. A comparative *in vitro* haemolytic analysis of QS, IM, and BGPNs revealed that IM, IGPNs, and BGPNs did not induce haemolysis (Figure 62). Although QS alone induced haemolysis even at a low concentration (50 µg/ml), IGPNs and BGPNs prepared using QS did not show haemolysis even at a much higher equivalent concentration of QS (450 µg/ml). The lipophilic aglycone moiety of QS which generally causes haemolysis [132] could have adhered to the lipid matrix of the SLNs. This will expose only the non-haemolytic hydrophilic polysaccharide groups to the outer aqueous medium which may have been the reason for the absence of haemolysis. Higher levels of IGPNs were also found to be non haemolytic indicating that SLNs prepared using QS as a surfactant and IM as the drug are safe for intravenous administration. Similar results were obtained for ISNs

(IM loaded solid lipid nanoparticles prepared using stearic acid as lipid carrier). When IGPNs were tested for haemolytic activity at concentrations several folds higher (e.g., 10 and 30 $\mu\text{g}/\text{ml}$) than its original C_{max} concentration (approximately 1 $\mu\text{g}/\text{ml}$) [184], haemolysis was not observed.

MTT assay was performed to evaluate the ability of IM, QS, IGPN3, Blank IGPN3, Blank IGPN3 + IM, B12-IGPN3, HAJ-IGPN3 and HAC-IGPN3 to inhibit the growth of MCF7 cells. Dose dependent cell growth inhibition was observed for all groups and % cell viability was decreased with an increase in the concentration of drug. As revealed from the results of MTT assay (Figure 64 and Table 22), HAC-IGPN3 showed highest inhibition against MCF7 cells. The IC_{50} of the samples increased in the following order: HAC-IGPN3 (0.91 μM) < HAJ-IGPN3 (1.25 μM) < B12-IGPN3 (1.45 μM), < IGPN3 (1.80 μM) < Blank IGPN3 + IM (2.21 μM) < Blank IGPN3 (6.31 μM) < IM (7.395 μM). These results reflect that IM encapsulated in solid lipid nanoparticles was more efficient in killing cancer cells than the free IM. Probably, this is due to the enhanced cellular uptake of lipid nanoparticles and/or a synergistic effect between QS (IC_{50} value = 8.167 $\mu\text{g}/\text{ml}$) and IM present in the IGPN3. Increased uptake of HA coated nanoparticles through CD44 mediated mechanism resulted in poor viability of cells [174]. Kesharwani et al. also reported poor viability of pancreatic cell lines when treated with HA conjugated dendrimer loaded with curcumin derivative [176]. HA coating further significantly improved the anticancer activity of HAC-IGPN3 through anticipated specific CD44 targeting mechanism on over expressed cells and it was the most potent formulation among all with the least IC_{50} concentration. The beneficial effect of HA coating onto the surface of mitoxantrone polymeric nanoparticles has been reported and the authors found that coated particles possessed lower IC_{50} than uncoated nanoparticles on MCF-7 cells [174]. The anticancer property of QS might be the reason for the higher cytotoxic potentials of BGPNS and BGPNS- IM mixture against MCF7 cells compared to IM.

On the other hand, when the RAW 264.7 cells (murine macrophages) were treated with the samples (IM, QS, IGPN3, BGNs, BGNs + IM mixture, B12-IGPN3, HAJ-IGPN3 and HAC-IGPN3), more than 90% cells were viable indicating that normal cells were not affected by the samples used (Figure 66). These results (Table 22) indicate that IM and QS targeted only the cancerous cells. Cytotoxic effect of saponins against MCF7 cells and its protective effect against RAW 264.7 cells have been previously reported [186,193]. Although the mechanism behind the specificity of QS to cancer cells is unknown, as IM (a tyrosine kinase inhibitor which specifically targets cancer cells expressing tyrosine kinase genes) was used, it did not show toxicity against RAW 264.7 cells [178].

Propidium iodide (PI) is a fluorescent intercalating agent which can be used for staining dead cells [180]. In the current study, PI was used as a DNA stain to evaluate the DNA damage and to visualise the nucleus and other DNA-containing organelles. To confirm if free IM, IGPN3 and HA-IGPN induces apoptosis in MCF 7 cells the nuclear condensation of the DNA was analysed by propidium iodide (PI) staining. In the control cells, which were treated only with PBS, PI positive cells were not observed indicating absence of apoptosis. But, in the cells exposed with IGPN3 and HA-IGPN for 24 h, the number of PI positive cells increased (Figure 67) when compared to the cells treated with IM alone (Figure 67 b). As PI can't cross the membrane of live cells the results indicate the death of the MCF 7 was due to apoptosis. The improved cytotoxicity of IGPN3 and HA-IGPN is possibly due to the smaller size of the SLNs.

7.7 SOLID LIPID NANOPARTICLES OF IMATINIB MESYLATE PREPARED USING GLYCERYL MONOSTEARATE AS LIPID CARRIER

The results from the experimental solubility studies, Hansen Hildebrand's total solubility parameters and QSSR studies indicated glycerylmonostearate to show highest solubility for IM. IM loaded solid lipid nanoparticles of glyceryl monostearate (IGMN) were prepared by hot melt homogenisation using a combination of high shear homogenisation and probe sonication. Homogenisation at high speeds and for longer duration or probe sonication for longer duration can generate high kinetic energy which can rupture the coating of the surfactant on the surface of the nanoparticles [63,194]. This ruptured particle surface can induce aggregation among the particles and consequently increased particle size. Additionally during these conditions, high amounts of heat will be generated which can further damage the particle surface. Hence, there should be optimum process parameters during the preparation of SLNs. For the preparation of IGMNs preliminary trials were conducted at different homogenizing conditions such as homogenising speeds of 10, 000 rpm- 15, 000 rpm, duration of homogenisation (2- 10 minutes) and duration of probe sonication (2- 10 minutes). Considering the stability, the process parameters for preparing IGMNs were optimised as follows: high shear homogenising at 15, 000 rpm for 4 minutes and probe sonication for 6 minutes.

Various batches of IGMNs were prepared by changing the amount of GMS and QS. The particle size of different batches of IGMNs as measured by dynamic light scattering ranged from 126.6 ± 6.1 – 740.9 ± 15.6 nm (Table 18). The smaller size of the nanoparticles could be attributed to the surfactant properties of the glyceryl monostearate [124,164], efficient solubilisation of IM in the lipid matrix and usage of high energy dispersive forces during the preparation of IGMNs. The particle size of IGMNs showed a negative correlation with the amount of lipid (GMS) and surfactant (QS) used. When the amount of QS was increased from 0.5% to 1.5%, the surface tension of the

medium could have reduced [131] and improved the dispersion of the lipid matrix in the water phase. Better dispersion of the lipid matrix could have facilitated reduction in the particle size of IGMNs. Due to the surface active properties of GMS, increased levels from 4% to 12 % could have facilitated reduction in the particle size similar to QS. Thus, for the formation of IGMNs with least particle size, it is favourable to use high amounts of QS (4%) and GMS (12%). The zeta potential of the IGMNs was in the range of -14.96 ± 0.8 mV to -2.92 ± 0.3 mV (Table 18). Due to the usage of QS, a non ionic surfactant in the preparation of IGMNs, the zeta potentials were neutral. The mild negative charges were due to the presence of ionised lipid moieties.

Analysis of the morphology using TEM showed aggregates of particles with a size around 150 nm. Size of the nanoparticles as visualised in TEM was found to be less when compared to the size obtained by Malvern particle size analyzer. Malvern particle size analyser uses the principle of dynamic light scattering, which measures the hydrodynamic diameter of the nanoparticles. But, TEM and AFM measures diameter of the dried nanoparticles. Hence, a smaller particle size was obtained using TEM. AFM images also showed clusters of nanoparticles aggregates. The results of AFM were in concordance with the results of TEM.

The entrapment efficiency of the formulations ranged from $41.9 \pm 1.1\%$ to $54.1 \pm 0.6\%$ (Table 18). Usage of a hydrophilic drug and GMS (a lipid with surfactant properties) and high temperatures during the preparation of IGMNs could have been the reason for poor entrapment efficiency values [124]. GMS and high temperatures could have enhanced the solubility of IM in the aqueous medium and also could have facilitated its entry into the aqueous phase. During the storage of the formulations in refrigerated conditions, creaming or cracking were observed in 30 days. Hence, additional studies were not performed for these formulations.

7.8 SOLID LIPID NANOPARTICLES OF IMATINIB MESYLATE PREPARED USING GELEOL MONO AND DIGLYCERIDES AS LIPID CARRIER

Geleol mono and diglycerides, which is composed of mono and diglycerides of stearic and palmitic acid was also used to prepare solid lipid nanoparticles of IM. A hot melt homogenisation method using high shear homogenisation and probe sonication were used to prepare IM loaded solid lipid nanoparticles of Geleol mono and diglycerides (IGEN). Preliminary trials were attempted at various conditions of high shear homogenisation (speed and duration) and probe sonication (duration). Considering the stability and particle size, the working parameters were optimised to high shear homogenisation at 15, 000 rpm for 2 minutes and probe sonication for 6 minutes. Different batches of IGEN were prepared by changing the amount of Geleol mono and diglycerides and QS.

The particle size of the formulations as measured by Malvern zeta sizer varied from 118.4 ± 5.1 nm to 653.9 ± 8.4 nm (Table 18). Although the composition of Geleol mono and diglycerides is majorly GMS, a particle size similar to the formulations prepared using GMS as a lipid carrier were not obtained as Geleol mono and diglycerides additionally contain diglycerides of stearic acid and palmitic acid apart from along with monoglycerides of stearic acid [195,196]. The composition of the lipid may have affected the particle size. The zeta potential of the formulations varied from -2.01 ± 0.1 mV to -12.03 ± 2.7 mV. Due to the usage of non ionic surfactant (QS) in the preparation of IGEN, the zeta potential of the formulations was neutral. A slight negative charge could be attributed to the ionisation of the fatty acid moieties [164,173].

The morphology of the SLNs was analysed using TEM and AFM. TEM images showed spherical shaped particles with few aggregates in TEM and AFM. The particle size results as observed in TEM and AFM was in concordance with the results obtained by analysis of particle size using Malvern particle size analyser.

The entrapment efficiencies of the formulations ranged from $47.0 \pm 1.2\%$ to $66.5 \pm 1.3\%$ (Table 18). Low entrapment efficiencies were poor due the usage of a hydrophilic drug and high speeds during homogenisation [65,197]. During the storage of the formulations in room temperature and refrigerated conditions, gelling was observed. Larger size of the nanoparticles and change of the physical state of the lipid carrier from amorphous to crystalline state could have caused expulsion of drug, which could have reduced the stability of the nanoparticles. Hence, additional studies were not performed for these formulations and usage of Geleol mono and diglycerides as lipid carrier for the preparation of solid lipid nanoparticles may not be suitable with the composition used in the current experimental studies.

7.9 PHARMACOKINETIC STUDIES TO QUANTIFY THE CONCENTRATION OF IMATINIB MESYLATE IN PLASMA AND SENTINAL LYMPH NODES

IM solubilised in pH 7.4 PBS (IM-PBS), ISN, HA-ISN, B12-ISN, IGPN, and HA-IGPN (sterile) were administered by subcutaneous route in female wistar rats to quantify the amount of IM present in the blood at different time points [181]. The $T_{1/2}$ of IM when administered using pH 7.4 PBS was 18.4 h. But, the $T_{1/2}$ of IM increased after administering it as an encapsulated form in solid lipid nanoparticles. Among the formulations used, hyaluronic acid coated solid lipid nanoparticles enhanced the $T_{1/2}$ of IM to nearly 42 h. B12-ISN increased the $T_{1/2}$ of IM to nearly 26 h. The C_{max} of IM administered via solid lipid nanoparticles was increased by 2-3 folds when compared to IM-PBS. Other parameters like AUC_{0-t} , $AUC_{0-\infty}$ and $AUMC_{0-t}$ and $AUMC_{0-\infty}$ also increased for IM after administration with solid lipid nanoparticles. The results (Table 23) indicate entry of the solid lipid nanoparticles loaded with IM to the lymphatics before being drained into the systemic circulation.

Subcutaneous administration enabled the test substances to reach the interstitial area beneath the dermis of the skin [198,199]. HA-ISN and HA-IGPN, whose particle size is below 100 nm could have been selectively absorbed to the regional lymphatics through the gaps present among the endothelial cells of the lymphatic capillaries. Additionally, the nanoparticles coated with hyaluronic acid bearing negative charge could have been pushed by the negatively charged glycosaminoglycans of the hyaluronan matrix to the lymphatics [94,174]. This is clearly justified by the increase in the half life, increase in T_{max} , and decrease in C_{max} of IM after administration by solid lipid nanoparticles. The enhanced concentration and half life of IM in the lymphatics can be helpful in killing the metastatic cancerous cells present in the lymph nodes.

There was only a slight increase in the $T_{1/2}$ of IM after administering through ISN, B12-ISN and IGPN. As their particle size is above 100 nm, they could have directly entered the systemic circulation after subcutaneous administration. Due to the presence of non ionic surfactant coating around the surface of the solid lipid nanoparticles, their half life could have been increased, which could have consequently increased the T_{max} , $MRT_{0-\infty}$, and $AUC_{0-\infty}$.

The drug concentration profile in sentinel lymph nodes was measured to estimate the concentration of IM present in the lymph nodes (the residing place of metastatic cancer cells) at different time intervals [200,201]. At all time points (Table 24), the amount of IM present in the lymph nodes was higher when administered subcutaneously as IGPN3 and HA-IGPN when compared to administration of IM solution. Additional coating of hyaluronic acid helped in the entry of higher levels of IM to the sentinel lymph nodes. The smaller sized nanoparticles and negatively charged matrix at the site of injection site could have propelled the transport of negatively charged HA-IGPN to the sentinel lymph nodes. Higher C_{max} was observed in the lymph nodes after administration of IGPNs and HA-IGPN when compared to the administration of IM in PBS solution. This clearly indicates that higher amounts of IM reached the sentinel lymph nodes after administration of HA-IGPN and IGPN.

Thus, the results of the pharmacokinetic studies reflect the fact that subcutaneous administration of solid lipid nanoparticles with a particle size below 100 nm could be used to target the regional lymphatics, the residing place of metastatic cancerous cells. Additional coating with hyaluronic acid could be used to enhance the uptake to the lymphatics and increase its retention time.

7.10 STABILITY STUDIES

Stability studies were carried out ISN3, HAC-ISN, B12-ISN, IGPN3, HAC-IGPN and B12-IGPN at room temperature (20 - 25°C) and refrigerated conditions (3 to 5 °C) over a period of 12 months. The stability was indicated by measuring some parameters like appearance of the formulations, particle size, polydispersity index, zeta potential and entrapment efficiency. The results indicated good stability when stored at refrigerated conditions than when stored in room temperature.

During storage at room temperature, large floccules were observed for the all the formulations after 3 months. After 6 months, sedimentation was observed and some formulations dispersed upon shaking. At the end of 9 months very large floccules were observed and were found difficult to disperse. The zeta potential of the formulations also gradually changed over a period of time. Entrapment efficiencies of the formulations also gradually decreased over a period of 12 months when stored at room temperature.

Whereas, for the formulations stored in refrigerated conditions, there were no floccules and sedimentation after 12 months. Very minimal increase in the particle size was observed (statistically insignificant). The zeta potential and entrapment efficiencies did not change when stored at refrigerated conditions.

During storage at room temperature, light and temperature provide extra energy to the nanoparticles [202,203]. This increased energy will enhance the Brownian motion and will consequently increase the collisions among them. Consequently, the outer surfactant coating will be eroded and leads to aggregation of particles. Thus, the particle size increases. This erosion of the surfactant will also change the values of zeta potentials. During storage,

the high energy lipid crystal matrix will transform to a low energy crystal form. This transformation usually causes expulsion of the drug from the matrix into the surrounding aqueous phase thereby leading to a reduction in the entrapment efficiencies of the SLNs. But, when stored at refrigerated conditions, which are devoid of light and high temperatures, a significant increase in the particle size or change in the zeta potential will not be observed. But, the entrapment efficiency may decrease as the lipids tend to change its crystalline state at any conditions.

Thus, it is favourable to store the SLNs at refrigerated conditions. Freeze drying of the SLN dispersion is also a good way to protect the particles against increasing particle size during storage.

Summary & Conclusion

8. SUMMARY AND CONCLUSION

The present work was proposed to develop ligand conjugated solid lipid nanoparticles of Imatinib mesylate (IM) to target the regional lymphatics of the breast to control metastasis of breast cancer. Efficient solubilisation of drugs in lipid is essential for successful development of lipid-based formulations (LBFs). Solubility of a drug in the lipid is a very important step in the development of LBFs. Examining the factors of lipids responsible for the solubility of drugs in the lipids and predicting the same can accelerate the development of LBFs. Through this research work, the role of chemical structures, polarity and various descriptors of the lipids which influenced in the solubilisation have been examined for the first time. Initially, the solubility of IM was experimentally quantified in various lipids. To correlate the quantitative solubility data with various forces connected to lipid-drug interaction, Hansen Hildebrand's total solubility parameters were calculated. To develop a relationship between the various molecular and physicochemical descriptors of the lipids and experimental solubility of IM in lipids (% w/w), quantitative structure-solubility relationship (QSSR) was used. Using MLR, a statistically valid model to theoretically predict the solubility of IM in the lipids was developed. IM showed good solubility in long chain fatty acids with a relative short alkyl chain length than long chain fatty acids with a relatively longer chain length. Monoglyceride (glyceride monostearate) derived from these long chain fatty acids showed highest solubilisation as they are more polar, which facilitates solubilisation of IM by forming hydrogen bonds. The results show that alkyl chain length and polarity of the lipids, index of cohesive interaction in solids ($AC \times DN^{0.5}/SA$), estimated number of hydrogen bonds that would be accepted by the solute from water molecules in an aqueous solution (accptHB), estimated number of hydrogen bonds that would be donated by the solute to water molecules in an aqueous solution (donorHB) and solvent accessible surface area (SASA) collectively play a significant role in solubilising IM in the lipids. It would be

ideal to have a good balance between the number of hydrogen bond acceptors and donors to favour the solubilisation of hydrophilic drugs in the lipids. The equation developed using MLR predicted the amount of IM that could be soluble in lipids with good accuracy ($R^2_{\text{pred}} = 0.912$).

IM loaded solid lipid nanoparticles were prepared using a combination of high shear homogenisation and ultrasonication techniques using different lipid carriers (stearic acid, palmitic acid, glyceryl palmitostearate, glyceryl monostearate and Geleol mono and di glycerides) and quillaja saponin (QS) as a surfactant. Hyaluronic acid and vitamin B 12 were used to modify the surface of the SLNs. Nearly fifty formulations were prepared by varying the lipids and amount of QS. The particle size, zeta potential, surface morphology, entrapment efficiency and the physical state of the entrapped drug were found out. *In vitro* release studies were performed using phosphate buffer saline (pH 7.4). The cytotoxicity of the free IM, the encapsulated form of IM in solid lipid nanoparticles and its ligand conjugated form were evaluated in MCF 7 breast cancer cell line. Apoptosis was found out using propidium iodide staining. Finally, *in vivo* pharmacokinetic studies were performed in female wistar rats after subcutaneous administration to estimate the concentration of IM in blood and lymph.

A least particle size of 92.1 ± 2.41 nm was observed for hyaluronic acid surface modified solid lipid nanoparticles of IM prepared using glyceryl palmitostearate as the lipid carrier (HAC-IGPN). These particles existed as nests containing 2-3 SLNs, with their outer surface intact. Additionally, with a neutral zeta potential, these nests of SLNs can reside in the lymphatics for a longer duration by evading opsonisation against macrophages and avoiding leakage outside the lymphatics. Usage of higher amount of QS generated SLNs with smaller size. As IM is a hydrophilic drug, the entrapment efficiencies of the formulations were low with a maximum of $65.9 \pm 0.6\%$ when glyceryl

palmitostearate were used as lipid carrier. The results of the *in vitro* release studies in phosphate buffer saline pH 7.4 showed that in almost 10 hours 100% of IM was released from the SLNs.

QS has an innate potential to cause haemolysis of red blood cells due to its lipophilic moiety. But, when it was used in the preparation of SLNs, the lipophilic moiety adhered to the lipid phase of the SLNs, and thereby exposing the hydrophilic portion to the aqueous phase. These results showed that SLNs prepared using QS as a surfactant can be used for intravenous administration. The anticancer properties of QS, smaller size of SLNs and usage of conjugating agents (like hyaluronic acid and vitamin B12) showed synergistic apoptotic effect against MCF 7 cell line by lowering the IC₅₀ value of IM loaded SLNs when compared to the free form of IM.

The amount of IM present in the blood and lymph nodes at different time points was tested after subcutaneous administration of free IM and IM encapsulated in SLNs (unconjugated and HA conjugated). The results showed a higher T_{1/2} in blood for IM encapsulated in SLNs than the free form. Additionally, subcutaneous administration of SLNs assisted in delivering higher loads of amounts of IM to the sentinel lymph nodes when administered via SLNs. A particle size below 100 nm, usage of a non-ionic surfactant and adhesion of hyaluronic acid around the surface of SLNs could have helped in delivering higher amounts of IM to the lymph nodes.

Thus, the results of the present study indicated that QSSR studies can be used as a tool to predict and study the role of lipids in solubilising IM. It was also shown for the first time that QS could be efficiently used as an emulsifier in the preparation of SLNs loaded with IM. Finally, subcutaneously administered hyaluronic acid coated SLNs (loaded with IM) with a particle size below 100 nm can enhance the amount of IM that can reach the lymphatics. These SLNs can specifically target and kill the cancerous cells in the lymphatics and prevent metastasis to other organs.

Impact of the Study

9. IMPACT OF THE STUDY

In the present scenario there are sufficient amount of anticancer drugs which can kill the tumor cells in the body. But, these drugs are equally toxic to the healthy cells of the body and cause several potential side effects, leading to reduced patient life and compliance. To avoid the possible side effects posed by the anticancer drugs, many people prefer surgical and radiation methods for the treatment. Though surgical removal of the tumor in breast cancer patients has been found to be beneficial, the incidence of recurrence of cancer to the other parts of the body (including breast) is very high and is attributed to metastasis of the cancer cells from the primary site through regional lymphatics. As metastasis of cancerous cells occurs in the regional lymphatics, it is essential for the drug to reach the regional lymphatics to arrest metastasis. In order to reach the lymphatics, the size of the particles should be in the range of 10- 100 nm, the uptake rate into the lymphatics should be high and the delivery route should be appropriate. Solid lipid nanoparticles (SLNs) can safely target and deliver anticancer drugs by subcutaneous administration to the regional lymphatics, the residing place of the metastatic cancer cells. Hence, the current doctoral research work has been planned to work on the development and evaluation of ligand conjugated SLNs of Imatinib mesylate (IM) which can specifically target and kill the tumor cells in the lymphatics. The development of SLNs requires solubilisation of the drug in the lipid carrier to achieve good entrapment efficiencies and stability. There is no model to predict the solubility of drugs in lipids. Hence, examining the various properties of lipids which influence their ability to solubilise the drugs has also been examined and a model has been developed to predict the solubility of IM in lipids for the first time. The utility of quillaja saponin (QS), a natural surfactant obtained from the bark of *Quillaja saponaria*, in the preparation of SLNs has also been evaluated for the first time.

Bibliography

BIBLIOGRAPHY

- [1] S. Ma, J. Huang, Y. Xie and N. Yi, Identification of Breast Cancer Prognosis Markers Using Integrative Sparse Boosting, *Methods Inf. Med.* 51 (2012), pp. 152–161.
- [2] J.E. Gershenwald, *CANCER: Targeting Lymphatic Metastasis*, *Science* (80). 296 (2002), pp. 1811–1812.
- [3] F. Yang, D.L. Fu, J. Long and Q.X. Ni, Magnetic lymphatic targeting drug delivery system using carbon nanotubes, *Med. Hypotheses* 70 (2008), pp. 765–767.
- [4] S. Ran, L. Volk, K. Hall and M.J. Flister, Lymphangiogenesis and lymphatic metastasis in breast cancer, *Pathophysiology* 17 (2010), pp. 229–251.
- [5] P.S. Steeg, Tumor metastasis: mechanistic insights and clinical challenges, *Nat. Med.* 12 (2006), pp. 895–904.
- [6] L. Qin, F. Zhang, X. Lu, X. Wei, J. Wang, X. Fang et al., Polymeric micelles for enhanced lymphatic drug delivery to treat metastatic tumors, *J. Control. Release* 171 (2013), pp. 133–142.
- [7] I. Singh, R. Swami, W. Khan and R. Sistla, Lymphatic system: a prospective area for advanced targeting of particulate drug carriers., *Expert Opin. Drug Deliv.* 11 (2014), pp. 211–29.
- [8] H.M. Patel, B. Katherine M. and R. Vaughan-Jones, Assessment of the potential uses of liposomes for lymphoscintigraphy and lymphatic drug delivery failure of 99m-technetium marker to represent intact liposomes in lymph nodes, *BBA - Gen. Subj.* 801 (1984), pp. 76–86.

- [9] M. A. Swartz, The physiology of the lymphatic system. [Review] [190 refs], *Adv. Drug Deliv. Rev.* 50 (2001), pp. 3–20.
- [10] Z. Yan, F. Wang, Z. Wen, C. Zhan, L. Feng, Y. Liu et al., LyP-1-conjugated PEGylated liposomes: A carrier system for targeted therapy of lymphatic metastatic tumor, *J. Control. Release* 157 (2012), pp. 118–125.
- [11] C.D. Kaur, M. Nahar and N.K. Jain, Lymphatic targeting of zidovudine using surface-engineered liposomes., *J. Drug Target.* 16 (2008), pp. 798–805.
- [12] S. Sonali, R.P. Singh, N. Singh, G. Sharma, M.R. Vijayakumar, B. Koch et al., Transferrin liposomes of docetaxel for brain targeted cancer applications: formulation and brain theranostics., *Drug Deliv.* 7544 (2016), pp. 1–37.
- [13] A. Schroeder, D. a. Heller, M.M. Winslow, J.E. Dahlman, G.W. Pratt, R. Langer et al., Treating metastatic cancer with nanotechnology, *Nat. Rev. Cancer* 12 (2011), pp. 39–50.
- [14] A.A. Khan, J. Mudassir, N. Mohtar and Y. Darwis, Advanced drug delivery to the lymphatic system: Lipid-based nanoformulations, *Int. J. Nanomedicine* 8 (2013), pp. 2733–2744.
- [15] C. Wang, Y. Wang, Y. Wang, M. Fan, F. Luo and Z. Qian, Characterization, pharmacokinetics and disposition of novel nanoscale preparations of paclitaxel, *Int. J. Pharm.* 414 (2011), pp. 251–259.
- [16] S. Kalepu, M. Manthina and V. Padavala, Oral lipid-based drug delivery systems – an overview, *Acta Pharm. Sin. B* 3 (2013), pp. 361–372.
- [17] S. Chakraborty, D. Shukla, B. Mishra and S. Singh, Lipid - An emerging platform for oral delivery of drugs with poor bioavailability, *Eur. J. Pharm. Biopharm.* 73 (2009), pp. 1–15.

- [18] W. Mehnert and K. Mäder, Solid lipid nanoparticles: Production, characterization and applications, *Adv. Drug Deliv. Rev.* 64 (2012), pp. 83–101.
- [19] R.H. Müller, K. Mäder and S. Gohla, Solid lipid nanoparticles (SLN) for controlled drug delivery - A review of the state of the art, *Eur. J. Pharm. Biopharm.* 50 (2000), pp. 161–177.
- [20] K. Cerpnjak, A. Zvonar, M. Gašperlin and F. Vrečer, Lipid-based systems as a promising approach for enhancing the bioavailability of poorly water-soluble drugs., *Acta Pharm.* 63 (2013), pp. 427–45.
- [21] M.L. Chen, Lipid excipients and delivery systems for pharmaceutical development: A regulatory perspective, *Adv. Drug Deliv. Rev.* 60 (2008), pp. 768–777.
- [22] C.M. O’Driscoll, Lipid-based formulations for intestinal lymphatic delivery, *Eur. J. Pharm. Sci.* 15 (2002), pp. 405–415.
- [23] G.A. Islan, P.C. Tornello, G.A. Abraham, N. Duran and G.R. Castro, Smart lipid nanoparticles containing levofloxacin and DNase for lung delivery. Design and characterization, *Colloids Surf B Biointerfaces* 143 (2016), pp. 168–176.
- [24] N.K. Han, D.H. Shin, J.S. Kim, K.Y. Weon, C.Y. Jang and J.S. Kim, Hyaluronan-conjugated liposomes encapsulating gemcitabine for breast cancer stem cells, *Int. J. Nanomedicine* 11 (2016), pp. 1413–1425.
- [25] L. Arana, C. Salado, S. Vega, O. Aizpurua-Olaizola, I. de la Arada, T. Suarez et al., Solid lipid nanoparticles for delivery of *Calendula officinalis* extract, *Colloids Surfaces B Biointerfaces* 135 (2015), pp. 18–26.

- [26] C.A.S. Bergström, W.N. Charman and C.J.H. Porter, Computational prediction of formulation strategies for beyond-rule-of-5 compounds, *Adv. Drug Deliv. Rev.* 101 (2015), pp. 6–21.
- [27] R.S. Kalhapure, S.J. Sonawane, D.R. Sikwal, M. Jadhav, S. Rambharose, C. Mocktar et al., Solid lipid nanoparticles of clotrimazole silver complex: An efficient nano antibacterial against *Staphylococcus aureus* and MRSA, *Colloids Surfaces B Biointerfaces* 136 (2015), pp. 651–658.
- [28] G. Wang, J. Wang, W. Wu, S. Shun, T. To, H. Zhao et al., Advances in lipid-based drug delivery: enhancing efficiency for hydrophobic drugs, *Expert Opin. Drug Deliv.* 12 (2015), pp. 1230-1332.
- [29] X. Wang, Q. Wang, Z. Liu and X. Zheng, Preparation, pharmacokinetics and tumour-suppressive activity of berberine liposomes, *J. Pharm. Pharmacol.* (2017), pp. 1–8.
- [30] S. Cai, Q. Yang, T.R. Bagby and M.L. Forrest, Lymphatic drug delivery using engineered liposomes and solid lipid nanoparticles, *Adv. Drug Deliv. Rev.* 63 (2011), pp. 901–908.
- [31] S.S. Nee Ling, al Sharon Sheue Nee Ling, E. Magosso, N. Abdul Karim Khan, K. Hay Yuen and S. Anne Barker, Enhanced Oral Bioavailability and Intestinal Lymphatic Transport of a Hydrophilic Drug Using Liposomes Evaluation of a Liposome System, *Drug Dev. Ind. Pharm.* 32 (2006), pp. 335–345.
- [32] D.M. Karpf, R. Holm, H.G. Kristensen and A. Müllertz, Influence of the type of surfactant and the degree of dispersion on the lymphatic transport of halofantrine in conscious rats, *Pharm. Res.* 21 (2004), pp. 1413–1418.
- [33] S.A. Wissing, O. Kayser and R.H. Müller, Solid lipid nanoparticles for parenteral drug delivery, *Adv. Drug Deliv. Rev.* 56 (2004), pp. 1257–1272.

- [34] C. Freitas and R.H. Müller, Spray-drying of solid lipid nanoparticles (SLN(TM)), *Eur. J. Pharm. Biopharm.* 46 (1998), pp. 145–151.
- [35] W. Mehnert and K. Mäder, Solid lipid nanoparticles: Production, characterization and applications, *Adv. Drug Deliv. Rev.* 64 (2012), pp. 83–101.
- [36] C. Schwarz and W. Mehnert, Freeze-drying of drug-free and drug-loaded solid lipid nanoparticles (SLN), *Int. J. Pharm.* 157 (1997), pp. 171–179.
- [37] A. Saupe, S.A. Wissing, A. Lenk, C. Schmidt and R.H. Müller, Solid lipid nanoparticles (SLN) and nanostructured lipid carriers (NLC) -- structural investigations on two different carrier systems, *Biomed Mater Eng* 15 (2005), pp. 393–402.
- [38] R.H. Müller, R.D. Petersen, A. Hommoss and J. Pardeike, Nanostructured lipid carriers (NLC) in cosmetic dermal products, *Adv. Drug Deliv. Rev.* 59 (2007), pp. 522–530.
- [39] M. Uner, Preparation, characterization and physico-chemical properties of solid lipid nanoparticles (SLN) and nanostructured lipid carriers (NLC): their benefits as colloidal drug carrier systems., *Pharmazie* 61 (2006), pp. 375–386.
- [40] C.C. Chen, T.H. Tsai, Z.R. Huang and J.Y. Fang, Effects of lipophilic emulsifiers on the oral administration of lovastatin from nanostructured lipid carriers: Physicochemical characterization and pharmacokinetics, *Eur. J. Pharm. Biopharm.* 74 (2010), pp. 474–482.
- [41] H. Shete, S. Chatterjee, A. De and V. Patravale, Long chain lipid based tamoxifen NLC. Part II: Pharmacokinetic, biodistribution and in vitro anticancer efficacy studies, *Int. J. Pharm.* 454 (2013), pp. 584–592.

- [42] T. Zhang, J. Chen, Y. Zhang, Q. Shen and W. Pan, Characterization and evaluation of nanostructured lipid carrier as a vehicle for oral delivery of etoposide, *Eur. J. Pharm. Sci.* 43 (2011), pp. 174–179.
- [43] C. Oussoren, M. Velinova, G. Scherphof, J.J. Van Der Want, N. Van Rooijen and G. Storm, Lymphatic uptake and biodistribution of liposomes after subcutaneous injection IV. Fate of liposomes in regional lymph nodes, *Biochim. Biophys. Acta - Biomembr.* 1370 (1998), pp. 259–272.
- [44] L. Kinman, T. Bui, K. Larsen, C. Tsai, D. Anderson, W.R. Morton et al., Optimization of Lipid Y Indinavir Complexes for Localization in Lymphoid Tissues of HIV-Infected Macaques, *J. Acquir. Immune Defic. Syndr.* 42 (2006), pp. 155–161.
- [45] A.S. Narang, D. Delmarre and D. Gao, Stable drug encapsulation in micelles and microemulsions, *Int. J. Pharm.* 345 (2007), pp. 9–25.
- [46] P.P. Constantinides, M. V. Chaubal and R. Shorr, Advances in lipid nanodispersions for parenteral drug delivery and targeting, *Adv. Drug Deliv. Rev.* 60 (2008), pp. 757–767.
- [47] R.G. Strickley, Solubilizing Excipients in Oral and Injectable Formulations, *Pharm. Res.* 21 (2004), pp. 201–230.
- [48] N. Anton, JP Benoit, P. Saulnier. Design and production of nanoparticles formulated from nano-emulsion templates-A review. *Journal of Controlled Release* 128 (2008), pp. 185-199.
- [49] J. Barauskas, H. Anderberg, A. Svendsen and T. Nylander, Thermomyces lanuginosus lipase-catalyzed hydrolysis of the lipid cubic liquid crystalline nanoparticles, *Colloids Surfaces B Biointerfaces* 137 (2016), pp. 50–59.

- [50] L.M. Negi, M. Jaggi and S. Talegaonkar, Development of protocol for screening the formulation components and the assessment of common quality problems of nano-structured lipid carriers, *Int. J. Pharm.* 461 (2014), pp. 403–410.
- [51] C. Oussoren and G. Storm, Liposomes to target the lymphatics by subcutaneous administration, *Adv. Drug Deliv. Rev.* 50 (2001), pp. 143–156.
- [52] S.M. Moghimi and M. Moghimi, Enhanced lymph node retention of subcutaneously injected IgG1-PEG2000-liposomes through pentameric IgM antibody-mediated vesicular aggregation, *Biochim. Biophys. Acta - Biomembr.* 1778 (2008), pp. 51–55.
- [53] H.L. Wong, R. Bendayan, A.M. Rauth, Y. Li and X.Y. Wu, Chemotherapy with anticancer drugs encapsulated in solid lipid nanoparticles, *Adv. Drug Deliv. Rev.* 59 (2007), pp. 491–504.
- [54] M.R. Aji Alex, A.J. Chacko, S. Jose and E.B. Souto, Lopinavir loaded solid lipid nanoparticles (SLN) for intestinal lymphatic targeting, *Eur. J. Pharm. Sci.* 42 (2011), pp. 11–18.
- [55] R. Paliwal, S. Rai, B. Vaidya, K. Khatri, A.K. Goyal, N. Mishra et al., Effect of lipid core material on characteristics of solid lipid nanoparticles designed for oral lymphatic delivery, *Nanomedicine Nanotechnology, Biol. Med.* 5 (2009), pp. 184–191.
- [56] U. Agrawal, G. Chashoo, P.R. Sharma, A. Kumar, A.K. Saxena and S.P. Vyas, Tailored polymer-lipid hybrid nanoparticles for the delivery of drug conjugate: Dual strategy for brain targeting, *Colloids Surfaces B Biointerfaces* 126 (2015), pp. 414–425.

- [57] C. Liang, Y. Yang, Y. Ling, Y. Huang, T. Li and X. Li, Improved therapeutic effect of folate-decorated PLGA-PEG nanoparticles for endometrial carcinoma, *Bioorganic Med. Chem.* 19 (2011), pp. 4057–4066.
- [58] X. yan Yang, Y. xia Li, M. Li, L. Zhang, L. xia Feng and N. Zhang, Hyaluronic acid-coated nanostructured lipid carriers for targeting paclitaxel to cancer, *Cancer Lett.* 334 (2013), pp. 338–345.
- [59] K. Becker, S. Salar-Behzadi and A. Zimmer, Solvent-Free Melting Techniques for the Preparation of Lipid-Based Solid Oral Formulations, *Pharm. Res.* 32 (2015), pp. 1519–1545.
- [60] K. Siram, V.R. Chellan, T. Natarajan, B. Krishnamoorthy, H.R. Mohamed Ebrahim, V. Karanam et al., Solid lipid nanoparticles of diethylcarbazine citrate for enhanced delivery to the lymphatics: in vitro and in vivo evaluation, *Expert Opin. Drug Deliv.* 11(9), pp.1351-1365..
- [61] A. Mishra, P.R. Vuddanda and S. Singh, Intestinal lymphatic delivery of praziquantel by solid lipid nanoparticles: Formulation design, in vitro and in vivo studies, *J. Nanotechnol.* 2014 (2014), pp. 1–12.
- [62] V.K. Venishetty, R. Komuravelli, M. Kuncha, R. Sistla and P. V. Diwan, Increased brain uptake of docetaxel and ketoconazole loaded folate-grafted solid lipid nanoparticles, *Nanomedicine Nanotechnology, Biol. Med.* 9 (2013), pp. 111–121.
- [63] C. Freitas and R.H. Müller, Correlation between long-term stability of solid lipid nanoparticles (SLNTM) and crystallinity of the lipid phase, *Eur. J. Pharm. Biopharm.* 47 (1999), pp. 125–132.
- [64] S. Cai, Q. Yang, T.R. Bagby and M.L. Forrest, Lymphatic drug delivery using engineered liposomes and solid lipid nanoparticles, *Adv. Drug Deliv. Rev.* 63 (2011), pp. 901–908.

- [65] M. Muchow, P. Maincent and R.H. Muller, Lipid Nanoparticles with a Solid Matrix (SLN®, NLC®, LDC®) for Oral Drug Delivery, *Drug Dev. Ind. Pharm.* 34 (2008), pp. 1394–1405.
- [66] H. Bunjes, and T. Unruh, Characterization of lipid nanoparticles by differential scanning calorimetry, X-ray and neutron scattering. 2007, 59(6), pp.379-402.
- [67] S.S. Rane and B.D. Anderson, What determines drug solubility in lipid vehicles: Is it predictable?, *Adv. Drug Deliv. Rev.* 60 (2008), pp. 638–656.
- [68] A.J. Almeida and E. Souto, Solid lipid nanoparticles as a drug delivery system for peptides and proteins, *Adv. Drug Deliv. Rev.* 59 (2007), pp. 478–490.
- [69] B. Ozturk and D.J. McClements, Progress in natural emulsifiers for utilization in food emulsions, *Curr. Opin. Food Sci.* 7 (2016), pp. 1–6.
- [70] F. Bakkali, S. Averbeck, D. Averbeck and M. Idaomar, Biological effects of essential oils - A review, *Food Chem. Toxicol.* 46 (2008), pp. 446–475.
- [71] M.R. Gasco, Lipid nanoparticles: perspectives and challenges, *Adv. Drug Deliv. Rev.* 59 (2007), pp. 377–378.
- [72] V. Jannin, J. Musakhanian and D. Marchaud, Approaches for the development of solid and semi-solid lipid-based formulations, *Adv. Drug Deliv. Rev.* 60 (2008), pp. 734–746.
- [73] N. Grimaldi, F. Andrade, N. Segovia, L. Ferrer-Tasies, S. Sala, J. Veciana and N. Ventosa, Lipid-based nanovesicles for nanomedicine. *Chemical Society Reviews*, 45 (2016), pp.6520-6545.

- [74] K.A. Shah, A.A. Date, M.D. Joshi and V.B. Patravale, Solid lipid nanoparticles (SLN) of tretinoin: Potential in topical delivery, *Int. J. Pharm.* 345 (2007), pp. 163–171.
- [75] D.J. Hauss, S.E. Fogal, J. V. Ficorilli, C.A. Price, T. Roy, A.A. Jayaraj et al., Lipid-based delivery systems for improving the bioavailability and lymphatic transport of a poorly water-soluble LTB₄ inhibitor, *J. Pharm. Sci.* 87 (1998), pp. 164–169.
- [76] R. Holm, H. Tonsberg, E.B. Jorgensen, P. Abedinpour, S. Farsad and A. Müllertz, Influence of bile on the absorption of halofantrine from lipid-based formulations, *Eur. J. Pharm. Biopharm.* 81 (2012), pp. 281–287.
- [77] R.H. Müller, M. Radtke and S.A. Wissing, Nanostructured lipid matrices for improved microencapsulation of drugs, *Int. J. Pharm.* 242 (2002), pp. 121–128.
- [78] W. Abdelwahed, G. Degobert, S. Stainmesse and H. Fessi, Freeze-drying of nanoparticles: Formulation, process and storage considerations, *Adv. Drug Deliv. Rev.* 58 (2006), pp. 1688–1713.
- [79] A. Pettenuzzo, R. Pigot and L. Ronconi, Vitamin B₁₂-Metal Conjugates for Targeted Chemotherapy and Diagnosis: Current Status and Future Prospects, *Eur. J. Inorg. Chem.* 20 (2017), pp. 1625–1638.
- [80] A. Verma, S. Sharma, P.K. Gupta, A. Singh, B.V. Teja, P. Dwivedi et al., Vitamin B₁₂ functionalized layer by layer calcium phosphate nanoparticles: A mucoadhesive and pH responsive carrier for improved oral delivery of insulin, *Acta Biomater.* 31 (2016), pp. 288–300.
- [81] F. Dosio, S. Arpicco, B. Stella and E. Fattal, Hyaluronic acid for anticancer drug and nucleic acid delivery, *Adv. Drug Deliv. Rev.* 97 (2016), pp. 204–236.

- [82] H. Shen, S. Shi, Z. Zhang, T. Gong and X. Sun, Coating solid lipid nanoparticles with hyaluronic acid enhances antitumor activity against melanoma stem-like cells, *Theranostics* 5 (2015), pp. 755–771.
- [83] Ö. Güçlü-Üstündağ and G. Mazza, Saponins: Properties, Applications and Processing, *Crit. Rev. Food Sci. Nutr.* 47 (2007), pp. 231–258.
- [84] R. Stanimirova, K. Marinova, S. Tcholakova, ND Denkov, S. Stoyanov, E. Pelan, Surface Rheology of Saponin Adsorption Layers, *Langmuir* 27 (2011), pp. 12486- 12498.
- [85] R. San Martin and R. Briones, Industrial Uses and Sustainable Supply of *Quillaja saponaria* (Rosaceae) Saponins, *Econ. Bot.* 53 (1999), pp. 302–311.
- [86] D. Pelah, Z. Abramovich, A. Markus and Z. Wiesman, The use of commercial saponin from *Quillaja saponaria* bark as a natural larvicidal agent against *Aedes aegypti* and *Culex pipiens*, *J. Ethnopharmacol.* 81 (2002), pp. 407–409.
- [87] I. Podolak, A. Galanty and D. Sobolewska, Saponins as cytotoxic agents: A review, *Phytochem. Rev.* 9 (2010), pp. 425–474.
- [88] C. Maier, J. Conrad, C.B. Steingass, U. Beifuss, R. Carle and R.M. Schweiggert, Quillajasides A and B: New Phenylpropanoid Sucrose Esters from the Inner Bark of *Quillaja saponaria* Molina, *J. Agric. Food Chem.* 63 (2015), pp. 8905–8911.
- [89] B. Tayyeb and M. Parvin, Pathogenesis of Breast Cancer Metastasis to Brain: a Comprehensive Approach to the Signaling Network, *Mol. Neurobiol.* 53 (2016), pp. 446–454.
- [90] B.M.M. Zwaans and D.R. Bielenberg, Potential therapeutic strategies for lymphatic metastasis, *Microvasc. Res.* 74 (2007), pp. 145–158.

- [91] H.-Y. Cho and Y.-B. Lee, Nano-Sized Drug Delivery Systems for Lymphatic Delivery, *J. Nanosci. Nanotechnol.* 14 (2014), pp. 868–880.
- [92] R. Liu, D.M. Gilmore, K.A. V Zubris, X. Xu, P.J. Catalano, R.F. Padera et al., Prevention of nodal metastases in breast cancer following the lymphatic migration of paclitaxel-loaded expansile nanoparticles, *Biomaterials* 34 (2013), pp. 1810–1819.
- [93] S.T. Reddy, A.J. van der Vlies, E. Simeoni, C.P. O’Neil, M.A. Swartz and J.A. Hubbell, Exploiting lymphatic transport and complement activation in nanoparticle vaccines, *Eur. Cells Mater.* 14 (2007), pp. 103.
- [94] A.E. Hawley, S.S. Davis and L. Illum, Targeting of colloids to lymph nodes: influence of lymphatic physiology and colloidal characteristics, *Adv. Drug Deliv. Rev.* 17 (1995), pp. 129–148.
- [95] L. Feng, L. Zhang, M. Liu, Z. Yan, C. Wang, B. Gu et al., Roles of dextrans on improving lymphatic drainage for liposomal drug delivery system., *J. Drug Target.* 18 (2010), pp. 168–178.
- [96] G.M. Mortimer, N.J. Butcher, A.W. Musumeci, Z.J. Deng, D.J. Martin and R.F. Minchin, Cryptic epitopes of albumin determine mononuclear phagocyte system clearance of nanomaterials, *ACS Nano* 8 (2014), pp. 3357–3366.
- [97] S.N. Mueller, S. Tian and J.M. Desimone, Rapid and persistent delivery of antigen by lymph node targeting PRINT nanoparticle vaccine carrier to promote humoral immunity, *Mol. Pharm.* 12 (2015), pp. 1356–1365.
- [98] L.M. Kaminskis, J. Kota, V.M. McLeod, B.D. Kelly, P. Karellas and C.J. Porter, PEGylation of polylysine dendrimers improves absorption and lymphatic targeting following SC administration in rats, *J. Control. Release* 140 (2009), pp. 108–116.

- [99] H.I. Chang and M.K. Yeh, Clinical development of liposome-based drugs: Formulation, characterization, and therapeutic efficacy, *Int. J. Nanomedicine* 7 (2012), pp. 49–60.
- [100] Y. Geng, P. Dalhaimer, S. Cai, R. Tsai, M. Tewari, T. Minko et al., Shape effects of filaments versus spherical particles in flow and drug delivery., *Nat. Nanotechnol.* 2 (2007), pp. 249–55.
- [101] C. Liu, Z. Chen, Y. Chen, J. Lu, Y. Li, S. Wang et al., Improving Oral Bioavailability of Sorafenib by Optimizing the “spring” and “parachute” Based on Molecular Interaction Mechanisms, *Mol. Pharm.* 13 (2016), pp. 599–608.
- [102] M. Joshi and V. Patravale, Formulation and evaluation of Nanostructured Lipid Carrier (NLC)-based gel of Valdecoxib., *Drug Dev. Ind. Pharm.* 32 (2006), pp. 911–918.
- [103] K.W. Kasongo, J. Pardeike, R.H. Müller and R.B. Walker, Selection and characterization of suitable lipid excipients for use in the manufacture of didanosine-loaded solid lipid nanoparticles and nanostructured lipid carriers, *J. Pharm. Sci.* 100 (2011), pp. 5185–5196.
- [104] Y. Geng and D.E. Discher, Hydrolytic degradation of poly(ethylene oxide)-block-polycaprolactone worm micelles, *J. Am. Chem. Soc.* 127 (2005), pp. 12780–12781.
- [105] T.S. Levchenko, R. Rammohan, A.N. Lukyanov, K.R. Whiteman and V.P. Torchilin, Liposome clearance in mice: The effect of a separate and combined presence of surface charge and polymer coating, *Int. J. Pharm.* 240 (2002), pp. 95–102.
- [106] V. Sanna, N. Pala and M. Sechi, Targeted therapy using nanotechnology: Focus on cancer, *Int. J. Nanomedicine* 9 (2014), pp. 467–483.

- [107] N. Kamaly, Z. Xiao, P.M. Valencia, A.F. Radovic-Moreno and O.C. Farokhzad, Targeted polymeric therapeutic nanoparticles: design, development and clinical translation., *Chem. Soc. Rev.* 41 (2012), pp. 2971–3010.
- [108] S.D. Li and L. Huang, Pharmacokinetics and biodistribution of nanoparticles, *Mol. Pharm.* 5 (2008), pp. 496–504.
- [109] V. Weissig, T.K. Pettinger and N. Murdock, Nanopharmaceuticals (part 1): products on the market, *Int. J. Nanomedicine* 9 (2014), pp. 4357–4373.
- [110] M. Joshi and V. Patravale, Nanostructured lipid carrier (NLC) based gel of celecoxib, *Int. J. Pharm.* 346 (2008), pp. 124–132.
- [111] H. Mu, R. Holm and A. Mullertz, Lipid-based formulations for oral administration of poorly water-soluble drugs, *Int. J. Pharm.* 453 (2013), pp. 215–224.
- [112] C.J.H. Porter and W.N. Charman, Intestinal lymphatic drug transport: An update, *Adv. Drug Deliv. Rev.* 50 (2001), pp. 61–80.
- [113] M.K. Shah, P. Madan and S. Lin, Preparation, in vitro evaluation and statistical optimization of carvedilol-loaded solid lipid nanoparticles for lymphatic absorption via oral administration, *Pharm. Dev. Technol.* 19 (2014), pp. 475–485.
- [114] C.M. O’Driscoll, Lipid-based formulations for intestinal lymphatic delivery, *Eur. J. Pharm. Sci.* 15 (2002), pp. 405–415.
- [115] H. Shete and V. Patravale, Long chain lipid based tamoxifen NLC. Part I: Preformulation studies, formulation development and physicochemical characterization, *Int. J. Pharm.* 454 (2013), pp. 573–583.

- [116] K. Yoshino, K. Nakamura, Y. Terajima, A. Kurita, T. Matsuzaki, K. Yamashita et al., Comparative studies of irinotecan-loaded polyethylene glycol-modified liposomes prepared using different PEG-modification methods, *Biochim. Biophys. Acta - Biomembr.* 1818 (2012), pp. 2901–2907.
- [117] C.K. Kim, M.K. Lee, J.H. Han and B.J. Lee, Pharmacokinetics and tissue distribution of methotrexate after intravenous injection of differently charged liposome-entrapped methotrexate to rats, *Int. J. Pharm.* 108 (1994), pp. 21–29.
- [118] S.K. Nune, P. Gunda, B.K. Majeti, P.K. Thallapally and M.L. Forrest, Advances in lymphatic imaging and drug delivery, *Adv. Drug Deliv. Rev.* 63 (2011), pp. 876–885.
- [119] Y. Nishioka and H. Yoshino, Lymphatic targeting with nanoparticulate system, *Adv. Drug Deliv. Rev.* 47 (2001), pp. 55–64.
- [120] V. Makwana, R. Jain, K. Patel, M. Nivsarkar and A. Joshi, Solid lipid nanoparticles (SLN) of Efavirenz as lymph targeting drug delivery system: Elucidation of mechanism of uptake using chylomicron flow blocking approach, *Int. J. Pharm.* 495 (2015), pp. 439–446.
- [121] B. Chauhan, S. Shimpi and A. Paradkar, Preparation and evaluation of glibenclamide-polyglycolized glycerides solid dispersions with silicon dioxide by spray drying technique, *Eur. J. Pharm. Sci.* 26 (2005), pp. 219–230.
- [122] E. Fahy, D. Cotter, M. Sud and S. Subramaniam, Lipid classification, structures and tools, *Biochim. Biophys. Acta - Mol. Cell Biol. Lipids* 1811 (2011), pp. 637–647.

- [123] Y. Wang and W. Wu, In situ evading of phagocytic uptake of stealth solid lipid nanoparticles by mouse peritoneal macrophages, *Drug Deliv* 13 (2006), pp. 189–192.
- [124] B. Rohit and K.I. Pal, A Method to Prepare Solid Lipid Nanoparticles with Improved Entrapment Efficiency of Hydrophilic Drugs, *Curr. Nanosci.* 9 (2013), pp. 211–220.
- [125] G. Bende, S. Kollipara, S. Movva, G. Moorthy and R. Saha, Validation of an HPLC method for determination of imatinib mesylate in rat serum and its application in a pharmacokinetic study., *J. Chromatogr. Sci.* 48 (2010), pp. 334–41.
- [126] G. Marslin, A.M. Revina, V.K.M. Khandelwal, K. Balakumar, J. Prakash, G. Franklin et al., Delivery as nanoparticles reduces imatinib mesylate-induced cardiotoxicity and improves anticancer activity, *Int. J. Nanomedicine* 10 (2015), pp. 3163–3170.
- [127] G. Guetens, G. De Boeck, M. Highley, H. Dumez, A.T. Van Oosterom and E.A. De Bruijn, Quantification of the anticancer agent STI-571 in erythrocytes and plasma by measurement of sediment technology and liquid chromatography-tandem mass spectrometry, *J. Chromatogr. A* 1020 (2003), pp. 27–34.
- [128] Y. Zhou, S. Wang, T. Ding, M. Wu, P. Geng, Q. Zhang et al., Pharmacokinetic interaction study of combining imatinib with dasatinib in rats by UPLC–MS/MS, *Drug Dev. Ind. Pharm.* 41 (2015), pp. 1948–1953.
- [129] B. Gupta, B.K. Poudel, T.H. Tran, R. Pradhan, H.J. Cho, J.H. Jeong et al., Modulation of Pharmacokinetic and Cytotoxicity Profile of Imatinib Base by Employing Optimized Nanostructured Lipid Carriers, *Pharm. Res.* 32 (2015), pp. 2912–2927.

- [130] I. Kralova and J. Sjoblom, Surfactants Used in Food Industry: A Review, *J. Dispers. Sci. Technol.* 30 (2009), pp. 1363–1383.
- [131] Y. Yang, M.E. Leser, A.A. Sher and D.J. McClements, Formation and stability of emulsions using a natural small molecule surfactant: Quillaja saponin (Q-Naturale), *Food Hydrocoll.* 30 (2013), pp. 589–596.
- [132] G. Francis, Z. Kerem, H.P.S. Makkar and K. Becker, The biological action of saponins in animal systems: a review, *Br. J. Nutr.* 88 (2002), pp. 587–605.
- [133] L.C. Alskär, C.J.H. Porter and C.A.S. Bergström, Tools for Early Prediction of Drug Loading in Lipid-Based Formulations, *Mol. Pharm.* 13 (2016), pp. 251–261.
- [134] L.A.D. Silva, F.V. Teixeira, R.C. Serpa, N.L. Esteves, R.R. Dos Santos, E.M. Lima et al., Evaluation of carvedilol compatibility with lipid excipients for the development of lipid-based drug delivery systems, *J. Therm. Anal. Calorim.* 123 (2016), pp. 2337–2344.
- [135] S. Umamatheswari, B. Balaji, M. Ramanathan and S. Kabilan, Synthesis, stereochemistry, antimicrobial evaluation and QSAR studies of 2,6-diaryltetrahydropyran-4-one thiosemicarbazones, *Eur. J. Med. Chem.* 46 (2011), pp. 1415–1424.
- [136] W. Zheng, A. Jain, D. Papoutsakis, R.M. Dannenfelser, R. Panicucci and S. Garad, Selection of oral bioavailability enhancing formulations during drug discovery, *Drug Dev Ind Pharm* 38 (2012), pp. 235–247.
- [137] D.B. Warren, D. King, H. Benameur, C.W. Pouton and D.K. Chalmers, Glyceride lipid formulations: Molecular dynamics modeling of phase behavior during dispersion and molecular interactions between drugs and excipients, *Pharm. Res.* 30 (2013), pp. 3238–3253.

- [138] L. Yang, C. Adam, G.S. Nichol and S.L. Cockroft, How much do van der Waals dispersion forces contribute to molecular recognition in solution, *Nat. Chem.* 5 (2013), pp. 1006–1010.
- [139] L.B. Jensen, E. Magnusson, L. Gunnarsson, C. Vermehren, H.M. Nielsen and K. Petersson, Corticosteroid solubility and lipid polarity control release from solid lipid nanoparticles, *Int. J. Pharm.* 390 (2010), pp. 53–60.
- [140] W.L. Jorgensen and E.M. Duffy, Prediction of drug solubility from Monte Carlo simulations., *Bioorg. Med. Chem. Lett.* 10 (2000), pp. 1155–8.
- [141] M. Sacchetti and E. Nejati, Prediction of drug solubility in lipid mixtures from the individual ingredients., *AAPS PharmSciTech* 13 (2012), pp. 1103–9.
- [142] Y. Li, N. Taulier, A.M. Rauth and X.Y. Wu, Screening of lipid carriers and characterization of drug-polymer-lipid interactions for the rational design of polymer-lipid hybrid nanoparticles (PLN), *Pharm. Res.* 23 (2006), pp. 1877–1887.
- [143] D.F. Ortwine and I. Aliagas, Physicochemical and DMPK in silico models: Facilitating their use by medicinal chemists, *Mol. Pharm.* 10 (2013), pp. 1153–1161.
- [144] C.A. Lipinski, F. Lombardo, B.W. Dominy and P.J. Feeney, Experimental and computational approaches to estimate solubility and permeability in drug discovery and development settings, *Adv. Drug Deliv. Rev.* 64 (2012), pp. 4–17.
- [145] A. Golbraikh and A. Tropsha, Beware of q^2 !, *J. Mol. Graph. Model.* 20 (2002), pp. 269–276.

- [146] D.J. Greenhalgh, A.C. Williams, P. Timmins and P. York, Solubility parameters as predictors of miscibility in solid dispersions, *J. Pharm. Sci.* 88 (1999), pp. 1182–1190.
- [147] M. Subashini, P. V. Devarajan, G.S. Sonavane and M. Doble, Molecular dynamics simulation of drug uptake by polymer, *J. Mol. Model.* 17 (2011), pp. 1141–1147.
- [148] X.Q. Chen, O.S. Gudmundsson and M.J. Hageman, Application of lipid-based formulations in drug discovery, *J. Med. Chem.* 55 (2012), pp. 7945–7956.
- [149] A. Cheng and K.M. Merz, Prediction of aqueous solubility of a diverse set of compounds using quantitative structure-property relationships, *J. Med. Chem.* 46 (2003), pp. 3572–3580.
- [150] S. V. Patel and S. Patel, Prediction of the solubility in lipidic solvent mixture: Investigation of the modeling approach and thermodynamic analysis of solubility, *Eur. J. Pharm. Sci.* 77 (2015), pp. 161–169.
- [151] L.C. Persson, C.J.H. Porter, W.N. Charman and C.A.S. Bergström, Computational prediction of drug solubility in lipid based formulation excipients, *Pharm. Res.* 30 (2013), pp. 3225–3237.
- [152] F. Chevillard, D. Lagorce, C. Reynès, B.O. Villoutreix, P. Vayer and M.A. Miteva, In silico prediction of aqueous solubility: A multimodel protocol based on chemical similarity, *Mol. Pharm.* 9 (2012), pp. 3127–3135.
- [153] L.Z. Benet, F. Broccatelli and T.I. Oprea, BDDCS applied to over 900 drugs., *AAPS J.* 13 (2011), pp. 519–47.

- [154] H. Ali, S.K. Singh and P.R.P. Verma, Preformulation and physicochemical interaction study of furosemide with different solid lipids, *J. Pharm. Investig.* 45 (2015), pp. 385–398.
- [155] S.S. Chalikwar, V.S. Belgamwar, V.R. Talele, S.J. Surana and M.U. Patil, Formulation and evaluation of Nimodipine-loaded solid lipid nanoparticles delivered via lymphatic transport system, *Colloids Surfaces B Biointerfaces* 97 (2012), pp. 109–116.
- [156] P. Bailon and C. Won, PEG-modified biopharmaceuticals, *In Vitro* (2009), pp. 1–16.
- [157] M. Garg, T. Dutta and N.K. Jain, Reduced hepatic toxicity, enhanced cellular uptake and altered pharmacokinetics of stavudine loaded galactosylated liposomes, *Eur. J. Pharm. Biopharm.* 67 (2007), pp. 76–85.
- [158] H. Yuan, J. Miao, Y.Z. Du, J. You, F.Q. Hu and S. Zeng, Cellular uptake of solid lipid nanoparticles and cytotoxicity of encapsulated paclitaxel in A549 cancer cells, *Int. J. Pharm.* 348 (2008), pp. 137–145.
- [159] S. Biswas, N.S. Dodwadkar, P.P. Deshpande, S. Parab and V.P. Torchilin, Surface functionalization of doxorubicin-loaded liposomes with octa-arginine for enhanced anticancer activity, *Eur. J. Pharm. Biopharm.* 84 (2013), pp. 517–525.
- [160] G.A. Edwards, C.J. Porter, S.M. Caliph, S.-M. Khoo and W. Charman, Animal models for the study of intestinal lymphatic drug transport, *Adv. Drug Deliv. Rev.* 50 (2001), pp. 45–60.
- [161] O.M. Feeney, M.F. Crum, C.L. McEvoy, N.L. Trevaskis, H.D. Williams, C.W. Pouton et al., 50 years of oral lipid-based formulations: Provenance, progress and future perspectives, *Adv. Drug Deliv. Rev.* 101 (2016), pp. 167–194.

- [162] Z. Wang, L. Wang, M.M. Xia, W. Sun, C.K. Huang, X. Cui et al., Pharmacokinetics interaction between imatinib and genistein in rats, *Biomed Res. Int.* 2015 (2015), .
- [163] M. Boyd, V. Risovic, P. Jull, E. Choo and K.M. Wasan, A stepwise surgical procedure to investigate the lymphatic transport of lipid-based oral drug formulations: Cannulation of the mesenteric and thoracic lymph ducts within the rat, *J. Pharmacol. Toxicol. Methods* 49 (2004), pp. 115–120.
- [164] P.K. Gaur, S. Mishra, M. Bajpai and A. Mishra, Enhanced oral bioavailability of Efavirenz by solid lipid nanoparticles: In vitro drug release and pharmacokinetics studies, *Biomed Res. Int.* 2014 (2014), pp. 363404.
- [165] L.C. Persson, C.J.H. Porter, W.N. Charman and C.A.S. Bergström, Computational prediction of drug solubility in lipid based formulation excipients, *Pharm. Res.* 30 (2013), pp. 3225–3237.
- [166] No Title. Available at <http://www.schrodinger.com/products/14/17/>.
- [167] P. Ramalingam and Y.T. Ko, Improved oral delivery of resveratrol from N-trimethyl chitosan-g-palmitic acid surface-modified solid lipid nanoparticles, *Colloids Surfaces B Biointerfaces* 139 (2016), pp. 52–61.
- [168] R. Swami, I. Singh, M.K. Jeengar, V.G.M. Naidu, W. Khan and R. Sistla, Adenosine conjugated lipidic nanoparticles for enhanced tumor targeting, *Int. J. Pharm.* 486 (2015), pp. 287–296.
- [169] Y. Sangsen, K. Wiwattanawongsa, K. Likhitwitayawuid, B. Sritularak and R. Wiwattanapatapee, Modification of oral absorption of oxyresveratrol using lipid based nanoparticles, *Colloids Surfaces B Biointerfaces* 131 (2015), pp. 182–190.

- [170] R.K. Subedi, K.W. Kang and H.-K. Choi, Preparation and characterization of solid lipid nanoparticles loaded with doxorubicin., *Eur. J. Pharm. Sci.* 37 (2009), pp. 508–513.
- [171] R. Cassano, S. Mellace, M. Marrelli, F. Conforti and S. Trombino, α -Tocopheryl linolenate solid lipid nanoparticles for the encapsulation, protection, and release of the omega-3 polyunsaturated fatty acid: in vitro anti-melanoma activity evaluation, *Colloids Surfaces B Biointerfaces* 151 (2017), pp. 128–133.
- [172] Y. Ma, X. Zhao, J. Li and Q. Shen, The comparison of different daidzein-PLGA nanoparticles in increasing its oral bioavailability, *Int. J. Nanomedicine* 7 (2012), pp. 559–570.
- [173] S. Honary and F. Zahir, Effect of zeta potential on the properties of nano-drug delivery systems - A review (Part 1), *Trop. J. Pharm. Res.* 12 (2013), pp. 255–264.
- [174] E. Muntimadugu, R. Kumar, S. Saladi, T.A. Rafeeqi and W. Khan, CD44 targeted chemotherapy for co-eradication of breast cancer stem cells and cancer cells using polymeric nanoparticles of salinomycin and paclitaxel, *Colloids Surfaces B Biointerfaces* 143 (2016), pp. 532–546.
- [175] E. Guzmán, M. Ferrari, E. Santini, L. Liggieri and F. Ravera, *Colloids and Surfaces B: Biointerfaces* Effect of silica nanoparticles on the interfacial properties of a canonical lipid mixture, *Colloids Surfaces B Biointerfaces* 136 (2015), pp. 971–980.
- [176] A. Jain, P. Kesharwani, N.K. Garg, A. Jain, S.A. Jain, A.K. Jain et al., Galactose engineered solid lipid nanoparticles for targeted delivery of doxorubicin, *Colloids Surfaces B Biointerfaces* 134 (2015), pp. 47–58.

- [177] A.R. Dixit, S.J. Rajput and S.G. Patel, Preparation and bioavailability assessment of SMEDDS containing valsartan., *AAPS PharmSciTech* 11 (2010), pp. 314–321.
- [178] V. Karanam, G. Marslin, B. Krishnamoorthy, V. Chellan, K. Siram, T. Natarajan et al., Poly (ϵ -caprolactone) nanoparticles of carboplatin: Preparation, characterization and in vitro cytotoxicity evaluation in U-87 MG cell lines, *Colloids Surfaces B Biointerfaces* 130 (2015), pp. 48–52.
- [179] N. Krishnakumar, N. Sulfikkarali, N. RajendraPrasad and S. Karthikeyan, Enhanced anticancer activity of naringenin-loaded nanoparticles in human cervical (HeLa) cancer cells, *Biomed. Prev. Nutr.* 1 (2011), pp. 223–231.
- [180] M. Ramar, B. Manikandan, P.N. Marimuthu, T. Raman, A. Mahalingam, P. Subramanian et al., Synthesis of silver nanoparticles using *Solanum trilobatum* fruits extract and its antibacterial, cytotoxic activity against human breast cancer cell line MCF 7, *Spectrochim. Acta - Part A Mol. Biomol. Spectrosc.* 140 (2015), pp. 223–228.
- [181] Y. Singh, A. Srinivas, M. Gangwar, J.G. Meher, S. Misra-Bhattacharya and M.K. Chourasia, Subcutaneously Administered Ultrafine PLGA Nanoparticles Containing Doxycycline Hydrochloride Target Lymphatic Filarial Parasites, *Mol. Pharm.* 13 (2016), pp. 2084–2094.
- [182] H. Mu, R. Holm and A. Müllertz, Lipid-based formulations for oral administration of poorly water-soluble drugs, *Int. J. Pharm.* 453 (2013), pp. 215–224.
- [183] B. Ozturk, S. Argin, M. Ozilgen and D.J. McClements, Formation and stabilization of nanoemulsion-based vitamin e delivery systems using natural surfactants: Quillaja saponin and lecithin, *J. Food Eng.* 142 (2014), pp. 57–63.

- [184] H.-P. Gschwind, U. Pfaar, F. Waldmeier, M. Zollinger, C. Sayer and G. Gross, Metabolism and Disposition of Imatinib Mesylate in Healthy Volunteers Abstract :, Drug Metab. Dispos. 33 (2005), pp. 1503–1512.
- [185] R. Singh and L.J. W., Nanoparticle-based targeted drug delivery, Exp. Mol. Pathol. 86 (2009), pp. 215–223.
- [186] R. Friedl, T. Moeslinger, B. Kopp and P.G. Spieckermann, Stimulation of nitric oxide synthesis by the aqueous extract of Panax ginseng root in RAW 264.7 cells., Br. J. Pharmacol. 134 (2001), pp. 1663–1670.
- [187] L. Tan, K.G. Neoh, E.T. Kang, W.S. Choe and X. Su, PEGylated anti-MUC1 aptamer-doxorubicin complex for targeted drug delivery to MCF7 breast cancer cells, Macromol. Biosci. 11 (2011), pp. 1331–1335.
- [188] D.D. Kumbhar and V.B. Pokharkar, Engineering of a nanostructured lipid carrier for the poorly water-soluble drug, bicalutamide: Physicochemical investigations, Colloids Surfaces A Physicochem. Eng. Asp. 416 (2013), pp. 32–42.
- [189] S. Karthik, C.V. Raghavan, G. Marslin, H. Rahman, D. Selvaraj, K. Balakumar et al., Quillaja saponin: A prospective emulsifier for the preparation of solid lipid nanoparticles, Colloids Surfaces B Biointerfaces 147 (2016), pp. 274–280.
- [190] N.V. Rao, H.Y. Yoon, H.S. Han, H. Ko, S. Son, M. Lee et al., Recent developments in hyaluronic acid-based nanomedicine for targeted cancer treatment., Expert Opin. Drug Deliv. 13 (2016), pp. 239–52.
- [191] V. Venkateswarlu and K. Manjunath, Preparation, characterization and in vitro release kinetics of clozapine solid lipid nanoparticles, J. Control. Release 95 (2004), pp. 627–638.

- [192] J. Akbari, M. Saeedi, K. Morteza-Semnani, S.S. Rostamkalaei, M. Asadi, K. Asare-Addo et al., The design of naproxen solid lipid nanoparticles to target skin layers, *Colloids Surfaces B Biointerfaces* 145 (2016), pp. 626–633.
- [193] M. Oh, Y.H. Choi, S.H. Choi, H.Y. Chung, K.W. Kim, S. Il Kim et al., Anti-proliferating effects of ginsenoside Rh2 on MCF-7 human breast cancer cells, *Int. J. Oncol.* 14 (1999), pp. 869–875.
- [194] S. Kumar and J.K. Randhawa, High melting lipid based approach for drug delivery: Solid lipid nanoparticles, *Mater. Sci. Eng. C* 33 (2013), pp. 1842–1852.
- [195] E.K. Noriega-Peláez, N. Mendoza-Muñoz, A. Ganem-Quintanar, D. Quintanar-Guerrero, Optimization of the emulsification and solvent displacement method for the preparation of solid lipid nanoparticles. *Drug Dev Ind Pharm.* 37(2011), pp. 160-166.
- [196] R. Yasmin, S. Rao, K.E. Bremmell and C.A. Prestidge, Porous Silica-Supported Solid Lipid Particles for Enhanced Solubilization of Poorly Soluble Drugs, *The AAPS journal*, 18(2016), pp.876-885.
- [197] C.J.H. Porter, N.L. Trevaskis and W.N. Charman, Lipids and lipid-based formulations: optimizing the oral delivery of lipophilic drugs., *Nat. Rev. Drug Discov.* 6 (2007), pp. 231–48.
- [198] L.M. Kaminskis and C.J.H. Porter, Targeting the lymphatics using dendritic polymers (dendrimers), *Adv. Drug Deliv. Rev.* 63 (2011), pp. 890–900.
- [199] C. Oussoren, J. Zuidema, D.J.A. Crommelin and G. Storm, Lymphatic uptake and biodistribution of liposomes after subcutaneous injection. II. Influence of liposomal size, lipid composition and lipid dose, *Biochim. Biophys. Acta - Biomembr.* 1328 (1997), pp. 261–272.

- [200] B. Lu, S.-B. Xiong, H. Yang, X.-D. Yin and R.-B. Chao, Solid lipid nanoparticles of mitoxantrone for local injection against breast cancer and its lymph node metastases., *Eur. J. Pharm. Sci.* 28 (2006), pp. 86–95.
- [201] R. Ling, Y. Li, Q. Yao, T. Chen, D. Zhu, Y. Jun et al., Lymphatic chemotherapy induces apoptosis in lymph node metastases in a rabbit breast carcinoma model., *J. Drug Target.* 13 (2005), pp. 137–42.
- [202] C. Freitas and R.H. Müller, Effect of light and temperature on zeta potential and physical stability in solid lipid nanoparticles (SLN TM) dispersions, *Int. J. Pharm.* 168 (1998), pp. 221–229.
- [203] D.P. Gaspar, V. Faria, L.M.D. Gonçalves, P. Taboada, C. Remuñán-López and A.J. Almeida, Rifabutin-loaded solid lipid nanoparticles for inhaled antitubercular therapy: Physicochemical and in vitro studies, *Int. J. Pharm.* 497 (2016), pp. 199–209.

Annexure I
Plagiarism Report

ANNEXURE -I

PLAGIARISM CERTIFICATE

This is to certify that this dissertation work titled **Development of Ligand Conjugated Nano Drug Delivery System to Prevent Lymphatic Metastasis of Breast Cancer** of the candidate **Siram Karthik** with registration Number **141440019** for the award of **Doctor of Philosophy** in the branch of **Pharmacy and Pharmaceutics** I personally verified the urkund.com website for the purpose of plagiarism Check. I found that the uploaded thesis file contains from introduction to conclusion pages and result shows **1** percentage of plagiarism in the dissertation.

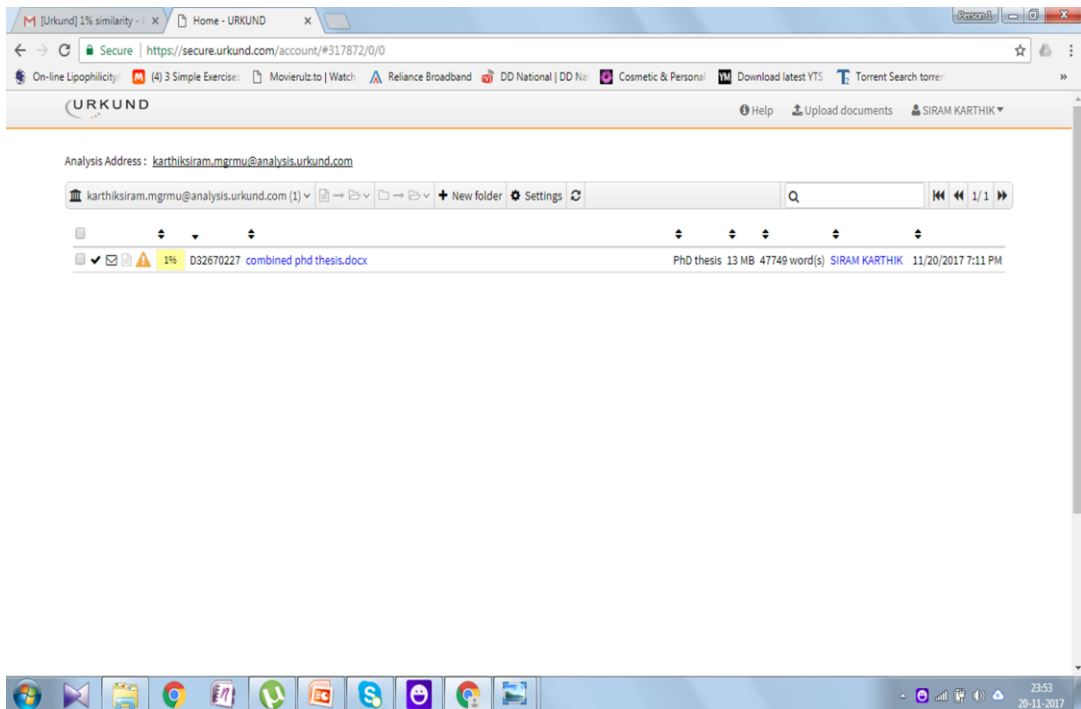
Guide & Supervisor sign with Seal.

Urkund Analysis Result

Analysed Document: combined phd thesis.docx (D32670227)
Submitted: 11/20/2017 7:11:00 PM
Submitted By: karthiksiram@gmail.com
Significance: 1 %

Sources included in the report:

<http://journals.plos.org/plosone/article?id=10.1371%2Fjournal.pone.0154926>
<https://helda.helsinki.fi/handle/10138/30100>
<https://www.sciencedirect.com/science/article/pii/S0378874102001381>
<https://www.sciencedirect.com/science/article/pii/S0927776516305677>
<https://books.google.co.uk/patents/US9387190>
<https://link.springer.com/article/10.1007/s11743-016-1871-2>
http://pubs.rsc.org/en/Content/ArticleLanding/2012/CS/C2CS15344K?_escaped_fragment_=divAbstract
<http://jprsolutions.info/newfiles/journal-file-5662ff4ea6e8e2.89313662.pdf>
<https://dash.harvard.edu/handle/1/29293168>
<https://link.springer.com/article/10.1007/s11095-013-1206-1>
<https://github.com/citation-style-language/schema/raw/master/csl-citation.json>





karthik siram <karthiksiram@gmail.com>

[Urkund] 1% similarity - karthiksiram@gmail.com

report@analysis.urkund.com <report@analysis.urkund.com>
To: karthiksiram@gmail.com

Mon, Nov 20, 2017 at 11:51 PM

Document sent by: karthiksiram@gmail.com
Document received: 11/20/2017 7:11:00 PM
Report generated 11/20/2017 7:21:16 PM by Urkund's system for automatic control.

Student message: combined PhD thesis.

Document : combined phd thesis.docx [D32670227]

IMPORTANT! The analysis contains 1 warning(s).

About 1% of this document consists of text similar to text found in 98 sources. The largest marking is 59 words long and is 96% similar to its primary source.

PLEASE NOTE that the above figures do not automatically mean that there is plagiarism in the document. There may be good reasons as to why parts of a text also appear in other sources. For a reasonable suspicion of academic dishonesty to present itself, the analysis, possibly found sources and the original document need to be examined closely.

Click here to open the analysis:
<https://secure.urkund.com/view/32256654-852399-373418>

Click here to download the document:
<https://secure.urkund.com/archive/download/32670227-930877-278325>

Annexure- II
Animal Ethical Committee
Certificate



PSG Institute of Medical Sciences & Research Institutional Animal Ethics Committee

Registration No. : 158 / PO / ReBi / SL / 99 / CPCSEA
POST BOX No. 1674, PEELAMEDU, COIMBATORE 641 004, TAMIL NADU, INDIA
Phone : 91 422 - 2570170, 2598822 Fax : 91 422 - 2594400 Email : psganimaethics@gmail.com

DATE: 17.06.2016

Title of the Project: Development of Ligand Conjugated Nano Drug Delivery System to Prevent Lymphatic Metastasis of Breast Cancer

Proposal Number: 211/2016/ IAEC

Name of the Applicant: Siram Karthik,

Approval date: 17.06.2016

Expiry date (Termination of the Project): 16.06.2017

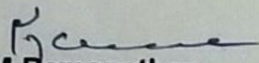
Methodology: Approved.

Name of species: Swiss albino mice/ Wistar rats/ Sprague Dawley rats/ Guinea pigs/ Newzealand White rabbits.

Male/Female/Both sex-----Renewed-----animals approved.

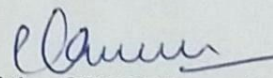
Signature of Chairperson

Date: 17.6.16


Dr.M.Ramanathan

Name of the chairperson

The Chair Person, CPCSEA
IAEC of PSGIMS&R
Coimbatore-641 004.


Signature of the CPCSEA nominee

Date: 17/6/2016

Dr.C.Kathirvelan

Name of IAEC/CPCSEA nominee

Main Nominee, CPCSEA
IAEC of PSGIMS&R
Coimbatore-641 004.

Annexure III
List of Awards, Publications
& Conferences Attended

ANNEXURE- III

LIST OF AWARDS, PUBLICATIONS AND CONFERENCES ATTENDED

List of awards and grants received:

- 1) Received **research grant** from **The Tamil Nadu State Council for Science and Technology**, Government of Tamil Nadu, India, under the scheme **Research Fund for Research Scholars** in support of my PhD work in 2015.
- 2) Received **travel fellowship** from **Science and Engineering Research Board (SERB)**, Department of Science and Technology, Government of India, for attending 2016 AAPS Annual Meeting and Exposition at Denver, Colorado, USA, during 13-17th November, 2016.
- 3) Awarded **1st prize for oral presentation** during **3rd International Conference on Drug Delivery**, organized by PSG College of Pharmacy, Coimbatore during 28th February- 1st March, 2014.
- 4) Research work entitled **“Development of Surface Modified Lipid Nanoparticles for Selective Targeting of Tumor Cells in Lymph Nodes to Prevent Metastasis and It’s Evaluation in BALB/c Mice Cancer Model”** was partially funded by **The Tamil Nadu Dr. MGR Medical University**. (grant not availed).
- 5) Received **travel fellowship** from **Centre for International Co-operation in Sciences (CICS)**, India for attending 5th World Congress on Bioavailability and Bioequivalence: Pharmaceutical R&D Summit from September 29th to October 01st 2014 at Baltimore USA. (grant not availed).
- 6) Awarded **1st prize for oral presentation** during 1st International Drug Delivery Congress 2017, held at RVS College of Pharmaceutical Sciences, Coimbatore, India during 20th- 21st January, 2017.
- 7) Awarded **best oral presentation** during National Conference on Current Perspectives in Novel drug Delivery Systems held at PSG College of Pharmacy, Coimbatore, India, during 16th- 17th June, 2017.

Publications

- 1) **Siram K**, Raghavan CV, Marslin G, Habibur Rahman, Divakar S, Balakumar K, Franklin G. Characterisation and toxicity evaluation of solid lipid nanoparticles prepared using Quillaja saponin as an emulsifier. *Colloids and Surfaces B: Biointerfaces*. 2016; 147:274-280. (Impact factor- 3.9).
- 2) **Siram K**, Marslin G, Raghavan CV, Balakumar K, Rahman H, Franklin. A brief perspective on the diverging theories of lymphatic targeting with colloids. *International Journal of Nanomedicine*. 2016;11:2867-2872. (Impact factor- 4.3).
- 3) **Siram K**, Chellan VR, Natarajan T, Krishnamoorthy B, Mohamed Ebrahim HR, Karanam V, Muthuswamy SS, Ranganathan HP. Solid lipid nanoparticles of diethylcarbamazine citrate for enhanced delivery to the lymphatics: in vitro and in vivo evaluation. *Expert Opinion on Drug Delivery*. 2014 Sept; 11(9): 1351-1365.
- 4) Marslin, G.; **Siram, K.**; Liu, X.; Khandelwal, V.K.M.; Xiaolei, S.; Xiang, W.; Franklin, G. Solid Lipid Nanoparticles of Albendazole for Enhancing Cellular Uptake and Cytotoxicity against U-87 MG Glioma Cell Lines. *Molecules* 2017, 22, 2040.

Book Chapters

S. M. Habibur Rahman, K. Balakumar, N. Tamilselvan, **Karthik Siram**, Sridhar Karthik, R. Hariprasad CH007: Nanomaterials in Drug Delivery: Existing Scenario and Potential Scope. *Nanobiomaterials in Drug Delivery*. Grumezescu. 197-228. Elsevier Publishers. May 2016. 978-0-323-42866-8. (DOI: 10.1016/B978-0-323-42866-8.00007-1).

Papers presented at conferences

- 1) Oral presentation during National Conference on Current Perspectives in Novel drug Delivery Systems held at PSG College of Pharmacy, Coimbatore during 16th- 17th June, 2017.

- 2) Oral presentation during 1st International Drug Delivery Congress 2017 held at RVS College of Pharmaceutical Sciences, Coimbatore, India during 20th- 21st January, 2017.
- 3) Oral presentation during “Two day symposium on Current trends in fundamental biochemical research: diverse applications from agriculture to human health” held at PSG Institute of Advanced Studies, Coimbatore during 13-14th December, 2016.
- 4) Presented a paper at “2016 American Association of Pharmaceutical Scientists Annual Meeting and Exposition”, Denver, United States of America during 13th- 17th November 2016.
- 5) Poster presentation at “Recent Advances in Neuropharmacology and Developmental Neurobiology”, RVS College of Pharmaceutical Sciences on 9th June, 2016.
- 6) Presented a poster at 67th Indian Pharmaceutical Congress, JSS University, Mysore during 19th- 21st December 2015.



ICODD 2014



3rd INTERNATIONAL CONFERENCE ON DRUG DELIVERY

Theme: "INNOVATIONS IN DRUG DELIVERY"

Organized by
PSG COLLEGE OF PHARMACY
Coimbatore, Tamil Nadu, India

Co - Sponsored by
DEPARTMENT OF BIOTECHNOLOGY
New Delhi, India

Certificate of Merit

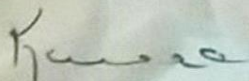
This is to certify that the scientific paper entitled LYMPHATIC TARGETING OF DIETHYLCARBAMAZINE

USING NANOPARTICLES

presented by Prof./Dr./Mr./Ms. SIRAM KARTHIK..... has been adjudged as the best paper

and secured FIRST..... place in oral / poster presentation of ICODD 2014 organized by PSG College of

Pharmacy, Coimbatore on 28th February - 1st March 2014.


Dr. M. Ramanathan
Chairman-LOC


Dr. C. Vijaya Raghavan
Convenor

**EXPERT
OPINION**

1. Introduction
2. Experimental section
3. Results and discussion
4. Conclusion

Solid lipid nanoparticles of diethylcarbamazine citrate for enhanced delivery to the lymphatics: *in vitro* and *in vivo* evaluation

Karthik Siram, Vijaya Raghavan Chellan[†], Tamilselvan Natarajan, Balakumar Krishnamoorthy, Habibur Rahman Mohamed Ebrahim, Vamshikrishna Karanam, Siva Selva Kumar Muthuswamy & Hari Prasad Ranganathan

[†]PSG College of Pharmacy, Department of Pharmaceutics, Coimbatore, Tamil Nadu, India

Objectives: The major objective is to target diethylcarbamazine citrate (DEC) to the lymphatics and to increase its retention time. The effect of various excipients on the physicochemical characteristics of the nanoparticles was also studied.

Materials and methods: Solid lipid nanoparticles (SLNs) of DEC were prepared by ultrasonication by varying the concentrations of Compritol 888 ATO, poloxamer 188 and soya lecithin. The SLNs were evaluated for size, shape, texture, surface charge, physical nature of the entrapped drug, entrapment efficiency and *in vitro* drug release. *In vivo* animal studies were carried out to estimate the pharmacokinetic parameters in blood and drug concentration in lymph after oral administration.

Results: The size of the spherical particles was in the range of 27.25 ± 3.43 nm to 179 ± 3.08 nm and a maximum entrapment efficiency of $68.63 \pm 1.53\%$ was observed. *In vitro* release studies in pH 7.4 PBS displayed a rapid release and the maximum time taken for the complete drug to release was 150 min. *In vivo* studies indicated an enhancement in the amount of drug that reached lymphatics when administered via SLNs.

Conclusion: Targeting of DEC to the lymphatics is possible through SLNs and the retention time in the lymphatics can also be enhanced.

Keywords: diethylcarbamazine citrate, filariasis, lymphatic targeting, mesenteric lymphatic duct, poloxamer 188, solid lipid nanoparticles

Expert Opin. Drug Deliv. [Early Online]

1. Introduction

The lymphatic system is an important repository for some diseases like filariasis [1], tuberculosis [2], AIDS [3], metastatic cancers [4], edema [5] and so on and also plays a role in the inflammatory processes [6]. The lymphatic system majorly modulates the immune system, and because of the complex nature and complex roles of the lymphatics, targeting of drugs to the lymphatics is challenging [7]. Thus, in order to target the drugs to the lymphatics and to further increase the residence time in the lymphatics, the moieties apart from reaching the lymphatic system should evade opsonization by reticuloendothelial system (RES), which can be possible by preparing particles of size > 100 nm [8].

Lymphatic filariasis is a vector-borne parasitic disease caused by three kinds of thread-like, parasitic filarial worms: *Wuchereria bancrofti*, *Brugia malayi* or *Brugia*

informa
healthcare

Article

Solid Lipid Nanoparticles of Albendazole for Enhancing Cellular Uptake and Cytotoxicity against U-87 MG Glioma Cell Lines

Gregory Marslin ^{1,*}, Karthik Siram ², Xiang Liu ¹, Vinoth Kumar Megraj Khandelwal ³, Shen Xiaolei ¹, Wang Xiang ¹ and Gregory Franklin ^{4,*}

¹ Chinese-German Joint Laboratory for Natural Product Research, Qinling-Bashan Mountains Bioresources Comprehensive Development C.I.C., College of Biological Science and Engineering, Shaanxi University of Technology, Hanzhong 723000, China; liuxiang8885@163.com (X.L.); 17809268805@163.com (S.X.); 15029541697@163.com (W.X.)

² Department of Pharmaceutics, PSG College of Pharmacy, Coimbatore, Tamilnadu, 641004, India; karthiksiram@gmail.com

³ Department of Translational Pharmacology, Consorzio Mario Negri Sud, Santa Maria Imbaro 66030, Italy; drvinothk@gmail.com

⁴ Department of Integrative Plant Biology, Institute of Plant Genetics of the Polish Academy of Sciences, Strzeszyńska 34, 60-479 Poznań, Wielkopolska, Poland

* Correspondence: marslingregory@gmail.com (G.M.); fgre@igr.poznan.pl (G.F.); Tel.: +86-150-2901-9373 (G.M.); +48-6-1655-0266 (G.F.)

Received: 27 October 2017; Accepted: 21 November 2017; Published: 22 November 2017

Abstract: Albendazole (ABZ) is an antihelminthic drug used for the treatment of several parasitic infestations. In addition to this, there are reports on the anticancer activity of ABZ against a wide range of cancer types. However, its effect on glioma has not yet been reported. In the present study, cytotoxicity of ABZ and ABZ loaded solid lipid nanoparticles (ASLNs) was tested in human glioma/astrocytoma cell line (U-87 MG). Using glyceryl trimyristate as lipid carrier and tween 80 as surfactant spherical ASLNs with an average size of 218.4 ± 5.1 nm were prepared by a combination of high shear homogenization and probe sonication methods. A biphasic in vitro release pattern of ABZ from ASLNs was observed, where 82% of ABZ was released in 24 h. In vitro cell line studies have shown that ABZ in the form of ASLNs was more cytotoxic ($IC_{50} = 4.90$ μ g/mL) to U-87 MG cells compared to ABZ in the free form ($IC_{50} = 13.30$ μ g/mL) due to the efficient uptake of the former by these cells.

Keywords: albendazole; solid lipid nanoparticles; U-87 MG cells; cytotoxicity; cellular uptake

1. Introduction

Development of new drugs with increased activity against cancer cells is the major focus of the pharmaceutical industry. Unfortunately, many of the new drugs are often toxic to the healthy cells as well. Hence, there is a space for the development of drugs that are toxic only to cancer cells. Although albendazole (ABZ) is known for its antihelminthic activity, recent studies show that it possesses significant anticancer activity as well. ABZ is an affordable drug, which exhibits antihelminthic activity even at a very low concentration (7.5 mg/kg) [1]. The ability of ABZ to destroy the β tubulin structures of the helminthes has also been exploited to kill tumor cells. Activities of ABZ against colorectal cancer and peritoneal carcinomatosis have been demonstrated respectively using HT-29 cell line and xenograft models [2]. Later, the ability of ABZ to inhibit cell proliferation, vascular endothelial growth factor and tumor growth was discovered [3]. In addition, ABZ could also arrest



Edited by
ALEXANDRU MIHAI GRUMEZESCU

NANOBIO MATERIALS IN DRUG DELIVERY

APPLICATIONS OF NANOBIO MATERIALS

Volume 9

Nanomaterials in drug delivery: existing scenario and potential scope

Habibur Rahman¹, Balakumar Krishnamoorthy¹, Natarajan Tamilselvan¹,
Karthik Siram¹, Sridhar Karthik¹ and Ranganathan Hariprasad²

¹*Department of Pharmaceutics, PSG College of Pharmacy, Coimbatore, Tamil Nadu, India*

²*Department of Pharmaceutical Analysis, PSG College of Pharmacy, Coimbatore, Tamil Nadu, India*

7.1 NANOTECHNOLOGY IN DRUG DELIVERY

Nanotechnology employs engineered materials or devices in the nanometer size range (1–1000 nm). Richard Feynman introduced the concept of nanotechnology as an important field of future scientific research in 1959 (Feynman, 1960). Nanotechnology applications in drug delivery are witnessed by many novel nano-devices. There has been substantial attention to the growth of novel drug delivery using nanotechnology. Nanoparticles (NPs) symbolize a promising drug-delivery scheme of controlled and targeted release. The advantages of nanoparticles as drug-delivery systems include reduced drug toxicity, time-controlled drug delivery, enhanced bioavailability, improved therapeutic efficacy, and biodistribution (Ravi Kumar, 2000). Nanotechnology also protects sensitive drugs from degradation by environmental factors, namely, stomach acid and enzymes (Jores et al., 2004). Polymeric nanoparticles are in the size range of 10–1000 nm (Kreuter, 2001), and can be tailored with diverse ligands, namely, antibodies to create a smart targeting delivery system. Polymeric nanoparticles in the size range of 300 nm or less with surfactant coatings have been proved to be able to transport drugs across the blood–brain barrier (BBB) (Schroeder et al., 1998). Recent advancements and applications of nanotechnology in drug delivery have proven effective for treating many diseases. Nanotechnology growth is unprecedented in the development of nanotherapeutics such as controlled drug-delivery systems, site-specific/targeted drug delivery, gene delivery, lipid-based delivery systems, implants, smart/intelligent drug-delivery systems, polymeric nanosystems, colloidal systems, etc.

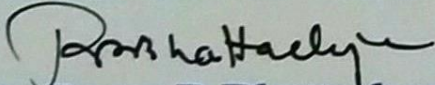
**Symposium on Current Trends in Fundamental Biochemical
Research: Diverse Applications from Agriculture to
Human Health**

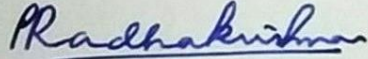


Certificate of Participation

This certificate is awarded to *Dr./Prof./Mr./Mrs./Ms. Karthik Siram*,
Research Scholar, PSG Pharmacy College, Coimbatore

for his/her active participation and oral/poster presentation entitled
Development of Hyaluronic Acid Coated Lipid Based Nanotherapeutics
against Metastasis of Breast Cancer in the National Symposium on
**“Current Trends in Fundamental Biochemical Research: Diverse
Applications from Agriculture to Human Health”** held on 13th and 14th
December 2016, organized by PSG Institute of Advanced Studies
and sponsored by SERB (Department of Science & Technology)
and ICMR (New Delhi).


Dr. Rama R. Bhattacharjee
Organizing Secretary


Prof. P. Radhakrishnan
Director, PSG IAS



Certificate of Presentation

This certificate acknowledges that

Karthik Siram

Presented a Poster Titled

Functionalization and Pharmacological Evaluation of Imatinib Mesylate Loaded Lipid Nanoshells Prepared Using Quillaja Saponin as Surfactant

2016 AAPS Annual Meeting and Exposition

November 13–17, 2016

A handwritten signature in black ink, appearing to read "Greg Amidon".

Gregory E. Amidon Ph.D.
AAPS President



RVS COLLEGE OF PHARMACEUTICAL SCIENCES



Affiliated to The Tamil Nadu Dr.M.G.R Medical University, Chennai
242-B, Trichy Road, Sulur, Coimbatore - 641402. TamilNadu, India
web: www.pharmacy.rvshs.ac.in

Certificate of Participation

This is to certify that

Dr./Mr./Ms. Sivam Karthik

has participated in one day

NATIONAL SEMINAR ON "Recent Advances in Neuropharmacology and Developmental Neurobiology"

*as a Speaker / Panel Member / Delegate / Presented a Poster In vivo testing of
Lipid Nanoshells in Wistar Rats* Held on 9th June 2016 at

RVS COLLEGE OF PHARMACEUTICAL SCIENCES SULUR, COIMBATORE

Dr.D. Benito Johnson
Convenor

Dr.R. Manavalan
Co-Chairman

Dr.R. Venkatanarayanan
Chairman



THEME
PHARMA
VISION
2020



इज्जतु भारत

PHARMACISTS FOR
A HEALTHY INDIA



67th Indian Pharmaceutical Congress
19-21 December 2015
Mysuru, India

Certificate of Participation

This is to certify that

Sriram Karthik

has participated as a Delegate
in the 67th IPC held at JSS University, Mysuru
19 - 21 December, 2015.

Dr. B. Suresh
Chairman, LOC
67th IPC, 2015

Dr. B. Manjunatha
Organising Secretary
67th IPC, 2015

Dr. (Lt Col) R. Vijaysimha
Chairman, Registration
67th IPC, 2015

The Scientific Program is recognised as 'Continuing Pharmacy Education' under Regulation 4.2(IV) of the Pharmacy Practice Regulations 2015



Pharmacy Council of India
New Delhi



Organised by
Indian Pharmaceutical Congress Association

Hosted by

Indian Hospital Pharmacists Association





THE TAMIL NADU Dr. M.G.R. MEDICAL UNIVERSITY

No.69, ANNA SALAI, GUINDY, CHENNAI - 600 032.

Website : www.tnmgrmu.ac.in
E-mail : mail@tnmgrmu.ac.in

☎ : 22353574, 22353576 - 79, 22301760 - 63, 22353094
Fax : 91-44-22353698

Dr. JHANSI CHARLES, MD.,
REGISTRAR.

SW(3)/30691/2014

Dated: 05/11/2014

To
Dr. C. Vijaya Raghavan,
Professor,
Department of Pharmaceutics,
PSG College of Pharmacy,
Peelamedu,
Coimbatore-4

Sir,

Sub: Student Welfare Section- The Tamil Nadu Dr. MGR Medical University -Project titled '**Development of surface modified lipid nanoparticles for selective targeting of tumor cells in lymph nodes to prevent metastasis and its evaluation in BALB/c mice cancer model**' - submitted before the University Research Council - Grants of fund for the year 2014-2015 Intimation- Regarding.

Ref :1. Letter dated 29.07.2014

2. Recommendation of the University Research Council meeting held on 17.09.2014.

I am by direction to inform that your project '**Development of surface modified lipid nanoparticles for selective targeting of tumor cells in lymph nodes to prevent metastasis and its evaluation in BALB/c mice cancer model**' submitted before the University Research Council of this University on 17.09.2014 for seeking research grant is approved. The sanctioned amount of **Rs.50,000/- (Rupees fifty thousands only)** will be released to the Principal Investigator through HOD/Guide. . The said grant will be sanctioned in 3 installment that is 50% as I stage balance 50% will be issued as 25% each in 2nd & last installment on production of Utilization Certificate.

Therefore you are instructed to follow rules in force as detailed below:-

1. Maximum duration of the Project is 2 years. If the project is not completed within the stipulated period, an extension of 6 Months may be allowed with justified reasons.



தமிழ்நாடு அறிவியல் தொழில்நுட்ப மாநில மன்றம்
TAMILNADU STATE COUNCIL FOR SCIENCE AND TECHNOLOGY

(Established by Government of Tamilnadu)

Directorate of Technical Education Campus, Chennai - 600 025

Phone : 044 - 2230 1428

Web : www.tanscst.nic.in

Telefax : 044 - 2230 1552

E-mail : enquiry.tanscst@nic.in / ms.tanscst@nic.in

DR. R. SRINIVASAN, M.Sc., Ph.D., F.I.C.S., M.A.C.S.(USA).
Member Secretary

Ref: TNSCST/RFRS/VR/08/2015-16

1068

12.04.2017

To

Sriram Karthik
Research Scholar
PSG College of Pharmacy
Peelamedu,
Coimbatore – 641 004

Sir/Madam,

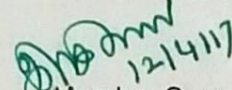
Sub: Programme to bridge the gap in research funding for research scholars in colleges (RFRS) – approval – reg.

Ref: 55th Meeting of Executive Committee conducted on 28.03.2017

With reference to the above, I am happy to inform that the research work of Sriram Karthik, Research Scholar, PSG College of Pharmacy, Peelamedu, Coimbatore – 641 004 has been approved for financial support under RFRS scheme of the Council (Medical sciences). A sum of Rs.3.00 lakhs (Rupees Three lakhs only) has been sanctioned for 2 years. The terms and conditions and other details of the grant is enclosed. Kindly send your acceptance to avail RFRS as per our terms and conditions within two weeks from receipt of this letter. Prof.V.Ramaswami, Associate Professor of the Council and Officer-in-charge of the above programme may be contacted for clarification (Ph:9444743052) if there is any.

With wishes,

Yours faithfully,


12/4/17
Member Secretary

Copy to:

The Principal
PSG College of Pharmacy
Peelamedu, Coimbatore – 641 004



Science and Engineering Research Board
International Travel Support Scheme

Established through an Act of Parliament: SERB Act 2008, Department of
Science & Technology, Government of India

Application No. - ITS/4017/2016-17

Dated: 30-09-2016

To

Mr. KARTHIK SIRAM

Research Scholar

Pharmaceutics

PSG COLLEGE OF PHARMACY

COIMBATORE-641004(TAMIL NADU)

Sub. : Financial Assistance to Mr. KARTHIK SIRAM for participating in 2016 AAPS ANNUAL MEETING AND EXPOSITION to be held from 13-11-2016 to 17-11-2016 in DENVER, UNITED STATES OF AMERICA.

Sir/Madam,

We are happy to inform you that your application seeking financial grant to attend the above mentioned international scientific event has been recommended for support by the Science and Engineering Research Board (SERB). We will provide to and fro economic class air-fare by the shortest route, airport tax, visa fees & registration fees. It is hoped that the support will give you an opportunity to interact with leading international experts in the area. The support, however, is subject to the following conditions.

1. You should not have received financial support during the last three years under this scheme.
2. The air tickets are to be booked in economy class by the shortest route in a national carrier i.e. Air India. In case you are traveling by other Airlines due to non-availability of tickets or service by Air India, you are requested to get a certificate from Air India indicating the actual position on that particular date/dates and sector/sectors. Without this certificate, it will not be possible to reimburse the air fare.
3. **The destination for which there is no direct Air India flight, you have to travel by Air India upto the nearest hub to the destination and after that services of any other airline may be utilized, preferably of Air India alliance partner.**
4. **E-ticket is acceptable provided the amount of the fare is clearly reflected on the ticket.**
5. The signed print copy of Claim Form along with the original Boarding passes and institute account details must be sent to the SERB immediately after completing the online Claim Form to the following address.

ITS Section

5 & 5A, Lower Ground Floor

Vasant Square Mall, Sector B, Pocket 5

Vasant Kunj, New Delhi, Delhi-110070

6. The account details must be in the format available at the home page of the online portal in the format section and it must be endorsed by the competent authority of the institute/university.

7. SERB will reimburse the grant after deducting the financial assistance received from any other sources, if any.
8. All other expenses such as per diem, taxi fare etc. will not be reimbursed by SERB.
9. You will have to make your own arrangements for foreign exchange required for the purpose.
10. You will not be treated as a delegate sponsored by the Government of India.
11. Based on this offer letter, your Institute may consider advancing necessary funds to enable you to attend the above event.
12. **We request you to either accept or decline this offer at the earliest online. On acceptance only, you will be able to submit the Claim Form. Please note that once you decline this offer, it will be assumed that you are not interested in availing this offer and no further communication will be entertained in this matter.**
13. **You must submit Claim Form and other documents online within 90 days of the Last Date of the Event, failing which SERB will not reimburse the Travel Grant.**

With kind regards,

Your's Faithfully

Monika Agarwal

Scientist-E

Email

:ms[DOT]its[At]serb[DOT]gov[DOT]in

Ph: 40000355(O)

**CENTRE FOR INTERNATIONAL CO-OPERATION IN SCIENCE (CICS)
REGISTERED SOCIETY**

(Promoted by Indian National Science Academy, New Delhi
in Association with Scientific Agencies and Departments)

**Dr. (Mrs) A. AMUDESWARI
Director**

DO\Dr. \TF-II\2014-15

18 July 2014

MR. SIRAM KARTHIK
RESEARCH SCHOLAR
PSG COLLEGE OF PHARMACY
PEELAMEDU
COIMBATORE-641004

Dear MR. SIRAM KARTHIK,

Sub: Travel support to attend 5TH WORLD CONGRESS ON BIOAVAILABILITY AND BIOEQUIVALENCE:
PHARMACEUTICAL R&D SUMMIT at BALTIMORE, USA during 29/09/2014 - 01/10/2014

We are extremely pleased to inform you that CICS will provide financial assistance of Rs.25,000/- **which is subject to actual expenditures and receipts from all other sources whichever is less**, towards partial travel / registration / accommodation for attending the above meeting/conference. Please confirm your acceptance of this offer within 15 days from the date of this letter, failing which the award will be forfeited.

In the event you are not able to utilise this grant for various reasons even after confirming your acceptance, please do inform us immediately so that the money can be transferred to waitlisted awardees.

The actual amount will be paid after your return from the Conference. Please find enclosed herewith a Proforma in which you will have to submit your claim along with a copy of

award letter
participation certificate
participation report & airticket
visa page

passport (first two pages)
passport size photograph
documents as specified in the terms & conditions
Award letter from other agencies

Your claim must be endorsed by the Head of the Institute / competent authority and should reach our office within one month after the completion of the scientific meeting / training. The payment will be made in favour of Head of organisation / Finance Controller of your organization.

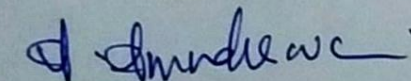
The grant is however subject to the consideration that you have not availed such offer from CICS (CCSTDS) during the last three years.

The grant is governed by Terms and Conditions (enclosed). The admissibility of the claim will be as per INSA/CICS norms.

In order to avoid delay in reimbursement of your claim, please do ensure that the terms and conditions are strictly adhered to.

With kind regards,

Yours sincerely,



(A. AMUDESWARI)

Encl: As above



IDG 2017



RVS GROUP
Building Independent Capital

1st INTERNATIONAL DRUG DELIVERY CONGRESS 2017 (IDG 2017)

Organized by: **RVS COLLEGE OF PHARMACEUTICAL SCIENCES & RVS PADMAVATHI AMMAL COLLEGE OF PHARMACY**

Theme: Exploring the Advances and Challenges in Drug Delivery with emphasis on Nano

CERTIFICATE OF MERIT

This is to certify that the scientific paper entitled *Development of A Novel Preformulation*

Method for Preparation of Lipid Based Formulations

presented by Prof. / Dr. / Mr. / Ms. SIRAM KARTHIK

has been adjudged as the *Best Paper in Oral / Poster Presentation* of IDG 2017 organized by RVS College of Pharmaceutical Sciences and RVS Padmavathi Ammal College of Pharmacy,

Sulur, Coimbatore from 20th - 21st January 2017.

R Manavalan

Dr. R. Manavalan
Convener

Sanjiv Kumar

Dr. H. Mohamed Mubarak
Secretary, RVS Educational Trust



Co-sponsors





PSG COLLEGE OF PHARMACY, COIMBATORE

**National Conference on
Current Perspectives in Novel Drug Delivery Systems**

16th & 17th JUNE 2017

Certificate of Merit


This is to certify that the scientific paper titled A COMPUTATIONAL APPROACH TO PREDICT
SOLUBILITY OF DRUGS IN LIPIDS

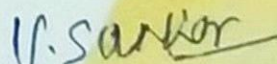
presented by Mr. /Ms. /Mrs KARTHIK SIRAM

Co authored by DIVAKAR.S, SM.HABIBUR RAHMAN, C.VIJAYA RAGHAVAN, V.SANKAR

has been awarded the BEST ORAL / ~~POSTER~~ presentation in the conference organized by

Department of Pharmaceutics.


Dr. M. Ramanathan
Chairman


Dr. V. Sankar
Convenor



Quillaja saponin: A prospective emulsifier for the preparation of solid lipid nanoparticles



Karthik Siram^a, Chellan Vijaya Raghavan^a, Gregory Marslin^b, Habibur Rahman^a, Divakar Selvaraj^c, Krishnamoorthy Balakumar^{a,1}, Gregory Franklin^{d,*,1}

^a Department of Pharmaceutics, PSG College of Pharmacy, Peelamedu, Coimbatore, 641004, India

^b Centre for the Research and Technology of Agro-Environment and Biological Sciences (CITAB), University of Minho, Braga 4710-057, Portugal

^c Department of Pharmacology, PSG College of Pharmacy, Peelamedu Coimbatore, 641004, India

^d Department of Integrative Plant Biology, Institute of Plant Genetics of the Polish Academy of Sciences, Strzeszyńska 34, 60-479 Poznań, Poland

ARTICLE INFO

Article history:

Received 22 March 2016

Received in revised form 3 July 2016

Accepted 31 July 2016

Available online 1 August 2016

Keywords:

Quillaja saponin

Stearic acid

Solid lipid nanoparticles

Imatinib mesylate

Haemolytic test

ABSTRACT

Quillaja saponin (QS) is a non-ionic amphiphilic surfactant of natural origin. In the present study, we evaluated its potential to form solid lipid nanoparticles (SLNs) in the presence of stearic acid (SA) as a lipid carrier and imatinib mesylate (IM) as a model drug. IM loaded solid lipid nanoparticles (IMSLNs) were prepared using the hot homogenisation method. Characterisation of IMSLNs revealed that they were quasi-spherical in shape, neutrally charged and 143.5–641.9 nm in size. Haemolysis, a toxicity issue of QS was not observed in SLNs. Comparative in vitro cytotoxicity analyses performed in human breast cancer cell line MCF7 revealed that IMSLNs were more toxic than IM. On the other hand, in vitro viability studies in the RAW264.7 cell line did not show any sign of toxicity by IMSLNs. Our results indicate that QS hold great potential in nano drug delivery as an emulsifier.

© 2016 Elsevier B.V. All rights reserved.

1. Introduction

Applications of solid lipid nanoparticles (SLNs) have increased tremendously in recent times due to their major advantages such as biocompatibility, biodegradability, ease of preparation, potential for scale up and cost effectiveness. SLNs consist of a solid lipid core dispersed in aqueous solutions of stabilisers or surfactants at room temperature [1]. Stearic acid, palmitic acid, glyceryl behenate, etc., are the commonly used lipids; whereas, poloxamers, polysorbates, phospholipids, bile salts, sodium oleate, cremophor EL, etc. are commonly used as stabilisers in the preparation of SLNs. In this communication, we report on the efficient preparation of SLNs loaded with an anticancer drug using Quillaja saponin (QS) for the first time.

QS is a non-ionic amphiphilic surfactant extracted from the bark of *Quillaja saponaria* (Soap bark tree). QS is a glycoside (Fig. 1) with a lipophilic backbone of quillaic acid and gypsogenic acid (a triterpene aglycone), to which hydrophilic polysaccharide moieties like

rhamnose, xylose, arabinose, galactose, fucose, and glucuronic acid are attached [2]. Thus, QS can perform the role of a surfactant by adsorbing at the oil and water interface to form an emulsion [3]. Despite the characterisation of the micellar properties of QS as early as 1800 AD and approval by the US Food and Drug Administration (FDA) [4], its application has not gained prominence in the pharmaceutical sector so far. In addition to its emulsifying property, QS also possesses many bioactivities (larvicidal, antitumor, antimicrobial etc.) and is used as a natural foaming agent in cosmetic products, and as an adjuvant in vaccine delivery [5–7]. Furthermore, a product based on the *Q. saponaria* bark extract is marketed under the trade name Q-Naturale and approved by FDA for use as emulsifier in beverages.

The aim of the present study was to investigate the possibility of using QS as a surfactant in the preparation of SLNs containing an anticancer drug. Briefly, we have used stearic acid (SA), an 18-carbon fatty acid as the lipid core to encapsulate imatinib mesylate (IM), a hydrophilic anticancer drug. The prepared SLNs, loaded with IM (IMSLN), were physicochemically characterised for particle size distribution, morphology, zeta potential, crystallinity, entrapment efficiency and drug release. In addition, they were analysed for in vitro haemolytic activity, cytotoxicity and viability using cell lines. Our results demonstrate that QS is an excellent stabiliser for the preparation of SLNs without any haematotoxicity.

* Corresponding author at: Department of Integrative Plant Biology, Institute of Plant Genetics of the Polish Academy of Sciences, Strzeszyńska 34, 60-479 Poznań, Poland.

E-mail address: fgre@igr.poznan.pl (G. Franklin).

¹ Contributed equally to this work.

A brief perspective on the diverging theories of lymphatic targeting with colloids

Karthik Siram¹
Gregory Marslin²
Chellan Vijaya Raghavan¹
Krishnamoorthy Balakumar¹
Habibur Rahman¹
Gregory Franklin³

¹Department of Pharmaceutics, PSG College of Pharmacy, Coimbatore, India; ²Centre for the Research and Technology of Agro-Environment and Biological Sciences, University of Minho, Braga, Portugal; ³Department of Integrative Plant Biology, Institute of Plant Genetics, Polish Academy of Sciences, Poznań, Poland

Correspondence: Chellan Vijaya Raghavan
Department of Pharmaceutics, PSG College of Pharmacy, Peelamedu, Coimbatore, India 641004
Tel +91 9843128373
Email drvijayaragha@gmail.com

Gregory Franklin
Department of Integrative Plant Biology, Institute of Plant Genetics, Polish Academy of Sciences, Strzeszyńska 34, 60-479 Poznań, Poland
Tel +48 61 655 0266
Fax +48 61 655 0301
Email fgfr@igr.poznan.pl

Abstract: For targeted delivery of colloids to the lymphatic system, the colloids should efficiently reach and remain in the lymphatics for a considerable period of time. As per the current knowledge, diffusion and phagocytosis are the two mechanisms through which colloids reach the lymphatic system. Several parameters including particle size and charge have been shown to affect the direct uptake of colloids by the lymphatic system. Although many researchers attached ligands on the surface of colloids to promote phagocytosis-mediated lymphatic delivery, another school of thought suggests avoidance of phagocytosis by use of carriers like polyethylene glycol (PEG)ylated colloids to impart stealth attributes and evade phagocytosis. In this perspective, we weigh up the paradoxical theories and approaches available in the literature to draw conclusions on the conditions favorable for achieving efficient lymphatic targeting of colloids.

Keywords: lymphatic targeting, colloids, PEGylation, phagocytosis

Introduction

The lymphatic system (lymphatics), which encompasses the circulating lymph, network of lymphatic pathways (lymphatic capillaries, collecting vessels, trunks, and ducts), and lymphatic organs (lymph nodes, thymus, bone marrow, tonsils, spleen, etc) is present throughout the body in conjunction with the systemic circulation. The lymph is formed by the transport of interstitial fluid surrounding the blood vessels into the lymphatic capillaries. Thus, the lipids, enzymes, and protein composition of lymph and plasma remain the same and vary only in concentrations.^{1,2} The lymphatic system removes foreign bodies from the body and maintains homeostasis. Apart from mediating the immune functions and tissue fluid balance, the lymphatics also act as a reservoir for human immunodeficiency virus, filariasis, tuberculosis, and metastatic cancer cells.³ Hence, lymphatic targeting of molecules, compounds, vaccines, and so on will be useful for diagnosis and therapy and eliciting immune responses. Colloids have emerged as an important class of drug carriers for targeted delivery into the complex lymphatic system.⁴ Targeting colloids to the lymphatics involves two major steps: first, the targeting material should reach the lymphatic structures and then it should reside there for a considerable period of time by evading the host immune trafficking mechanisms. A plethora of articles on lymphatic targeting using colloids suggests that several parameters such as surface charge, particle size, molecular weight, route of administration, nature of the colloid and its surface properties (hydrophilicity and lipophilicity), and so on play a role in targeting colloids to the lymphatics, and a discussion on each of those factors is out of focus of this perspective as it would be a mere repetition of the already established facts. However, the role of phagocytosis and polyethylene glycol (PEG) attachment to colloids (PEGylation) on lymphatic